Western Australian School of Mines
Department of Mining Engineering & Metallurgical Engineering

Characterising Coarse Particle Gangue Densimetric Separation Response in Gold Bearing Sulfide Ore Broken by Different Fine Crushing Modes

Paul Bode

This thesis is presented for the Degree of
Master of Philosophy
of
Curtin University

February 2022

ABSTRACT

Fine crushing regime test-work and techniques for gravity separation performance characterisation of gold-bearing ores are powerful tools in proving confidence in the design and performance of coarse-scale (millimetres) gravity circuits. Achieving successful early-stage rejection of low-grade uneconomic material can increase the valuable metal units within the mass fed to energy and water-intensive tumble milling circuit. This research describes interpretative techniques to characterise crushed gold-bearing sulfide ore's inherent propensity for density-based metal pre-concentration by coarse particle gangue rejection. Coarse gangue rejection aims to concentrate the waste mineral in ore feed into lower density fractions by removing the liberated gangue produced during fine crushing. Knowledge of an ore's amenability for early-stage gangue rejection can reduce waste mineral mass fed to a tumble milling circuit. This knowledge benefits the mining where a predicted decline in head grade trajectory for future gold-bearing ore deposit projects is attributed to a rising proportion of gangue minerals in run-off mine ore that require tumble milling. However, until this study, a method for quantitatively measuring laboratory gravity separation performance at a coarse scale on crushed gold-bearing ores was inadequate. As a result, the economic potential of gravity-based coarse-scale gangue mineral rejection or pre-concentration to improve the economic potential of some ore deposits is overlooked.

The Gangue Rejection Amenability Test (GRAT) method, described by McGrath, Eksteen, and Bode (2018), yielded a promising path for evaluating the propensity of gold-bearing sulfide ores to preferentially concentrate metal by combined size and density classification of finely crushed material below five (5) millimetres. However, Bode, McGrath & Eksteen (2019) reported that previous laboratory gravity methods for separating particle sizes of ≥1.18 mm were inadequately identified for gold ores.

This thesis investigated empirical data derived from using the GRAT gravity separation method to process selected gold-bearing sulfide ores after breakage by various crushing modes. These ores were from orogenic and porphyry copper-gold ore-deposit styles supplied as samples by Ballarat Castlemaine Goldfields Limited,

Victoria, Australia, and Cadia East NSW, Australia, respectively. Representative sub-samples of Ballarat and Cadia ore were stage-crushed using specified crushing modes and screened to 100 percent, with passing sizes of 2.00 mm and 4.75 mm, respectively. Crushing modes used were the laboratory-scale Sala mortar Cone crusher, SELFRAG Lab Selective Fragmentation (SELFRAG), Rolls crusher, High Pressure Grinding Rolls (HPGR) and Vertical Shaft Impactor (VSI) modes. The GRAT classification technique investigated the interaction of specific gold-bearing sulfide ores with different crushing modes to provide information for predicting mineral gravity separation performance. The variability in quantity for metal-rich and gangue particles in the GRAT specific density fractions after ore breakage determines the extent of the enrichment ratio and preferential grade by density deportment response.

The thesis demonstrates a mathematical approach capable of characterising the GRAT gravity separation empirical data. This dissertation developed three metallurgy parameters to describe gravity separation metallurgical efficiency of metal concentration for particle sizes of ≤4.75 mm. These parameters were coined the rejection enrichment ratio (RER), enrichment deportment response (EDR) and enrichment deportment index (EDI). The RER and EDR parameters provided a statistically robust prediction of the grade enrichment ratio and preferential grade by density deportment response within sink fractions during gangue removal. A method of least squares estimated the EDI parameter value by using the slope coefficient of the natural log of the metal RER and the accumulative mass pull into the sink fractions. The EDI value enables the calculation of grade and metal yield partition curves for different specific separation operations over a range of mass pulls into sinks fractions. Statistical comparison of partition yield values into sinks against the GRAT Ballarat and Cadia densimetric results provided good agreement, demonstrating the EDI parameter as a robust prediction of crushed gold-bearing sulfide ore overall magnitude of grade deportment by density response into sinks. Thereby, using the EDI parameter ore signature to improve resource efficiency and productivity in waste mineral rejection through coarse particle gravity separation offers a substantial opportunity for present mine operating philosophy.

DECLARATION BY AUTHOR

To the best of my knowledge and belief, this thesis contains no material previously published by any other person except where due acknowledgment has been made.

This thesis contains no material which has been accepted for the award of any other degree or diploma in any university.

Name: Paul Bode

Signature: ……..

Date: 19th October 2021

ACKNOWLEDGMENT

The author wishes to thank the AMIRA P420F sponsors (AngloGold Ashanti, Australian Gold Reagents, Barrick Gold, Evolution, FLSmidth, Gekko Systems, Gold Fields, Kemix, Lhoist, Newcrest Mining, Newmont Mining, Northern Star Resources, Orica, Pionera and Vega industries) and the Western Australian School of Mines: Minerals, Energy and Chemical Engineering at Curtin University for financial and technical support. Coarse particle gangue rejection is a research objective of the AMIRA P420F Gold Processing Technology project; much of the density separation results used in this thesis have been taken from AMIRA P420F project work, reported on by Eksteen (2015). The author is particularly appreciative to Castlemaine Goldfields Limited and Newcrest Mining for the provision of ore samples.

This research would not have been possible without the financial support from The Cooperative Research Centre for Optimising Resource Extraction (CRC ORE). CRC ORE is part of the Government's Cooperative Research Centre (CRC) Program, which is made possible through the investment and ongoing support of the Australian Government. The CRC Program supports industry-led collaborations between industry, researchers, and the community.

My sincere appreciation is extended to Professor Jacques Eksteen and Dr Teresa McGrath for their guidance and technical support during my MPhil studies at Curtin University. I am also grateful to Mr Jim Cupitt for his support and our conversations regarding geostatistical techniques while undertaking this research. Finally, I also am thankful to Prof. Ryan Loxton for discussions on statistical analysis and Mr Jeff McGrath for his support in laboratory test work.

List of Definitions and Acronyms

a	((practical) range)
Alpha or α	(significance level)
AMIRA	(Australian Mineral Industries Research Association)
As	(arsenic)
Au	(gold)
b	(slope)
β	(population slope)
c	(sill)
c_0	(nugget)
CI	(confidence interval)
Cu	(copper)
CVO	(Cadia Valley Operations)
CPGR	(coarse particle gangue rejection)
CM	(cumulative mass)
CW	(cumulative weight)
DF or df	(degrees of freedom)
Ɛ	(error or residual)
Ep	(Ecart probable)
EDR	(enrichment deportment response)
EDI	(enrichment deportment index)
f	(feed grade)
Fe	(iron)
g	(grams)
GRAT	(Gangue Rejection Amenability Test)
GTG	(Curtin university gold technology group)
g/t	(grams per tonne)
h	(parametric displacement or lag distance)
HPGR	(high pressure grinding roll)
HLS	(heavy liquid separation)

HV	(high voltage)
i	(the i-th point in suggestive order)
j	(set to 1 at the first observed state)
Kg	(kilogram)
ln	(natural log)
LST	(lithium heteropolytungstates)
LLS	(linear least squares)
ME	(mean error)
MFP	(mining multifactor productivity)
Mo	(molybdenum)
n	(total number of separation points)
N or n	(total number of individuals in a sample)
O/S	(oversize)
p-value	(probability value)
P_{xx}	(xx percentage passing size of product)
ppb	(parts per billion)
ppm	(parts per million)
PSD	(particle size distribution)
r	(correlation coefficient)
R^2 or r^2	(coefficient of determination)
RER	(rejection enrichment ratio)
RMSE	(root-mean square error)
ROM	(run-off mine)
S	(sulfur)
SD or S	(standard deviation of a sample)
SELFRAG	(Selective Fragmentation)
SEM	(standard error of the mean)
SG	(specific gravity)
SPT	(sodium polytungstate)
SST	(total sum of squares)

SSW	(sum of squares within groups)
S_b	(standard error of the slopes)
$S^2_{y.x}$	(standard error)
$SE_{(\bar{y}_1 - \bar{y}_2)}$or $SE_{\mathrm{x-y}}$	(standard error of the differences between two means)
S^2	(error variance)
S^2_{Res}	(variance of the pooled residuals)
S_r	(standard error of r)
sW	(variance within groups)
t	(tail grade)
t_α	(t-value, sourced from the t-distribution)
UCS	(unconfined compressive strength)
U/S	(undersize)
Upg ratio	(upgrade ratio)
VSI	(vertical shaft impactor)
w	(tail fraction to feed mass ratio)
Wt	(weight)
x_i $or x_j$	(independent variable on the x-axis)
y_i or y_j	(dependent variable on the y-axis)
$\widehat{y_j}$	(fitted model y_j predicted dependent variable)
γ	(semivariance)
μ or $\bar{x}$ or $\bar{y}$	(arithmetic mean)
μm	(micron)
Σ	(sum of x_i or x_j or y_i or y_j variables)
%	(percent)

Publications during candidature

McGrath, T.D.H., Eksteen, J.J. and Bode, P., 2018. Assessing the amenability of a free milling gold ore to coarse particle gangue rejection. Minerals Engineering, 120, pp.110-117.

Contributor	Statement of contribution
Dr Teresa McGrath Signature.	Designed experiments (100%) Methodology & data acquisition (80%) Analysis of data (50%) Wrote the paper (60%)
Prof Jacques Eksteen Signature.	Wrote the paper (5%)

Bode, P., McGrath, T., & Eksteen, J., (2019). Characterising the effect of different modes of particle breakage on coarse gangue rejection for orogenic gold ore. In World Gold Conference, Perth, WA, 11-13 September 2019 (pp. 285-302).

Contributor	Statement of contribution
Dr Teresa McGrath Signature.	Designed experiments (100%) Methodology & data acquisition (20%) Wrote the paper (5%) Edition and revision (90%)
Prof Jacques Eksteen Signature.	Edition and revision (10%)

Bode, P., McGrath, T.D.H. and Eksteen, J.J., 2019. Characterising the effect of different modes of particle breakage on coarse gangue rejection for an orogenic gold ore. Mineral Processing and Extractive Metallurgy, pp.1-14.

Contributor	Statement of contribution
Dr Teresa McGrath Signature.	Designed experiments (100%) Methodology & data acquisition (20%) Wrote the paper (5%) Edition and revision (90%)
Prof Jacques Eksteen Signature.	Edition and revision (10%)

Contributions by others to the thesis

This thesis forms part of a larger research project, AMIRA Project P420F – Gold Processing Technology sponsored by the mining industry and the Australian government through The Australian Mineral Industries Research Association Limited (AMIRA) and Cooperative Research Centre for Optimising Resource Extraction (CRC ORE). The conception and design of the research project were created by Prof Jacques Eksteen, Dr Teresa McGrath, and many others whose individual contributions helped deliver this thesis.

Author contribution statement

As the primary author of two out of three publications produced from this thesis, the MPhil candidate conducted a part of the planning and the experiments, collected, organised, processed, and interpreted the experimental data, and took the lead in writing and revising the manuscript for two of the publications. Prof Jacques Eksteen and Dr Teresa McGrath provided constructive design and critical comments, as well as conducted a part of the writing, data analysis, interpreted the experimental data and revised the manuscript.

For the third publication, the MPhil candidate is the third co-author from a total of three authors. The candidate conducted a large part of the experiments, as well as contributed to the data analysis and interpretation, writing and revision of the manuscript.

A signed statement of contribution to the published works from this thesis is attached in Appendix 4.

TABLE OF CONTENTS

TABLE OF FIGURES

LIST OF TABLES

Chapter 1. Introduction

This chapter provides context and introduces the topic, highlighting the gaps in the present literature and the reasons for this thesis project. It describes the overall aim and delimitation of the thesis and the resultant hypotheses, objectives, and thesis structure.

1.1 Context

A successful interpretative technique for optimally applying gold-bearing sulfide ore gravity separation in removing coarse particle gangue or pre-concentrate metal justifies ongoing research. This research supports efforts to remove a high proportion of liberated gangue ahead of tumble milling, reduces grinding energy and water consumed in milling gangue, and improves unit metal productivity. Reducing energy and water intensity, and thereby cost, in metal production improves productivity in mining operations (ABS, 2012; ABS, 2016; ABS, 2018). However, the mining industry faces energy and water efficiency and productivity challenges (Aldrich, 2013; Eksteen; 2015). Therefore, a better understanding of the proportion of gangue removal can be an essential driver in improving mine productivity used to generate a single unit of metal product (Topp et al., 2008).

Several researchers have reported that host rock mineralogy and spatial grade heterogeneity influences metal pre-concentration through preferential grade deportment into specific size fractions in the broad range between 5 mm to 125 mm, after ore breakage (Bamber et al., 2008; Dominy, Murphy, & Gray, 2011; Bearman, 2013; Sakuhuni, Tong, & Klein, 2014; Bowman & Bearman, 2014; Carrasco et al., 2017; McGrath, Eksteen, & Bode, 2018). In addition, Carrasco, Keeney, & Napier-Munn (2016a) also reported on coarse particle separation where value component pre-concentration by particle size relies on the inherent propensity of the value to deport into specific size fractions after breakage. This phenomenon was referred to by Carrasco et al. (2016a) as preferential grade deportment by size. As a result, Carrasco, Keeney, Napier-Munn, & Bode (2017) found that removing the size of already highly liberated coarse gangue particles in grinding feed significantly reduces the amount of energy used in comminution. In addition, Grigg & Delemontex (2014) and Wang & Forssberg (2007) reported that amenable ores minimise the mass of gangue requiring comminution above a particle size one-millimetre lowering grinding energy consumption significantly. Therefore, the proportion of uneconomic material or gangue removal can be an important driver in improving mine productivity used to generate a single unit of metal product (Topp

et al., 2008). Still, few publications describe and characterise gravity separation response in metal pre-concentration by coarse gangue removal after crushing ore to exploit natural preferential intergranular breakage (Laplante, Woodcock, & Huang, 2000; Dominy et al., 2011; McGrath et al., 2018).

The Curtin university Gold Technology Group (GTG) has developed a new laboratory gravity test methodology, coined the gangue rejection amenability test (GRAT) (McGrath et al., 2018). The GRAT methodology evaluates the amenability of finely crushed gold-bearing ore products for coarse-scale gangue removal or pre-concentration, above a particle size of 1.18 mm (McGrath et al., 2018). The GRAT densimetric data provides information to evaluate the deportment of selected metal into the sink and float products yielding a recovery versus mass pull relationship (McGrath et al., 2018). Particles of different sizes and densities are separated due to the differential settling rates in the heavy liquid medium whose density can be controlled. The GRAT method classifies particles by size and heavy liquid specific gravity (SG) segregation processes into multiple fractions within a particle size range of -4.75/+0.30 mm. The minus 0.3 mm particles were removed to reduce the risk of misclassification during HLS sink–float processes due to insufficient forces to separate the very fine particles. (Aktaş, Karacan, & Olcay, 1998; McGrath et al., 2018). McGrath et al. (2018) reported the successful application of the GRAT methodology for gravity separation of orogenic gold-bearing ore, crushed by various mechanical or non-mechanical fine crushing modes in assessing their breakage pattern liberating coarse gangue. McGrath et al., 2018 reported that the degree of liberation could be inferred by altering the heavy liquid separation (HLS) density split. Bode, McGrath, & Eksteen (2019) reported that the ease with which a waste mineral is liberated from its host rock and recovered is influenced by the method of crushing and the variability in gravity separation parameters. This thesis described data collected experimentally via sieving and HLS techniques using the GRAT methodology as gravity concentration data and resulting gravity separation behaviour.

Mukherjee (2009) identified a weakness in present metallurgy efficiency parameters to quantify and characterise ore for gravity separation performance in metal pre-concentration by coarse gangue rejection. Bode, McGrath & Eksteen (2019) reported that before the GRAT methodology, previous laboratory gravity test methods for characterising gold-bearing ores differences in density separation performance were restricted to particle sizes of ≥1.18 mm.

In describing separation performance, metallurgists are usually interested in two aspects of the process behaviour: the extent of enrichment achieved and the recovery of the valuable component into the concentrate. However, laboratory test empirical results seldom provide the exact ore resource characterising measures for separation efficiency needed for a process application, so some form of interpolation is typically required (Holland-Batt, 1990).

Empirical data from the application of the GRAT method is sought from the interaction between specific gold-bearing sulfide ores and different fine crushing regimes to answer knowledge gaps highlighted in the Chapter 2 literature review, identified as:

(1) There is limited published information for orogenic and porphyry copper-gold ore styles describing how gangue and preferential metal transportation across the HLS density increments are selective for different rock liberation patterns within a particle size range of 4.75/+0.30 mm.

(2) There is limited published information on evaluating the interaction between different gold-bearing sulfide ore geological styles, mechanical and non-mechanical crushing modes and gravity separation.

(3) A mathematical methodology for quantitatively predicting separation performance in heavy liquid specific gravity (SG) separation processes into multiple fractions within a particle size of 4.75/+0.30 mm is inadequate for fine crushed ores.

This work develops and employs quantitative prediction and characterisation methodologies and statistical techniques to answer the research hypothesis.

1.2 Problem statement

It is critical to characterise gold-bearing sulfide ores for their propensity to reject coarse particle gangue after fine crushing to assess their amenability in gravity separation performance. As consequently, this may increase effective run-off mine ore grades, strengthening the economic viability of some deposits. However, mathematically derived parameters that quantitatively predict preferential metal deportment between metal-rich and gangue particles in specific density fractions remain inadequate, principally for particle sizes above approximately 1.18 millimetres.

1.3 Aim

This thesis aims to develop a mathematical methodology capable of quantitatively predicting the propensity of some gold-bearing sulfide ores to reject coarse particle gangue and pre-concentrate metal (grade) by preferential grade by density deportment response as an attribute of the interaction between ore type, crushing mode and gravity separation technique.

1.3.1 Objectives of the study

This thesis seeks to characterise and mathematically evaluate gold-bearing sulfide ores preferential grade by density deportment response during breakage by different fine crushing breakage mechanisms. Where ore breakage would contribute to the greater liberation favouring the preferential deportment of minerals by gravity separation within a crushed particle size range of -4.75/+0.30 mm. The obtained results will benefit mining companies to select the most appropriate crushing mode for a given gold-bearing ore type. Further, it will benefit mining companies to understand the impact of the interaction between specific gold-bearing sulfide ores, different fine crushing modes and gravity separation techniques on metal upgrade and recovery during coarse gangue removal or pre-concentration. The following are the primary objectives of the thesis:

(1) Experimentally obtained laboratory gravity concentration data for mass and grade distribution across size and density fractions, for different gold-bearing sulfide ore mineral styles, crushing modes, and the GRAT sieving and heavy liquid separation (HLS) techniques, described in Section 3.3.

(2) Develop a mathematical method for measuring gravity separation performance using metallurgy parameters to quantify grade enrichment ratio, preferential grade by density deportment response, and the overall magnitude of grade deportment by density response into sinks.

(3) Analyze and differentiate gravity separation performance for variation of separation density with mineral particle size in selected gold-bearing sulfide ore-deposit styles and the impact of the findings on both interpretative technique and implied liberation induced by specific crushing modes.

(4) Use existing statistical analysis techniques to identify, compare, and evaluate the significance of differences in metallurgy parameter results for gravity separation performance produced from the interaction between ore type, crushing mode and gravity separation technique.

(5) Validate the EDI parameter prediction in modelling mass and grade distribution across size and density fractions against the actual gravity experimental results.

1.4 Hypothesis

The following hypothesis was developed (after a review of the literature as presented in Chapter 2) through this thesis:

- If you mathematically characterise preferential grade deportment response between metal-rich and gangue particles in specific density fractions, after ore coarse-scale (millimetres) breakage. Then, you will be able to quantitatively measure the enrichment ratio and magnitude of grade deportment by density response in a gravity separation operation for a gold-bearing ore after breakage by various fine crushing mechanisms.

1.5 Scope

A comprehensive literature review, provided in Chapter 2, has identified knowledge gaps on the effects of the fine crushing mechanism on gravity separation preferential grade by density deportment response within HLS density increments after the fine crushing of gold ores. This literature review finding is particularly true for laboratory research using gravity separation techniques for predicting the effect of coarse crushing on preferential grade deportment in particle sizes ≥1.18 mm. The main scope of this thesis is to characterise and quantify the variability in preferential grade deportment by density response, at a coarse scale (millimetres), influenced by the methods of crushing, and controlled by natural variability in mineralogy and textures present in the ore-deposit style itself.

Specifically, in the first part of the thesis, information came from the GRAT experimental program treating selected dissimilar crushed gold ore sample products produced by different crushing modes. The GRAT methodology is used to concentrate metal preferentially by varying the density of the heavy liquid separation (HLS) for selected particle-sized feed

materials to provide densimetric data for evaluating particle density separation performance. Crushing modes examined were laboratory-scale Sala mortar Cone crusher (Cone), SELFRAG Lab Selective Fragmentation (SELFRAG), Rolls crusher (Rolls), high pressure grinding roll (HPGR) and Vertical Shaft Impactor (VSI) crushing modes. With gold ore samples represented by orogenic ore from Ballarat Castlemaine Goldfields Limited (CGT) in Victoria, Australia, and a porphyry copper-gold ore, from Cadia Valley Operation (CVO) in New South Wales, Australia. These ores were crushed to a product particle size range of -2.00/+0.30 mm and -4.75/+0.30 mm, respectively. In addition, this research analysed information from two GRAT experimental examples to establish metallurgy parameters to characterise the relationship between ore type changes of the crushing mode and the separation technique. Chapter 3 describes the GRAT experimental program test work conditions for the methodology producing data for this study. Charts figures, tables, and non-textual forms characterised the GRAT empirical size and density data to evaluate metal pre-concentration by gangue rejection response, linked to the interaction between crushing mode, ore type and separation operation.

In the first part of this thesis, the GRAT empirical densimetric data for grade-by-size and grade-by-density deportment response was graphically characterised and interpreted. The Least Squares Regression (LSR) modelling technique was a mathematical tool used in data analysis. This technique allowed better characterisation of the relationship between metal (grade) versus mass recovery, influenced by ore crushing mode and separation technique.

The second part of this thesis quantified the propensity to increase grade in studied gold-bearing sulfide ores while removing coarse particulate gangue during physical separation processes by developing metallurgy parameters. Metallurgy parameters are mathematically derived that quantitatively predict the GRAT size and density classification metal upgrade and the overall preferential grade by density deportment response, relative to the ore abundance, accounting for gangue removal. In this study, these parameters characterise the interaction between selected gold ore types, specified fine crushing mode, and separation technique.

In the third part of this thesis, existing F-test, Student's t-test, and error and reliability analysis statistical techniques are used to conduct comparative analyses and significance testing on metallurgy parameter data derived from this thesis densimetric experimental study.

Statistical methods evaluated changes in preferential grade deportment into multiple density fractions, linked to the interaction between crushing mode, ore type and separation operation.

In the fourth part of this thesis, the applicability of a single EDI parameter to characterise ore preferential grade by density deportment response for an SG sequential separation operation, as a function of the interaction between ore, crushing mode and separation technique.

1.6 Overview

This thesis is in seven chapters to provide first a context, research motivation, methodology, analysis, and application for this research, described by:

Chapter 1 presents the background, problem statement, hypothesis, objectives, and scope of this thesis.

Chapter 2 provides the literature review on the gold industry mining trends, unit metal productivity and energy and water efficiency, coarse particle pre-concentration research, current laboratory gravity testing methods, and gaps in knowledge.

Chapter 3 describes selected ores mineralisation, crushing regime, experimental classification methodology, regression modelling methods, mathematical method description parameters, and statistical techniques used in this thesis.

Chapter 4 presents the mathematical method for characterising grade deportment response in metal pre-concentration during gangue rejection, following the interaction between selected gold-bearing ore types, fine crushing modes, and separation techniques.

Chapter 5 presents the statistical analysis results of metallurgical parameters as a function of the specified ore type, crushing mode, and separation technique.

Chapter 6 presents the application of a single Enrichment Deportment Index (EDI) parameter to describe a uniform response value for preferential grade by density deportment responses to selected density fractions during gravity separation of crushed gold-bearing ore.

Chapter 7 describes the final thesis conclusion and recommendations.

Chapter 2. Literature review

The literature review introduces the need for gold mining productivity improvements. It discusses present size and gravity coarse gangue separation methods in metal pre-concentration of ore. It identifies the role and the advantages of having a laboratory gravity separation method to characterise sequential density separation of coarse particles at a particle size of ≤4.75 mm. It highlights the lack of an analytical approach to describe the separation performance of a coarse particle gravity circuit, influenced by the interaction between ore type, crushing mode and classification technique.

2.1 Introduction

A literature review is based on the research objectives described in Chapter 1, ahead of this study. The literature review covers the need for productivity improvements in gold-bearing ore resource exploitation. Areas focused on in the literature review include trends in mine ore grade and overall productivity and water consumption and energy metal unit intensity in micron-scale comminution. Further focus areas included coarse gangue removal and existing ore gravity test procedures. The literature review focuses on the need to pre-concentrate future gold ores, the effect of crushing comminution on ore gangue and valuable component liberation and coarse particle gangue rejection techniques. In addition to characterising metallurgical parameters for gravity separation performance in metal concentration via coarse particle gangue rejection. This chapter's principal aims are to:

1. Support understanding of the need for productivity changes in the exploitation of gold-bearing ore resources.

2. Prove the gap in knowledge for the implication of change in concentration of valuable components into specific density fractions by CPGR following breakage of a gold-bearing sulfide ore by different fine crushing modes.

2.2 Need for gold mining productivity improvements

The standard metric used to represent the gold grade of ore is grams per tonne, inferring gold-bearing ores contain a high proportion of uneconomic or gangue material. Indicated by the World Gold Council (WGC) defines a high-quality underground mine as having a gold-bearing ore grade between 8 and 10 g/t, while a low-quality underground mine has a gold-bearing ore grade of 1 to 4 g/t (Hanusch et al., 2019). Furthermore, treating gangue wastes

energy and water in tumble milling comminution by delivering no value in grinding it (Bracey, 2012). Therefore, removing coarse particle gangue in the early stages of gold-bearing ore mineral processing would reduce the total cost of production by increasing the ore grade concentration, plus reducing energy and water consumption per unit of gold produced.

High all-in-costs reflect the total cost of production in the Australian gold mining industry, indicated in Figure 2-1, which presents a risk for investment in Australia's gold mining projects through a loss of cost competitiveness (Topp, 2008; Mitchell et al., 2014; Minerals Council of Australia, 2017). The all-in costs measure the total expenses and interest included in a financial transaction, such as a loan or equipment purchase and varying costs of producing metal over the life cycle of a mine. The average all-in costs rose close to 18 % between 2005 and 2011 (Minerals Council of Australia, 2017). Rising all-in expenses have not been off-set by either mine productivity gains, through the introduction of new technology, or by increased gold production, which is predicted to half by 2027 and continue trending lower through to 2055, as shown by Figure 2-1 (Topp, 2008; Giurco, Prior, Mudd, Mason, & Behrisch, 2010; Prior, et al., 2012; Mitchell et al., 2014; Schodde, 2017). Presently, increased expenditure in the Australian gold mining industry has not been combated by increased run-off mine (ROM) average ore grades or by raising the production scale of operations (Mudd, 2007a, 2007b; Prior et al., 2012; Topp, 2008). Instead, the Australian gold mining MFP is reduced by lower average ore grades, where the lower grade contributes to the loss of cost competitiveness and lower metal production (Topp, 2008; Prior et al., 2012; Schodde, 2017).

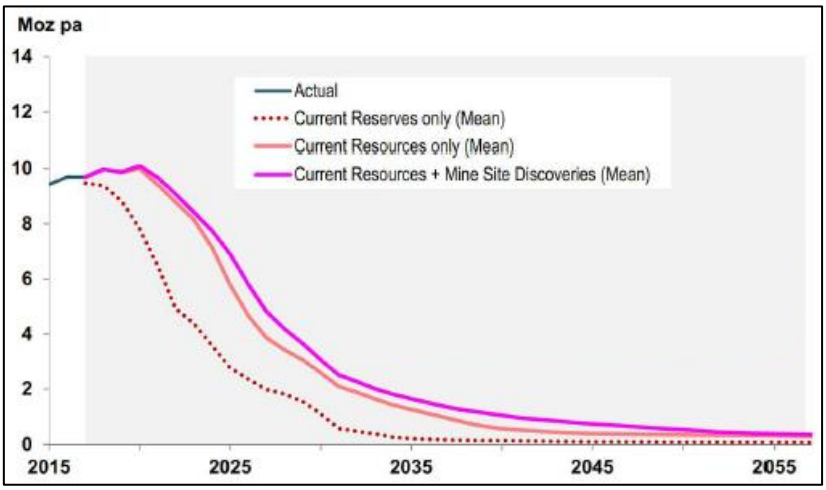

Figure 2-1. Forecast Australia gold production rate under differing assumptions of resource availability: 2017-2057 (Schodde, 2017)

Novak & Moran (2011), ABS (2016), and Mitchell & Steen, 2017 reported that the Australian mining industry MFP declined roughly 50% between approximately 2002 and 2013, as described in Figure 2-2. Over a similar period, Mitchell & Steen, 2017 reported that the South African gold mining industry MFP showed a similar downward trend in mine productivity. These Trends in Figure 2-2 and Figure 2-3, after 2000, suggest that the gold mining industry is suffering from lower productivity than the mining industry in general. Comparing the MFP trends in Figure 2-2 and Figure 2-3 suggests that the gold mining industry has a significantly lower production efficiency than the overall mining industry.

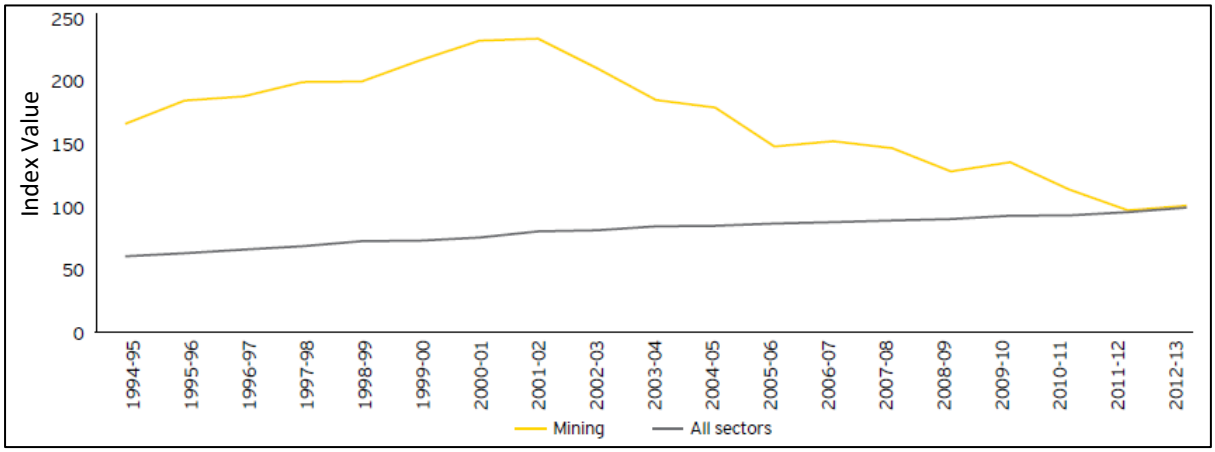

Figure 2-2. Mining sector productivity between 1994 to 2013 (Mitchell & Steen, 2017)

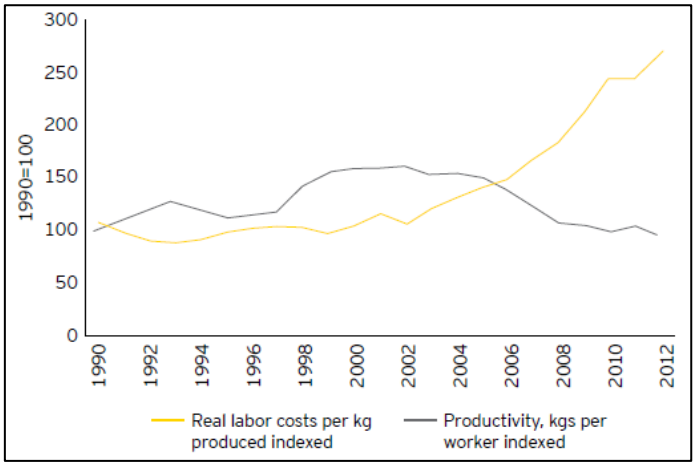

Figure 2-3. Labour productivity (kilograms produced per employee) and real labour costs per kilogram of gold produced between 1990 to 2012 (Mitchell & Steen, 2017)

The ABS (2018) reported that since 2011 the Australian mining industry's multifactor productivity has stagnated, as shown in Figure 2-4. Figure 2-4 also identified that the mining industry chain volume is measured as gross value added (GVA). In addition, the capital investment in new mining capacity has also declined. Since 2011, evidence shown in Figure

2-4 suggests that lower production and capital investment have reduced productivity (ABS, 2018; Novak and Moran, 2011).

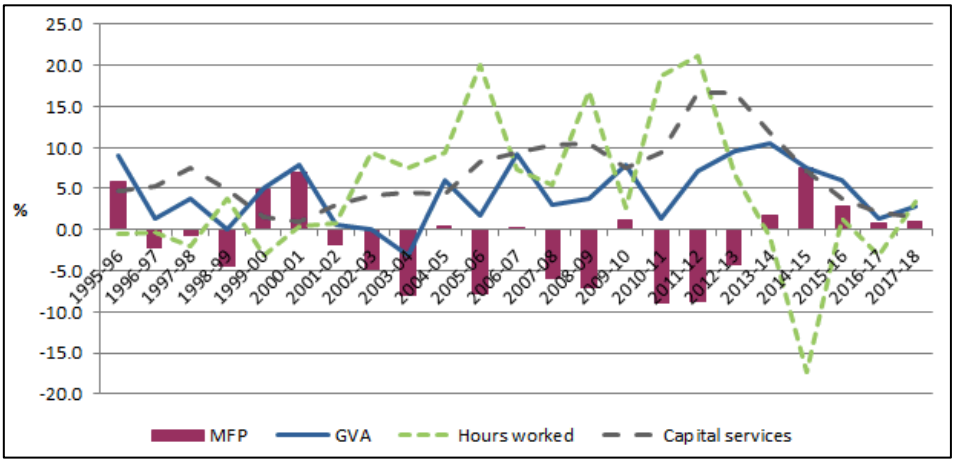

Figure 2-4. Yearly mining sector productivity and components between 1995 to 2018 (ABS, 2018)

The decline in the gold mining industry productivity since 2001 and following stagnation since 2011 is primarily explained by the dropping mine production efficiency. Reducing mine production efficiency is strongly linked to the treatment of lower metal head grade ores (Mudd, 2007a, 2007b; Topp, 2008; Topp et al., 2008; Giurco et al., 2010; Prior et al., 2012; Foggiatto, Bueno, Lane, McLean, & Chandramohan, 2014). Topp et al. (2008) cited that a key explanatory factor in MFP decline was ore treatment with lower head grades linked to resource depletion, as described in Figure 2-5 for 2000-01 and 2007-08. Topp (2008) identified an essential factor in the decline of the MFP metric is the increasing difficulty of mining and processing ores with lower ore head grades.

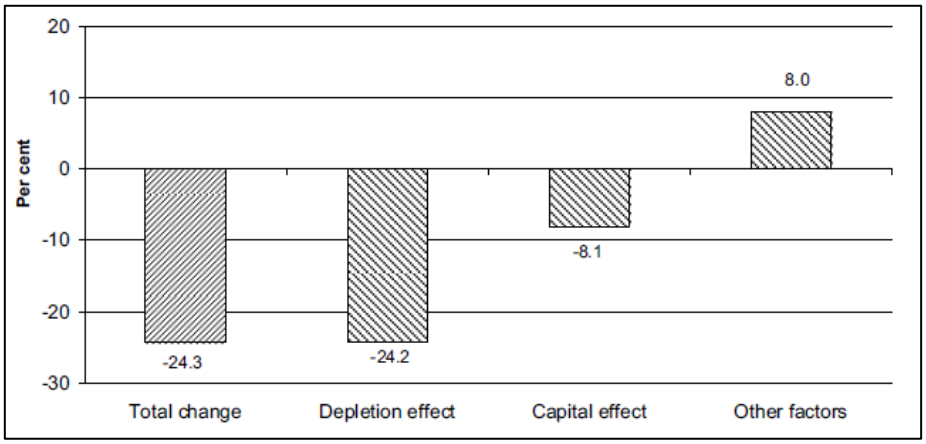

Figure 2-5. Contribution factors to the decline in mining MFP between 2000-01 and 2006-07 (Topp et al., 2008)

The gold-bearing ore grade mined and utilised in beneficiation can decline over time as ore resource exploitation moves from the rock with the highest gold content to the rock with the lower content (Mudd, 2009; Ericsson et al., 2019). Schodde (2017) has reported a decreasing trend in the total forecasted mined ore weighted average gold head grade over the next forty years from existing mines and predicted discoveries. Schodde (2017) shows in Figure 2-6 that the mined actual average head grade has already declined from 2.44 g/t Au in 2006 to 1.83g/t in 2017. Schodde (2017) predicts that the forecast total weighted average gold head grade drops over the next decade to 1.02 g/t by 2029, as shown in Figure 2-6. The lower predicted head grade means that a significantly higher proportion of gangue is present in the ore feed supplied to the processing plant.

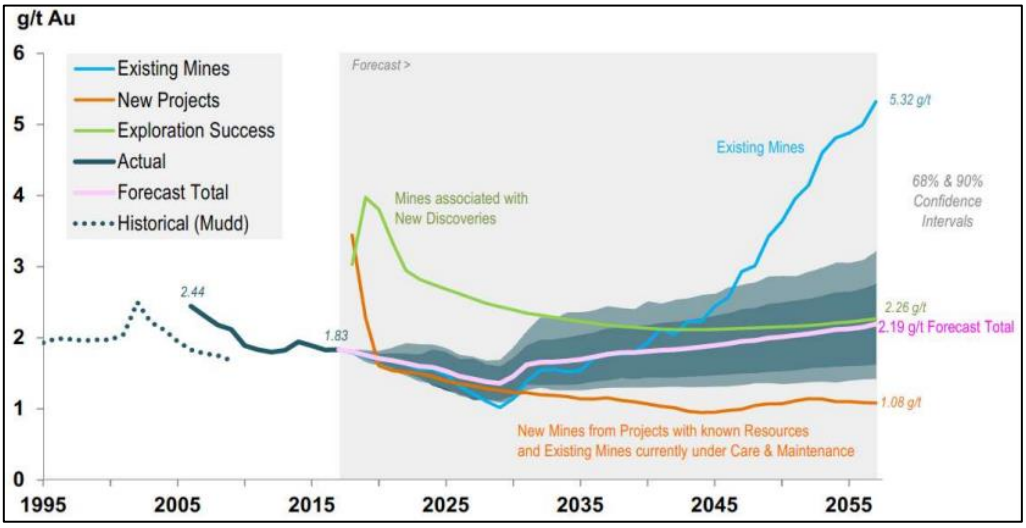

Figure 2-6. Forecast gold head grade trajectory over time predicted from existing mines and new projects (Schodde, 2017)

2.2.1 Metal unit productivity trend and energy consumption in comminution

Mudd (2007b) reported that a decline in mine head grade would require higher volumes of gangue material to be mined to produce the same quantity of valuable components, described in Figure 2-7. A common strategy to counter the declining average grade in gold-bearing ore is the scale of mining operations and the intensity of inputs required in gold production (Sandu & Syed, 2008). Subsequently, as the gold-bearing ore grade declines in feed to the grinding circuit, the silicate content increases as a percentage of the contained ore mass. Silicates, which typically occur in a higher proportion of the mineral composition in lower-yielding deposit ore, are typically harder, more competent, and likely more abrasive than the valuable component, consuming a higher proportion of energy, liners and media in

tumbling mill comminution processes (Wilson & Hawk, 1999; Aldrich, 2013; Eksteen, 2015). Therefore, low-grade ores, with a high proportion of gangue in the ore, increase the metal unit production intensity required to generate a valuable product output. Increased intensity of supplied inputs, particularly energy, negatively impacts the mining MFP, as demonstrated over the last decade.

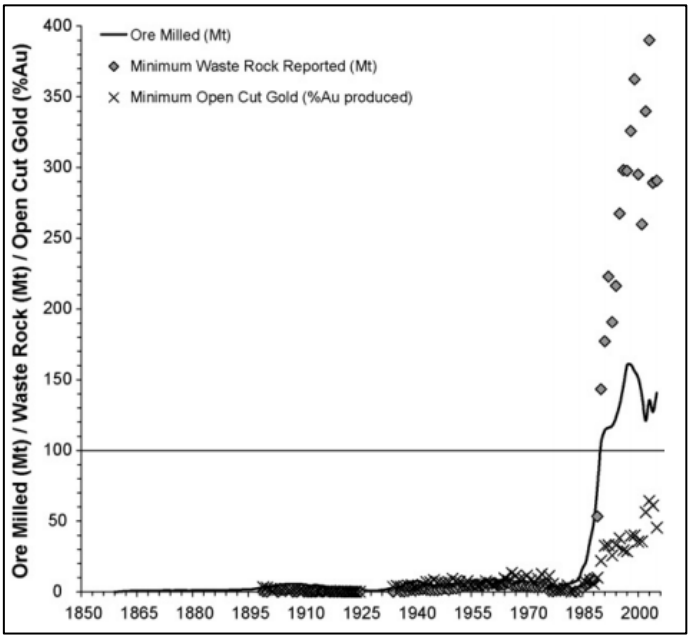

Figure 2-7. Average (milled) gold production ore milled and waste rock (Mudd, 2007b)

Typically, gangue is composed of mainly silicate minerals, such as quartz or quartzite materials that are being processed by energy and water-intensive tumbling mills (Norgate & Lovel, 2004; Marsden and House, 2006; Mudd, 2007a, 2007b; Norgate & Haque, 2010; Norgate et al., 2010). Silicates consume a higher proportion of energy, liners, and media in tumbling mill comminution processes (Wilson & Hawk, 1999; Aldrich, 2013; Eksteen, 2015). The implications in tumble milling specific energy consumption, measured in kWh/t units, of low-grade gold-bearing ores, were indicted by the Australian Mineral Industries Research Association (AMIRA) P420 Industry Practices Survey data on gold mine production (Eksteen, 2015). The AMIRA P420 data identified that energy consumption increases exponentially per unit of gold produced, as gold head grade falls below one (1) g/t for the sites surveyed (Eksteen, 2015; McGrath et al., 2018). Mudd (2007a) reported an exponential relationship between a declining head grade in gold-bearing ore, increased ore milled, and increased metal unit consumption of energy, shown in Figure 2-8. Similarly, Eksteen (2015) reported that energy consumption per unit of gold produced increases exponentially as milled ore

grade falls, as shown in Figure 2-9. Further, Mudd (2007a) stated an exponential relationship between declining milled gold-bearing ore head grade and increased metal unit consumption of water, described in Figure 2-10.

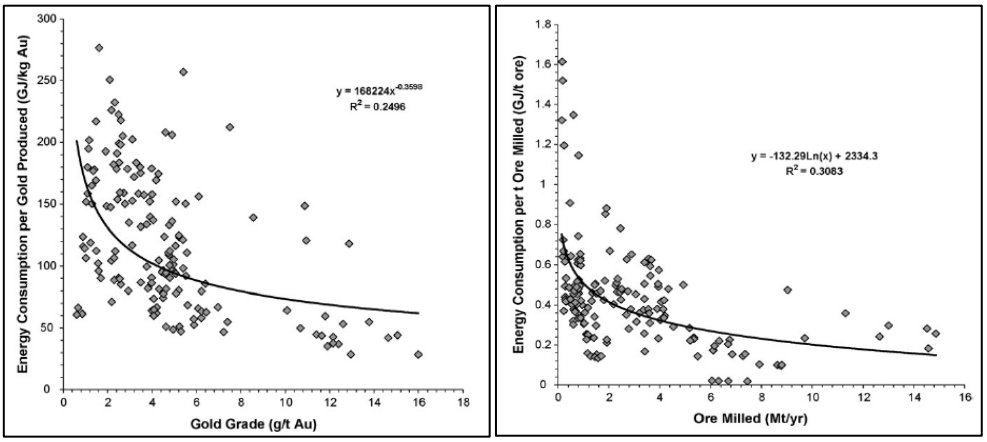

Figure 2-8. Energy consumption in Australian gold mining as a function of milled head grade and milled tonnes (per unit gold and unit ore) (Mudd, 2007a)

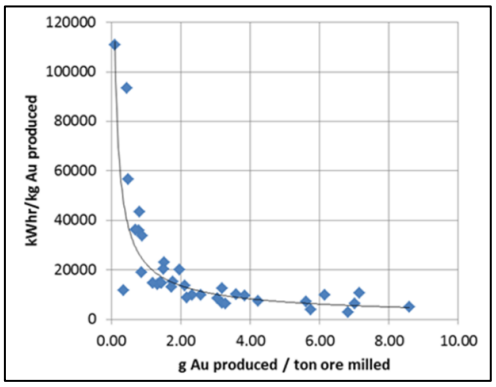

Figure 2-9. Specific electrical energy consumption versus gold grade in ore on a kWh per kg gold produced basis (Eksteen, 2015)

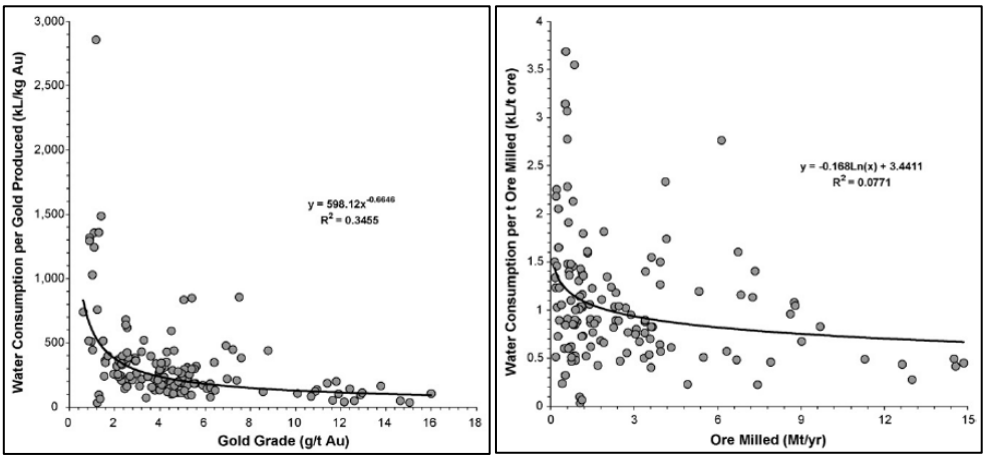

Figure 2-10. Water consumption in Australian gold mining as a function of milled head grade and milled tonnes (per unit gold and unit ore) (Mudd, 2007a)

Typically, tumbling mill comminution processes are used to achieve high liberation of the valuable component at a micron-scale before mineral beneficiation. Still, gangue may be liberated and separated at the millimetre scale during the crushing breakage of rock. Tumbling mills account for approximately 30 to 53 percent of the average mine site energy consumed and represent 4.9 percent of Australia's energy consumption overall, as described in Figure 2-11 (Norgate et al., 2007; Norgate et al., 2010; Norgate & Haque, 2010; Aldrich, 2013; Australian Industry Report, 2016). However, Carrasco et al. (2017) reported that a significant amount of energy in comminution is directed towards inefficient size reduction of already highly liberated coarse economically worthless waste or gangue material. Subsequentially, the mining MFP is improved by early-stage or coarse particle gangue rejection, primarily by reducing metal unit consumption of energy in the tumbling milling stage. (Syed, Grafton, & Kalirajan, 2013; Prior et al., 2012; Topp, 2008). In addition, coarse particle gangue rejection can achieve higher metal unit productivity by reducing the mass of gangue subjected to energy-intensive tumble milling processes in the presence of sulfide and non-sulfide minerals (Bamber et al., 2008; Dominy et al., 2011; Dominy, Murphy et al., 2011; Bearman, 2013; Sakuhuni, Tong et al., 2014; Bowman & Bearman, 2014; Carrasco et al., 2017; McGrath et al., 2018).

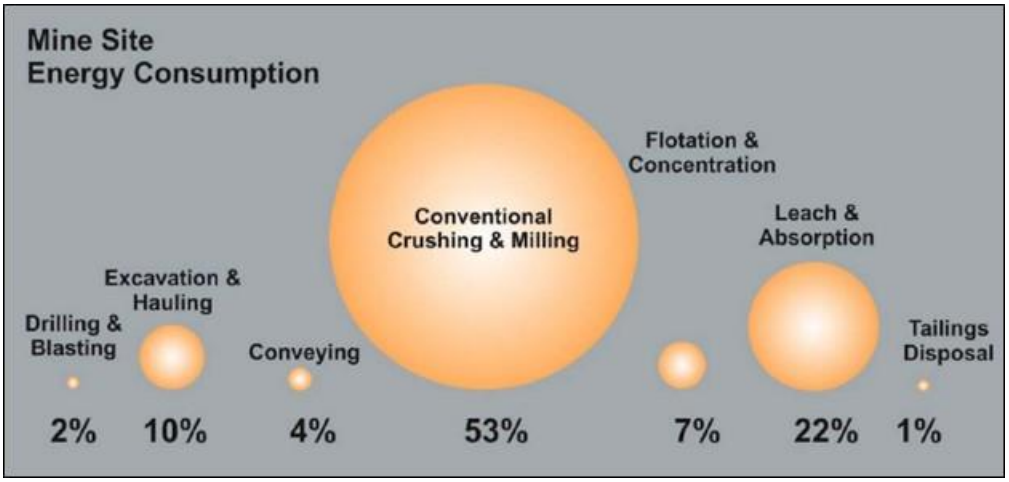

Figure 2-11. Energy consumption breakdown distribution at typical mining operations (modified from http://www.visualcapitalist.com)

2.3 Geometallurgical ore characterisation

Geometallurgy focuses on optimising mine operations and processing facilities by combining geoscientific studies with mineral processing and mining (Dominy et al., 2012). The main objectives are to understand the metallurgical processing attributes of geological material

and reduce the technical risks in treating new mine deposits or expansions (Baumgartner, 2012; Zhou and Gu, 2016). Understanding and inferring critical differences in ore properties and behaviour that will affect comminution and separation are being investigated by the AMIRA P843 Geometallurgical Mapping and Mine Modelling (GeM^{III}) project (Bonnici et al.,2008; Vatandoost et al.,2009; Hunt et al., 2010). The AMIRA P843 GeM^{III} is a major Australian project that combines geoscientific investigations with mining, metallurgical, environmental, and economic information (Baumgartner, 2012; Chibaya, 2013). The AMIRA P843 GeMIII project aims to maximise an ore deposit's Net Present Value (NPV) (Baumgartner, 2012; Chibaya, 2013). Physical ore characteristics from a gold deportment study, associated with a geometallurgy approach, are essential to any gold-bearing ore project. The information produced from such a study can assist in optimising cost and operating efficiency in process selection and flowsheet design (Zhou and Gu, 2016). Many reported studies emphasise the importance of early geometallurgical intervention in mining project development.

Geometallurgy is an approach to ore characterisation that is quantified and spatially constrained in relation to critical processing performance behaviours and ore textural drivers for separation performance in a variable and complex ore body (Tungpalan et al., 2021). Bonnici et al., 2008 reported that “texture can be a critical influence for a wide range of mineral processing behaviours, e.g., comminution, liberation, recovery” (p. 415). Subsequently, quantifying mineralogical and textural connections that affect mineral processing (e.g., liberation and recovery) is important for geometallurgy. This information must be incorporated into the mining and mineral processing planning processes (Hunt, 2011). Methodologies for geological characterisation concentrate on deposit genesis to discover new mineralised zones, whereas metallurgical characterisation identifies characteristics required for processing plant engineering design (Keeney and Walters, 2011). However, Bonnici (2012) reported that there are currently only a few ways for routinely analysing and characterising mineralogical and textural properties before mining to predict variability in mineral processing behaviour. Keeney and Walters (2011) also reported that although doing an integrated geological and metallurgical investigation is not new, few publications provide integrated methodologies, and current geometallurgical integration approaches have significant technical problems. Walters (2011) reported that the emerging

'geometallurgy' discipline is rapidly gaining recognition as a discrete and high-value activity. Geometallurgy links ore mineralogical, texture, and spatial grade heterogeneity to metallurgical beneficiation separation attributes. A more quantitative methodology for predicting and characterising preferential grade deportment response during sequential size or density separation of finely crushed gold-bearing sulfide ore can be developed to link these areas.

2.4 Crushing Mode Influence on Host Rock Breakage and Mineral Liberation

Guldris Leon et al. (2020) identified that relatively few comminution studies have tried to address mineral liberation in relatively coarse particle sizes, such as the research of Bazin et al. (1994), Carrasco et al. (2016a, 2016c). The propensity of some ores to deport metal into specific size fractions can, in some cases, allow the early rejection of low-grade materials or pre-concentration during selective coarse comminution (Carrasco et al., 2016a; Carrasco et al., 2016c; Guldris Leon et al., 2020). The early-stage gangue rejection or pre-concentration could reduce energy and water intensity in a mining operation but is rarely implemented in industrial practice. Guldris Leon et al. (2020) reported, “most ores are not suitable since they display weak fractionation of valuable minerals during comminution, or the liberation of ore-bearing particles occurs at very fine grain sizes” (p. 18). However, the potential for early gangue rejection to benefit the mining industry in preferential grade-by-size or grade by density deportment is rarely considered in process flowsheet design due to the focus on tumble milling achieving liberation. Still, mechanical comminution modes may exploit ore spatial grade heterogeneity to achieve preferential liberation of the gangue minerals, principally by selective intergranular breakage (Carrasco et al., 2017).

Carrasco et al. (2017) described crushing devices that can influence the degree of gangue liberation and preferential metal by size deportment among broken particles. Parapari et al. (2020) reported that the main rock breakage properties of mechanical strength, toughness, and brittleness strongly influenced the product shape, size distribution, and mineral liberation. Mineral liberation based on the breakage device mode has been expressed as random and non-random breakage (Parapari et al., 2020). The breakage mode is random when independent of mineral texture and non-random breakage when it depends on the mineral texture (Parapari et al., 2020). Parian, Mwanga, Lamberg, & Rosenkranz, 2018

reported that “ore texture refers to volume, grain size, shape, spatial distribution and association of each mineral in the ore” (p. 57). However, the potential of mineral comminution mechanisms may not consistently deliver the optimum energy efficiency in the liberation of the gangue and valuable components from mineral assemblages (Pérez-Barnuevo, Pirard, & Castroviejo, 2012). King (1994) classified non-random breakage in an ore as selective breakage.

Particle breakage in comminution begins with crack induction and propagation, with the breakage mode determining the path of cracks, which is either preferential in phase breakage or phase boundary breakage (Parapari, Parian, & Rosenkranz, 2020; Parapari et al., 2020). The crack formation behaviour is affected by ore texture and operational conditions, such as loading mechanisms produced by different comminution regimes (Mariano & Evans, 2018; Parapari et al., 2020). At the nano- and micro-scales, ore texture heterogeneity is an inherent component of geological material (Parapari et al., 2020). King (1979), Choi (1986), Choi, Adel, & Yoon (1987), Choi, Adel, & Yoon (1988), Barbery & Leroux (1988), Guimarães & Durãao (2003), and Gay (2004) reported that mineral liberation models are influenced by comminution and the geological style or characteristics of the ore. Also, Guldris et al. (2015) reported that “the liberation of ore minerals is a function of the rock texture and the difference in size and mechanical properties of the valuable minerals relative to gangue minerals and they may fracture in certain grain sizes if they behave differently during comminution” (p. 164). The two main parameters that influence ore crack formation and, consequentially, the ore breakage mode and mineral liberation are ore texture type and loading displacement rate (Parapari et al., 2020). Loading displacement in the rock is associated with the comminution technology used in the breakage mode. Knowing how minerals break down makes it possible to identify the factors that affect mineral liberation and optimise them for greater liberation, even in coarser grain-sized fractions (Parapari, Parian, & Rosenkranz, 2020).

Resabal (2017) reported that the interaction between the ore characteristics and the comminution mode breakage mechanism could significantly affect how particles respond to size reduction and changes in mineral liberation. Ore characteristics are associated with variability in mineral composition, spatial grade heterogeneity, texture, particle feed size, and the mechanical properties of the valuable minerals in ore relative to waste minerals. Limited

published information exists on how host-rock gangue liberation properties respond to different crushing modes below five (5) millimetres (Carrasco et al., 2016a; Carrasco et al., 2016c; Guldris Leon et al., 2020).

McGrath et al. (2018) and Bode et al. (2019) identified that the selection and addition of either mechanical or non-mechanical devices in mineral processing circuits could aid in selective intergranular breakage so that a high percentage of mineral particles are liberated. In ores with a significant difference in density between the valuable component and the waste, gravity separation can be employed in processing for early-stage gangue rejection or valuable component pre-concentration by coarse particle gauge rejection before energy-intensive comminution treatment (Andres et al., 2001). Mechanical crushing modes examined in this thesis were the Sala mortar cone (cone) crusher, rolls crusher, High Pressure Grinding Rolls (HPGR), and Vertical Shaft Impactor (VSI). Crusher mechanisms achieve rock breakage by different combinations of impact and compression fragmentation.

The cone crushers function as a compressing crusher, with particle breakage, either interparticle or single particle, and a higher loading displacement rate than the HPGR or roll crusher technology (Bengtsson, Svedensten, & Evertsson, 2006; Drozdiak, 2011; Solomon, 2011, Parian, 2020; Yamashita, Thivierge & Euzébio, 2021). Evertsson (2000) reported on cone crushers as compressing crushers in which the rock particles are broken by squeezing between two surfaces.

For the roll crusher and HPGR modes, compression fracture predominates as breakage occurs between two surfaces relatively slower than particle impact breakage mechanisms like the VSI (Loveday, 2004; Solomon, 2011). The roll crusher and high pressure grinding roll (HPGR) breakage mode are used for slow compression rates (Parapari et al., 2018). Ghorbani et al. (2013) reported, “in the HPGR, contrary to conventional crushing rolls, the particles are broken by compression in a packed particle bed, and not by direct nipping of the particles between the two rolls” (p. 3). This particle bed is created between two choke-fed, counter-rotating rolls. Between these rolls, a particle bed is pressed to a density of up to roughly 85% of the actual material density (Schönert et al., 1988; Schneider et al., 2009; Aydoğan et al., 2006). As a result, the product from an HPGR is different (Aydoğan et al., 2006) and may be expected to have different behaviour in downstream processes. Garcia et al. (2009) found

liberation improves due to phase boundary breakage mode when the loading displacement rate is slow, conducive with the HPGR and rolls crusher breakage mode. The HPGR demonstrated higher liberation in coarser particle sizes above 53 microns (Daniel, 2007).

The vertical shaft impact (VSI) crusher is a common comminution technology used in the aggregate production of cubical particles in overall fraction sizes. However, VSIs typically produce a larger fine aggregate than other technologies such as the cone crusher (Bengtsson and Evertsson, 2008). The VSI mode rock breakage mechanisms are a bimodal function between attrition and cleavage, with impact fracture dominating comminution. The application rate is rapid, and breakage is by instantaneous particle collisions (Loveday, 2004; Bengtsson and Evertsson, 2008). The breakage behaviour in comminution depends on the rock type. However, little research has been done in modelling the interaction between the ore characteristics and the VSI comminution mode breakage mechanism (Bengtsson and Evertsson, 2008). The main industry focus has been on predicting the VSI outcome of the product size distribution (Bengtsson and Evertsson, 2008).

Novel non-mechanical modes, such as the SELFRAG comminution device, have emerged as an energy-efficient alternative to mechanical comminution techniques. The SELFRAG mode achieves breakage differentially from mechanical crushing modes. Scott (2006), Vizcarra et al. (2010), and Wang et al. (2012) have reported that the SELFRAG regime can produce higher mineral liberation in ores by more efficient preferential intergranular breakage. The SELFRAG breakage mode uses high-voltage pulses to shatter rock particles by creating stress concentrations around pores and flaws by electrical charge build-up at grain boundaries (Zuo et al., 2015). Parvaz, Weh, & Mosaddeghi (2015) reported that the selectivity of the SELFRAG process arose from the way the electricity and shockwaves interact with both the electrical and acoustic rock material properties. Research from SELFRAG mineral processing indicates a pre-concentration potential of the process by the selective accumulation of comminution energy towards electrically conductive phases (Zhou, Jago, & Martin, 2004; Shi et al., 2015). SELFRAG AG (Kerzers, Switzerland) in Switzerland (Zhou et al. 2004) is involved in promoting the industrialisation of the SELFRAG process.

2.5 Metal pre-concentration by coarse gangue rejection

Much emphasis has been placed on coarse-scale (millimetre) size-based characterisation methodologies in run-off mine grade pre-concentration literature. These characterisation methodologies have helped understand ore size deportment separation performance characteristics associated with screening, differential blasting, bulk, and particle-based sensing approaches. Recent emphases have been on a better understanding of ore particle size by grade deportment characteristics related to screening, differential blasting, bulk, and particle-based sensing approaches. Carrasco et al. (2016a, 2016b, 2016c) and Carrasco et al. (2017) reported screening approaches to improve run-off mine ore grade quality. At the same time, Keeney and Walters (2011) and Redwood and Scott (2016) reported on a strategy to enable blast design optimisation for size-based pre-concentration by exploiting orebody natural grade heterogeneity at the blast-hole scale and natural deportment of grade into different particle sizes. Ore sensing approaches in selective pre-concentration of coarse particle ore streams have focussed on rapid online elemental and mineralogical characterisation by various methods, including Mid-Infrared (Mid-IR) and Laser-Induced Breakdown Spectroscopy (LIBS), etc. (Weatherwax, 2007; Iyakwari, 2014). Nonetheless, gravity approaches have not received the same level of reported research as the previously mentioned pre-concentration approaches.

2.5.1 Gravity separation sorting benefits to industry

Gravity separation beneficiation is among the oldest methods used to recover valuable components from a broken rock. The beneficiation method separates minerals and metals based on their different densities, typically in liquid media or suspended heavy fine media. Burt (1984) reported that effective gravity separation requires a good understanding of the ore's natural mineralisation heterogeneity. The gold mining industry has extensively used gravity, or centrifugal, separators to process gold-bearing ores for over 20 years, significantly increasing the recovery of fines (-106 μm) free gold (Zhou, 2016). However, its application on coarse-scale (millimetre) size particles does have limitations. One of the main limitations has been a laboratory gravity separation methodology for predicting coarse-scale gold-bearing sulfide ore grade deportment by density response for particles sizes ≥1.18 mm. Still, Gravity separation processes are known to separate coarse mineral particles and generally employ relatively simple equipment technology, with typically few moving parts, which lowers mine

operating cost. Consequently, coarse particle gravity separation methods in the mining industry have gained increased interest because of their potential in early-stage coarse gangue rejection ahead of energy and water-intensive tumble milling and beneficiation stages.

2.5.2 Previous research in coarse particle metal pre-concentration

In the gold industry, metal pre-concentration by coarse particle gangue rejection is topical. Coarse particle gangue liberation and early-stage gangue rejection to a waste stream are topical today due to the potential benefit of removing a significant fraction of gangue before fine grinding. Where the ore spatial grade heterogeneity and its amenability to liberate gangue by fine crushing may be exploited. Where lower head grade deposits are treated in future mining, there will be increased levels of gangue content in feed stream inputs to mining comminution and beneficiation operations without a pre-concentration strategy (Dominy et al., 2011). Shirley (2009) described exploiting the rock's physical properties to produce preferential breakage liberation patterns during coarse particle comminution to achieve coarse particle metal pre-concentration by selective gangue removal.

Both size and density-based classification processes may allow a CPGR response to promote metal pre-concentration in run-off mine ore from low-grade natural resources, following coarse scale (millimetre) breakage (Bamber et al., 2008; Bearman, 2013; Bowman & Bearman, 2014; Carrasco et al., 2016a; Carrasco et al., 2016c; Carrasco et al., 2017; McGrath et al., 2018). Grigg and Delemontex (2014) reported the benefits of pre-concentration or gangue rejection processes when considering the treatment of marginal ore deposits, reducing metal unit production intensity at a coarse crush size. Grigg and Delemontex (2014) described the result of this pre-concentration step as a largely metal-free gangue product and a non-liberated valuable component phase. With metal units, productivity benefits are achieved by concentrating the valuable component into a smaller mass yield product stream.

Carrasco et al. (2016a, 2016c) and Carrasco et al. (2017) reported on crushed gold and base metal ores, in the particle size range of 125 mm and down to 0.32 mm, investigations by size classification processes, for preferential grade-by-size-based deportment to predict metal pre-concentration response. Gray, Davies, & Theletsane (2014), Wielen et al. (2014) and Grigg and Delemontex (2014) reported on the relationship between pre-concentration responses

and different fine crushing mechanisms, such as HPGR, SELFRAG and VSI, as regimes that can liberate valuable components at their coarsest size. Further, these comminution technologies have also been reported by other researchers as highly efficient in releasing Sulfide particles and metallic gold along their natural grain boundaries. Dunne (1996) reported that the HPGR achieved great liberation of coarse sulfide minerals, significantly improving gravity pre-concentration beneficiation operations. Grigg and Delemontex (2014) said that VSI effectively crushes with relatively low operating costs and has a unique breakage style. Grigg and Delemontex (2014) commended that the VSI is a 'metallurgical tool' to produce a 'cubic shape' coarse mineral particle, with a lower proportion of micron-scale fines, ahead of a continuous gravity concentration circuit. Gray et al. (2014) indicated that the VSI produced similar benefits to the HPGR but reduced cost.

Understanding various crushing modes influence preferential rock breakage to release significant amounts of gangue, followed by gravity separation to separate gangue and pre-concentrate the valuable component is of great interest to the gold mining industry. This interest in coarse particle metal pre-concentration comes, in part, from the potential to reduce the metal unit energy and water intensities of production and create additional economic value for a mining operation (Burns & Grimes, 1986; Von Ketelhodt, 2009; Carrasco et al., 2016a; Carrasco et al., 2017). However, up until recently, reported literature suggests there existed no widely accepted and standardised laboratory gravity test for metal pre-concentration by CPGR, above a particle size of 1.18 mm (Laplante, Shu, & Marois, 1996; Laplante & Dunne, 2002b; Dominy et al., 2011; Murphy, van Zyl, & Domingo, 2012; Sakuhuni et al., 2014).

2.6 New laboratory gravity test methodology for gold-bearing ores

Several researchers have reported laboratory gravity test methodologies for characterising gold-bearing ore propensity to concentrate gold at different densities, up to a particle size of around 1.18 mm. However, until the new gangue rejection amenability test (GRAT) methodology, described by McGrath et al. (2018), no small sample mass (≤50 kg) test method adequately characterised gold-bearing Sulfide ores for the level of gravity amenable gangue rejection or gold separation above a 1.18 mm particle size.

Other laboratory characterisation procedures reported on by researchers for gravity amenability assessment of gold-bearing ores include the Gravity Recoverable Gold (GRG) (Banisi, Laplante, & Marois, 1991; Laplante & Shu, 1992; Woodcock & Laplante, 1993; Laplante, Woodcock and Huang, 2000; Dominy et al., 2011); the Multi-Pass Test (Ghaffari, 2004); and the continuous gravity recovery (CGR) (Dominy et al., 2011; Sakuhuni et al., 2014). The GRG, CGR and the multi-pass test do not typically assess particles above a maximum particle size of approximately 1.18 mm (Laplante et al., 2000; Laplante, 2000; Dominy et al., 2011). As well, an important gravity recoverable gold test methodology, the GRG methodology, is limited to micron-scale feed samples and cannot evaluate sulfide-locked gold-bearing ore (Laplante et al., 2000; Laplante, 2000; Laplante & Dunne, 2002a; Laplante & Dunne, 2002b; Sakuhuni, Altun, Klein, & Tong, 2016). Further, the GRG test methodology is limited by; a low concentrate fraction mass yield of typically less than one percent of the potential liberated gold particles, test feed particle maximum size below 0.850 mm, and not being suitable for testing sulfide-locked gold-bearing ores (Dominy et al., 2011; Laplante et al., 2000; Laplante, 2000). Subsequentially, neither the GRG, CGR or the multi-pass test methodologies can fully consider metal processing cost and productivity benefit gains from millimetre scale CPGR and subsequent gold pre-concentration above a 1.18-millimetre particle separation operation. However, a new laboratory coarse particle gravity test, developed by the Curtin university Gold Technology Group (GTG), named the gangue rejection amenability test (GRAT) methodology, can classify particles above 1.18 millimetres. This methodology produced grade deportment by gravity classification scheme information for selected gold-bearing sulfide ores after breakage by specified crushing modes. McGrath et al. (2018) reported the new GRAT methodology characterises sequential density increment preferential grade by density deportment into specific density fractions at a particle size range between 0.3 mm to 4.75 mm. McGrath et al. (2018) reported on minus 0.30 mm particles removed in the present GRAT methodology due to that material having poor heavy liquid classification efficiency and risk of misclassification between float and sink fractions.

The GRAT methodology investigates responses in gold-bearing ores by quantifying the mass and grade changes in heavy liquid separation (HLS) sink and float products (McGrath et al., 2018). The GRAT classification data is achievable by characterising gangue and valuable metal liberation in gold-bearing ores, including sulfide-locked gold-bearing ores. The GRAT HLS

density increment sink and float fractions estimate the extent of gangue and valuable component liberation in gold-bearing ores through the variability in mass and grade content within separation fractions.

The HLS approach is selective, rejecting low-density particles to float and high-density particles into sinks, with the separation performance dependent on both heavy liquid density or apparent SG and the treated particle SG distribution. For example, the quartz and quartzite have SG's of 2.65 and 2.68, respectively; and the pyrite and pyrrhotite minerals have SG's of 4.06 and 4.04, respectively. Marsden and House (2006) reported average free gold SG's greater than (>) 15 g/cm3 (at a density of 15 g/cm3, the silver content of the gold particle is approximately 28 % and is more akin to electrum). Therefore, liberated gold predominately reports to the sink fraction during HLS (Cui and Forssberg, 2003). If quartz and quartzite, typical gangue components in gold-bearing ores, are liberated, they predominately report to the float fraction for any separation performed at an SG higher than that of the mineral (approximately 2.65) (McGrath et al., 2018). Subsequently, a simple mass balance of grade by mass contained in the sink–float fractions, at sequential density increments, indicates the degree of gangue and valuable component liberation by the extent of value grade enrichment and recovery with product fractions.

2.7 Coarse gangue separation characterisation methodologies

Characterisation research reported by Carrasco et al. (2014) and Carrasco et al. (2016a) for broken ore preferential grade-by-size deportment response via screen classification suggests an ore characterisation database for preferential grade by density deportment response can be created. However, Mukherjee (2009) reported a lack of metallurgical parameter functions suitable for calculating enrichment and preferential grade by density deportment linked to gangue rejection. These parameters characterise the propensity of crushed material to preferentially concentrate value components into multiple density fractions during coarse gangue rejection. Preferential grade by density refers to the propensity of some ores to naturally concentrate metal into specific density fractions during breakage, with the parameter indicators able to qualify and quantify rock following coarse-scale (millimetre-scale) breakage by different fine crushing modes. Mukherjee (2009) reported on numerous mathematical expressions to calculate gravity separation performance. Still, these are

typically considered only the recovery of the values in the concentrate alone. However, gangue rejection in the reject stream is correspondingly significant. Thus, a practical methodology may lead to processing ores previously categorised as uneconomic and increase the valuable component recovered from a deposit.

Carrasco et al. (2014) and Carrasco et al. (2016a) reported on a mathematical method to describe particle size separation performance for elemental deportment within size fractions. Carrasco et al. (2016a) and Carrasco, Keeney, Napier-Munn & François-Bongarçon (2016b) reported on a parameter metric to characterise a comminuted ore overall preferential grade-by-size deportment response, called a Ranking Response, "RR". The RR parameter mathematically described the relationship between screen separation metal upgrade (Upg) and the cumulative screen product fraction, typically screen undersize, cumulative weight (CW) percent, but did not focus on gangue rejection (Carrasco et al., 2016a; Carrasco et al., 2016b).

Traditionally, the "Concentration Criterion" value in gravity separation has been used to indicate amenability to gravity concentration (Taggart, 1951). The "Concentration Criterion", C, is defined by Taggart (1951) as a function of the specific gravity of the valuable mineral, waste mineral and the fluid medium in which gravity separation occurs. The higher the gravity differential ratio, described by C, the easier the gravity separation (Aplan, 1985). The partition curve provides information on the partition coefficient, representing the percentage of feed material of an SG that reports to the sink's product plotted against SG (Taggart, 1951). The partition curve identifies key performance factors, including the separation SG cutpoint and Ecart probable (Ep). The Ep value describes misplaced valuable component material or sharpness of separation (slope of the curve) as a likely error number (Taggart, 1951). The Partition curve or Tromp curve shows the amount of material, with a particular quality, based on the mass split at different medium densities, that appeared in the product (or reject) compared to how much of that same material was in the feed. Therefore, the central measured values are mass split at different densities and the SG of the valuable components, waste mineral and the fluid medium. Subsequentially, density and mass splits are not always an adequate measure of operating separation performance due to the risk that despite generally satisfactory values, the distribution can be unsatisfactory indicators of inter-grade deportment within sink–float density fractions.

Holland-Batt (1990) described an equation for separation performance, E, function based on the value component recovery. The value of the function, E, represents the amount of the valuable component present in the feed recovered to the concentrate in its pure form. Holland-Batt (1990) showed that plots of efficiency against mass recovery could show the efficient separation of a spiral concentrator gravity operation. However, the 'E value' that Holland-Batt (1990) explained did not consider the proportion to value component lost to the gangue that would occur during CPGR.

The GRAT laboratory gold-bearing ore testing and separation method are better for ore process evaluation above a particle size of 1.18 mm, up to 4.75 mm. However, the GRAT method does not provide a mathematical approach to describe particle size or density separation performance by calculated parameters for enrichment response and metallurgical efficiency of the concentration operation parameters. Therefore, the GRAT methodology focuses on the separation method and not on a mathematical approach for characterising separation performance.

2.8 Mine sample source process flowsheet

The Ballarat Castlemaine Goldfields Limited (CGT) and Cadia Valley Operation (CVO) operations are underground mines with extracted mined ore sent to primary crushers for coarse comminution. Ballarat and Cadia comminutions circuits are indicated in Figure 2-12 and Figure 2-13, respectively. The material used in this research was ore of about 30 mm in size and was removed from respective CGT and CVO crushing circuits. This research evaluated CGT and CVO ores by various fine crushing modes for pre-concentration by gangue rejection response. In the CGT and CVO, existing circuits optimised mechanical or non-mechanical fine crushing and pre-concentration by gangue rejection may offer downstream benefits that have not been thoroughly investigated. These benefits may include reducing cut-off grade and reducing grinding media consumption and mineral beneficiation energy and water costs. Therefore, it is important to characterise the benefits that coarse comminution techniques offer in early-stage gangue rejection and choose a technique that best exploits downstream benefits.

The existing CGT processing plant, shown in Figure 2-12, consists of two-stage crushing, with fine crushing, via a VSI crusher, to liberate the sulfide minerals at a millimetre-scale (Petrie,

Hernan, & Valle, 2017). The two crushing stages aim to achieve good gold and sulfide minerals liberation before gravity recovery (Petrie et al., 2017). Grigg and Delemontex (2014) reported CGT ore gravity test results which identified that coarse gold liberation and recovery are achievable with gold concentrated into 5 to 10 percent of the mass at a grind 80 % passing (P_{80}) size of 600 µm.

The existing Cadia ore processing facility, shown in Figure 2-13, receives crushed underground ore, which is conveyed to a surface stockpile, and then fed into two comminution circuits (Akerstrom, Waters, Bubnich, & Seaman, 2018). In one processing train, the stockpiled ore feeds a secondary Cone and tertiary High-Pressure Grinding Rolls (HPGR) circuit, which produces a crushed product as feed to a 40' SAG mill, feeding three parallel ball mill lines (Akerstrom et al., 2018). In addition, the stockpiled ore feeds a newly constructed secondary and tertiary Cone crushing circuit (Akerstrom et al., 2018). Each train has gravity gold recovery and flash flotation on the comminution circuit cyclone underflow (Akerstrom et al., 2018).

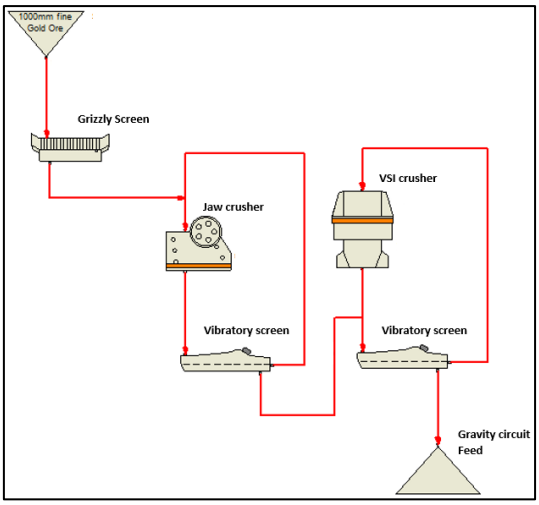

Figure 2-12. The CGT comminution circuit (adapted from Baines et al., 2017)

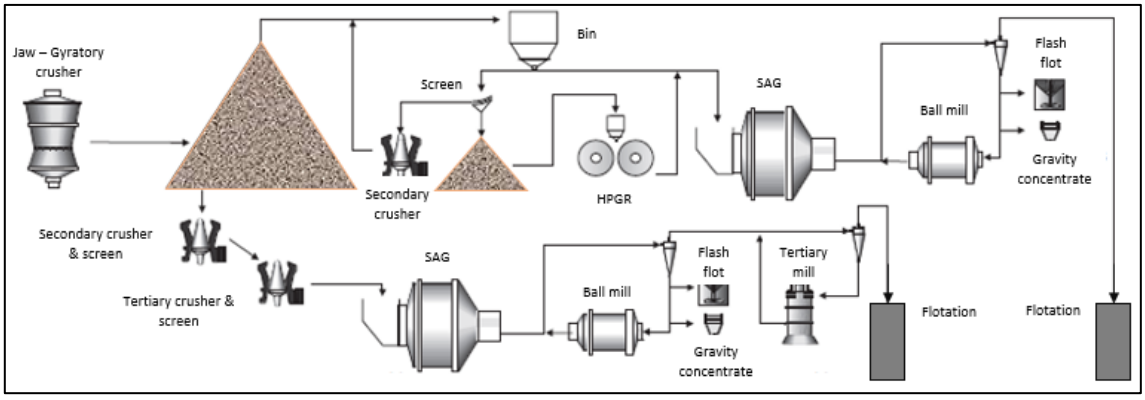

Figure 2-13. The CVO comminution circuit (adapted from Akerstrom et al., 2018)

The Ballarat and Cadia comminution circuits would benefit from removing gangue in the early stages of mineral processing. In both Ballarat and Cadia circuits, reducing the coarse gangue mass to the concentrator would reduce energy and water intensity in metal production. The gangue material usually contains little to no valuable minerals. It is often made up of harder materials, such as silica, which results in a large amount of energy being wasted on grinding it (Bracey, 2012).

2.9 Summary

In mining operations, the principal purpose of comminution ore processing is typically to liberate valuable minerals. In contrast to this, this thesis focuses on liberating gangue and rejecting gangue at a coarse scale (millimetres) using a gravity separation methodology. At the ore resource level, removing a high proportion of liberated gangue ahead of tumble milling reduces grinding energy and water consumption per unit of metal produced. Thus, reducing energy, water intensity, and thereby cost in metal production improves productivity in mining operations (ABS, 2012; ABS, 2012; ABS, 2018). However, the gold mining industry faces energy and water efficiency and productivity challenges (Aldrich, 2013; Eksteen; 2015).

Syed et al. (2013) reported that mine productivity is reduced due to higher proportions of waste rock in the feed ore stream into grinding circuits associated with treating lower grade ore. Mudd (2007a) and Eksteen (2015) reported this increase in grinding energy and water intensity, who identified lower head grade ore and increased energy and water consumption. Mining multifactor productivity (MFP) is a useful measure of productivity performance in the mining industry. The MFP measures the output-input efficiency of capital, materials, energy, labour, and services to generate a unit of product (Prior et al., 2012). Novak & Moran (2011) and ABS (2016) reported that the MFP has declined in the last 20 years by up to approximately 30-40 percent. MFP is heavily impacted by natural resource inputs, including a decline in ore grade and resource quality (Prior et al., 2012; Topp, 2008). A reduction in ore body quality increases the use of energy and water per unit of output and therefore increases production unit metal cost (Norgate et al., 2007; Norgate & Haque, 2010; Norgate et al., 2010; Walters, 2016). Consequentially, the economic viability of some gold mining projects is at risk due to the forecast extraction of lower head grade gold from mined resources (Mudd & Ward, 2008; Prior, Giurco, Mudd, Mason, & Behrisch, 2012; Schodde, 2017).

One way to reverse the decline in MFP and improve metal unit productivity is by characterising and quantifying gold-bearing ore amenability for early-stage coarse particle gangue rejection (Norgate et al., 2007; Norgate & Haque, 2010; Norgate et al., 2010; Walters, 2016). For low-grade ores, early-stage coarse particle gangue separation by size and density processes has been previously reported as an important operational advance to increase unit metal productivity and MFP output-input efficiency (Bamber et al., 2008; Bearman, 2013; Bowman & Bearman, 2014; Carrasco et al., 2016a, 2016c; Carrasco et al., 2017; McGrath et al., 2018). Notably, a significant amount of energy in comminution may be directed towards inefficient size reduction of already highly liberated coarse gangue (Carrasco et al., 2016c; Carrasco et al., 2017). As a result, a lack of understanding of the impact of the crushing mode on coarse gangue liberation and separation efficiency can lead to flaws in the strategic approach to resource beneficiation required to achieve profitable exploitation of the ore deposit.

In Chapter 2, several authors have reported on size-based metal pre-concentration by gangue rejection on low-grade ores in a broad particle size range between 5 mm to 125 mm. However, important laboratory gravity ore methods, including the GRG, CGR and the multi-pass test, were limited to ore particle top size of ≤1.18 mm. Still, McGrath et al. (2018) reported on a new laboratory gravity separation methodology, called the GRAT method, tested in the particle size range of -4.75/+0.30 mm. McGrath et al. (2018) reported on minus 0.30 mm particles being removed in the present GRAT methodology due to that material having poor classification efficiency and risk of misclassification between float and sink fractions. The GRAT method was reported as capable of treating various fine crushed comminuted gold-bearing sulfide ores. The GRAT test data demonstrated metal pre-concentration during gangue removal by sequential density separation responses for combined size by density separation processes.

According to the literature, robust metallurgical parameters are necessary for forecasting the preferential grade by density deportment response in metal pre-concentration by rejecting coarse gangue. Still, this issue remains unresolved at the time of this study. (Mukherjee, 2009). Existing metallurgical parameters quantify changes in enrichment and metal (grade) deportment density separation processes, typically only by considering the recovery of the values in the concentrate alone. However, gangue liberation and rejection into the reject

stream are significant, as unremoved gangue typically consumes energy and water in the grinding stage to achieve liberation, increasing mine costs.

McGrath et al. (2018) reported that little published evidence existed on a mathematical method for characterising the propensity of fine crushed ore to concentrate metal into multiple density fractions between minus 4.75 mm plus 1.18 mm particle size range during gangue rejection. Therefore, this research into a mathematical method will increase understanding of exploiting preferential breakage and associated metal (grade) deportment, subject to the interaction between a rock's natural spatial grade heterogeneity, crushing mechanism, and separation technique.

The literature review underscored limited published information on the degree that fine (millimetre scale) crushing mechanical and non-mechanical electric pulse SELFRAG Lab Selective Fragmentation (SELFRAG) devices influence changes in ore coarse particle gangue liberation. Subsequently, the interaction between ore type and breakage mechanisms influences changes in early-stage coarse gangue rejection and metal pre-concentration during density separation processes is not well understood.

The critical research question for consideration in this thesis is:

- What metallurgy parameters characterise metallurgical efficiency of metal concentration during gravity separation for a crushed gold-bearing sulfide ore at a laboratory scale by quantifying the grade enrichment ratio, preferential grade by density deportment response, and the overall magnitude of grade deportment by density response across various geological style deposits, different fine crushing modes, and gravity separation technique?

Based on the literature review and critical research question, the main objectives of this research are to:

(1) Characterise the interaction between the ore’s spatial grade heterogeneity and the influence of various fine crushing modes on changes in preferential grade by density deportment, as imparted by size and density separation processes, within a particle size range of -4.75/+0.30 mm.

(2) Determine a mathematical approach using metallurgy parameters that quantitively measures grade enrichment and magnitude of grade deportment by density response into sinks after ore fine crushing breakage and gangue rejection.

This research was undertaken to know that the results could be helpful to both the CGT and CVO mine sites in their process flowsheet development. Identifying crushing modes that improve gangue liberation and early-stage rejection allows less waste mineral requiring micron-scale tumble milling, significantly reducing the energy and water expended in processing rock with no economic value.

Chapter 3. Experimental methodology

This chapter documents the experimental and mathematical methods used in this research. This work builds on data collected in the AMIRA P420F Gold Processing Technology project undertaken by the Curtin university Gold Technology Group (GTG). The experimental test plan, testwork flowsheets, scenarios and mathematical method are described in detail within the chapter to allow it to be reproduced and built upon by future research studies.

3.1 Background

The literature review in Chapter 2 has identified that ore breakage patterns, particle body breakage or surface breakage can respond differently to size reduction comminution methods, where changes are related to the extent of the value and gangue mineral component liberation. Therefore, it is important to recognise how different crushing modes in rock particle breakage interact with the ore's natural mineralisation heterogeneity. This interaction can significantly influence gangue liberation patterns and the subsequent gangue removal through a classification technique, such as gravity separation. Consequently, an improved understanding of changes in breakage patterns that liberate gangue by the selection of a crushing mode may subsequently achieve better coarse particle gangue rejection (CPGR) and metal (grade) pre-concentration by gravity separation processes.

Previous researchers have reported that some gold-bearing ores are amenable to pre-concentration by targeted gangue liberation and removal to a waste stream by size separation techniques. McGrath et al. (2018) reported on a new laboratory gravity separation method coined the gangue rejection amenability test (GRAT). The GRAT gravity separation

methodology was developed by the Curtin university Gold Technology Group (GTG) (McGrath et al., 2018). The GRAT method successfully separated millimetre scale particles by size and heavy liquid specific gravity (SG) segregation into multiple fractions for finely crushed particle sizes in the minus 4.75 mm plus 0.3 mm range (McGrath et al., 2018).

The literature review in Chapter 2 found that crushing mechanisms can influence selective intergranular breakage so that a high percentage of gangue particles are liberated in gold-bearing sulfide ores. Also, according to the literature review, large amounts of energy and water are consumed to commute waste minerals during milling, negatively impacting mine operating costs. However, characterising an ore's amenability to liberate gangue and valuable material during coarse breakage has uncertainty in the extent and significance of the ore separation response. Ores studied were orogenic or free milling ore from Ballarat Castlemaine Goldfields Limited (CGT) in Victoria, Australia, and a porphyry copper-gold ore, from Cadia Valley Operation (CVO) in New South Wales, Australia. Most gold is produced from orogenic and porphyry copper-gold deposit ores in Australia (Geoscience Australia, 2009). Therefore, understanding coarse liberation attributes in gold-bearing sulfide rock is an important challenge to better design the gold separation processes.

The two gold-bearing ore samples are characterised by a laboratory-scale densimetric analysis using heavy liquids of varying densities (Maré, Beven, & Crisafio, 2015). The data produced include grade and mass concentrations by size and by density. This data is used to calculate gravity separation performance for enrichment response and metallurgical efficiency of the concentration operation by analysing the percentages of feed material of given size and densities that report into the sinks and floats.

This research aims to develop a novel gravity separation characterisation methodology to measure finely crushed gold-bearing ore separation performance. Where the method mathematically describes preferential metal (grade) by density deportment response for different crushed gold-bearing sulfide ore crushed products undergoing gravity separation. The methodology for analysing and characterising the propensity of grade deportment by density response from GRAT experimental observations was undertaken with the knowledge that the results would be helpful to Ballarat and Cadia operations. Results included metallurgy parameters that characterised the ore propensity for early process stage metal pre-

concentration by CPGR, following fine crushing by a selected mechanism. With different crushing modes assessed principally to determine their potential influence on changes in coarse gangue liberation as an ore attribute. The following methodology is specific to the gold mining industry, but modified versions apply to all types of mineral ores.

3.2 Ore mineralogy

Petrie et al. (2017) reported that Ballarat mineralisation has significant amounts of coarse gold (greater than (>) 80 % at plus 100-micron gold particles), as well as very coarse gold (locally >50%, plus 1,000-micron gold) hosted within the quartz veins. Gold in the Ballarat ore type occurs as liberated gold particles or in mineral associations with pyrite, arsenopyrite, and silicates (Phillips & Hughes, 1996). High spatial grade variability, partly associated with nugget effects, is observed in the deposit, where gold grades change over small distances and may reach over 50 g/t Au or drop to a few g/t Au from the high-grade zones (Clark, 2010; Petrie et al., 2017). As well, it is reported that "gold may occur within fractures within Sulfide minerals or be deposited on the margins of Sulfide grains" (Petrie et al., 2017). The appearance of coarse, often visible gold (>100 µm in size) in ore imparts a degree of risk in representative ore sampling due to grade variations that cannot be anticipated easily (Petrie et al., 2017). Petrie et al. (2017) identified only valuable metal in the ore is gold, while the significant non-valuable minerals are quartz and muscovite.

Cadia ore deposits primarily contain native gold with some electrum (Akerstrom et al., 2018). The gold grains have a fine texture, with liberation sensitive to grind size (Akerstrom et al., 2018). Gold occurrence in the gold (Au) and copper (Cu) ore is likely to vary from finely disseminated gold particles to those locked within minerals such as copper and iron sulfides (Akerstrom et al., 2018). The most valuable mineralisation at Cadia is chalcopyrite, which has a copper grade of around 0.28 percent. A further valuable component of Cadia ore is native gold, with a grade of about 0.98 grams/tonne. Gold and copper are valuable components in pyrite, chalcopyrite and lesser extent, bornite (PorterGeo, 2018). Akerstrom et al. (2018) identified the major non-valuable minerals are siderite, quartz, muscovite, and plagioclase. The fine texture of the Cadia ore gold grains suggests beneficiation metal recovery is sensitive to grind size and liberation (Akerstrom et al., 2018).

Bureau Veritas Minerals Pty. Ltd. (Bureau Veritas), using a quantitative X-ray powder diffraction (QXRD) analysis (crystalline phases) techniques, determined the Ballarat and Cadia bulk ore sample mineralogy. The QXRD results for the Ballarat and Cadia bulk ore sample mineralogy are shown in Table 3-1 and Table 3-2, respectively. Mineral SG values shown in Table 3-1 and Table 3-2 were reported by Drzymala (2007), where the SG is a dimensionless quantity and therefore not expressed in units.

Table 3-1. QXRD and SG analysis of Ballarat orogenic gold-bearing ore ([a]Drzymala, 2007)

Mineral		**Ballarat ore**	
		% Volume	SG
Quartz	SiO_2	61	2.65[a]
Mica group	$X_2Y_{4-6}Z_8O_{20}(OH,F)_4$	23	2.80[a]
Chlorite group	$A_{4-6}Z_4O_{10}(OH, O)_8$	<1	2.50[a]
Pyrite	FeS_2	<1	5.01[a]
Kaolinite	$Al_2Si_2O_5(OH)_4$	4	2.60[a]
Ankerite	$Ca(Mg, Fe)(CO_3)_2$	5	3.05[a]
Siderite	$Fe(CO_3)$	5	3.96[a]
Plagioclase	$(Na, Ca)Al(Al, Si)Si_2O_8$	2	2.69[a]

Table 3-2. QXRD and specific SG of Cadia porphyry copper-gold ore ([a]Drzymala, 2007)

Mineral		**Cadia ore**	
		% Volume	SG
Quartz	SiO_2	20	2.65[a]
Mica group	$X_2Y_{4-6}Z_8O_{20}(OH,F)_4$	11	2.80[a]
Chlorite group	$A_{4-6}Z_4O_{10}(OH, O)_8$	7	2.50[a]
Calcite	$Ca(CO_3)$	5	2.71[a]
Ankerite	$Ca(Mg, Fe)(CO_3)_2$	<1	3.05[a]
Siderite	$Fe(CO_3)$	44	3.96[a]
Plagioclase	$(Na, Ca)Al(Al, Si)Si_2O_8$	11	2.69[a]
Bornite	Cu_5FeS_4	<1	5.10[a]
Chalcopyrite	$CuFeS_2$	<1	4.20[a]
Pyrite	FeS_2	<1	5.01[a]
Molybdenite	MoS_2	<1	5.50[a]

The primary gold carrier in the Ballarat ore is coarse gold particles or gold in mineral associations with pyrite, arsenopyrite, and silicates. The major gold carriers in the Cadia ore are native fine texture gold grains, with some electrum, and gold in mineral associations with pyrite, arsenopyrite, base metal sulfides and silicates (Bonnici et al., 2008). Marsden and House (2006) quoted the average free gold density as> 15 g/cm^3. At a density of 15 g/cm^3, the silver content of the particle is around 28%, indicating the material is electrum. Other

valuable mineral components in Cadia ore are copper, chalcopyrite, bornite, and molybdenum.

Waste minerals from Ballarat and Cadia with no valuable metals have SG's ranging from 2.50 to 5.01, as shown in Tables 3 1 and 3 2. If gold particles are liberated from non-sulfide gangue at particle sizes of 10 µm, they can be recovered into the sink fraction at a separation SG of 3.0. (Marsden and House, 2006). Similarly, Okrusch (2018) reported that liberated pyrite and other sulfide gangue minerals enable them to recover into the SG of 3.0 sink fraction due to their high SG's, albeit at coarser particle sizes than free gold. Thus, the Ballarat and Cadia ore mineralogy's SG differences between waste mineral and valuable components suggest that metal will separate into multiple density sink fractions, described in Sections 3.4.3.2 and 3.4.3.3, dependent on the extent of gangue and valuable component liberation.

3.3 Ore sample preparation and test program flowsheet

Castlemaine Goldfields Limited and Newcrest Mining Limited mining operations supplied approximately 250 kilograms of Ballarat orogenic ore and Cadia porphyry copper-gold ore samples from respective crushing circuits. Ore samples received from CGT and CVO mining operations with a minus (-) 30 mm rock particle top size were supplied for this project. The as-received samples were oven-dried, blended by coning mixing technique, weighed, and placed in storage bags. Because it was assumed that the CGT and CVO samples received were not homogeneous, they were blended in this study.

The crushing comminution method involved a 'stage crush' approach, with screening between each pass through the crusher. This approach was used to minimise the generation of minus 0.3 mm particle fines produced during crushing by over-crushing sub sized material. It is considered unlikely in gravity separation that the 0.3 mm particles would be coarse enough for SG separations in a typical gravity separation plant process. The progressive screening was also applied to prevent unaccounted changes in particle breakage pattern and liberation by over crushing particles—the screening equipment used in sizing included 200 mm test sieves well suited for the large sample masses. Figure 3-1 describes the simplified experimental test program flowsheet. Ballarat CGT and CVO crusher products were produced and investigated at particle size ranges of -2.00/+0.30 and -4.75/+0.30 mm, respectively.

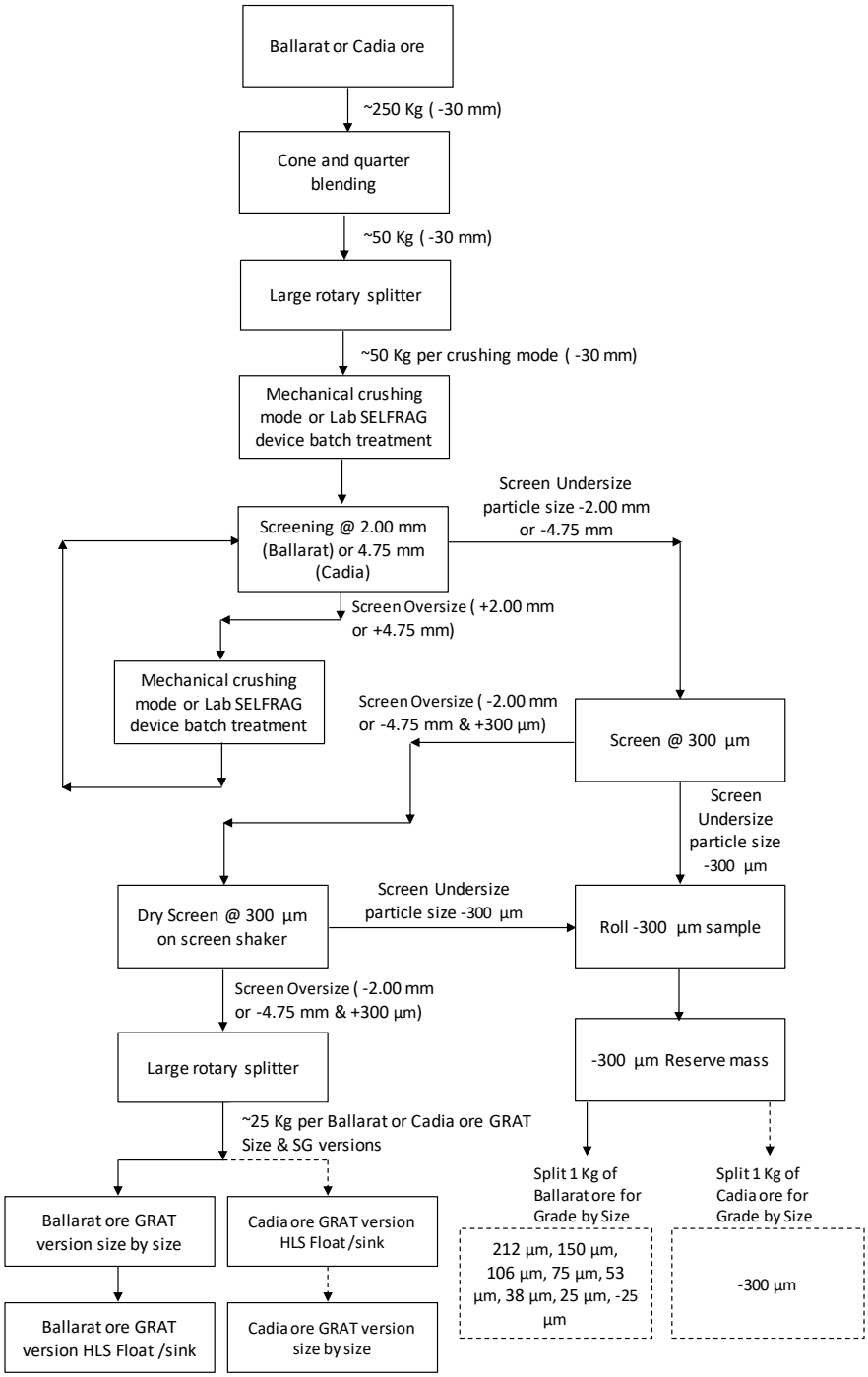

Figure 3-1. Simplified experimental test program flowsheet for the GRAT processing of gold-bearing ores (adapted from Curtin University, Gold Technology Group)

3.3.1 Sampling error

Natural ore heterogeneity and grade distribution can cause sampling error in subsampling (Pitard, 1993). The more heterogeneous the ore material sampled, the harder it is to obtain a representative subsample and infer geological and metallurgical characteristics of the sample (Ehrig, Liebezeit, & Macmillan, 2017). Therefore, it is crucial to consider the accuracy

of analytical and measured result errors in ore subsamples. There are several sampling procedures for splitting a large sample to obtain representative sub-samples. In this research, the first stage of subsampling to split the large Ballarat and Cadia sample masses provided by the mine sites was a coning and quartering technique. Next, cone and quartered samples were crushed and subsequently split by rotary sample divider, shown in Figure 3-2, a method to provide representative smaller subsample masses for screen fractionation and sink-float, respectively.

Figure 3-2. Rotary sample divider (RSD)

Pleysier (2018) reported a sampling nomogram plot for different ores, shown in Appendix 1, including gold and metal-bearing sulfide ores. The nomogram ensures representative mass sampling of ores while considering the ore particle size distribution (Minnitt & Assibey-Bonsu, 2009). Minnitt & Assibey-Bonsu (2009) said that the sampling nomogram, derived from the Gy (1992) formula proposed for determining the relative variance (σ2) of the fundamental sampling error (FSE), predicts the sampling error or design thresholds. Consequently, the sampling nomogram plot in Appendix 1 is a risk sampling diagram whereby the design threshold is described for different ores by curves in the plot. The curves predict the minimum sampling mass required to obtain a representative sample. The Appendix 1 sampling nomogram plot indicates that both the Ballarat Castlemaine Goldfields Limited (CGT) and Cadia Valley Operation (CVO) copper-gold ore sample masses and sub-sample masses are within response design thresholds. Therefore, the potential uncertainty of the results reported in this thesis, caused by bias in subsampling, is reduced.

3.4 Experimental methodology

3.4.1 Crushing Comminution methodology

The study evaluated laboratory-scale mechanical crushing and non-mechanical SELFRAG Lab Selective Fragmentation (SELFRAG) device fragmentation techniques for particle reduction on material sub-samples of the as-received gold-bearing ores received from the Ballarat CGT and Cadia CVO mining operations. In this case, crushing was induced by a Sala mortar cone (cone) crusher, SELFRAG Lab Selective Fragmentation (SELFRAG), rolls crusher, High Pressure Grinding Rolls (HPGR) and Vertical Shaft Impactor (VSI) crusher mechanisms. The cone crusher equipment was operated at the CSIRO Minerals Laboratory, Waterford, Western Australia. A laboratory rolls crusher was operated by Gekko Systems Pty. Ltd. (Gekko). The laboratory VSI equipment was operated by Gekko, with the principal control variable in achieving a nominal two (2) millimetres product top size being the rotational speed, established through trial investigations. SGS Minerals Pty. Ltd. operated the HPGR equipment in Australia. These breakage regimes were investigated to compare changes in gold pre-concentration linked to gangue liberation and removal by combined size and density separation processes of particle size up to ≤4.75 mm.

Crushing from 30 mm to 2.00 mm and 4.75 mm for Ballarat and Cadia ores, respectively, is very unusual in a single pass and requires the gold-bearing ore samples to be screened and oversize recycled to avoid over crushing at size particles. It is also of note that many small-scale crushing units do not typically perform in a manner representative of larger commercial machines. It is generally acknowledged that there is a risk of indirectly scaling results from laboratory crushing equipment to plant performance, given the small sample sizes and potential that laboratory crushing equipment is operated in an atypical manner. In the broader sense, there is potential for such atypical behaviour to invalidate the outcomes of commercial operations. For example, VSI crushers can use varying degrees of particle-particle breakage depending on the internal arrangement of the chamber, which can introduce variability in the results produced between the laboratory and commercial-scale equipment. Notwithstanding, despite laboratory-scale breakage regimes and energy levels not being typical of commercial equipment, this does not negate the concept used in this study to analyse and characterise the effect of different crushing modes on ore particle breakage in liberating gangue.

3.4.1.1 Crushed product size control methodology

In this research, the mechanical crushing operation was operated in a closed circuit. The crushed product was screened at target particle sizes of 2.00 mm for Ballarat ore and 4.75 mm for Cadia ore. The screen oversize was returned to the crusher feed until all the crushed material passed the selected target sizes. Closed-circuit crushing and screening were used to avoid "over crushing" of particles of a certain size fraction and decrease the fines yield in the Ballarat and Cadia ore studies. The SELFRAG approach avoids over-breaking the target minerals by a process that uses interchangeable sieve bottoms in the process vessel through which the target fragmented material passed (Wang et al., 2011). Because liberation is linked to particle size during comminution, comparing comminution methods is crucial in this study. A size control methodology is employed to minimise over crushing particles by removing at-size material after breakage. In addition, preventing over-crushing of ore particles allows improved understanding of the interaction between the crushing mode and ore geological style on the breakage mechanism influence on mineral liberation.

3.4.1.1 Sala mortar cone crusher method

A small laboratory cone crusher comminuted the Ballarat CGT and Cadia CVO gold-bearing ore samples. The laboratory cone crusher has a rolling breakage rather than a squeezing action seen in an industrial cone crusher.

The laboratory cone crusher test was completed on the sample as received, pre-screened to remove the minus 0.3 millimetres fraction. At its selected set pestle position, the crusher can reduce 25 mm feed material to 2 mm crushed product at a possible feed rate of more than 50 kg/h. The cone crusher used for this testwork is shown in Figure 3-3.

Figure 3-3. Laboratory Sala mortar cone crusher located at CSIRO

3.4.1.2 Rolls crusher method

The Ballarat CGT ore sample was comminuted by a Lab-scale rolls crusher, operated by Gekko Systems Pty. Ltd. (Gekko). The rolls crusher breakage test was completed on the sample as received, minus 0.3 mm. The rolls crusher was set up to generate a 2 mm particle product top size with the gap between the rolls established for ore through trial runs between 2.5 mm to 2 mm gap size. The rolls are held in the gap position by rams charged with nitrogen to prevent or limit movement. In comparison, a commercial HPGR crusher's Rolls are positioned by hydraulic pressure and may flex during operation reducing crushing efficiency. The laboratory rolls crusher used for this testwork is shown in Figure 3-4.

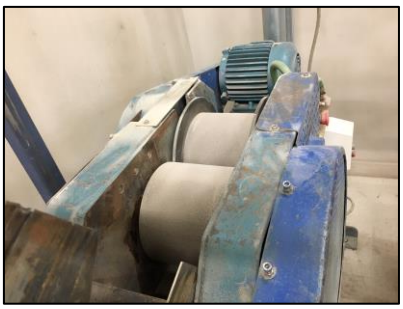

Figure 3-4. Roller crusher located at Gekko Pty Ltd

The rolls crusher's dominant mechanism of breakage is by compression and shear through a nipping function as mineral particles pass between the rolls, as opposed to an interparticle breakage function in a commercial HPGR crusher (Anticoi et al., 2018). Therefore, where interparticle breakage in the compression zone between the rollers is achieved by choke feeding the solids, the Gekko equipment functions as an HPGR; otherwise, the HPGR runs like a conventional rolls crusher (Keller-wessel, 1990). Still, Gekko operated the rolls crusher as a single particle crusher.

3.4.1.3 HPGR method

The Cadia ore sample was comminuted by a Lab-scale HPGR mechanism, operated by SGS Australia Pty. Ltd. (SGS). The HPGR breakage regime involves a flow of coarsely crushed ore finely ground between two rotating rolls. In this process, the Rolls are pressed to each other by a hydraulic system, thereby reaching a very high (specific) pressure in the grinding zone between the rolls, approaching and exceeding the unconfined compressive strength (UCS) of the rock. Unlike Rolls crushing, HPGR achieves a size reduction because of inter-particle compression within the particle bed and not by contact crushing of coarse particles between the roll surfaces. The Lab-scale HPGR used was a Polysius SMALLWAL HPGR model, with a roll

diameter of 0.50 m and a roll width of 0.30 m, equipped with a stud-lined roll surface and maximum feed size of 16 mm, shown in Figure 3-5. The estimated HPGR test conditions are shown in Table 3 3.

Figure 3-5. Polysius SMALLWAL HPGR unit located at SGS Australia Pty Ltd

Table 3-3. Summary of HPGR estimated test conditions ([a] SGS Australia Pty Ltd, 2018)

Test	Unit	Ore
HPGR Product Classification	mm	4.75
Moisture Content	%	3.0
Specific Pressure	N/mm^2	1.76[a]
Throughput	t/h	2.7[a]
Specific Throughput	ts/hm^3	238[a]
Net Specific Energy	kWh/t	1.38[a]

3.4.1.4 VSI crusher method

The Ballarat CGT and Cadia CVO samples were fragmented by a small laboratory sized VSI, operated by Gekko. The VSI breakage test was completed on the sample as received, minus 0.3 mm material. The feed to the VSI was deliberately choke fed to ensure rock on rock breakage during the test. The principal control variable in achieving a nominal 2 mm product top size from this unit is rotational speed, established through trial investigations to determine single pass amenability. The laboratory VSI used for this testwork is shown in Figure 3-6.

Figure 3-6. VSI crusher located at Gekko Pty Ltd

3.4.1.5 High voltage electrical comminution method

In this research, electrical comminution tests were undertaken with a SELFRAG AG (Kerzers, Switzerland) manufactured specific SELFRAG device. The SELFRAG device is a high voltage pulse (HVP) generator technology. The SELFRAG was operated at the John de Laeter Centre (JdLC), Western Australia. The SELFRAG breakage action may be regarded as producing close to ideal liberation in so far as mineral particles are discretely separated along grain boundaries. The SELFRAG instrument achieves electrical comminution using a high voltage pulse (HVP) power generator with a single-particle-test-vessel (Parvaz et al., 2015). Shi et al. 2013 described the SELFRAG rock breakage comminution method in detail.

The SELFRAG uses an HVP generator to apply electrical discharges to particles located between two device electrodes, resulting in extensive micro-fracturing (weakening) and complete particle fragmentation, dependent on the applied energy (Zhou et al., 2004). The generator unit converts a continuous flow of electricity into power pulses by storing electricity in capacitor banks and spark gaps (Parvaz et al., 2015). A steel mesh screen with an aperture of 0.3 mm was placed at the bottom of the reaction vessel, and the sample was processed, using high-voltage pulse fragmentation (HVPF), typically 150-160 kV, to break down the sample until 100 % passing the size of the steel mesh. Generally, the starting material was introduced as particles of about 30 mm in size, with sample batches of approximately 0.5 kg processed at any one time. In the SELFRAG device, deionised water is typically used for the fragmentation of mineral samples to avoid a high level of dissolved ions. A high level of ions in the solution will cause the electric pulse to pass through the ions but not through the sample, and the sample will not be a fragment. The SELFRAG test generator uses four parameters as setpoints for the electrical fragmentation process: voltage, pulse rate, no. of pulses, and the gap between the electrode tip and the bottom counter electrode. The working limits are shown in Table 3-4.

Table 3-4. SELFRAG test-generator device operating range and operating conditions for tests (adapted from JdLC)

	Operating range
Voltage	90 – 200 kV
Pulse rate	Number of Pulses: operator controlling factor: typically, 2.0 – 3.0 Hz
Electrode gap	10 – 40 mm
Batch capacity	1 Kg

In the SELFRAG devise to avoid over-breaking the minerals, the process vessel has interchangeable sieve bottoms with sieve apertures from 4 to 0.3 mm. Deionised water or low ion-containing water is used in sample material fragmentation, so the equipment generated electric pulse does not pass through the water ions but through the sample material. Figure 3-7 shows the JdLC laboratory SELFRAG equipment.

Figure 3-7. SELFRAG process vessel in association with the electrode located at the JdLC

3.4.2 Laboratory size classification method

It is understood through the literature review, described in Chapter 2, that size-based separation may also achieve preferential valuable metal pre-concentration within specific particle size fractions, as defined by Carrasco et al. (2016a); Carrasco et al. (2016b); Carrasco et al. (2016c), which can be exploited through screening strategies. The interaction between crushing mode and ore type generates the fragmentation pattern and subsequent particle size distribution (PSD) in the crushed product. However, it is not just the mass transfer between the size fractions that is important, but also the grade within size classes. Both the grade and mass provide information on the extent of particle liberation and likely metal enrichment recovery in a screening size-based classification or density-based separation. Due

to the very high SG of gold, the transfer of even small amounts of gold in particles can significantly impact density separations.

Chapter 2 has described that the mechanism of ore breakage and resultant particle size distribution can impose limitations on coarse particle stage-wise preferential grade-by-size increment deportment. The GRAT screen classification results characterise elemental deportment (principally gold) to the oversize (O/S) and undersize (U/S) screen fractions during breakage. In addition, the GRAT results allow investigation of whether gangue and key metals can be liberated from the rock within specific size fractions and the extent to which gangue material can be preferentially rejected within the screen O/S fraction. And conversely, the metal is preferentially reduced to fines by breakage. Various mechanical and SELFRAG comminution modes were investigated in this thesis to produce breakage.

Understanding the breakage between crushing mode and ore type on crushed particle size distribution (PSD) changes is important. The PSD can influence coarse particle removal of gangue during a classification operation. However, it is not just the mass transfer between the size fractions that is important, but also the grade of material within size classes that gives information about particle liberation and likely metal enrichment recovery in a classification operation.

Mineral grain density-based particle separation efficiency through preferential grade-by-density-based elemental deportment relies on substantial-grade variability across particle size fractions. Particles were screened into size ranges on crushed Ballarat and Cadia products as part of the GRAT methodology to improve gravity separation performance by reducing the influence of various particle settling rates during separation. Grade analysis of the screen mass fractions supplied information caused by size on mass recovery and elemental recovery in screen classification fractions. Of interest is evidence for preferential grade-by-size recovery, relative to mass recovery, which may be exploitable by screen-based classification during breakage. By separating an ore sample into size fractions, the particle size distribution of the material can be determined, and after assay, the particle size at which valuable components are contained can also be measured.

Size-based classification for preferential grade-by-size elemental deportment requires quality and quantity characterisation to understand the expected benefit in gravity separation

processes. Particle size distribution can limit ore physical gravity separation due to well-known factors, including relative density, shape, and extent of liberation. The presence of physical separation limiting factors may contribute to low classification efficiency for small particles and lower potential for the full liberation of gangue components in coarser particles. The GRAT screen classification results characterise mass and elemental deportment (principally gold) to the O/S and U/S screen fractions during breakage.

3.4.3 Laboratory gravity classification method

Curtin university Gold Technology Group (GTG) developed a new laboratory gravity test method for the gravity classification of gold-bearing ores (McGrath et al., 2018). The GTG test, called the GRAT, was a combined size and SG classification method previously reported by McGrath et al. (2018). The GRAT methodology assessed coarse gold liberation and deportment characteristics for maximum ore particle size ≤4.75 mm, and sample masses of ≤50 kg (McGrath et al., 2018). The characterisation methodology was developed to assess how different fine crushing rock breakage modes influence coarse particle gangue rejection (CPGR) response and subsequent metal pre-concentration heavy liquid separation (HLS) segregation. Grade deportment is the distribution of the element of interest against the overall particle distribution. The GRAT Gravity concentration data is influenced by the inherent specific ore geological variability and preferential separation between metal-rich and gangue particles in specific density fractions during different crushing mode breakage.

The GRAT HLS separation philosophy involves crushed material fed into an HLS medium of a set density that results in particles with a bulk SG higher than the medium to sink and those with a lower SG float (‘float’). Typically, the float removes low-density particles when the particles are below the heavy liquid density. Conversely, gold and sulfide minerals report to the sink with a higher density than the heavy liquid media. Then by altering the HLS density, the degree of liberation and preferential deportment response of gangue and gold can be evaluated in metallurgical terms by analysing HLS fraction mass by grade by recovery changes (Sakuhuni et al., 2014; McGrath et al., 2018). The GRAT methodology sink-float testing employed two types of water-based heavy liquid solutions. The first heavy liquid composition was a sodium polytungstate (SPT), and the second was lithium heteropolytungstates (LST) or Fastfloat®.

This thesis evaluated two different versions of the GRAT methodology for Ballarat and CVO ores, respectively. The GRAT method was modified, namely in the number of SGs splits, point of ore sample introduction, initial sample mass, and the crushed particle top size used. The Cadia version of the GRAT approach had screening after the sink/float separation, whereas the Ballarat GRAT approach gravity separated sized material. Changes in the GRAT experimental method between the Ballarat ore procedure completed first, and the following Cadia ore procedure, resulted in a reduction in the duration and cost of the process while still achieving sufficient separation characterisation data for each rock feed material. In each version of the GRAT methodology, the crushed ore product was screened at 0.3 mm, with the plus 0.3 mm fraction used in HLS studies. It is considered unlikely in gravity separation that the 0.3 mm particles would be coarse enough for SG separations in a typical plant process. However, the minus 0.3 mm material is considered in metallurgical balancing for this research on gangue rejection. Sections 3.3.2.2 and 3.3.2.3 describe variants of the Ballarat and Cadia ores GRAT experimental assessment methodology, respectively.

3.4.3.1 The GRAT heavy liquid separation procedure

The GRAT classification efficiency was investigated for various laboratory-scale fine crushing mechanical and electric pulse SELFRAG Lab devices. The GRAT separation fractions were analysed for changes in the CPGR response on specified gold-bearing sulfide ores crushed between minus 2.00 mm plus 0.3 mm and minus 4.75 mm plus 0.3 mm particle size ranges for Ballarat and Cadia sample materials, respectively. The GRAT test approach removed the minus 0.3-millimetre particles to reduce the risk of misclassification of HLS sink–float fractions due to anticipated insufficient forces to separate the very fine particles (Aktaş et al., 1998; McGrath et al., 2018).

McGrath et al. (2018) described GRAT produce as a heavy liquid targeted separation density established by evaporative removal of water from the saturated heavy liquid (HL) solution, shown in Figure 3-8, A, while measurement of the solution density using a standard calibrated hydrometer. Once the heavy liquid achieves the target density for solids separation, it is temperature-controlled, at approximately 48^{o}C. Temperature controlling the heavy liquid maintains a lower liquid viscosity, which is critical in separating the particulate solids, by the process described in Figure 3-8, B. The separation method involved adding solids in controlled amounts into a beaker of heavy liquid and then allowing the particulate material to separate,

as shown in Figure 3-9, A. The removal of float solids is carefully completed either by a vacuum suction method, shown in Figure 3-9, B or by removing float solids by spatula onto filter paper. Figure 3-10, A and B give an example of separated float and sink products.

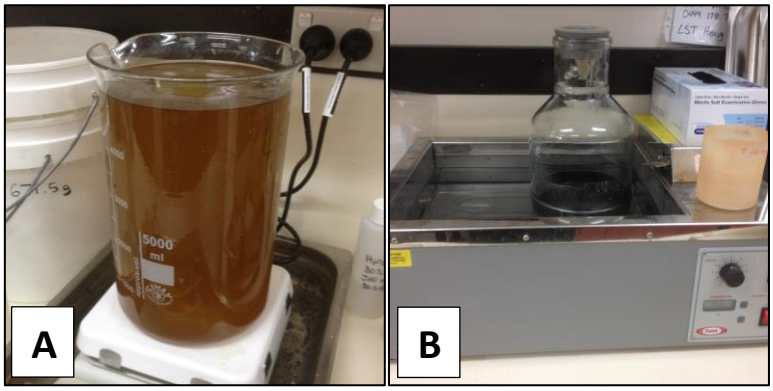

Figure 3-8.Images A and B show HL density control by evaporation and HL viscosity control by hot-bath temperature maintenance method

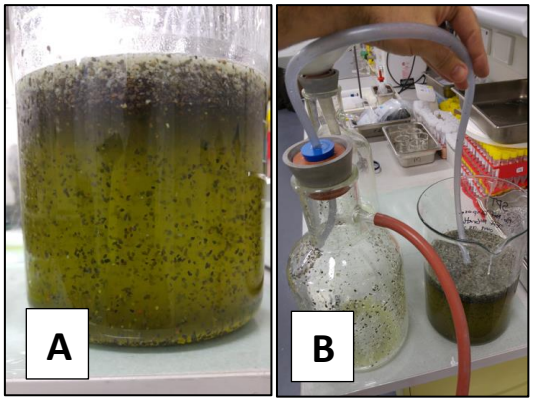

Figure 3-9. Images A and B show HL separation of solids and float vacuum removal method

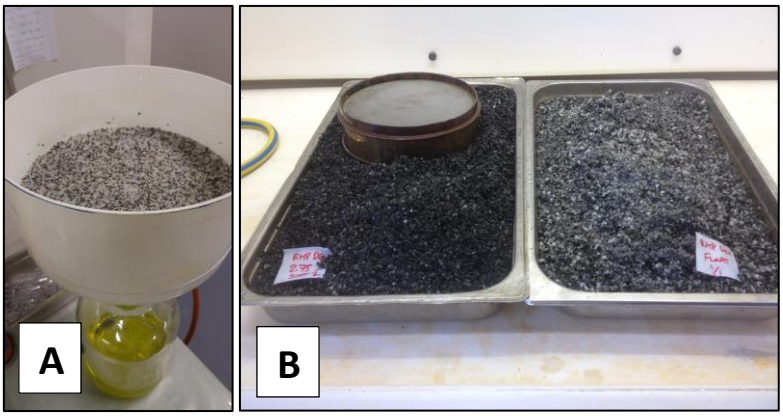

Figure 3-10. Images A and B show float solids filtering and sink–float method

3.4.3.2 Ballarat ore GRAT classification process flowsheet

Approximately 250 kg of ≤30 mm of orogenic ore sample yielded several sub-samples of ≤50 kg in the Ballarat version of the GRAT methodology. The ore sample was sub-divided by the procedure described in Section 3.3.1 and commuted by particle breakage modes described in Section 3.4.1. In the Ballarat version of the GRAT methodology, shown in Figure 3-11, the sub-sample was crushed to a particle size P100 of 2.00 mm. The crushed material is classified into screen size fractions, then sequential separated by HLS, at specified SG's.

shows the Ballarat crushed ore size and density classification method. The HLS product fractions were measured for elemental grade and weight recovered from each sink and float fractions. The Ballarat GRAT methodology sought to reduce the influence of coarse particle size in the HLS operation by screening crushed material into four size fractions to improve separation performance. In this way, the HLS classification process demonstrates coarse gangue rejection into HLS float primarily through differences in particle density (McGrath et al., 2018). It is predicted that particles with the same or near the same SG as that of the heavy liquid may have an improved chance of reporting into the right sink or float fraction by separating particles in narrow size distribution.

The HLS classification operation relies on differences in mass to separate minerals. In classification, the GRAT density separation selectivity is dependent on the size of particles and the particle size distribution (PSD), so particle size classification ahead of HLS is important in separation efficiency.

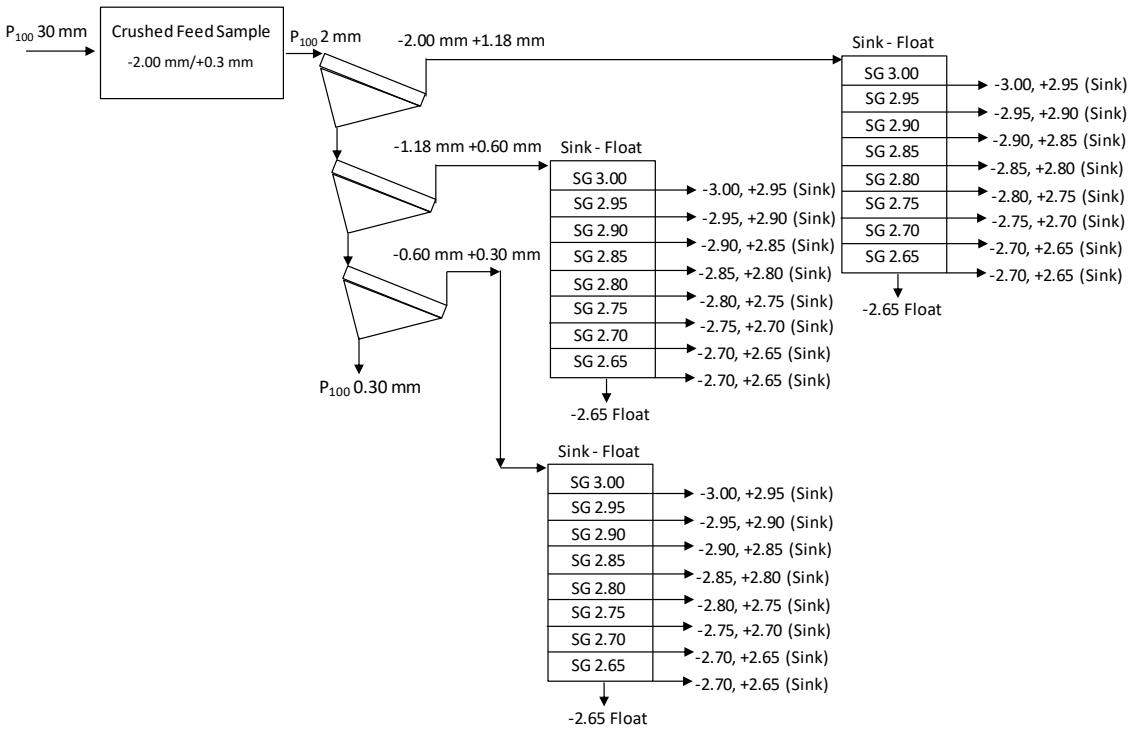

Figure 3-11. Ballarat ore GRAT methodology flowsheet (adapted from McGrath et al., 2018)

3.4.3.3 Cadia ore GRAT classification process flowsheet

In the Cadia version of the GRAT methodology, a homogenising coning and quartering process split approximately 250 kg of ≤30 mm of porphyry copper-gold ore sample to yield several sub-samples of ≤50 kg. The ore sample was sub-divided by the procedure described in Section 3.3.1 and commuted by particle breakage modes described in Section 3.4.1. In the Cadia version of the GRAT methodology, the sub-sample was fragmented to a particle size P_{100} of 4.75 mm. Crushed ore material was separated into density and size fractions described in Figure 3-12. Each separation product has grade and mass recovery measured. The density and size classification method specified in Figure 3-12 treated Cadia crushing mode product.

The Cadia GRAT method, shown in Figure 3-12, sought to achieve cost and test-time improvements on the previous Ballarat GRAT classification method. The Cadia method also sought to reduce the number of HLS stages and limit the potential particles misreporting separation errors caused by inefficiencies within the heavy liquid gravity separation process. As well, product specification identifies that the Cadia method heavy liquid LST solution had a lower viscosity than the Ballarat SPT heavy liquid, at higher SG, and therefore allowed faster separations and easier filtration. However, the LST only achieved separation up to a density of 2.95, as opposed to SPT, which could separate at an SG of 3.00.

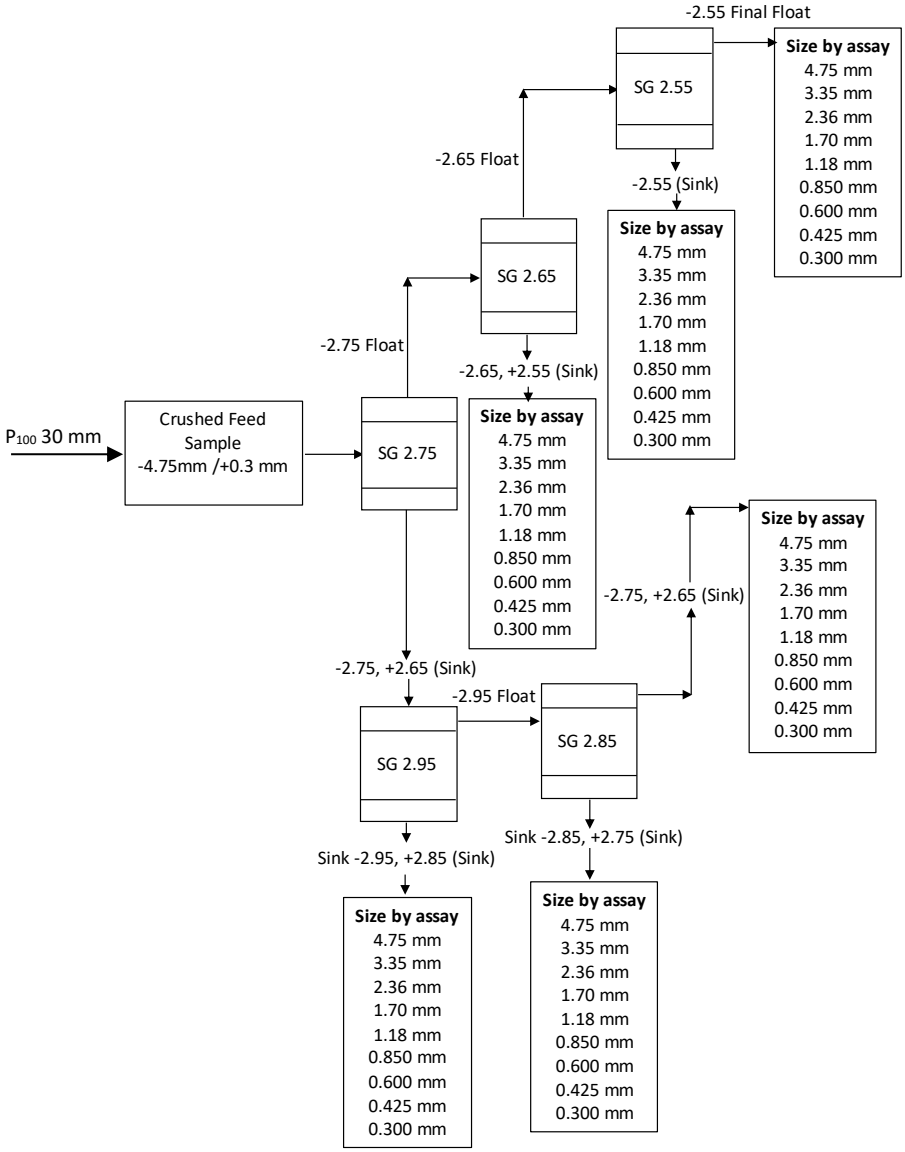

Figure 3-12. Cadia ore GRAT methodology flowsheet (adapted from GTG)

3.5 Sample assaying method

Following the GRAT procedure, samples less than 2 kg were milled, split in a riffle splitter, and submitted for assay at Bureau Veritas. Occasionally, ore samples are larger than 2 kg; they are split and recombined until sub-samples of approximately 2kg are achieved. Where sample mass permitted, gold assays were performed in duplicate, generating data to understand statistical variance as determined by the Student's t-test (t-test) for paired samples.

The elemental grades were determined by fire assay for gold (Au) analysis, inductively coupled plasma (ICP) for iron and arsenic, gas chromatography (GC) for sulfur and mixed acid digestion with ICP finish for sulfate (sulfide by difference). The fire assay method gold detection limit is one (1) part per billion (ppb). Elements that have a concentration of less

than one weight percent (wt%) of the associated data are treated as indicative only. All other key elements were determined by multi-acid digest, with the elemental detection limits described below:

- Copper (Cu), five parts per million (ppm)
- Molybdenum (Mo), 0.5 ppm
- Arsenic (As), one ppm
- Iron (Fe), 0.01 %
- Sulphur (S), 0.01 %
- Sulfate (SO_4), 0.005% (HCl digest only)

The Bureau Veritas analytical procedures to establish accuracy and precision include the inclusion of “blanks”, or standard reference materials, and two random repeats per batch. Gold, due to its “nuggety” nature, behaves differently from other elements in terms of reproducibility, and hence different protocols apply.

Bureau Veritas automatically investigates suspicious assay results (repeat assays vary more than a few percentage points) further by running repeat assays. When results are near the detection limit, Bureau Veritas typically allows a spread of two detection limit increments; otherwise, the lab dilutes and repeats the assays. Ballarat CGT material analytical results were reported for Au, Fe, As, and S. The Cadia CVO solids were reported for Au, Cu, Mo, Fe and S.

Before Ballarat and Cadia ore sample mineralogy is determined QXRD analysis technique, the samples were micro-milled for 10 minutes, with ethanol as the grinding liquid. The resultant samples were then lightly pressed into a back-packed sample holder. The mineral identification was undertaken using the X’Pert HighScore Plus search/match software. Rietveld quantitative analysis was performed on the XRD data using the commercial package, Highscore Plus version 4.6, and the Inorganic Crystal Structure Database (ICSD). The standard ICSD is used to identify and estimate mineral abundances in the sample material. The QXRD analysis level of accuracy, for results, is shown in Table 3-1 and Table 3-2, as reported by Bureau Veritas, and is around ± three (3) weight (wt) % (absolute) at the 95 % confidence level.

3.6 Comparison of normalised assay feed grades

Ideally, the head grades from the Ballarat CGT and Cadia CVO ore sub-samples used in this research should be the same, which would allow a better direct analytical comparison for analysis between equipment breakage modes evaluated (Drzymala, Tyson, & Wheelock (2007)). However, there is a grade variation between the Ballarat and Cadia ore sub-sample material, shown in Table 3-5 and Table 3-6, respectively, typically due to the natural grade heterogeneity of the ore.

Table 3-5. Ballarat ore sub-sample gold, arsenic, iron and sulfur grade values

Crushing Mechanism	Ore Subsample Feed Grade			
	Au ppm	As ppm	Fe %	S %
Cone crusher	1.64	2426	3.78	0.36
SELFRAG	3.60	2932	3.39	0.42
Rolls crusher	1.97	2343	3.49	0.39
VSI	2.92	2703	4.04	0.46
Statistic				
Sample standard deviation, SD	0.90	269	0.29	0.05
Mean (μ)	2.53	2601	3.68	0.41
Standard error of the mean (SEM)	0.45	134	0.15	0.02

Table 3-6. Cadia ore sub-sample gold, copper, molybdenum, iron and sulfur grade values

Crushing Mechanism	Ore Sub-sample Feed Grade				
	Au ppb	Cu ppm	Mo ppm	Fe %	S %
Cone crusher	1102	3094	12.07	4.36	0.60
SELFRAG	996	3129	10.88	4.18	0.55
Rolls crusher	1158	2909	12.88	4.34	0.55
VSI	1146	3067	11.66	4.41	0.61
Statistic					
Sample standard deviation, SD	74	97	0.83	0.10	0.03
Mean (μ)	1101	3050	11.87	4.32	0.58
Standard error of the mean (SEM)	37	49	0.42	0.05	0.01

Grade variation in ore sub-sample material is typically due to individual ores natural grade heterogeneity and the variability caused by the sub-sampling methodology. The standard deviation (SD) and the standard error of the mean (SEM) infer the sub-sample head grade precision and sample sub-division reliability, respectively. The SEM value, determined by Equation 1, considers both the value of the SD and the sample size (n) (Napier-Munn, 2014).

$$SEM = \left(\frac{SD}{\sqrt{n}} \right) \quad (1)$$

Both the SD and the SEM values provide different statistical information on the quality and representativity of the subsampled material based on a variation of the grade. The SD value measures how much the subsample head grade assays vary from each other and is a measure of the spread or variability of a given sample's grade from the mean grade (Napier-Munn, 2014). The SEM value provides inferential information about how accurately the sub-sample mean grades represent a true population mean (Napier-Munn, 2014).

Table 3-5 SD and SEM values show the gold variability is larger when compared to other elemental results, which suggests higher inaccuracy in the sub-sample gold mean representing the true population mean. However, for free milling gold-bearing ores, larger gold SD and SEM values may be expected as they suggest the influence of a "nugget" effect in the sub-sample assays, which is typical of this ore type (Clark, 2010; Goodall, 2008; Zhou et al., 2004). Overall, the magnitude of the SD and SEM elemental values for different crushing mode feed sub-sample assays do not infer an issue in the sub-sampling quality, inferring the sub-samples are suitable for the weight normalising method.

Table 3-6 SD and SEM values for gold and other elemental grades are relatively small. Overall, the results in Table 3-6 suggest good quality in sub-sampling the ore sample. Therefore, the Cadia ore sub-samples indicate a higher degree of homogeneity in the natural mineralogy than observed in the Ballarat ore sub-samples.

A weight normalisation technique may reduce the influence of ore sample natural grade heterogeneity in comparing results for ore subsamples. For this study, the feed head grade of the sub-samples has been feed grade normalised to the same elemental values by a method adapted from Drzymala et al. (2007). This approach allows better direct comparison between preferential grade by separation technique response, influenced by ore type and crushing mode. The technique calculates the same normalised ore feed grade for each sub-sample, taken from the same ore, using the sample masses and elemental unit quantities in a weighted averaging method. The weight normalised approach used in this study accounted for the minus 0.3mm screen fraction removed ahead of HLS classification.

The Ballarat sub-samples, weight normalised head grade assays were 2.48 ppm gold, 2611 ppm arsenic, 3.63 % iron and 0.39 % sulfur. The Cadia sub-samples, weight normalised head grade assays were 1106 ppb gold, 3043 ppm arsenic, 12 ppm molybdenum, 4.33 % iron and 0.58 % sulfur. Both Ballarat and Cadia weight normalised elemental grades lie within ±2 standard deviations, or about 95 % of the true theoretical population means, providing reasonable confidence in their use for metallurgical evaluations. Weight normalised sub-sample assay values allowed direct comparison of ore crushing mode GRAT classification results for analysis on an equal basis.

3.7 Ore sample test work replication

GRAT classification sink–float tests were dissimilar between Ballarat and Cadia investigations in this research and are not comparable. Limitations in laboratory resources, including sample material supplied, financial resources, and experimental program time restrictions in reporting, prevented test replication. However, this did not significantly impact the research emphasis in this study in developing a characterisation methodology, with parameters indices describing grade by density deportment. Still, the statistical comparison of means could only be made on four (4) crushing mode product head-grade assays. The small number of sample material head-grade assays available for analytical comparison negated the statistical value of calculating confidence intervals (CI) for assays, as Napier-Munn (2014) indicated. The Chapter 2 literature review showed that other researchers with similar experimental limitations in similar gravity separation studies have not always reported duplicate results.

3.8 Rosin-Rammler particle size distribution modelling

Particle size distribution can impose a limitation on density separation operations. Density separation limitations are primarily due to well-known factors, including small particle separation performance and lower potential for the full liberation of gangue components in coarser particles (Eksteen, 2015; McGrath et al., 2018). Both these factors contribute to misclassification in density separation processes.

This study collected and screened broken gold-bearing ore particles by specified size meshes. The particle size distribution of the broken ores was studied and compared for different crushing modes using a Rosin-Rammler (RR) distribution function. A line of best fit for the GRAT size-based data from the RR function. The RR technique provides a mathematical form

for the breakage size distribution, as reported by Rosin and Rammler (1933). The application of the RR technique to characterise the distribution to particle size analysis of comminution processes is regularly used (Wills & Finch, 2015). The relationships and influences between the ore type, inherent breakage pattern, and separation technique were characterised by the RR distributions, referenced against selected crushing modes. Based on this analysis, a particle size distribution Rosin-Rammler curve was created as a graph of the cumulative percent of retained grains versus the particle size, which is referenced to the crushing mode technique. The shape and extent of the curves provide visual information regarding changes in the breakage pattern, linked to size mass deportment changes and the method used in crushing the ore.

This thesis shows the Rosin-Rammler equation (RR) distribution function by equation two (2). The RR function describes the relationship between screened material cumulative percent retained and particle size (Rosin & Rammler, 1933; Fraser, 2020).

$$\mathrm{R} = e^{-\left(\frac{\mathrm{D}}{\mathrm{D}n}\right)^{\mathrm{n}}} \tag{2}$$

Where Fraser (2020) describes the R value as the cumulative percent retained at a particle size, D. Fraser (2020) further describes the regression fitting parameters as exponent n, which affects the spread of the distribution, and $\mathrm{D}n$, which is a fitting parameter affecting the mean particle size of the distribution.

3.9 Least-squares regression modelling of densimetric data

This thesis tests seven standard model fitting formulas, shown by equations 3 to 9, as described by Goovaerts (1997), Webster & Oliver (2007) and Bohling (2007). These formulas are tested in regression modelling to derive the best fitting line through the points representing data produced from the GRAT classification scheme, both for the observed and calculated data. For better accuracy, formulas as tested using a least-squares regression (LSR) model fitting technique. The least-squares regression (LSR) technical optimises the fitted line to both measured and calculated variable x-y axis data produced in this study, with model equations described for linear, power, exponential, Gaussian, and spherical formula.

Linear: $\gamma(h) = c_0 + \mathrm{b}h$ (3)

Power: $\gamma(h) = c \cdot h^{\omega} \quad with\ 0 < \omega < 2$ (4)

Gaussian (1): $\gamma(h) = c \cdot (1 - exp(\frac{-3h^2}{a^2}))$ (5)

Gaussian (2): $\gamma(h) = c_0 + c \cdot (1 - exp(\frac{-3h^2}{a^2}))$ (6)

Exponential (1): $\gamma(h) = c \cdot (1 - exp(\frac{-3h}{a}))$ (7)

Exponential (2): $\gamma(h) = c_0 + c \cdot (1 - exp(\frac{-3h}{a}))$ (8)

Spherical: $\gamma(h) = c \cdot (1.5(\frac{h}{a}) - 0.5(\frac{h}{a})^3) \quad if\ h < a$ (9)

The aim consists of adjusting the model function parameters to fit a data set best. Where b equals the regression line slope. The exponent parameter ω is a dimensionless quantity that describes the intensity of the process, which relates to the curvature and must lie strictly between 0 and 2 where the value of ω = 1 yields a straight line (Webster, 2005).

3.10 Graphical characterisation of grade deportment by size

Carrasco et al. (2016a) characterised preferential grade-by-size deportment by a diagram of cumulative weight passing (%) against cumulative metal recovery (%) for each size fraction, where the diagrams cumulative weight left to the right describes fine to coarse size fractions. In the diagram, the 45° response line indicates no size preference for metal deportment (Carrasco et al., 2016a). However, the further the response is from this line, the stronger the response level per size (Carrasco et al., 2016a).

This research analysed gravity experimental GRAT results for size class fraction grade and mass variations in individual segregation products by selected LSR modelling techniques, utilising equations presented in Section 3.9. This methodology allowed graphical characterisation of the relationship between metal (grade) versus mass recovery by size deportment. The LSR equations used in this study were Power and Gaussian functions. These functions were determined, by experimental investigation, to minimise the sum of squared errors best in predicting the lines of best fit to the GRAT size-based classification results.

The shape and extent of the LSR best fit line is a visual measure of gold's propensity to be preferentially concentrated by particle size into the screen O/S fractions. The shape and extent of the curves also provide visual information regarding changes in the breakage pattern resulting from the application of different crushing modes. The lines of best fit

indicate the degree of gold pre-concentration by gangue rejection at each size interval, relative to mass pull into the O/S.

Understanding whether gold will preferentially deport into the screen O/S or U/S fractions is dependent on the position and shape of the curve above or below a diagonal line. The diagonal partition line implies the region of the chart where gold follows mass transfer across screen sizes, or as an example, where 50 % of the mass contains 50 % of the gold. Therefore, the distance of a curved line above or below the diagonal line suggests the strength of preferential gold enrichment response into either the screen O/S material or the screen U/S material, respectively.

3.11 Graphical characterisation of grade deportment by density

This study used an LSR modelling technique to analyse gravity gold-bearing ore experimental GRAT findings for density class fraction grade and mass variations in individual segregation products, utilising equations presented in Section 3.9. This methodology allowed characterisation of the relationship between metal (grade) versus mass recovery by density deportment.

In the graphical analysis, the cumulative mass (CM) and grade accepted into the HLS sink and float, as a function of the specified GRAT HLS density range, for the Ballarat and Cadia ores, were plotted as curves for different crushing modes. The shape and extent of these plotted curves estimate the propensity of elements to preferentially concentrate via particles reporting into either sink or float fractions and evidence for the extent of coarse particle liberation between the value component and gangue.

The silicate minerals have a much lower SG than gold or sulfide minerals. Therefore, silicate mineral associations with gold and sulfide minerals result in lower particle densities than liberated gold or sulfide minerals alone. As an example, where recovery of gold into HLS sink products is very high and mass yield low, particularly in high SGs splits, the extent of gold liberation from silicates is high. Conversely, relatively lower gold deportment into sink fractions indicates a higher proportion of gold is associated with silicates in binary particles. Therefore, the gold grade and mass yield into the HLS sink and float fractions indicate the extent of the liberation of valuable components and waste materials.

Typically, a highly liberated particle of either gold or sulfide mineral will report into the HLS sink because the gold and metal sulfides have a higher SG than the media. However, fine-grained (< 10 µm) gold particles and poorly liberated gold, metal sulfides in mineral associations with low SG waste mineral, such as silicates, will predominately report into the HLS float, when the bulk particle density is below that of the media (McGrath et al., 2018).

3.11.1 Gravity separation performance metallurgical parameters

This thesis develops and evaluates three new metallurgical parameters. New parameters predict the enrichment ratio, separation operation preferential grade by density deportment response, and gravity process magnitude of grade deportment by density response during gangue rejection. In addition, these parameters predict and index the propensity of valuable component pre-concentration by early-stage coarse particle gangue rejection (CPGR) influenced by the selected ore type, crushing breakage mode, and classification process. The essential requirements of the parameters were to evaluate the separation efficiency of the gravity separation process under conditions of:

i. Unbiased to ore feed characteristics; measures recovery of values from the available values in the feed.
ii. Grade improvement-oriented; considers the recovery loss of the value component in the gangue contained in the reject fraction.
iii. The recovery-based indicator considers the recovery of the value component in the respective product and waste fractions.

Equation 2 shows a mathematical function that describes a new metallurgical parameter coined the Rejection Enrichment Ratio (RER). This thesis uses the RER on Ballarat and Cadia GRAT experimental observations to calculate the grade enrichment during gangue rejection for screen size or HLS density separation operations. The equation is adapted from previous research by Holland-Batt (1990), Carrasco et al. (2016a), Carrasco et al. (2016b) and Carrasco et al. (2016c) on the upgrade ratio. It is analogous to the enrichment ratio (RE), a parameter described by Wills & Napier-Munn (2006). The RER parameter is a measure of the “efficiency of the separation process”, as defined by Wills & Finch (2015), for a classification operation (size or SG) separation point and is equivalent to the upgrade ratio response in a separation product. The RER parameter calculation, shown by equation 10, produces a dimensionless

value, which is a quantitative prediction of the fractional efficiency of a selected element's separation and enrichment process into a nominated concentrate product while accounting for the chosen element loss in the gangue fraction of the separation operation. Therefore, the RER value represents the metal upgrade ratio of the weight of the selected valuable component recovered in the nominated concentrate component to 100% of the same constituent in the feed during gangue rejection in a separation operation.

$$\mathrm{RER}_i = \sum_{i=1}^{n}\left(\frac{\left(f - t_i \ \mathrm{x}\, w_i\right)}{\left(1 - w_i\right)}\right)\mathrm{x}\,\frac{1}{f} \tag{10}$$

Where i refers to the classification operation (size or SG) separation point, in consecutive order of increasing HLS SG or reducing screen size and n is the total number of separation measurement points in the classification operation. The f and t parameters refer to the specified ore feed grade and the combined product tail grade at the separation point i. The w metric refers to the mass ratio for a specified tail fraction mass i and the total mass of all separation points.

The cumulative RER measures the efficiency of the separation process, accounting for the selected element loss in the tail (Wills & Napier-Munn, 2006). The RER is related to the extent of waste mineral liberation and preferential value component deportment into the selected concentrate fraction. The larger the RER value raises above one (1), the greater the value component ratio of concentration or the higher mass proportion rejection of gangue material during the separation operation. Conversely, an RER value of 1 implies no preferential grade by separation operation deportment or no increase in the ratio of metal concentration into the specified concentrate fraction. An RER value around 1 indicates poor value component liberation from waste minerals (Wills & Napier-Munn, 2006). The RER parameter is independent of recovery during the separation process and, therefore, does not provide information on the metallurgical separation performance of the concentration operation. The extent of liberation in the gangue and value component strongly influences the separation efficiency of the classification process (Finch and Gomez, 1989).

The second parameter, coined the Enrichment Deportment Response (EDR) parameter, is a function of the RER value and product cumulative weight recovery, calculated for each separation operation. The EDR is a quantitative prediction of an elemental component

metallurgical separation performance of the concentration operation described by Wills & Finch (2015) for each separation process. The EDR parameter quantifies the ore preferential grade by density deportment response for each classification size or SG increment as a function of gangue rejection (Wills & Napier-Munn, 2006). The EDR parameter is analogous to the ore Ranking Response (RR) parameter reported by Carrasco et al. (2016a), Carrasco et al. (2016b), and Carrasco et al. (2016c). In this study, the EDR value is representative of the magnitude of preferential grade deportment by density response for a separation operation for a selected ore during comminution. Where Equations 11 describes the EDR function.

$$\mathrm{EDR}_i = \sum_{i=1}^{n} \left| \left(\frac{\ln\left(\mathrm{RER}_i\right)}{\ln\left(\mathrm{CW}_i\right)} \right) \right| \mathrm{x100} \tag{11}$$

The CW metric refers to the specified sinks, concentrate cumulative weight at a progressive separation fraction point, i, in the suggestive order, and the parameter n identifies the total number of classification fractions.

The EDR parameter is a dimensionless value that is affected by the interaction of rock mineralogy and heterogeneity, mode of breakage, and separation process. The EDR parameter is shown as an absolute value that indicates the numeral displacement from zero for the magnitude of selected metal deportment by density response into sinks during a density separation operation. Where a zero value identifies no preferential deportment or separation response relative to changes in mass displacement during the separation operation, the EDR value quantifies the extent of the metallurgical efficiency of the concentration operation response from a specified separation cut with values in the range of $0 \geq \mathrm{EDR} \leq 100$. An EDR value of 100 corresponds to 100 % of the feed element recovered into a specified concentrate fraction to represent 100 percent of the concentrated mass. Conversely, an EDR value of 0 indicates no preferential deportment of the valuable component into the specified concentrate fraction during separation.

The third parameter, coined the Enrichment Deportment Index (EDI), provides a uniform response value for the EDR parameter values. The EDI parameter is a gravity separation performance measure to identify the overall magnitude of grade deportment by density response as a relative index value. The metallurgical basis of the EDI parameter to evaluate separation performance is described by:

- Grade enrichment-oriented: An efficient beneficiation process rejects maximum gangue minerals and minimum value components in the tail. In other words, the indicator measures the preferential recovery of values available in the feed as a function of gangue minerals rejected.

The EDI parameter is derived from the linear least squares (LLS) regression technique Napier-Munn (2014) described. This process gives a linear fit in the slope, where information about the slope estimator of that line is used to produce the EDI parameter. The slope of the LLS line estimates the strength of the mean grade deportment change in the dependent RER variable when the independent variable or explanatory variable, sinks accumulative weight percentage, is increased. The EDI parameter is a dimensionless value derived from the LLS slope through a simple scaling process to calculate a value between 0 to 100.

An EDI value of 100 implies a perfect separation of valuable components into a separation product fraction, with no contained waste mineral. Conversely, an EDI value of 0 implies no separation between the valuable component and waste minerals during classification operation. Subsequentially, after the EDI equals 100 percent, the gravity classification efficiency must decline in proportion to the progressive addition of waste minerals to the metal value concentrate. Therefore, the EDI parameter is a suitable interpretative technique for ore gravity separation performance characterisation. The EDI parameter describes the separation behaviour for the magnitude of the gravity classification change in grade across density separation fractions as a cumulative response that can be indexed and racked.

The EDI parameter provides a uniform response value for a separation sequence of individual separation operation EDR parameter values, calculated from densimetric empirical data. Therefore, the EDI value does not indicate the variability that may exist within separate heavy separation processes. The EDI parameter is directly related to the collective mean of the EDR responses for individual separation processes. Described another way the EDI parameter predicts a broken ores gravity classification overall preferential grade by density deportment response in sinks during gangue rejection, influenced by the interaction between ore type, crushing mode and gravity separation technique. Therefore, the EDI value represents the gravity separation process's overall extent of preferential metal deportment by density potential for a specified ore during comminution.

3.11.2 Practical analysis with the metallurgy parameter methodology

The RER, EDR and EDI parameters describe the extent of gangue and value component liberation as a measurable rock property that is a function of both particle breakage mode and downstream separation technique. These parameters are used in a characterising method in this thesis. This method is created to evaluate and classify the GRAT classification data for the propensity of gold-bearing sulfide ore to preferentially concentrate metal into the specific size or density fractions during millimetre-scale breakage by the specified crushing mode selected gold-bearing ores. Where metal deportment propensity is a function of the ore type, crushing mode and separations technique. An important part of this methodology is the creation of functions that predict metallurgy parameters that can index and rank preferential grade by density responses. The research characterising methodology includes:

1. plotted data charts with modelled lines of best fit to compare separation performance, metal recovery, and metal enrichment against mass;
2. developing and applying mathematically described preferential metal (grade) by density deportment response parameters for the RER, EDR and EDI metrics;
3. using existing statistical analysis techniques to identify the reliability of the research bivariate data analysis and classification performance measures; and
4. demonstrating the applicability and accuracy of the EDI parameter to describe and model gold deportment in density-based separations as a relative index value.

The first ore parameter coined, RER, is adapted from the upgrade ratio (Upg ratio) metrics described by Holland-Batt (1990), Carrasco et al. (2016a, 2016b, 2016c) and is analogous to the enrichment ratio (RE), a parameter described by Wills (2006). The RER parameter specifies the concentration ratio of a valuable component in a specified product relative to the ore abundance of that component. The second parameter coined, EDR, is a function of the RER value and particle weight attainment in an SG product fractions. The EDR is used to describe the extent of the metallurgical efficiency of the concentration operation into a specified concentrate fraction (Wills, 2006). The third ore characterising parameter, the EDI, is used to predict the separation efficiency or performance of the overall gravity HLS sink–float

response. The EDI value represents the metallurgical performance of the gravity concentration operation for all separation points. The EDI parameter value represents the amount of a specific valuable component present in the crushed ore feed that is recovered to the concentrate/product in its pure form after gangue rejection.

The RER, EDR, and EDI parameters allow characterisation of the influence on the liberation and gravity separation performance between waste and valuable components following comminution by various fine crushing modes on a selected gold-bearing ore. It is noted that the plotted data charts are in line with the usual standards for mineral classification characterisation, where the RER, EDR and EDI parameters are newly described characterisation parameters developed and applied in this research. This thesis shows the applicability of the EDI parameter in predictive modelling of partition curves showing variation in element grade and yield into sinks at varying sink mass pulls. Successful interpretation of the GRAT results by the EDI increases understanding of how ore type, densimetric classification processes, and selected crushing mode breakage influence gravity separation performance. Ultimately the EDI may be used in characterising separation performance in gravity or gravity separation processes, influenced by the type of ore and mode of breakage, to convert previously uneconomic gangue to valuable ore.

This research focused on demonstrating the applicability of the EDI parameter to estimate the relationship between gold (grade) deportment into a float and sink fraction versus gold yield into sinks. This relationship evaluation is achieved by using the EDI value to predict grade and yield partition curves generated at varying mass yields accepted into the sink. In addition, the RER, EDR and EDI parameters may be useful in other metal gravity assessments for different ore types, such as base metals, with little modification in their notation or procedural methodology.

3.12 Statistical error and reliability analysis

This research applies a statistical error and reliability analysis methodology for bias, accuracy, and precision in data analysis. This thesis methodology quantitatively estimates bivariate data regression models' reliability or measurement errors (Goovaerts, 1997). These estimates indicate the strength of the developed mathematical regression models to predict the relationship between the variable (x) and a response variable (y). In this thesis, the regression

models find the line of best fit (or trend line) to predict the behaviour between x and y variables by the method of least squares. The x and y variables describe each Cartesian coordinate point (x, y) of data in a scatterplot. With the scatterplot trend line detailing the estimated value of the dependent variable, y read as "y hat" (ŷ). The least-squares method minimises the sum of the residuals or error between the response variable, y, and corresponding points from the plotted trend line. Napier-Munn (2014) reported that the least squares regression (LSR) technique predicts the behaviour of the dependent variable by minimising the sum of the squares of the errors between the observed and model-predicted value. Napier-Munn (2014) reported that bivariate analysis modelling predicts a result as an estimate, not a prescriptive measure. Therefore, a measure of bias, accuracy, and precision characteristics provides information on how well a regression model estimator performs (Goovaerts, 1997).

Esmaeelnejad, Siavashi, Seyedmohammadi, & Shabanpour (2016) reported statistical quality measures for the mean error (ME) and root mean square error (RMSE) characterise bias and different model accuracy in regression modelling, respectively. Low ME and RMSE values suggest low bias and good accuracy or total precision with low prediction errors when comparing different models for a variable, such as crushing mode. Esmaeelnejad et al. (2016) described ME in equation 12:

$$ME = \frac{1}{n}\sum_{j=1}^{n}(y_j - \hat{y}_j) \tag{12}$$

Where j represents the index of summation, incremented by 1 for each successive term, stopping when $j = n$, n is the number of data points, y_j represents observed values, and $\hat{y}_j$ represents predicted values.

Esmaeelnejad et al. (2016) described RMSE by equation 13. The RMSE metric characterises the model precision or scattering around the mean and should be as small as possible for unbiased and precise prediction. The RMSE values suggest the degree of spread in the errors of the model predictions, and therefore model "precision".

$$\mathrm{RMSE} = \frac{1}{n}\sum_{j=1}^{n}(y_j - \hat{y}_j)^{0.5} \tag{13}$$

Napier-Munn (2014) reported the coefficient of determination, R-squared (R^2), as a standard approach to indicate how much variance two variables share and as an overall measure of the accuracy of the regression model. The R^2 shows the goodness of fit for the linear regression model or variability of the observed dependent variable around the trendline (Bowerman and O'Connell, 1990). The R^2 variability between the regression model predicted and the observed value was measured on a 0 to 100 % scale (Bowerman and O'Connell, 1990). R^2 values approaching 1.00 suggest a good fit for the prediction. Napier-Munn (2014) described R^2 by equation 14:

$$\mathrm{R}^2 = \frac{\sum\left(\hat{y}_j - \bar{y}\right)^2}{\sum\left(y_j - \bar{y}\right)^2}. \tag{14}$$

Where $\bar{y}$ represents the observed values mean.

Using empirical data and metallurgical parameters developed as a result of this research. Existing statistical methods evaluate the significance of changes in metal enrichment and preferential grade by density deportment. Statistical methods applied are analysis of variance (ANOVA) F-test and t-test analysis of regression line slopes techniques. These statistical techniques identify the significance of changes in classification results linked to the selected crushing mode influence on the extent of gangue and value component breakage liberation.

3.13 Experimental separation performance data comparison

Appendix 2 and Appendix 3 provide the GRAT sieve size and HLS sink–float grade and mass classification for Ballarat and Cadia ore results. The sieve pan minus 0.3 mm particles were removed to reduce the risk of misclassification during the heavy liquid separation (HLS) sink–float processes. The 0.3 mm material assays and mass used with HLS sink–float grade and mass in feed grade normalised the classification results. These feed grade normalised mass balanced results allowed better comparison of variability in density separation performance and other data comparisons due to the influence of different crushing modes for specific ore styles investigated in this thesis. The RER, EDR and EDI characterisation metallurgy parameters are determined using feed grade normalised mass balanced results in Appendix 2 and Appendix 3 data.

3.14 Summary

The emphasis in this thesis is on the method of separation efficiency calculation and its implication for gravity process evaluation of gold-bearing ore, broken by different crushing modes. The principal focus of this research is the development of a successful methodology for characterising gravity separation behaviour of gangue in pre-concentration of fine crushed gold-bearing sulfide ore, using densimetric data produced by the GRAT methodology. The GRAT methodology was developed by Curtin university Gold Technology Group (GTG). This methodology aims to show how the preferential transportation of gangue and metal across the HLS density increments is selective for different rock breakage liberation patterns caused by crushing. In this thesis, crushing is either by mechanical or non-mechanical mode producing coarse scale (millimetre) breakage up to a particle top size of ≤4.75 mm.

The GRAT methodology separated particles by size and heavy liquid specific gravity (SG) segregation into multiple fractions to enhance and exploit coarse gangue rejection to float and increase effective feed grades to sink fractions. The GRAT float and sink fraction data produced within each density increment indicate the degree of gangue and valuable component particle liberation (McGrath et al., 2018). Furthermore, the GRAT data suggests the impact of variations in gangue liberation patterns by selected crushing modes on value component pre-concentration by gangue removal (McGrath et al., 2018). Where the extent of liberation in the gangue and value component strongly influences the separation efficiency of the classification process (Finch and Gomez, 1989).

The GRAT methodology is an advancement over previous laboratory GRG, CGR or the multi-pass test techniques, unable to treat particle sizes much above 1.18 mm (McGrath et al., 2018). This study used densimetric data obtained from Ballarat and Cadia gold-bearing sulfide ores, using versions of the GRAT methodology. Both the Ballarat and Cadia ore versions of the GRAT methodology allowed assessment of gold pre-concentration potential principally by particle SG, subject to gangue rejection.

The gold-bearing ore samples studied were orogenic and porphyry copper-gold materials provided by the Ballarat Castlemaine Goldfields Limited (CGT) and Cadia Valley Operation (CVO) mines. The Ballarat gold-bearing ore sample was crushed by laboratory scale cone crusher, rolls crusher, SELFRAG and VSI modes. Laboratory scale cone crusher, HPGR,

SELFRAG and VSI modes were used for crushing Cadia copper-gold ore sub-samples. During crushing, particle top sizes were controlled at ≤2.00 mm for Ballarat orogenic ore and ≤4.75 mm for Cadia porphyry copper-gold ore through a staged screening technique, ahead of the GRAT sequential separation process. The staged screening technique was employed to avoid crushing particles at size to fines. In the GRAT classification process, feed particle size ranges investigated are -2.00/+0.30 mm for the orogenic ore and particle sizes of -4.75/+0.30 mm for the porphyry copper-gold ore. The GRAT methodology removed the minus 0.3-millimetre material to reduce the potential influence of particle size in misclassification between the float and sink fractions, particularly of fine particles of low SG particles of silica that have long settling rates (McGrath et al., 2018). The minus 0.3 mm particles were removed to reduce the risk of misclassification during heavy liquid separation (HLS) sink–float processes, but assays and mass were used in balancing classification results. McGrath et al. (2018) reported that the liberation response is both a rock characteristic and a response to the selected fine crushing mode used in rock breakage.

The Ballarat and Cadia ore sample preparation and simplified experimental test program flow sheets are provided in Section 3.3. In addition, the Ballarat and Cadia ore versions of the GRAT classification process flowsheets are described in Section 3.4.3.2 and Section 3.4.3.3, respectively. The two principal areas of difference between the Ballarat and Cadia GRAT versions are:

1. Respective Ballarat and Cadia crushed ore particle top size of 2.00 mm, versus 4.75 mm for gravity separation; and
2. Cadia version sizing of the sink–float products following density separation, as opposed to Ballarat crushed ore size fractionation ahead of density classification.

The primary study objective was to understand and characterise the propensity of gold-bearing ores to exhibit preferential breakage leading to the concentration of minerals in specific density fractions. The interpretative approach describes the subsequent inherent propensity to pre-concentrate metal values, influenced by implied liberation induced by the selected crushing mode used in breakage. Importantly, this interpretative approach includes metallurgy parameters to predict preferential grade (principally gold) by density deportment responses, representing the interaction between crushing mode, ore and separation process.

In this study, a mathematical methodology was developed to derive metallurgy parameters, which indicate the propensity for the crushed gold-bearing ore to separate gangue and preferentially upgrade and recover the valuable component into a concentrate while transporting gangue and metal across multiple density fractions. These parameters were coined RER, EDR, and EDI. The parameters are used to categorise, index, and rank the extent of liberation and efficiency of a gravity separation process. In addition, the parameters allow characterisation of the influence on the liberation and gravity separation efficiency between waste and valuable components during separation processes for different fine crushing mode products.

The RER is a dimensionless value, which is a quantitative prediction of the fractional efficiency of a selected element's separation and enrichment process into a nominated concentrate product while accounting for the chosen element loss in the gangue fraction of the separation operation. An RER separation operation response value well above 1 implies a strong enrichment response of valuable components into either a sieve fine or HLS sink fraction. Conversely, an RER value below 1 shows a tendency for the element to enrich in the coarse fraction material or float material. A value component RER value of approximately one (1) has either no or weaker element upgrade ratio response during separation within a designated product fraction. Therefore, the RER value is representative of a metal upgrade ratio within sink fractions.

The EDR is a quantitative prediction of the metallurgical efficiency of the grade concentration operation within a separation process. The EDR metric value represents the propensity of the valuable component in feed material to concentrate into the sinks during gangue rejection for a specific density separation process. Thus, the EDR value is a quantified measure of the preferential metal deportment by density response, linked to the interaction between an ore type, specific crushing mode, and gravity separation technique.

The EDR value is calculated as a function of the metal and mass content ratio in the separation process fractions per separation operation. Where the EDR value:

1. Ranges between any real number from 0 to 100.

2. At or near 0 implies little or no preferential grade by density deportment response during the separation process. This response result means that the sinks grade equals the feed assay associated with the value component.

3. Close to 100 implies an excellent preferential grade by density deportment response, where the grade is associated with the value component.

The EDI parameter value is determined using a linear line of best fit LSR modelling method, with the value estimated by the slope of a regression line. The slope of the LSR line represents the rate of change in the natural log of the valuable component enrichment ratio or RER and the accumulative mass pull into the sink fractions during gravity separation. The line slope of the bivariate regression is determined over the GRAT density separation range investigated for each selected gold-bearing ore examined in this thesis. The predicted model best-fit line shape and extent is a visual measure of the overall propensity of selected metal to preferentially concentrate into the sinks during gravity separation. Determining the EDI parameter represents a methodology for transforming raw density and assay data into a set of cumulative responses that can be used to index and rank the magnitude of preferential metal deportment. Therefore, providing a uniform response value for systematic change in grade across density fractions.

The EDI value represents the propensity for valuable components present in the ore feed to be recovered into the overall gravity separation concentrate (sinks) in its elemental form, during gangue removal, and is a measure of the metallurgical efficiency of metal concentration. An EDI value of 100 implies a perfect separation of valuable components into a separation product fraction, with no contained waste mineral. An EDI value of 0 means no separation between the valuable component and waste minerals during classification operation. If there is only one density separation operation in a study; there is no difference between the EDI value and the EDR response. Therefore, the EDI parameter can rank and compare the magnitude of preferential deportment responses produced by the interaction between ore type, crushing mode, and density separation process.

The EDI is a function that can predict gravity separation partition curves for the sinks grade, and yield changes for specific elements over a cumulative mass pull range produced at selected sequential density intervals. Furthermore, the findings of actual laboratory gravity

separation experiments, including those described in this thesis, can be utilised to verify the predicted partition curves.

Existing statistical analysis techniques are employed in this study to model, compare, and show the significance of data associated and error on validity and reliability. The mean error (ME) and root mean square error (RMSE) values measure the statistical estimates for bias and accuracy. The RMSE value is a valuable measure of the total precision of the model trend line. The R^2 measure predicts the overall accuracy of the regression model. The analysis of variance (ANOVA) and t-tests were statistical techniques used to test for equal means, variances, and the significance of the slope of the regression lines for the GRAT research data to compare various crushing mode influences on gravity separation performance.

Successful interpretation of the GRAT results for CPGR and metal deportment by density responses are anticipated to increase understanding of how changes in gold-bearing ore type and crushing mode influence natural ore breakage patterns, gangue liberation, and early-stage gangue removal to a waste stream. Ultimately, this will aid the mining industry in converting previously uneconomic low-grade ore to valuable ore and enrichment of the ore feed ahead of comminution.

Chapter 4. Crushing mode effect on metal deportment

The Chapter 2 literature review has identified that crushing rock breakage causes variations in preferential grade-by-size-based deportment in many types of ores. This research has characterised coarse particle density separation performance by density classification after different crushing mode breakage. A characterisation methodology is investigated for a coarse particle-sized sequential density separation by gravity separation techniques. For this reason, sized sequential density separation and fine crushing breakage behaviour tests were conducted on the Ballarat and Cadia ore samples. These tests evaluated the comminution effects of various mechanical and SELFRAG Lab devices. The gangue rejection amenability test (GRAT) method provided data for characterising variation in metal (grade) by density deportment response.

4.1 Background

The research evaluated empirical gravity data obtained from laboratory scale mechanical and electric pulse SELFRAG comminution tests conducted on the Castlemaine Goldfields Limited (CGT) and Cadia Valley Operation (CVO) gold-bearing sulfide ores. Each ore was treated by a different version of the gangue rejection amenability test (GRAT) methodology, described in Chapter 3. The GRAT methodology characterised deportment by quantifying the mass and grade of each combined size and density fraction.

The Chapter 2 literature review revealed a scarcity of published information in characterising gold-bearing sulfide ore amenability for valuable metal pre-concentration via coarse particle gangue rejection (CPGR) during gravity separation of particles larger than 1.18 mm. Still, the Chapter 2 literature review identified that published research by Carrasco et al. (2016a, 2016b, 2016c) and other researchers reported size-based pre-concentration research into preferential grade-by-size deportment in comminute ores particles above 1.18 mm. This size-based research developed methodologies to predict, index, and rank separation performance for preferential grade deportment within specific particle size fractions typically between 5 mm to 100 mm (Bamber et al., 2008; Bearman, 2013; Bowman & Bearman, 2014; Carrasco et al., 2016a; Carrasco et al., 2016b; Carrasco et al., 2016c; and Carrasco et al., 2017). These researchers had also identified that the mass transfer and the grade of material between the size fractions provided information on gangue and value component particle liberation and, consequently, their ability to be preferentially separated.

The interaction between crushing mode and ore type generates the fragmentation pattern and subsequent crushed product particle size distribution (PSD). However, it is not just the mass transfer between the size fractions that is important, but also the grade within size classes. This relationship provides information about particle liberation and likely metal enrichment recovery in a screening size-based classification or density-based separation. Furthermore, particle Specific Gravity (SG) substantially influences the settling velocity and, consequently, the density separation performance (Sarkar et al., 2008). Notwithstanding, the extent to which different crushing modes and ore types may influence rock gangue fragmentation patterns and subsequent preferential grade by density deportment during SG stage-wise separation is not well understood.

The crushed Ballarat orogenic gold-bearing sulfide ore and Cadia porphyry gold (Au) and copper (Cu) polymetallic ore samples were subjected to the GRAT classification scheme, described by the Chapter 3 testwork programs. A key element evaluated in the test work for the Ballarat ore was gold as the valuable component. Other elements assessed in the grade-by-size analysis for Ballarat ore were arsenic (As), iron (Fe) and sulfur (S) to determine the association with sulfide minerals. Key elements evaluated for Cadia ore were gold and copper as the valuable components. Other Cadia ore elements evaluated in the grade-by-size analysis were molybdenum (Mo), Fe and S, given their association with sulfide minerals. The GRAT classification scheme testwork results were mass balanced, with the minus 0.30 mm material included in the mass balancing calculation. As described in Section 3.6, a feed grade normalisation method was applied to the GRAT research data to directly compare balanced metallurgical results for a selected ore type, broken by different crushing modes.

This study employs Chapter 3 Ballarat and Cadia GRAT methodologies to generate measured observations for selected gold-bearing sulfide ore's propensity to concentrate chosen metal into density fractions during gangue rejection, following different modes of crushing influence on ore breakage pattern. This study evaluates the crushed gold-bearing sulfide ore product by particle size distribution and the sequential grade by density response within separation fractions to determine the metallurgical efficiency of metal concentration and interpret coarse particle scale rejection and metal pre-concentration responses.

4.2 Ballarat ore size and density classification analysis

4.2.1 Background

A metallurgical analysis of the Ballarat crushed ore samples, produced by the laboratory Sala mortar cone crusher (Cone), rolls crusher (Rolls), SELFRAG Lab Selective Fragmentation (SELFRAG) and Vertical Shaft Impactor (VSI) modes were assessed. This assessment investigated changes in the propensity for the fragmented ore to preferentially concentrate gold into the specific size and density fractions after breakage. The changes are a function of the interaction between a gold-bearing sulfide ore type, fine crushing mode, and a classification scheme.

4.2.2 Particle size distribution by Rosin-Rammler modelling technique

The Rosin-Rammler (RR) method describes the particle size distribution (PSD) in the cone crusher, rolls crusher, SELFRAG and VSI comminuted gold-bearing ore products. The

mathematical form of the different crushing mode RR distributions is shown, in Figure 4-1 for the cumulative mass percent of retained grains versus the particle size.

In comparing the PSD of the Ballarat ore crushing mode products, shown in Figure 4-1, it is observed that there is a significant difference in the fragmentation pattern produced by the SELFRAG and the mechanical modes. Figure 4-1 shows particle size distribution Rosin-Rammler response curves created as a graph of cumulative percent of retained grains versus the particle size for different fine crushing modes treating Ballarat ore. A comparison of the Ballarat mass retained response curves suggests a minimal size difference between the cone, HPGR and VSI modes. Therefore, the cone crusher rolls crusher and VSI results indicate that the different breakage modes produce similar fragmentation particle size distributions on a size-by-size basis. Thus, the observed difference for the SELFRAG curve PSD is likely linked to the SELFRAG high voltage electric comminution particle breakage method, which differs significantly from the mechanical particle fracturing mechanism of the other crushing modes investigated.

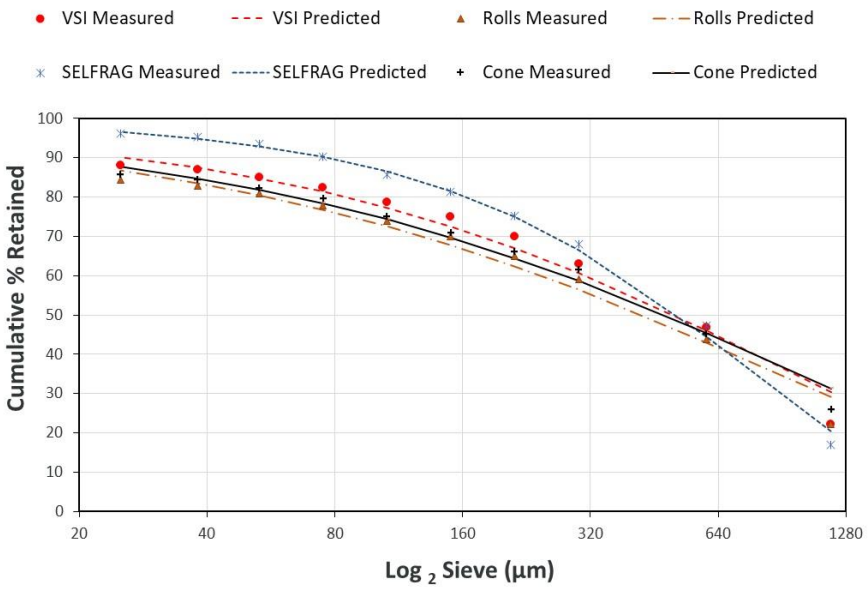

Figure 4-1. Ballarat ore mass distribution for different size fractions by crushing mode

Observations and conclusions from the analysis are that:

- The roll crusher is the most suitable for efficiently reducing the size of the material over most of the size distribution, except in particles larger than approximately 0.6 mm, where the SELFRAG is more efficient in size reduction.

- Over most of the size distribution, the VSI mode produces a coarser PSD in the crushed product than PSD's determined in either the rolls crusher or the cone crusher products.
- The rolls crusher PSD curve shape and extent suggest the crusher is acting as a single particle crusher, as opposed to a typical HPGR inter-particle size distribution curve, which is typically flatter, as reported by Drozdiak, Klein, Nadolski, & Bamber, 2011 and Anticoi et al. (2018).

The statistical quality measures in Table 4-1 indicate the goodness of fit of the cumulative PSD against the RR model predictions. Table 4-1 shows all the RR particle trajectories of different particle sizes produced low ME and RMSE values, which indicate low bias and good accuracy. The high R^2 values indicated low unexplained variability and good agreement between predicted and measured results. However, as a rule, RMSE values between 0.2 and 0.5 show that a model can predict the data accurately. So, the RR results suggest moderate prediction errors for each crushing mode, with the SELFRAG showing the best accuracy and the VSI crusher the lowest.

Table 4-1: Rosin-Rammler modelling descriptive statistics

Statistic	Cone	SELFRAG	Rolls	VSI
ME	1.637	1.035	2.121	2.224
RMSE	0.704	0.486	0.885	0.974
R^2	0.988	0.996	0.983	0.980

4.2.2.1 Gold deportment by size analysis

The cumulative 80 % and 50 % passing (P_{80} and P_{50}) for crushed ore sample mass distribution and gold (Au) distribution, by particle size, are listed in Table 4-2 and Table 4-3. The extent of the difference between the mass and metal passing size figures in Table 4-2 and Table 4-3 indicates the strength of the preferential grade-by-size deportment tendency during crushing. Table 4-2 and Table 4-3 results showed weak preferential deportment of gold into fines for the cone crusher, with slightly better deportment of gold by size into the coarse particles evident for the rolls crusher, VSI and SELFRAG modes. Usually, if the P_{80} values between the PSD and grade are similar, it is concluded that the breakage behaviour comminution efficiencies are the same. Detailed supporting data is provided in Appendix 2.

Table 4-2: Ballarat ore 80 % passing particle size and gold distributions by crushing mode

Size (µm)	Crushing Mode	PSD P_{80} (µm)	Au P_{80} (µm)
P_{80}	Cone	1350	1168
P_{80}	Rolls	1251	1528
P_{80}	VSI	1252	1223
P_{80}	SELFRAG	1117	1417

Table 4-3: Ballarat ore 50 % passing particle size and gold (Au) distributions by crushing mode

Size (µm)	Crushing Mode	PSD P_{50} (µm)	Au P_{50} (µm)
P_{50}	Cone	502	410
P_{50}	Rolls	465	746
P_{50}	VSI	534	691
P_{50}	SELFRAG	558	537

The rolls crusher P_{80} and P_{50} particle size results in Table 4-2 and Table 4-3 show the stronger the natural gold grade by size follows a slightly different distribution than the overall particle size distribution (PSD). There is an indication that the gold was not preferentially reduced to fines over gangue and remains in the coarse size fraction. Table 4-2 and Table 4-3 show evidence that the rolls crushing mode product have a higher proportion of gold in coarser particles. Similarly, there is evidence that the SELFRAG also preferentially deports gold into coarser particles, while the cone crusher preferential deports gold into finer particles.

4.2.3 Cumulative grade-by-size analysis

Representative sub-samples of Ballarat CGT gold-bearing sulfide ore underwent comminution by different laboratory-scale fine crushing modes, identified in Figure 4-2. Figure 4-2 these crushing modes as cone crusher, rolls crusher, VSI and SELFRAG mechanisms. Section 3.2 describes that the Ballarat gold-bearing ore had a free-milling mineralogical style. Gold is either liberated gold particles or gold in mineral associations with pyrite, arsenopyrite, or silicates. The charts in Figure 4-2 infer preferential grade deportment as the relative transport of gold, sulfur and mass deportment into size fractions linked to the interaction between a specific ore and crushing mode.

The cone, rolls crusher, and VSI crushing modes achieve rock breakage patterns and mineral liberation by different combinations of impact and compression fragmentation. The SELFRAG technology achieves breakage patterns and liberation by high voltage electrical comminution. It is understood from Chapter 3 that mineral liberation is linked to the interaction between the inherent ore mineralogical and textural characteristics and crushing mode balance between particle body breakage or surface breakage mechanisms. Middlemiss (2004) identified that particle surface breakage increased the degree of liberation in the value or gangue mineral components by distinctive intergranular breakage. Whereas Middlemiss (2004) identified random breakage as associated with particle body breakage and reduced overall liberation during comminution. The relative grade-by-size transport analysis, shown in Figure 4-2, produces grade distribution versus cumulative mass pull relationships for specified breakage modes treating Ballarat gold-bearing sulfide ore. Cumulative percentage passing curve trajectories describe in figure 4-2 grade-by-size relationships.

Different crushing modes have distinct intergranular breakage characteristics that can influence the extent of gangue liberation and, as a result, preferential mass and grade-by-size deportment among broken particles (see Section 2.3). However, the potential breakage from mechanical and electrical comminution modes may not consistently deliver the optimum energy efficiency in the liberation of the gangue or valuable components from host rock mineral assemblages. So, each crushing mode must be evaluated on a specified ore style and compared. The charts in Figure 4-2 suggest variations in mineral liberation by particle size for the various mechanical and electrical comminution modes investigated. Different breakage mechanisms have contributed differently to the ability of the Ballarat gold-bearing ore samples to reject coarse particle gangue and pre-concentrate metal (grade) by particle size, as shown in Figure 4-2.

According to Section 2.3, ore mineral liberation may improve in crushing modes with a dominant phase boundary breakage comminution mechanism, which is typically produced when the loading displacement rate is slow. Section 2.3 identifies that the type of breakage mode associated with particle breakage by a slow compression loading mechanism is associated with the rolls crusher and High Pressure Grinding Rolls (HPGR). The HPGR produces a slow compression rate, with two breakage mechanisms, single-particle compression and bed particle compression, which may increase comminution in some ores (Anticoi et al.,

2019). Comparatively, in the VSI mode, impact fracture dominates in comminution. The rate of application is rapid, and breakage is by instantaneous particle collisions, producing a 'cubic shape' coarse mineral particle with a lower proportion of micron-scale fines (Grigg and Delemontex, 2014). The cone crusher functions as a compressing crusher, with particle breakage through a combination of interparticle or single-particle compression and a higher loading displacement rate. The cone crusher breakage mode, in part, suggests a faster loading displacement rate over a breakage mechanism like a rolls crusher, indicating a greater potential for particle body breakage and subsequentially lower liberation (see Section 2.3). The SELFRAG utilises high voltage pulses to interact with ore properties in the fracture of particles and liberation of minerals, with the electricity and shockwaves interacting with the minerals (Bru et al., 2018). Subsequentially, variances in mineralogical heterogeneity and differences in fine particle dispersion gold or sulfide minerals assemblages in the Ballarat ore may reduce the selectivity of the SELFRAG process in pre-weakening of mineral ores and liberation in some size classes (Bru et al., 2018; Lakshmanan and Gorain, 2019).

Charts A, B, C, and D, as shown in Figure 4-2, describe grade distribution by size for the cone, rolls, VSI, and SELFRAG comminution of the Ballarat ore. These charts show that the gold and sulfur tendency is to preferential transport into the coarser or finer particle sizes. In addition, the shape and extent of metal and sulfur curves relative to the mass deportment response curve suggest the strength of the preferential deportment response by size.

The Ballarat gold-bearing ore A, B, C, and D charts in Figure 4-2 indicate that different crushing mode products have different ore breakage patterns, evident by the variations in the slope and extent of the grade curves and the overall particle distribution curves. These different breakage patterns suggest changes in the preferential distribution of gold and sulfur grade-by-size deportment response within particle size classes. For example, in Figure 4-2 charts, where the grade curve moves above the overall particle distribution curve, the grade preferentially deports into screen passing size particles or finer particles. Conversely, Where the grade curve moves below the overall particle distribution curve, the grade preferentially deports into screen retained size particles or coarser particles. Therefore, there may be an opportunity for gangue rejection or metal pre-concentration within individual size classes, which may have mine operational significance in pre-concentration by size classification.

Figure 4-2 grade by size curves for different crushing modes suggests that the HPGR results produced a higher preferential gold by size-based deportment response, with the gold deporting into the coarse particles more than the sulfide minerals. The VSI results show a weaker tendency for gold to preferential deport into coarse particles at a similar rate to the sulfide minerals. The Cone crusher curves suggest that gold is slowly reduced into finer particle sizes above 0.30 mm during screening. The SELFRAG mode curve indicates a tendency for gold to preferential deportment into the coarser particle sizes above 0.6 mm. The SELFRAG mode minus 0.30 mm data suggests there is evidence that the gold particles are less liberated due to the shape and extent of the gold by mass deportment response curve.

Generally, Figure 4-2 plots suggest that selected crushing mode breakage patterns produce weak gold and sulfur preferential grade by size-based deportment response, offering little opportunity for metal pre-concentration. However, there may be an opportunity for metal pre-concentration within individual size classes through preferential grade by size deportment, which may have operational significance.

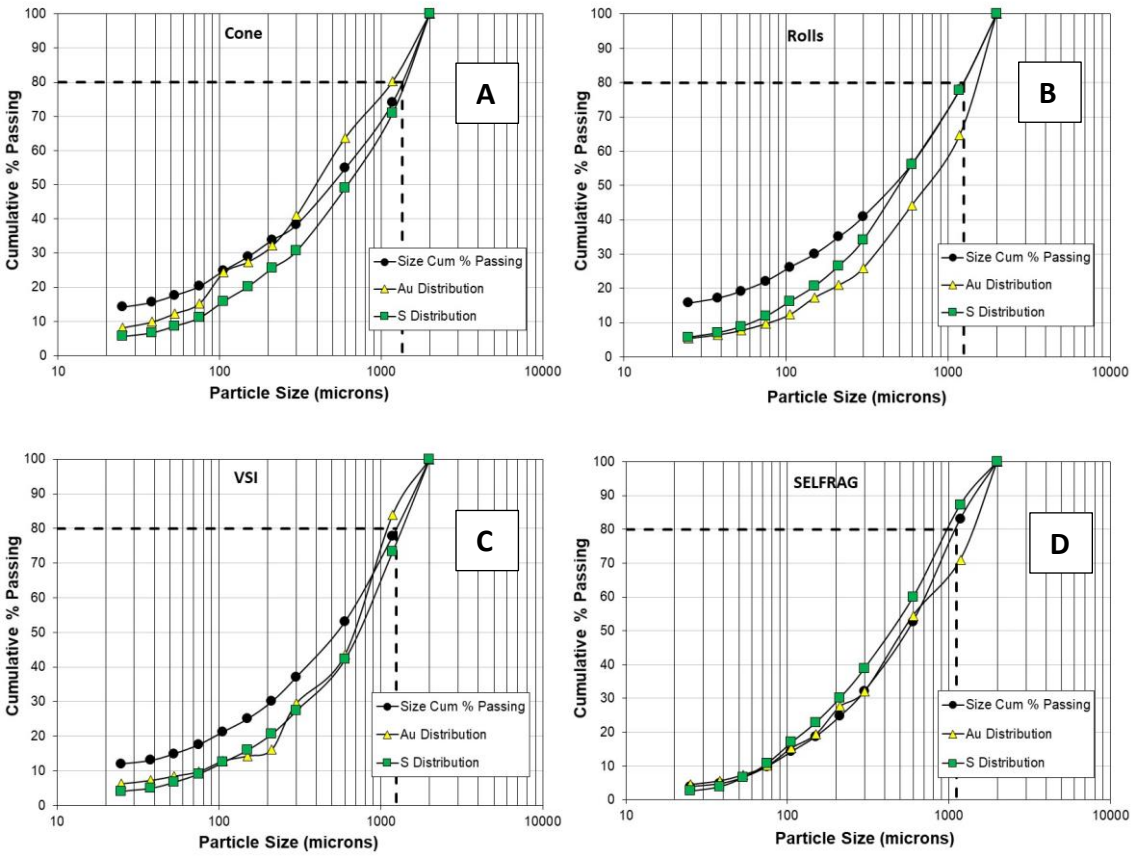

Figure 4-2. Ballarat particle mass, gold and sulfur distributions by size for (A) Cone crusher, (B) Rolls crusher, (C) VSI, and (D) SELFRAG crushing modes

Figure 4-3 A and B charts describe fine crushing mode influences on the sequential separation of gold within size classes. The graphs compare the separation performance of gold within size classes for different crushing modes. Gold grade deportment within individual size classes for selected crushing modes is described in Figure 4-3 A and B charts. Figure 4-3 A and B charts show that gold grade is higher in coarser size classes, above 150 microns. Also, Figure 4-3 B chart shows that crushing mode strongly influences gold content in coarser size classes. Figure 4-3 B shows that both the rolls crusher and SELFRAG modes suggest strong gold deportment into coarser particles between the -2.0/+1.18 mm size range. The VSI -1.18/+0.60 mm particle size range had >40 % of the sample gold content. From an operational perspective, selective separation of size classes by screening may be an effective strategy for metal pre-concentration by size.

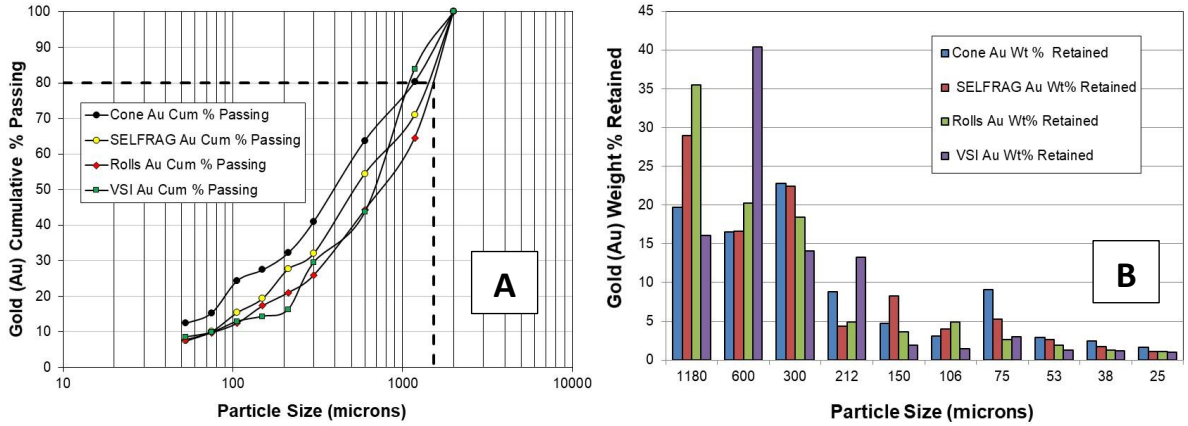

Figure 4-3. Ballarat gold grade-by-size deportment for screen undersize (A) passing sample and screen retained sample (B) responses by crushing mode

Table 4-4 shows different crushing mode product grade deportment by size results for elements associated with sulfur (S) in sulfide minerals. These results describe an elemental grade-by-size-frequency distribution for various crushing mode products produced from Ballarat ore. In gold-bearing sulfide ores, arsenic (As) is typically contained in an arsenic sulfide mineral, like Arsenopyrite is an iron (Fe) arsenic sulfide (FeAsS). Therefore, it is important to understand how arsenic preferential deportment within process separation fractions, where the mineral may contain gold (Marsden and House, 2009). Table 4-4 shows that the distribution and grade of arsenic, iron, and sulfur in the dominant sulfide minerals in the Ballarat ore preferentially deport into coarser particles larger than 300 microns. Comparing results in Figure 4-3 and Table 4-4 shows that the overall gold and arsenic contained in the feed preferentially deport into particle size fractions above 212 microns.

Table 4-4. Frequency distributions of the Ballarat mass and elemental deportment variability within crushed products

Mass and Metal Yield Distributions						
Size Fraction	Cone Crusher			SELFRAG		
(µm)	Arsenic Rec.	Iron Rec.	Sulfur Rec.	Arsenic Rec.	Iron Rec.	Sulfur Rec.
-2000 + 1800	23.7%	20.7%	29.0%	12.5%	14.7%	12.8%
-1800 +600	23.9%	16.2%	21.9%	27.4%	27.1%	27.4%
-600 +300	23.2%	25.1%	18.5%	26.4%	20.8%	21.0%
-300 +212	5.9%	4.4%	5.0%	9.3%	7.8%	8.7%
-212 +150	5.8%	5.0%	5.4%	7.1%	6.5%	7.3%
-150 +106	4.1%	4.0%	4.3%	5.1%	5.0%	5.9%
-106 +75	4.4%	4.6%	4.8%	4.6%	5.2%	6.2%
-75 +53	2.0%	2.7%	2.4%	3.0%	4.2%	4.2%
-53 +38	1.6%	2.4%	2.0%	1.8%	2.7%	2.7%
-38 +25	0.8%	1.5%	1.1%	1.0%	1.4%	1.4%
-25	4.6%	13.5%	5.6%	1.9%	4.6%	2.6%
Mass and Metal Yield Distributions						
Size Fraction	Rolls			VSI		
(µm)	Arsenic Rec.	Iron Rec.	Sulfur Rec.	Arsenic Rec.	Iron Rec.	Sulfur Rec.
-2000 + 1800	20.2%	19.4%	22.4%	19.8%	25.8%	26.8%
-1800 +600	22.3%	19.0%	21.6%	29.8%	30.0%	31.0%
-600 +300	26.5%	20.2%	22.1%	20.3%	9.7%	14.9%
-300 +212	7.8%	6.2%	7.5%	7.9%	6.3%	6.7%
-212 +150	5.9%	5.2%	6.0%	5.7%	4.4%	4.7%
-150 +106	4.0%	3.9%	4.4%	3.9%	3.5%	3.5%
-106 +75	3.9%	4.2%	4.4%	3.6%	3.5%	3.3%
-75 +53	2.3%	3.1%	2.9%	2.5%	2.7%	2.4%
-53 +38	1.4%	2.2%	1.8%	1.8%	2.1%	1.7%
-38 +25	1.1%	1.7%	1.4%	0.9%	1.1%	0.9%
-25	4.7%	14.9%	5.7%	3.9%	10.9%	4.1%

4.2.4 Graphical analysis of gold deportment by size

Comparative response changes for the accumulative gold deportment by mass into screen oversize (O/S) material are shown for crushed Ballarat gold ore by partition lines for different crushing modes in Figure 4-4 chart. These lines are predicted by least squares regression (LSR) modelling equations, described in section 3.9. The position and shape of the lines above or below the chart diagonal line determine whether the gold preferentially concentrates into the screen oversize (O/S) or undersize (U/S) and the line distance from the 45° diagonal line is the strength of concentration. For example, the 45-degree diagonal partition line implies the region of the diagram where gold follows mass transfer across screen sizes with no preferential metal deportment, i.e., 50 % of the mass contains 50 % of the gold. Therefore, the distance of a crushing mode line above or below the diagonal line suggests the preferential gold enrichment response strength into the screen O/S material during comminution. The charted results describe the preferential gold deportment by mass relationship to measure the grade variability across specified GRAT size class intervals investigated.

In Figure 4-4, a Power function (section 3.9, equation 4) technique predicts the lines of best fit for the cone, SELFRAG and Rolls crushing modes. The Gaussian function (section 3.9, equation 5) predicts the VSI crushing mode line of best fit. The selected LSR equations predict the mathematical form of the relationship between accumulative percentage gold versus mass deportment into screen oversize. Lines are determined from the results produced from gravity test work in this study for the laboratory-scale cone crusher, rolls crusher, SELFRAG and VSI mode products, classified by the Ballarat GRAT size separation technique.

Figure 4-4 information indicates that both the cone and SELFRAG crushing modes produce only marginal influence over the gold preferential deportment into the screen O/S (or coarser fraction) particles by size. The particle size distribution evidence in the diagram does not show an improvement in size-by-size grade relative to feed grade (i.e., upgrade ratio) when the coarse fraction is screened out. However, the HPGR and VSI modes show a higher degree of preferential metal by size deportment response, with a stronger gangue rejection into the screen O/S.

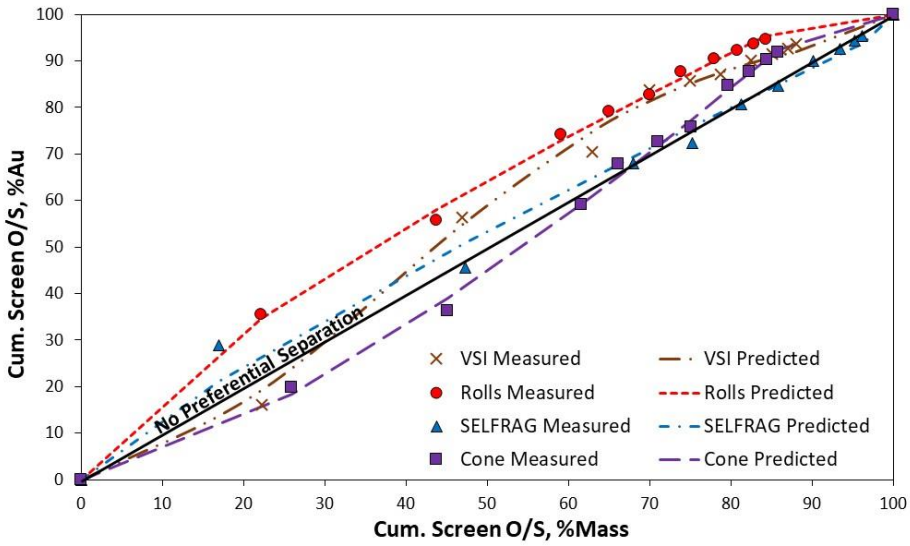

Figure 4-4. Ballarat crushed ore gold grade versus mass yield curves by size for different crushing modes

Table 4-5 shows descriptive statistics that indicate Figure 4-4 gold line of best fit models achieves good agreement between the measured and predicted values, with overall high accuracy. The Ballarat SELFRAG LSR modelling results showed moderate error; this error may be reduced by applying a different LSR equation in modelling. Low ME and RMSE values

indicate low bias and good accuracy, with high R^2 indicating low unexplained variability, suggesting good reliability of the model function predictions.

Table 4-5: Ballarat crushed size class gold by size descriptive statistics

Statistic	Cone	SELFRAG	Rolls	VSI
ME	0.014	0.269	0.001	0.000
RMSE	0.464	1.068	0.329	0.653
R^2	0.995	0.969	0.996	0.992

4.2.5 Ballarat Heavy liquid separation by crushing mode

4.2.5.1 Analysis of float-sink grade separation and recovery

Figure 4-5 shows the Ballarat ore sample HLS sink–float separation float product cumulative weight rejected and contained gold (Au), arsenic (As), iron (Fe) and sulfur (S) grades recovered for the different crushing modes products. Sequential specific gravity (SG) separation float products produced in the range from 3.0 to 2.65 SG provided elemental grade and masses. Interpretation of these Figure 4-5 results indicated that the cone crusher mode showed lower gold recovery into the sink fractions across part of the GRAT density partition range investigated. This moderate recovery is likely the consequence of having a higher proportion of silicate present in composite particles in binary contact with gold. The VSI crushing mode produces the highest mass pull into the sink fractions and is evidence of strong gold and arsenic recoveries into sinks. This evidence suggests that the VSI sink product contains a higher proportion of high-density gold composites particles in binary contact with metal sulfide and silicates. Both the cone and VSI crushing mechanisms produced a higher ratio of gold loss and mass yield to float, suggesting a lower degree of particle liberation. Conversely, the SELFRAG has the lowest portion of gold misclassified in composite particles with silicates, closely followed by the HPGR crushing mode.

Overall, the sink gold recovery into sinks is very high at >80 %, irrespective of the crushing method. The arsenic demonstrated low recovery into the float, suggesting high arsenic sulfide particle liberation, reducing gold loss, where gold is associated with arsenic sulfide particles. The iron recovery into floats is high, indicating a high proportion of low-density iron-containing composite particles.

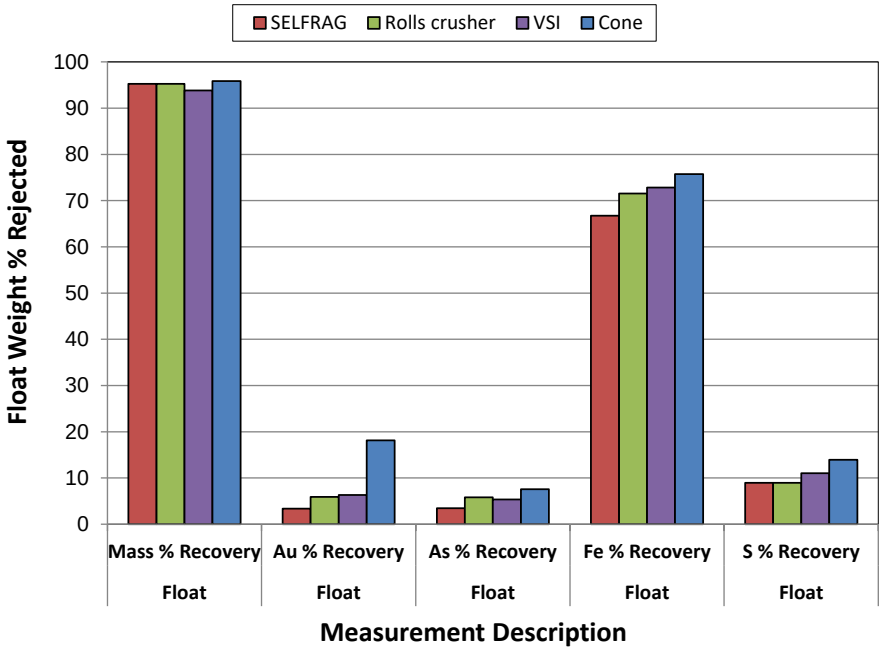

Figure 4-5. Ballarat ore accumulative HLS float mass and grade recovery by crushing mode

Figure 4-6 directly compares Ballarat ore sample HLS cumulative weight percent and gold recovered or accepted into the HLS sink as a function of density and crushing mode. Figure 4-6 analysis excludes minus 0.3-millimetre material.

In Figure 4-6 chart B, the higher the proportion of feed gold contained in the sinks during separation, the closer the gold grade trajectory curve remains to the horizontal plane at or near 100 percent gold acceptance. Consequentially, the degree to which the curve slope decreases from 100% suggests the extent that which gold is lost into the floats as composite or non-liberated particles. In chart A, the mass trajectory curves indicate the combined accumulative mass percentage of higher SG value components and lower SG gangue minerals in the sinks at different specific density fractions. Therefore, a change in the trajectory curve slope ratio suggests a change in the proportion of composite valuable components and lower SG gangue minerals versus liberated particles of higher SG value component material contained in particles within the sinks. Subsequentially, change in the accumulative mass percentage in sinks between density splits of SG 2.65 to SG 3.00 is associated with rejection into floats of metal-rich particles, as lighter gangue-rich composite (non-liberated) particles are removed first. Therefore together, chart A and B, trajectory curves provide information on the preferential separation between metal-rich and gangue particles in specific density

fractions, linked to the proportion of composites and liberated particles present after comminution.

It is observed that the mass in chart 'A' and gold deportment curves in chart 'B' are similar for the rolls crusher and SELFRAG over part of the HLS density partition range examined. Similar trend lines within chart 'B' suggest a similar degree of liberation. Therefore, gangue liberation is comparable between the rolls crusher and SELFRAG modes. The SELFRAG and rolls crusher produce a similar, lower proportion of composite or incompletely liberated gangue particles than the cone and VSI products. Consequently, the rolls crusher and SELFRAG modes produce a higher degree of liberation of silicates, demonstrated by a lower gold loss at high mass pull to the float. Conversely, the cone crushing mode provides the weakest recovery of gold into sink fractions, indicating a relatively higher proportion of silicate in mineral associations with gold particles. Experimental evidence suggests that the propensity for gold by density deportment into the sink fractions decreases in the following order of breakage mechanism applied in comminution mode: SELFRAG>Rolls>VSI>Cone crusher.

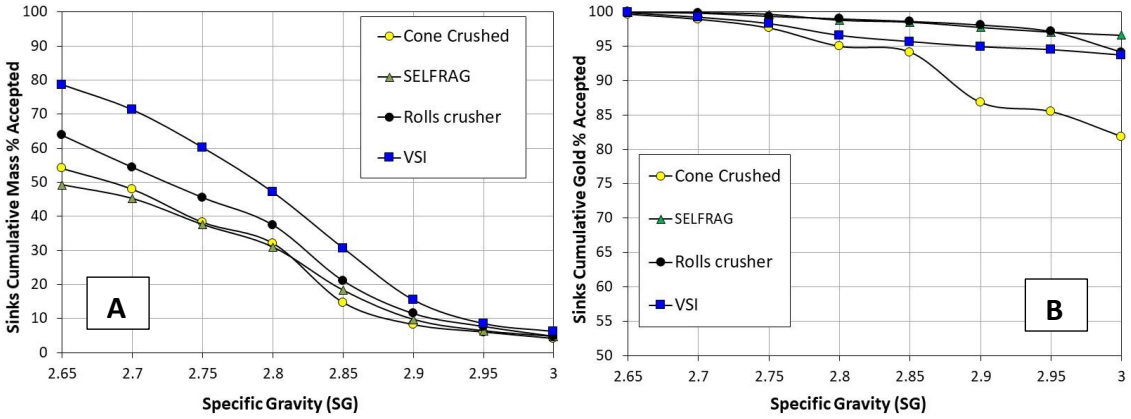

Figure 4-6. (A) Mass and (B) gold percentage accepted into sink versus specific gravity by crushing mode

Figure 4-7 describes gold deportment into the sink as grade-recovery curves produced by both mechanical and SELFRAG crushing modes. The curves support the opportunity indicated by Figure 4-5 and Figure 4-6 for significant gold pre-concentration by coarse gangue mass rejection. The relationship between the curves suggests that both the rolls crusher and SELFRAG modes produce a superior and similar performance on the Ballarat gold-bearing ore examined.

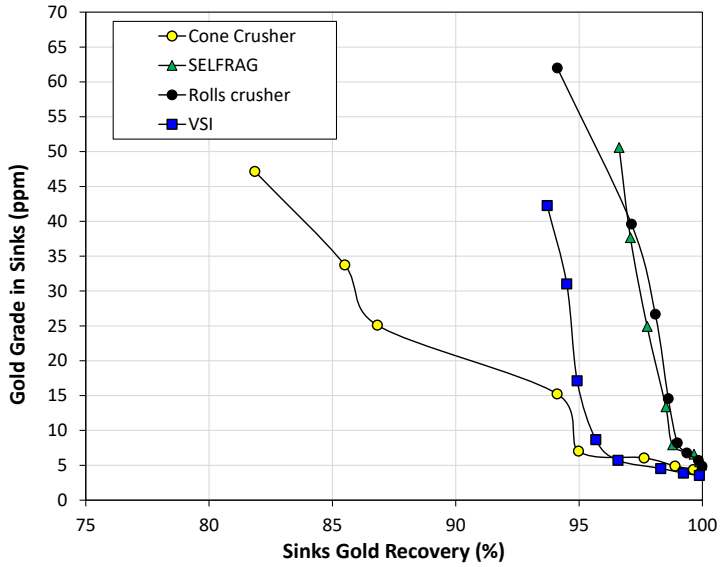

Figure 4-7. Gold grade versus recovery into sinks by crushing mode (excluding minus 0.30 mm material)

4.2.5.2 Gold deportment by size and density surface charts

Figure 4-8 and Figure 4-9 show the crushed Ballarat gold grade and distribution across the different sizes and SG fractions. The grade surface chart suggests that the cone crusher produces a higher proportion of composite particles, with a lower gold grade than the other crushing modes. Cone crusher data suggests the garnet is usually spread across the entire size spectrum below two millimetres, with some preferential deportment to the coarse particles. Conversely, the SELFRAG and rolls crusher grade and recovery plots indicate a higher proportion of coarse, highly liberated, gold-containing particles, with a high gold grade, between 600 to 1800 microns. Figure 4-8 and Figure 4-9 charts indicate that the VSI has a relatively higher comparative potential to pre-concentrate gold by size separation and recovery in a size class of around 600 microns. Consequently, the cone crushing mode demonstrates a lower potential for selective pre-concentration by size and density classification. Correspondingly, the rolls crusher, SELFRAG and VSI modes have a comparatively higher potential to pre-concentrate gold, with preferential deportment to the coarse particles.

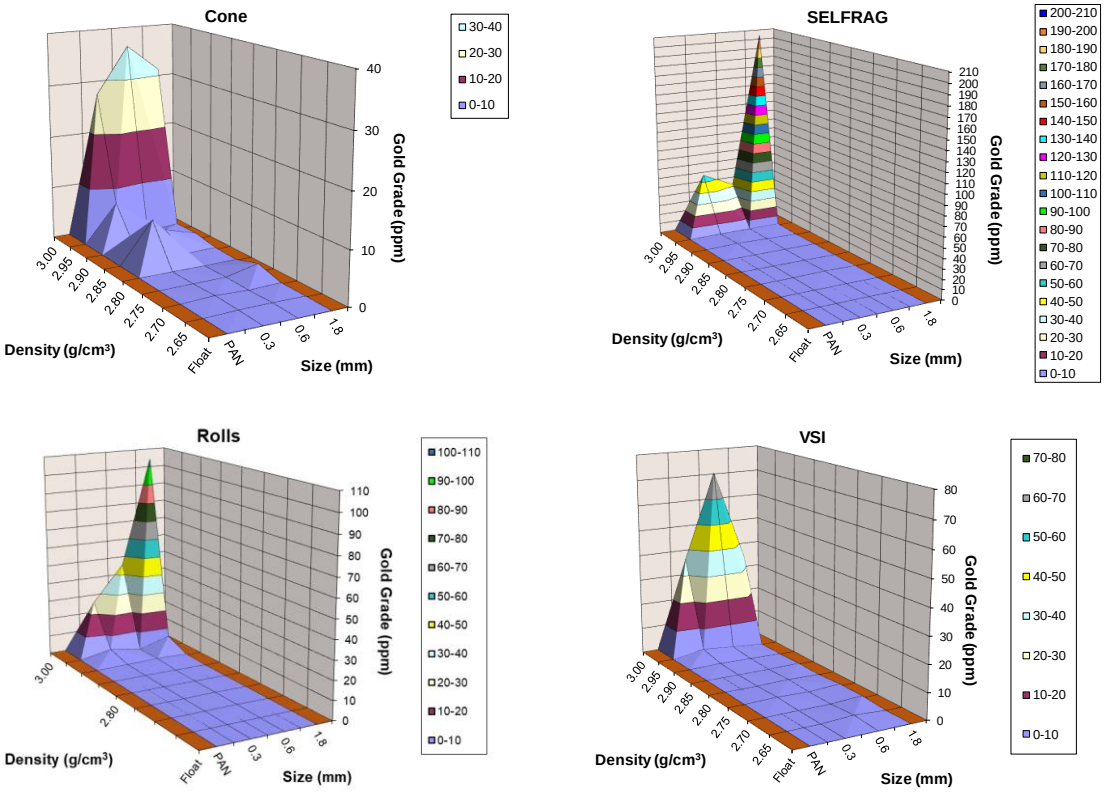

Figure 4-8. Ballarat ore gold grade across SG and size by crushing mode (Bode et al., 2019)

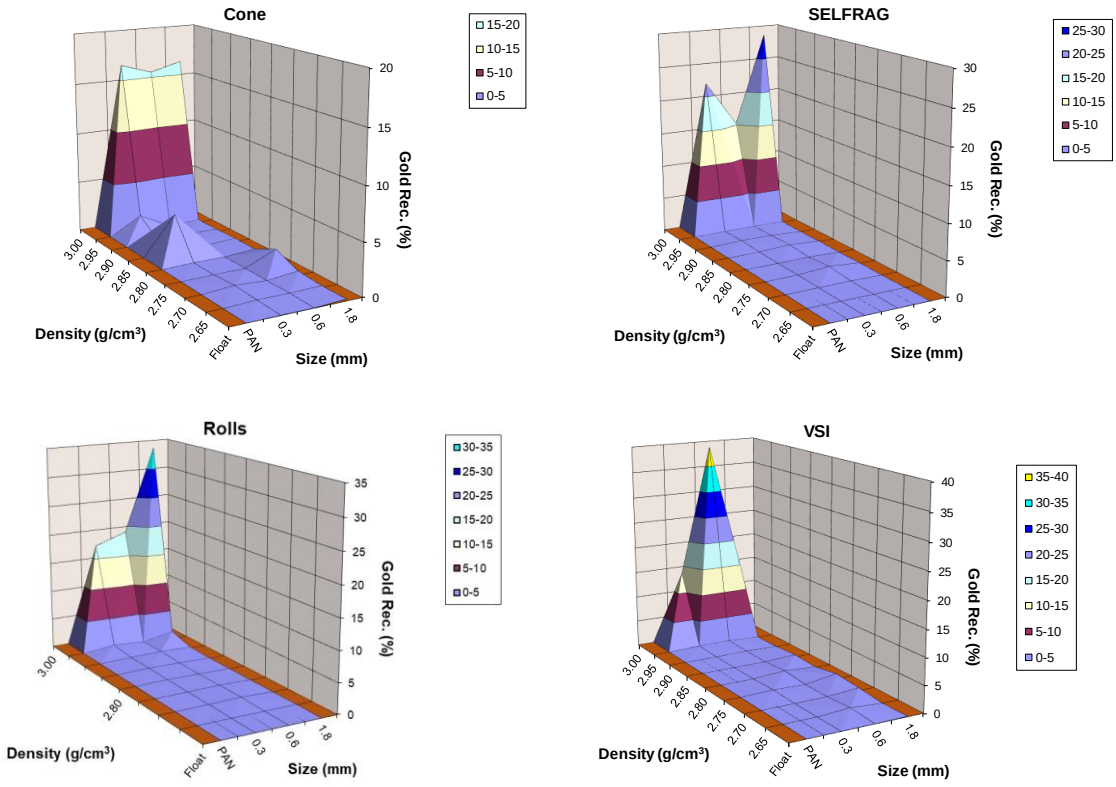

Figure 4-9. Ballarat ore gold recovery across SG and size by crushing mode (Bode et al., 2019)

4.2.5.3 Coarse particle density pre-concentration separation response

Coarse particle gangue rejection can achieve higher metal unit productivity by reducing the proportion of waste or gangue rock subjected to downstream mineral processing energy-intensive micron-scale comminution. CPGR separation under GRAT HLS conditions characterises the elemental deportment response into float products for each density fraction and constitutes a metal loss versus mass pull relationship.

The comparative response produced by different crushing modes for the relationship between metal recovery and mass pull percentage is characterised in Figure 4-10 for Ballarat ore GRAT density separation operations. The Ballarat ore GRAT density separation results indicate strong potential for coarse gangue rejection and pre-concentration by recovering a large proportion of gold in the feed into the product sink fraction. The SELFRAG and rolls crusher modes suggest the best potential for gold pre-concentration, and the VSI and cone crusher has a lower potential. However, overall, all crushing modes show good gold pre-concentration potential.

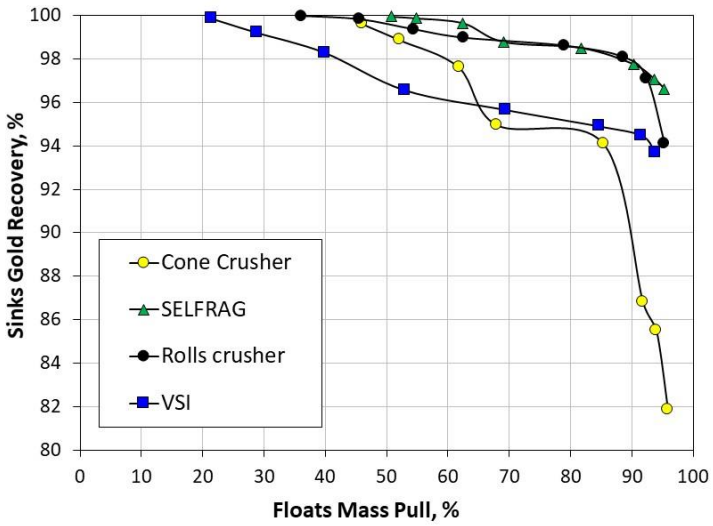

Figure 4-10. Ballarat HLS float mass pull versus gold recovery to concentrate by crushing mode (excluding minus 0.30 mm material)

Similarly, to Figure 4-10, Figure 4-11 provides comparative response evidence of gold and gangue coarse particle liberation by the extent of gold deportment into the HLS float via gold loss or deportment to float. Figure 4-11 shows how the crusher type selection may exploit the ore natural grade heterogeneity to liberate coarse particulate gangue and allow density-based rejection. In Figure 4-11, the rolls crusher and SELFRAG modes demonstrate comparable cumulative mass rejection and gold loss to the heavy liquid float for a large

portion of the same HLS float mass pull percentage range. Conversely, the cone crushing and VSI crushing mechanisms produce a higher proportion of the gold loss at an earlier accumulative mass pull rejected into the float, suggesting a higher relative proportion of low-grade composite particles than either the SELFRAG or rolls crusher modes. The cone crushing mode produced the highest gold loss to float relative to accumulative mass pull. The shape and extent of the rolls crusher and SELFRAG crushing mode curves indicate that good density-based separation is achievable, evidenced by the low gold loss with high cumulative mass pull into the HLS float. In Figure 4-11, the rolls crusher and SELFRAG crushing modes show that approximately 2 % gold loss at 90 % mass rejection into the float is possible for the Ballarat gold-bearing ore. In comparison, 5 % and 10 % gold loss to float for the VSI and cone crushing modes, respectively, were observed.

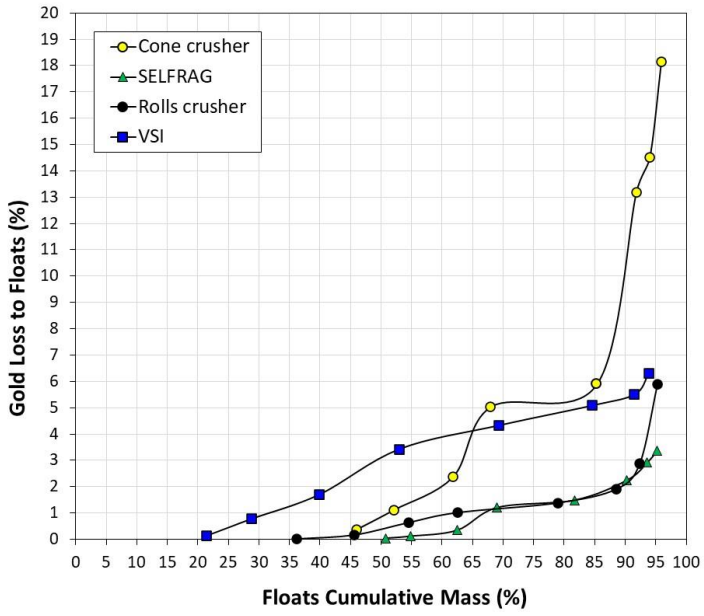

Figure 4-11. Percentage gold loss in float versus ore mass rejected into float by crushing mode (excluding minus 0.30 mm material) (adapted from McGrath et al., 2018)

Figure 4-12 shows charted results of LSR modelling applied to the GRAT float recovery and mass pull data, from Ballarat ore crushed products, for comparison of the magnitude of variability for CPGR and metal pre-concentration response. Two model function types predict the lines of best fit; these were exponential and Gaussian functions. The exponential function (section 3.9, equation 7) LSR technique predicted lines of best fit for the cone crusher and a second exponential function for the SELFRAG (section 3.9, equation 8). Both the rolls crusher

and the VSI model functions had a line of best fit determined by a Gaussian function (section 3.9, equation 6).

It is observed in Figure 4-12 that the rolls crusher curve is comparable to that of SELFRAG over part of the GRAT density partition range investigated. The rolls crusher and SELFRAG curves suggest a similar degree of silicate liberation from gold particles, with a strong CPGR potential during gravity separation. The shape and extent of the rolls crusher and SELFRAG crushing mode curves indicate that good density-based CPGR separation is achievable, evidenced by the low gold loss with high cumulative weight (CW) pull into the HLS float. By comparison, the cone crusher, and to a much lesser extent, the VSI crushing mode, shows a higher proportion of gold loss into the float, increasing CW pulls. Thereby, these crushers have a subsequently poorer CPGR response.

Figure 4-12 suggests that the VSI mode produces a higher percentage of incompletely liberated or composite sulfide and gold-containing particles. The assumption is that the cone and VSI crushing modes produce a higher proportion of low-grade gold composite particles than either the SELFRAG or HPGR crushed products, based on comparative response evidence shown in Figure 4-12. Above floats, CW mass pull of approximately 65 percent, the cone crusher material exhibits gold losses to float that significantly exceeds those of the SELFRAG, HPGR, and, to a lesser extent, VSI. The cone mode predicted curve flattens out early, extending gold losses to float and indicating a higher portion of gold misclassified in composite particles. The steep VSI model curve suggests a higher proportion of gold composite particles spread from low to high grade than contained in the SELFRAG, rolls crusher or cone crusher products. The SELFRAG and rolls crusher show the steepest curves, suggesting the lowest proportion of gold composite particles.

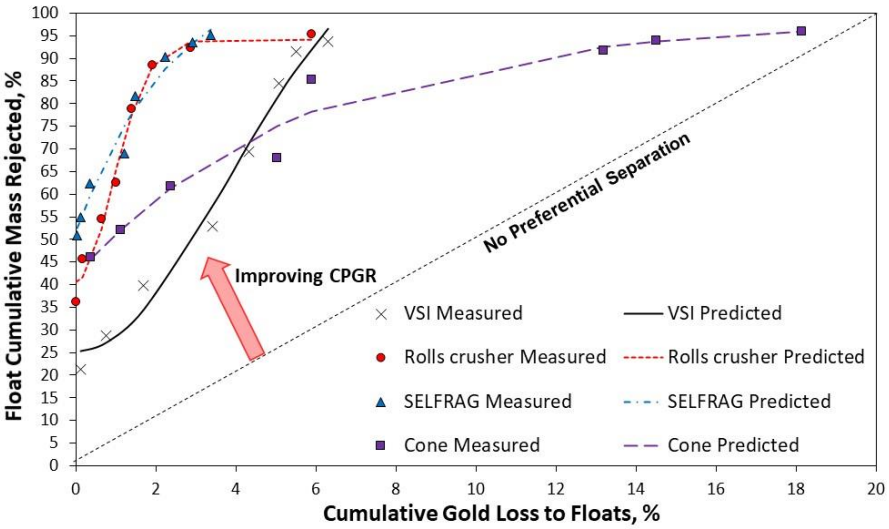

Figure 4-12. Ballarat ore model fitted lines for HLS float gold loss versus cumulative mass rejection by crushing mode (excluding minus 0.30 mm material) (Bode et al., 2019)

The statically quality of Figure 4-12 LSR fitted curves produced from the GRAT density separation data on Ballarat crushed ore products is shown in Table 4-6. The results shown in this table indicate the good strength of fit for the developed models. In addition, the ME and RMSE correlation coefficients suggest that the models developed can estimate the relationship between the gold percentage loss into floats versus mass pull to float response.

Table 4-6: Descriptive statistics for Ballarat ore HLS float gold loss versus mass pull model fitted lines by crushing mode

Statistic	Cone	SELFRAG	Rolls	VSI
ME	0.000002	0.000051	0.000029	-0.000009
RMSE	1.257	0.998	0.933	1.259
R^2	0.9550	0.9641	0.9807	0.9790

4.3 Cadia ore size and density classification analysis

4.3.1 Background

Representative sub-samples of Cadia CVO gold-bearing sulfide ore were crushed by laboratory scale cone crusher, HPGR, SELFRAG and VSI, modes to produce materials for the GRAT process. The results of this analysis were assessed for changes in the propensity for the fragmented ore to preferentially concentrate gold and copper into the specific size and density fractions after breakage. Ore samples were crushed to a particle size of -4.75 mm. The minus 0.3 mm particles were removed from crushed material to reduce the risk of misclassification during heavy liquid separation (HLS) sink–float processes. The GRAT method

classifies particles by size and heavy liquid specific gravity (SG) segregation processes into multiple fractions. Variations in the GRAT classification experimental results. The changes are a function of the interaction between a gold-bearing sulfide ore type, fine crushing mode, and a gravity separation scheme.

4.3.2 Particle size distribution by Rosin-Rammler modelling technique

Comparing the PSD of the Cadia ore crushing mode products, shown in Figure 4-13, the most significant difference in the fragmentation breakage patterns is between the SELFRAG and the mechanical modes, indicated by the observed difference in their respective PSD's. Similarly, the HPGR crusher and VSI and cone crushing modes show differences in their respective PSD's. Figure 4-13 curves suggest that the HPGR crusher produces a finer PSD across the size classes investigated compared to other crushing modes. There is evidence that the SELFRAG provides a coarser PSD across all size classes compared to different crushing modes. The curves in Figure 4-13 suggest that the mechanical breakage pattern produced in Cadia ore by the VSI and cone crushing modes are similar.

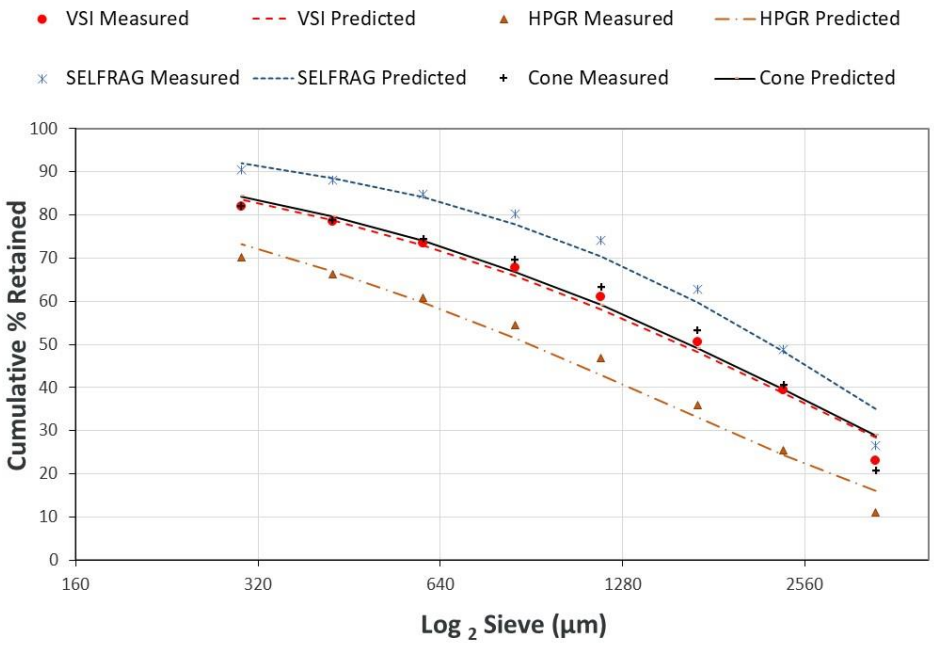

Figure 4-13. Cadia ore mass distribution for different size fractions by crushing mode

Table 4-7 shows statistical quality information on the goodness-of-fit statistical measures between the Rosin-Rammler (RR) distribution model predicted values and the Cadia copper-gold ore crushing mode measured data. The Cadia ME results indicate a slightly higher bias in the crushing mode measured data. The RMSE values suggest that little spread exists in the

errors of the Cadia model predictions, therefore good overall RR model “precision" for the different crushing modes. However, as a rule, RMSE values between 0.2 and 0.5 show that a model can relatively predict the data accurately. The RR results suggest moderate prediction errors for each crushing mode, with the VSI showing the best accuracy and the cone crusher the lowest. Good agreement between model predictions and measured results is supported by good correlation coefficients R^2 values for the Cadia crushing mode results. Table 4-7 demonstrates a generally good agreement between the measured and Rosin-Rammler modelled predicted values, with reasonable accuracy.

Table 4-7. Cadia crushing mode Rosin-Rammler distribution descriptive statistics

Statistic	Cone	SELFRAG	HPGR	VSI
ME	3.004	2.612	2.649	1.925
RMSE	1.353	1.286	1.071	0.859
R^2	0.9741	0.9754	0.9869	0.9893

4.3.2.1 Gold and copper deportment by size analysis

Mineral liberation is linked to the interaction between the inherent ore mineralogical and textural characteristics. The crushing mode's distinctive intergranular breakage influences the balance of particle body breakage or surface breakage mechanisms, according to Chapter 3 and sections 2.3 and 4.2.3. In comparison, particle surface breakage increased the degree of liberation, and particle body breakage was associated with a decreased overall liberation during comminution. The relative grade-by-size transport trajectory curves, shown in Figure 4-14, represent grade distribution versus cumulative mass pull relationships for specified breakage modes treating Caida gold-bearing sulfide ore.

Figure 4-14 charts A, B, C, and D describe grade distribution by size for the cone, HPGR, VSI, and SELFRAG comminution of the Cadia ore. These charts show that the gold, copper, and sulfur tendency is to preferential transport into either the coarser or finer particle sizes. The shape and extent of metal and sulfur curves relative to the mass deportment response curve suggest the strength of the preferential deportment response by size. Where the grade curve moves above the overall particle distribution curve, the grade preferentially deports into screen passing size particles or finer particles. Conversely, Where the grade curve moves below the overall particle distribution curve, the grade preferentially deports into screen retained size particles or coarser particles. Therefore, there may be an opportunity for gangue

rejection or metal pre-concentration within individual size classes through preferential grade-by-size deportment, which may have mine operational significance in pre-concentration by size classification.

Figure 4-14 shows the comparative response of the accumulative gold, copper, and sulfur grade distributions into the screen undersize for specified size fractions by different crushing mode test results on Cadia gold-bearing ore. The variations in the slope and extent of the distribution curves, concerning the overall particle distribution curve, suggest changes in preferential grade deportment by size, linked to differences in breakage patterns during comminution. There is evidence that the HPGR and SELFRAG breakage modes have a stronger preferential deportment response for gold, copper, and sulfide particles into fine-grain sizes than the other crushing modes. As a result, the SELFRAG product results indicate that the mode produces more gold-bearing mineral liberation in fine particles due to more efficient preferential intergranular breakage, with a higher proportion of metal and sulfides deporting into finer particles than the other modes. Conversely, the cone crusher product deportment response curve suggests a lower strength in the metal and sulfide preferential deportment response by size. Figure 4-14 shows the HPGR comminution product produces a stronger preferential deportment response for gold, copper and sulfide particles into coarser particles than observed for the cone, SELFRAG, and VSI mode products. The gold industry understands that coarser particles in feed can improve gravity classification, benefiting overall metal separation performance.

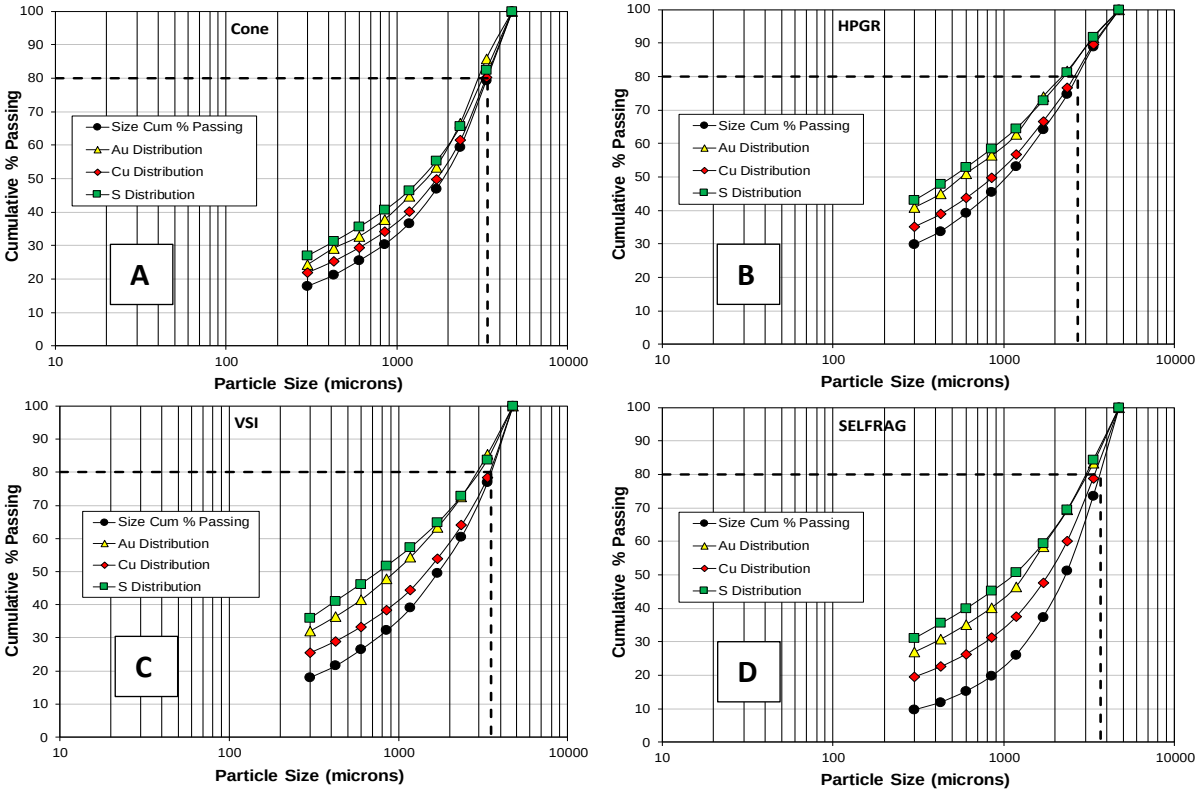

Figure 4-14. Cadia crushing mode particle gold, copper, and sulfur distributions by size for (A) Cone crusher, (B) HPGR, (C) VSI, and (D) SELFRAG crushing modes

Table 4-8 and Table 4-9 show the cumulative 80 % and 50 % material passing particle sizes for mass, gold, and copper, respectively. Also, Table 4-8 and Table 4-9 show a modest preferential reduction of gold into finer particle sizes below 0.30 mm for the SELFRAG, VSI and HPGR modes. However, a weaker gold by size deportment into fines is demonstrated during cone crusher comminution. Similarly, the copper mineral is reduced to fines on crushing by the various modes but has a lower deportment tendency in the HPGR product.

Table 4-8: Cadia crushed ore 80 % passing size for size, gold and copper distributions by crushing mode

Size (µm)	Crushing Mode	PSD (µm)	Au (µm)	Cu (µm)
P_{80}	Cone	3392	3038	3335
P_{80}	HPGR	2710	2196	2601
P_{80}	VSI	3534	2908	3451
P_{80}	SELFRAG	3688	3098	3417

Table 4-9: Cadia crushed ore 50 % passing size for size, gold and copper distributions by crushing mode

Size (µm)	Crushing Mode	PSD (µm)	Au (µm)	Cu (µm)
P_{50}	Cone	1862	1484	1715
P_{50}	HPGR	1028	568	862
P_{50}	VSI	1725	954	1453
P_{50}	SELFRAG	2305	1324	1818

4.3.3 Cumulative grade-by-size analysis

Figure 4-15 A and B describe comparative responses for the influence on Cadia ore of specific crushing mode breakage on preferential gold deportment between screen size O/S and U/S fractions. Figure 4-15 A shows that, when compared to the other crushing modes, the HPGR mode appears to have a slight comparative advantage in producing a finer, higher grade gold U/S product. From the size fractions result shown in Figure 4-15 B, it is observed that the cone crusher produces a higher gold deportment within the minus 3.35 mm to plus 1.70 mm size range compared to other crushing modes. The cone crusher grade by size metal deportment results may aid selective gravity separation operations benefited by separating coarser particles.

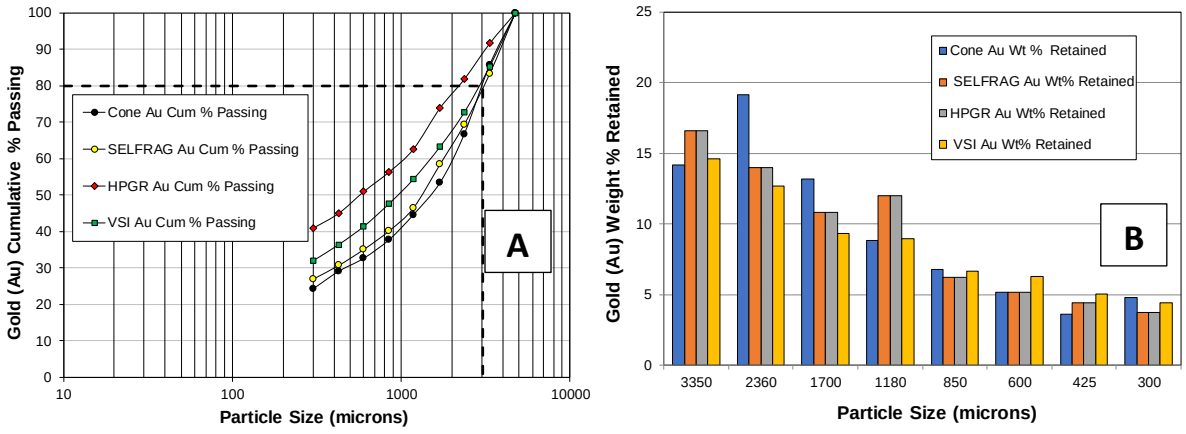

Figure 4-15. Cadia gold grade-by-size deportment for screen undersize (A) passing and screen retained (B) responses by crushing mode

Investigation of fine crushing mode influences on the sequential separation of copper within size classes is described in Figure 4-16 A and B comparative response charts for Cadia ore. Figure 4-16 A chart results suggest that the HPGR crushing mode product produces a high proportion of copper passing to fines by size-based separation. In Figure 4-16 B chart, the VSI

crushing mode results suggest a higher proportion of copper in the plus-size 3350 microns fraction. Figure 4-16 B chart shows the HPGR and SELFRAG both have a strong tendency for copper to report into the screen O/S down to approximately 1180 microns, the cone crusher producing similar results. Overall, Figure 4-16 results suggest different crushing mode products produce moderate preferential grade deportment by size responses.

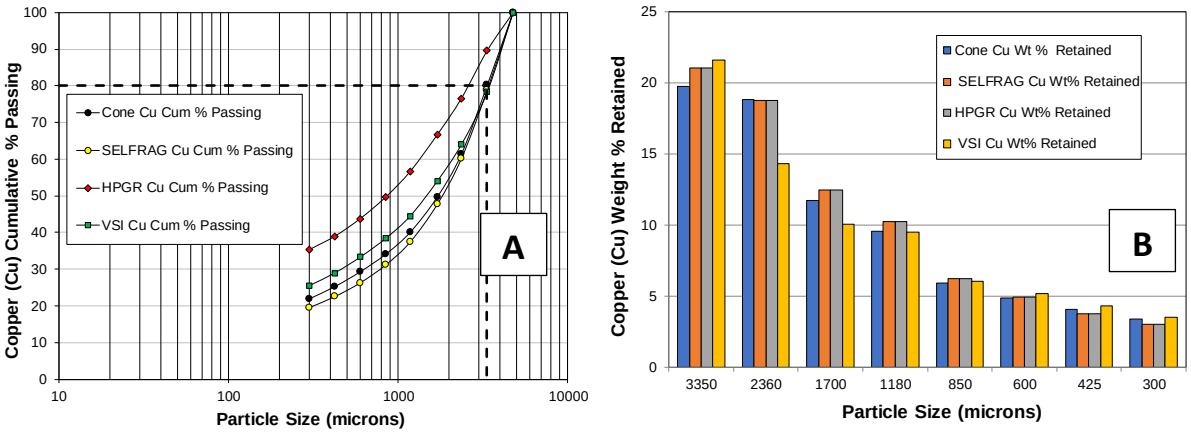

Figure 4-16. Cadia copper grade-by-size-based deportment for screen undersize (A) passing and screen retained (B) responses by crushing mode

Table 4-10 shows that for the Cadia copper-gold ore sample, the SELFRAG mode of ore breakage produces the best potential to concentrate molybdenum and iron grade by size into coarser particles larger than 1700 microns, followed by the Cone crusher mode of ore breakage. Other crushing modes show weaker evidence for the preferential concentration of molybdenum in the minus 0.30 mm material fraction is weaker. Iron by size deportment shows a similar transfer relationship with molybdenum deportment within size fractions but has a weaker pre-concentration tendency.

Table 4-10. Frequency distributions of the Cadia mass and elemental deportment variability within the crushed product

Mass and Metal Yield Distributions						
Size Fraction	Cone Crusher			SELFRAG		
(µm)	Molybdenum Rec.	Iron Rec.	Sulfur Rec.	Molybdenum Rec.	Iron Rec.	Sulfur Rec.
-4750 +3350	18.9%	19.9%	17.5%	21.2%	24.8%	15.6%
-3350 +2360	17.5%	19.4%	16.8%	24.8%	20.8%	14.8%
-2360 +1700	12.3%	12.2%	10.5%	11.2%	13.3%	10.1%
-1700 +1180	11.4%	9.9%	8.7%	9.5%	10.8%	8.8%
-1180 +850	6.5%	6.1%	5.8%	5.2%	6.0%	5.5%
-850 +600	4.5%	4.9%	5.1%	3.7%	4.5%	5.2%
-600 +425	3.5%	4.1%	4.4%	2.7%	3.3%	4.5%
-425 +300	2.5%	3.3%	4.1%	1.5%	2.5%	4.3%
-300	22.8%	20.1%	27.1%	20.1%	14.0%	31.1%
Size Fraction	HPGR			VSI		
(µm)	Molybdenum Rec.	Iron Rec.	Sulfur Rec.	Molybdenum Rec.	Iron Rec.	Sulfur Rec.
-4750 +3350	11.1%	10.2%	8.1%	22.9%	22.9%	16.2%
-3350 +2360	14.4%	13.3%	10.6%	13.3%	15.4%	10.9%
-2360 +1700	12.1%	9.8%	8.5%	8.9%	10.3%	8.2%
-1700 +1180	9.8%	10.0%	8.3%	8.2%	9.7%	7.4%
-1180 +850	7.3%	7.0%	6.0%	5.2%	6.5%	5.6%
-850 +600	5.2%	5.9%	5.7%	4.8%	5.5%	5.5%
-600 +425	4.0%	4.9%	5.1%	3.8%	4.6%	5.1%
-425 +300	3.1%	3.6%	4.7%	2.4%	3.7%	5.2%
-300	33.0%	35.1%	43.1%	30.4%	21.5%	35.9%

4.3.4 Graphical analysis of gold and copper deportment by size

Comparative response of the accumulative gold and copper deportment by mass into screen oversize (O/S) material is shown for crushed Cadia gold-bearing ore by partition lines for different crushing modes in Figure 4-17 and Figure 4-18 charts, respectively. These lines are predicted by least squares regression (LSR) modelling equations, described in section 3.9. The position and shape of the partition lines, above or below the diagonal diagram line, determine whether the metal preferentially concentrates into either the screen oversize (O/S) or undersize (U/S) and the strength of concentration. For example, the chart 45° response line indicates the region of the diagram where metal follows mass transfer across screen sizes with no preferential metal deportment, i.e., 50 % of the mass contains 50 % of the gold. Therefore, the distance of a crushing mode line above the diagonal line suggests the preferential metal enrichment response strength into the screen O/S or coarse particles. Conversely, the distance of a crushing mode line below the diagonal line indicates the preferential metal enrichment response strength into the screen U/S or fines.

The charted results describe the preferential metal deportment by mass relationship as a measure of the grade variability across specified GRAT size class intervals investigated. The LSR modelling used the power function (section 3.9, equation 2) LSR technique to predict lines

of best fit for the cone crusher, SELFRAG, HPGR crusher and VSI crushing modes experimental data.

The results shown in Figure 4-17 indicate the gold preferentially reported into the fine fraction for all crush mode products studied by the GRAT size classification. The SELFRAG mode produces the strongest gold deportment tendency into fines, followed by the VSI crusher, HPGR, and cone crusher in the order of deportment strength.

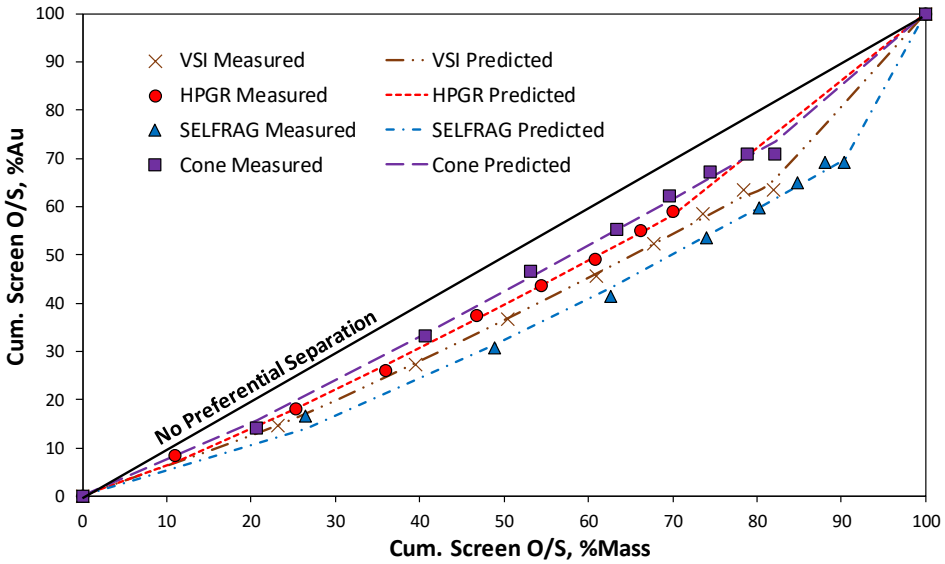

Figure 4-17. Cadia ore size-by-size gold grade versus mass yield curves by crushing mode

Table 4-11 indicates that Cadia Figure 4-17 gold lines of best fit models achieve good agreement between the measured and predicted values, with overall high accuracy. In addition, low ME and RMSE values indicate low bias and good accuracy, with high R^2 showing low unexplained variability, suggesting good reliability of the model function predictions.

Table 4-11: Cadia crush mode gold by size descriptive statistics

Statistic	Cone	SELFRAG	HPGR	VSI
ME	-0.077	0.098	0.076	0.000
RMSE	0.420	0.416	0.230	0.653
R^2	0.995	0.995	0.998	0.992

The copper curves shown in Figure 4-18 were produced by a power model function (section 3.9, equation 2) LSR technique to predict lines of best fit to the cone, SELFRAG, HPGR, and VSI crushing mode observed data. Figure 4-18 predicted that best fit lines describe copper deportment by size. The lines of best fit suggest minimal opportunity to exploit a size-based

preferential separation for copper across the size intervals investigated. The strongest copper deportment tendency into fines is from the SELFRAG product and followed to a lesser extent in order of deportment tendency reduction by the VSI, HPGR and cone crusher.

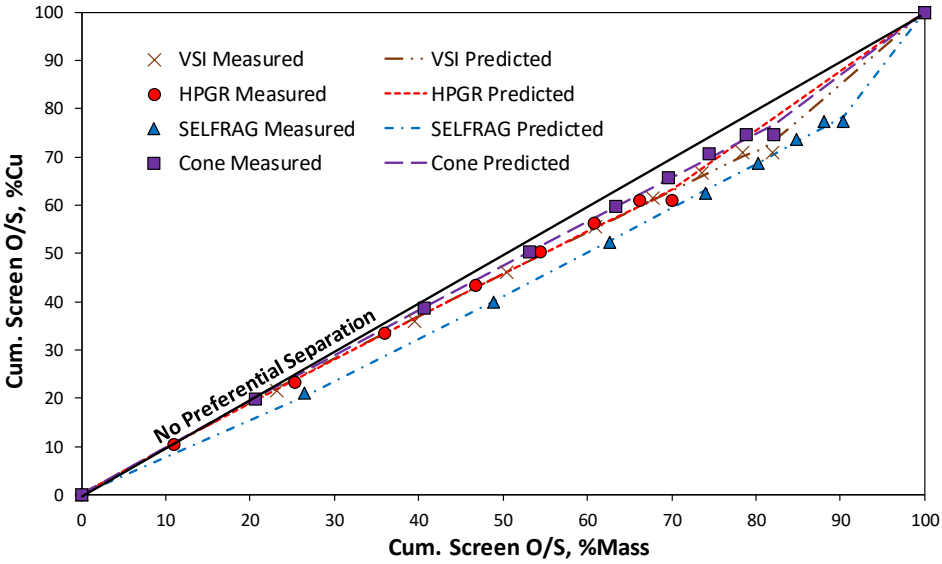

Figure 4-18. Size-by-size copper grade versus mass yield curves for Cadia ore by crushing mode

The descriptive statistics, shown in Table 4-12, indicate that Cadia Figure 4-18 copper lines of best fit models achieve good agreement between the measured and predicted values, with overall high accuracy. In addition, low ME and RMSE values indicate low bias and good accuracy, with high R^2 showing low unexplained variability, suggesting good reliability of the model function predictions.

Table 4-12: Cadia crush mode copper by size descriptive statistics

Statistic	Cone	SELFRAG	HPGR	VSI
ME	-0.018	0.016	-0.040	0.000
RMSE	0.276	0.200	0.315	0.653
R^2	0.998	0.999	0.997	0.992

4.3.5 Heavy liquid separation by crushing mode

4.3.5.1 Analysis of float-sink grade separation and recovery

Figure 4-19 shows the Cadia ore sequential HLS sink–float results. These results report cumulative float product gold (Au), copper (Cu), molybdenum (Mo), iron (Fe), and sulfur (S) content and the mass recovered in combined separation products in the SG separation range

between 2.75 to 2.55, for each crushing mode. In the test work methodology, an upper splitting density of SG 2.75 was selected in this analysis as it produced the most significant relative difference in separation performance to compare the crushing mode gangue liberation potential.

The highest relative gold and copper recoveries occurred in the float products for the SELFRAG and VSI crush modes. These float products suggest a higher proportion of composite particles in crushed produced after rock breakage, relative to the other crushing modes investigated. Molybdenum demonstrated relatively high recovery loss in the SELFRAG, HPGR, and VSI mode float products, indicating that the molybdenum sulfide particles were poorly liberated. Similarly, the iron recovery into SELFRAG, HPGR, and VSI float products is relatively high, suggesting a high proportion of low-grade iron-containing composite particles. The cone crusher product offers the lowest proportion of selected elemental losses in composite particles in the float, indicating the best relative separation performance.

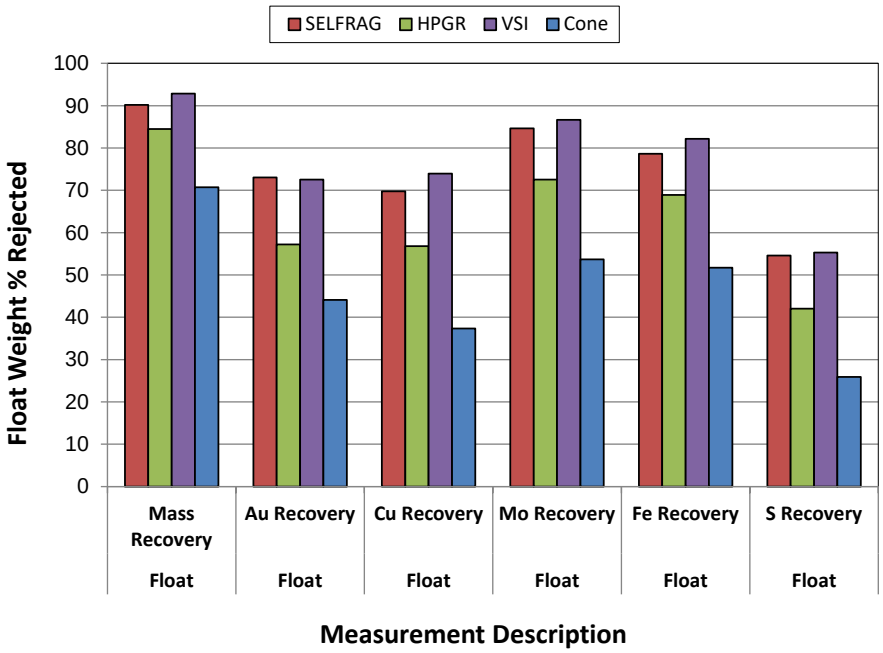

Figure 4-19. Cadia crushed product heavy liquid float recovery and mass pull at SG 2.75 by crushing mode

Figure 4-20 directly compares Cadia ore sample HLS cumulative mass, gold and copper recovered, or proportion of metal accepted into the HLS sinks fractions as a function of density separation and crushing mode. The mass in chart 'A' and the gold and copper deportment curves in charts 'B' and 'C' are similar for the SELFRAG, and VSI over part of the HLS density partition range examined. Similar trend lines suggest that these modes produce

a similar degree of liberation. However, the extent of the mass, gold and copper curves demonstrate low to moderate preferential gold by density deportment response, compared to the other breakage modes shown in Figure 4-20. Conversely, the SELFRAG crushing mode produces the lowest recovery of gold and copper into the sink fractions, indicating a relatively higher proportion of gangue minerals associated with gold.

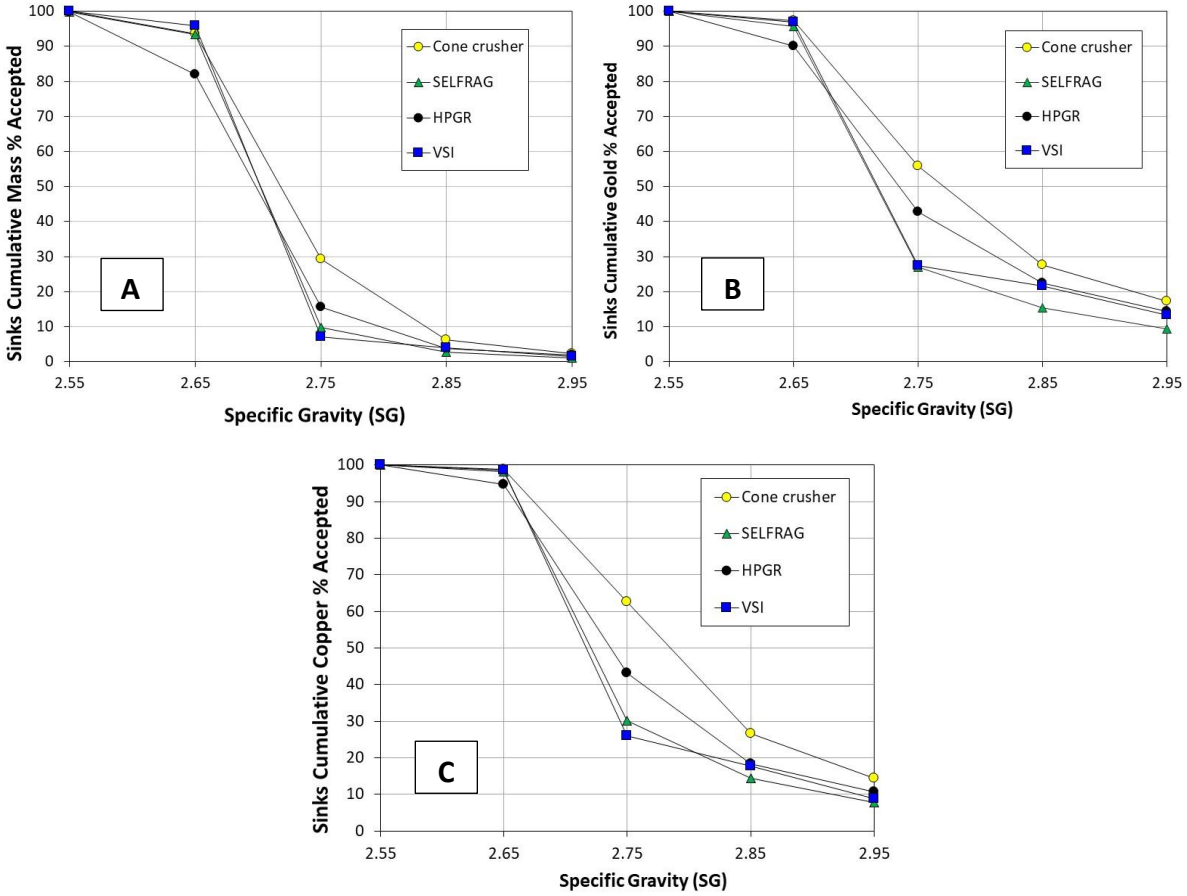

Figure 4-20. (A) Mass, (B) gold and (C) copper percentage accepted into sink vs. specific gravity by crushing mode (excluding minus 0.30 mm material)

Figure 4-21 describes gold and copper deportment into the sink through grade-recovery curves produced by mechanical and SELFRAG crush types. The shape and extent of the curves support the findings related to Figure 4-19 and Figure 4-20 in achieving a low to moderate gold and copper pre-concentration by coarse gangue mass rejection. After breakage, the cone crusher findings show the strongest preferential deportment of metal into specified density sink fractions. This evidence suggests a relatively low proportion of silicate in mineral associations with gold-bearing sulfide particles. A comparison of the curves indicates that both the cone crusher and HPGR crusher modes produce both superior and similar

performance in the pre-concentration of gold and copper. The propensity for preferential metal (grade) deportment into the sink fractions, influenced by the different crushing modes, decreases in the following order: Cone >HPGR>VSI>SELFRAG.

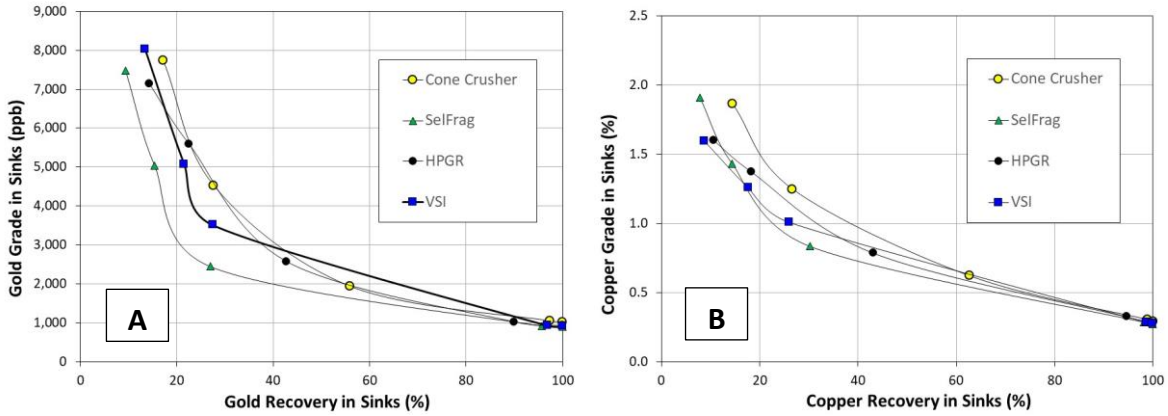

Figure 4-21. Gold (A) and copper (B) grade versus metal recovery into sinks by crushing mode (excluding minus 0.30 mm material)

The GRAT methodology allows the assessment of gold and copper pre-concentration potential principally by particle SG and size-based separation. The gold deportment surface charts are shown in Figure 4-22, and Figure 4-23 suggests that the SELFRAG crusher produces a higher proportion of composite particles with lower gold content. Conversely, it is observed that the cone crusher and HPGR crusher grade and recovery plots suggest a higher proportion of composite particles, with relatively higher gold content, compared to other crushing mode results. Figure 4-22 and Figure 4-23 charts indicate that the cone crushing mode has a higher comparative potential to pre-concentrate gold by size in a size range around 2.36 mm.

4.3.5.2 Gold and copper deportment by size and density surface charts

The copper deportment surface charts are shown in Figure 4-24, and Figure 4-25 suggests similar copper deportment responses to gold, as influenced by the different crushing modes identified in Figure 4-23 and Figure 4-24. The principal copper deportment mechanism into sinks is coarse enriched grade composite particles.

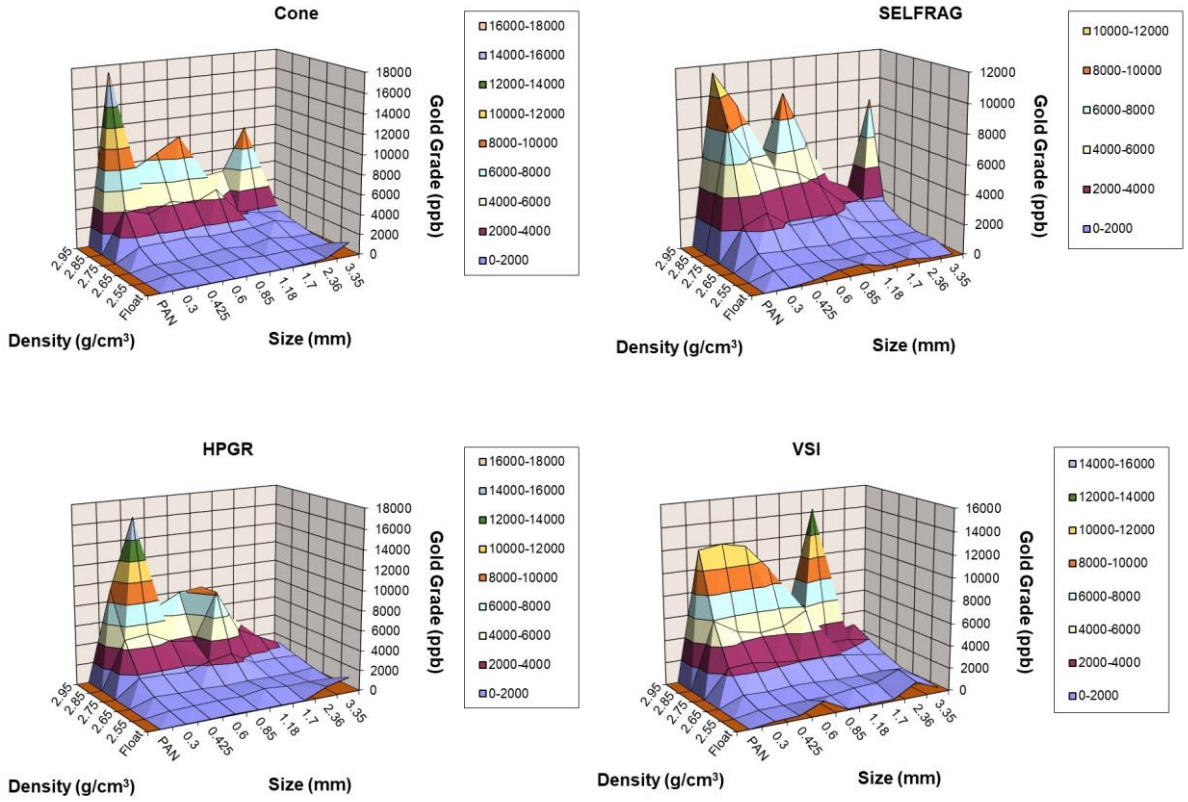

Figure 4-22. Cadia ore gold grade across SG and size by crushing mode

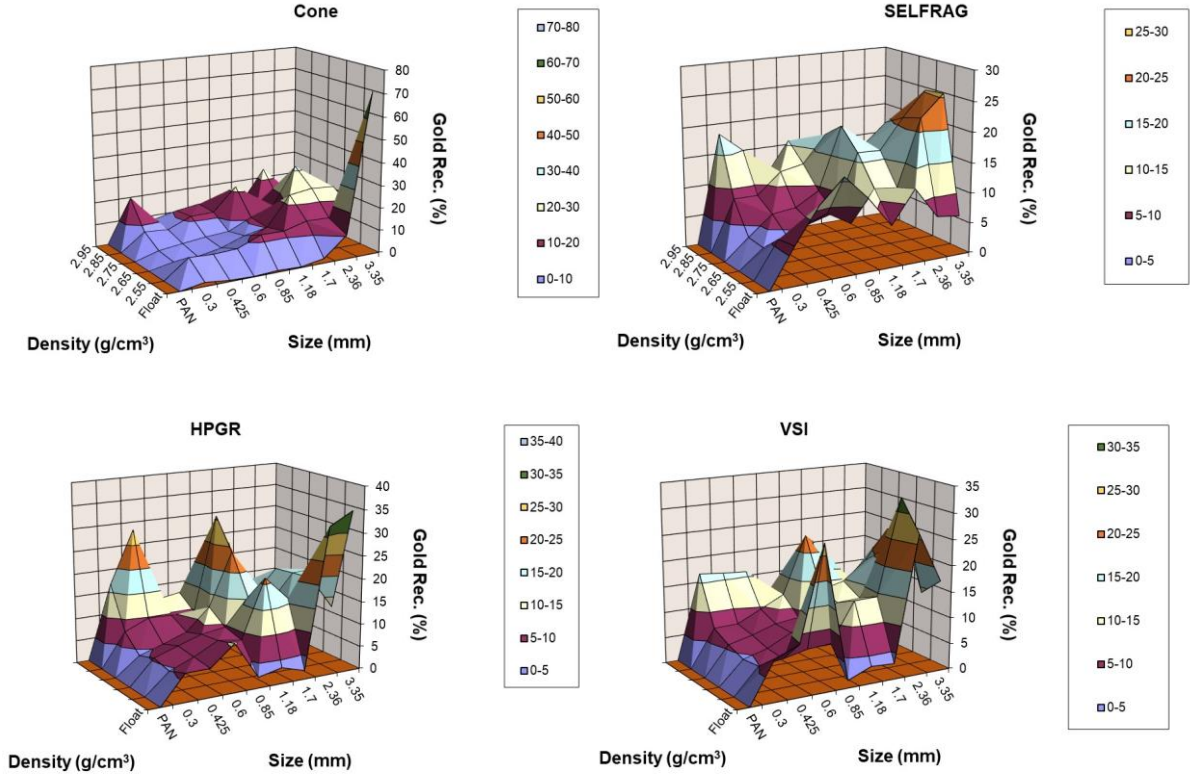

Figure 4-23. Cadia ore gold recovery across SG and size by crushing mode

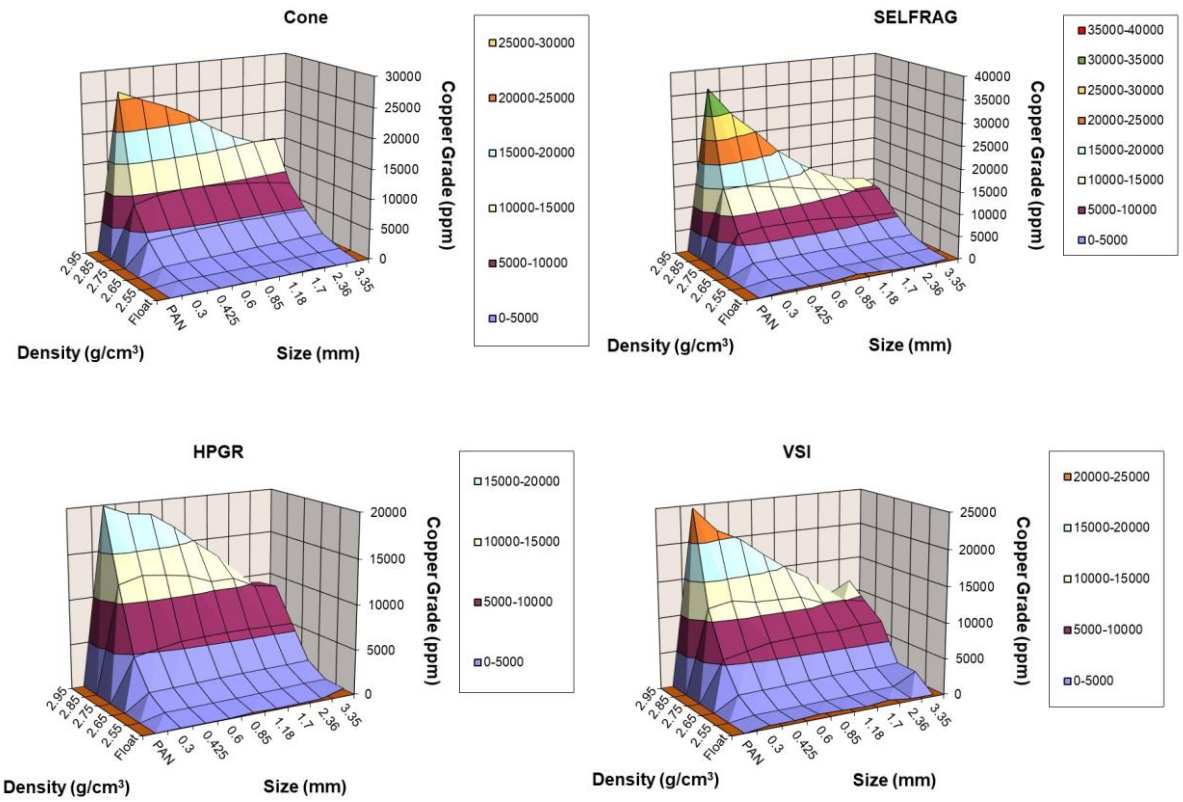

Figure 4-24. Cadia ore copper grade across SG and size by crushing mode

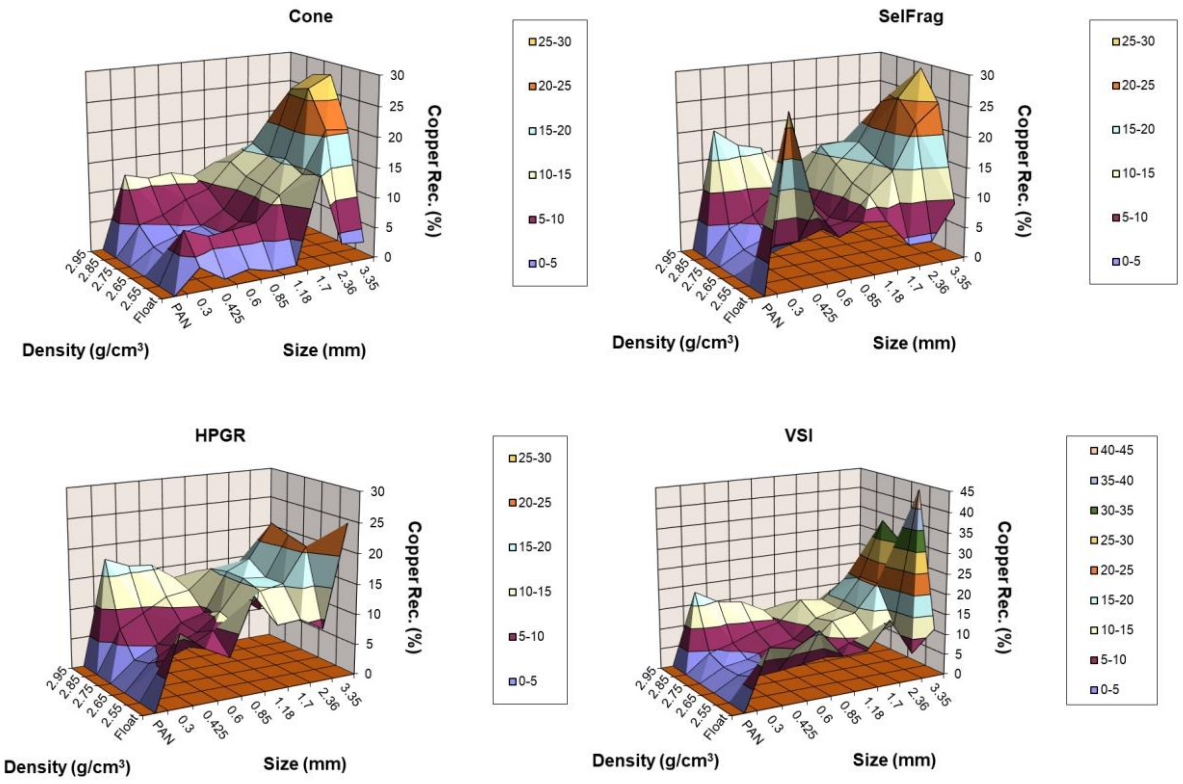

Figure 4-25. Cadia ore copper recovery across SG and size by crushing mode

4.3.5.3 Gold and copper deportment by heavy liquid float mass pull separation relationships

Figure 4-26 shows comparative response by least square regression model fitted lines for Cadia ore GRAT HLS float mass pull versus gold and copper recovery in sinks during gangue rejection into floats, for various density separation splits, by different crushing modes. This analysis excludes the minus 0.30 mm material. The plots for lines of best fit indicate the propensity of gold and copper to concentrate into the sink, following the rejection of gangue into float during density separation. In addition, these plots show that the VSI and SELFRAG modes show the lowest propensity for gold and copper pre-concentrating potential across most of the mass pull range. Conversely, the cone and HPGR crusher modes show the highest, relative to all crushing modes shown in Figure 4-26.

The mass versus elemental recovery curves in Figure 4-26 suggests that the cone crusher and HPGR products have a higher degree of liberation than other crushing modes' results. In addition, with the cone crusher and HPGR gold and copper, metal distributions are higher over part of the density fraction splits. This evidence suggests that the cone breakage mode can achieve a higher preferential grade by density deportment response relative to other crushing modes.

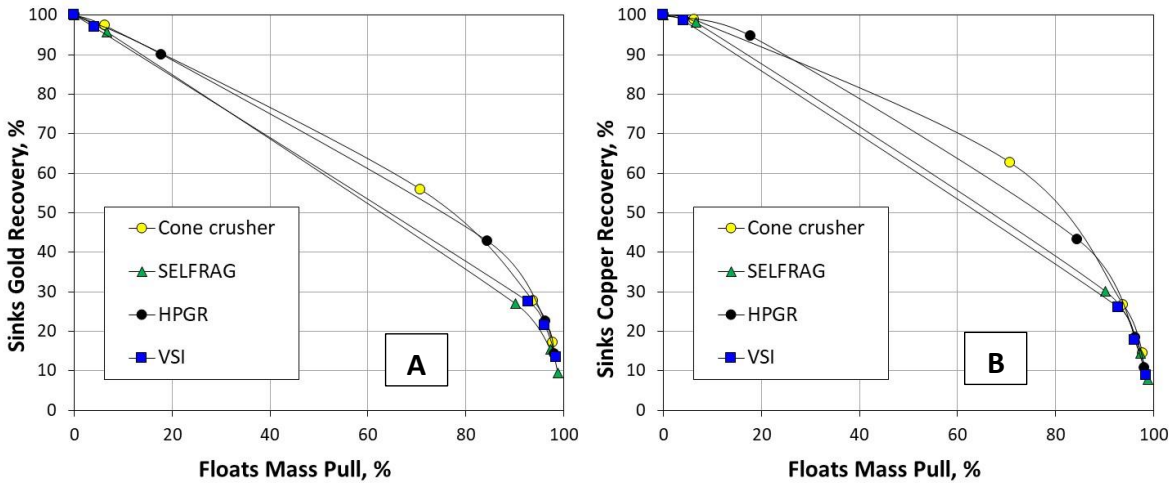

Figure 4-26. Cadia HLS float mass pull versus gold and copper recovery to concentrate relationship by crushing mode (excluding minus 0.30 mm material)

Cadia ore produced comparative response least square regression model fitted lines are shown in Figure 4-27 that estimate the GRAT HLS float gold and copper loss versus cumulative mass rejection for different crushing modes. This figure excludes minus 0.30 mm material produced in the product of different crushing modes. The plots for lines of best fit indicate the propensity that gold and copper follow mass transfer across sequential density splits,

influenced by the ore breakage crushing mode on mineral liberation. Overall, the coarse gangue rejection to float response is weak for all crushing modes observed. Still, the cone crushing mode has the highest propensity and the SELFRAG mode the lowest.

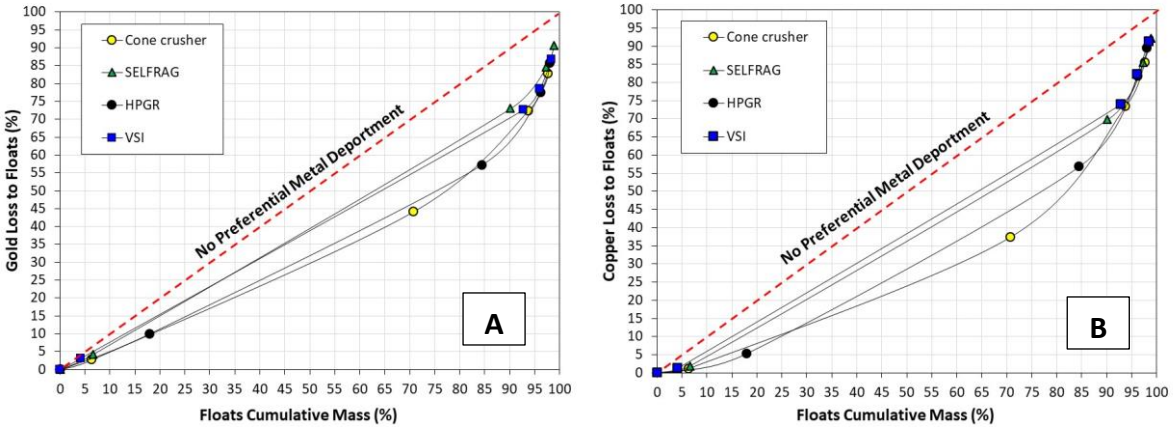

Figure 4-27. Percentage gold (A) and copper (B) loss in float versus ore mass rejected into float relationship by crushing mode (excluding minus 0.30 mm material)

Figure 4-28 and Figure 4-29 show comparative response plots of gold and copper loss versus cumulative mass rejection into the float as a function of the four different comminution modes adopted for Cadia ore. The shape and the extent of the different crushing modes generated LSR model predicted lines of best fit characterise the gold and copper deportment relationship versus cumulative mass pull rejection into the float fractions. Furthermore, the lines of best fit suggest the ore amenability and extent for coarse particle gangue separation through the GRAT methodology. In addition, the lines of best fit describe the magnitude and variability for CPGR and metal pre-concentration by the preferential grade by density deportment responses. The models used in Figure 4-28 and Figure 4-29 were exponential (section 3.9, equation 8) and Gaussian (section 3.9, equation 5) functions with an LSR technique to predict lines of best fit.

For the Cadia ore type, it is observed in Figure 4-28 and Figure 4-29 that the SELFRAG curve is comparable to that of VSI over part of the GRAT HLS density partition range investigated. The cone crusher and HPGR crusher line of best fit suggest a similar degree of silicate waste liberation from valuable mineral sulfide or gold component particles. Similarly, the best fit SELFRAG and VSI lines are comparable but indicate a lower degree of silicate waste liberation. The shape and extent of the SELFRAG and VSI crushing mode lines of best fit indicate a low density-based separation response, indicated by elevated gold and copper loss with high CW

mass pull into the HLS float. Overall, the HLS observations results indicate a low degree of liberation of metal-bearing sulfide particles for all crushed material. The assumption is that all crushing modes produce a very high proportion of low-grade copper, gold, and mineral sulfide composite particles. However, the cone crusher and HPGR crusher produce relatively higher-grade metal composite particles than observed in either the SELFRAG or VSI crushed products.

The statical quality of Figure 4-28 and Figure 4-29 LSR fitted lines of best fit are shown in Table 4-13 and Table 4-14. The results in these tables indicate good strength of fit for the developed models. The ME, RMSE and correlation coefficients suggest that the developed models can estimate gold and copper percentage loss to float response as a function of mass pull. In the Cadia modelling, an exponential function (section 3.9, equation 7) produced a predicted best fit line for the cone and SELFRAG modes. A Gaussian function (section 3.9, equation 5) LSR technique predicted lines of best fit for the HPGR crusher and VSI bivariate GRAT data.

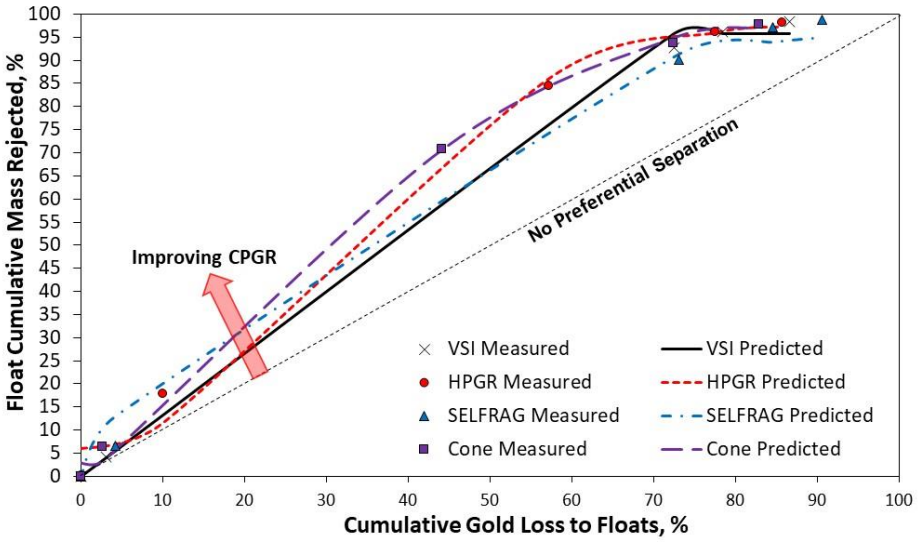

Figure 4-28. Cadia ore model fitted lines for HLS float gold loss versus cumulative mass rejection by crushing mode

Table 4-13: Cadia ore HLS float gold loss versus mass pull LSR model fitted lines descriptive statistics by crushing mode

Statistic	Cone	SELFRAG	HPGR	VSI
ME	0.000013	0.000007	0.000013	0.000033
RMSE	0.865	1.641	1.771	0.800
R^2	0.9979	0.9934	0.9910	0.9985

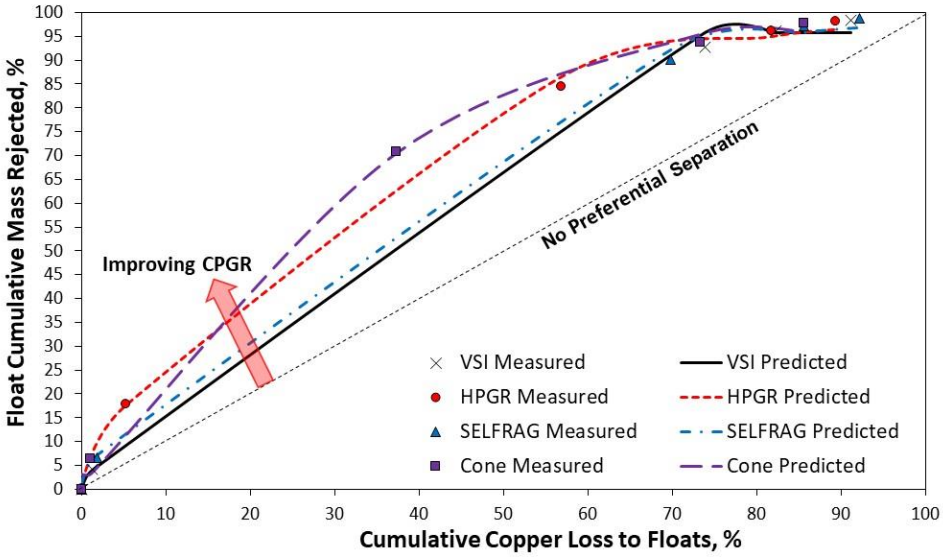

Figure 4-29. Cadia ore model fitted lines for HLS float copper loss versus cumulative mass rejection by crushing mode

Table 4-14: Cadia ore HLS float copper loss versus mass pull LSR model fitted lines descriptive statistics by crushing mode

Statistic	Cone	SELFRAG	HPGR	VSI
ME	-0.000006	-0.000004	0.000005	-0.000005
RMSE	1.000	0.660	0.647	0.800
R^2	0.9972	0.9989	0.9988	0.9985

4.4 Metallurgy parameter characterisation of separation operations

4.4.1 Ballarat ore grade enrichment by size response

The Ballarat gold-bearing ore GRAT grade deportment by size classification results provides data for calculating the Rejection Enrichment Ratio (RER) metallurgical parameters, shown in Table 4-15. In this investigation, the enrichment ratio, described by the RER parameter, is associated with grade deportment into the screen U/S fraction. Thus, the RER parameter

defines the enrichment response for each size class, with the RER calculation described in section 3.11.1 where the RER value is a function of the U/S size fraction grade to the ore feed grade abundance (Wills & Finch, 2015).

Table 4-15 shows the Ballarat ore GRAT size-by-size classification for gold by RER (metal upgrade ratio) quantitative predictions for different crushing modes. In crushed particles <0.60 mm, the SELFRAG RER values indicate a low gold deportment potential into the sieve U/S, where the HPGR favours gold deportment into the screen O/S or coarse fraction across all size classes. However, the cone RER values indicate a mix of preferential gold deportment between O/S and the U/S fractions. The VSI RER values are similar to the HPGR, with a weak tendency for gold to preferential deport into coarse particles. However, the HPGR RER values indicate a better opportunity for gold pre-concentration by size. Table 4-15 RER values for size-by-size fractions in crushed Ballarat orogenic gold-bearing ore show that metal pre-concentration by size is generally low in all crushing mode products.

Table 4-15. Ballarat gold RER response in screen U/S fractions by size class

Screen Passing Size (µm)	Cone Gold RER	SELFRAG Gold RER	Rolls Gold RER	VSI Gold RER
- 1180	1.08	0.86	0.83	1.08
- 600	1.16	1.03	0.79	0.82
- 300	1.07	1.00	0.63	0.80
- 212	0.89	1.12	0.95	0.68
- 150	0.89	1.04	0.91	0.72
- 106	0.91	1.08	0.75	0.76
- 75	0.71	1.03	0.69	0.70
- 53	0.65	1.13	0.64	0.72
- 38	0.59	1.19	0.59	0.70
- 25	0.54	1.17	0.54	0.66

4.4.2 Cadia ore grade enrichment by size response

The Cadia gold and copper ore GRAT size classification grade deportment results provided data for calculating the different RER's or metal upgrade ratios, shown in Table 4-16 and Table 4-17, respectively. All crushing modes investigated produced strong gold and copper preferential grade by size responses into the screen undersize (U/S) based on RER values. The SELFRAG RER indicate a stronger gold and copper propensity to concentrate metal into screen U/S fractions, particularly in the finer screen size fractions over other modes investigated.

Conversely, the cone crusher, rolls crusher, and VSI had a good but lower tendency to concentrate metal into screen U/S preferentially. Overall, the Cadia copper-gold ore demonstrated that the gold had a stronger preferential grade by size deportment response than copper for the different crushing modes investigated.

Table 4-16. Cadia Copper-gold RER response in screen U/S fractions by size class

Screen Passing Size (µm)	Cone Gold RER	SELFRAG Gold RER	HPGR Gold RER	VSI Gold RER
- 3350	1.08	1.13	1.03	1.11
- 2360	1.12	1.36	1.10	1.20
- 1700	1.14	1.57	1.15	1.28
- 1180	1.22	1.79	1.18	1.40
- 850	1.24	2.05	1.24	1.48
- 600	1.28	2.32	1.30	1.57
- 425	1.37	2.60	1.33	1.69
- 300	1.36	2.82	1.37	1.78

Table 4-17. Cadia copper RER response in screen U/S fractions by size class

Screen Passing Size (µm)	Cone Copper RER	SELFRAG Copper RER	HPGR Copper RER	VSI Copper RER
- 3350	1.01	1.07	1.01	1.02
- 2360	1.03	1.18	1.03	1.06
- 1700	1.06	1.28	1.04	1.09
- 1180	1.10	1.44	1.07	1.14
- 850	1.12	1.59	1.09	1.19
- 600	1.15	1.74	1.12	1.26
- 425	1.20	1.90	1.15	1.34
- 300	1.23	2.04	1.18	1.41

4.4.3 Metal deportment and enrichment graphical characterisation

The GRAT method involves screening crushed ore at a 0.3 mm sieve size. The propensity of Ballarat and Cadia ores to preferentially deport gold and copper into specific size fractions above and below 0.30 mm is compared in this section. This comparison is shown for different particle breakage modes in Figure 4-30, **Error! Reference source not found.**Figure 4-31 and Figure 4-32. These figures show changes in the RER parameter metal upgrade against the proportion of metal mass contained in specific size fractions above and below 0.30 mm, by specified crushing mode. Figure 4-30 and Figure 4-31 plots show gold deportment into the

0.30 mm fractions for the Ballarat and Caida ores, respectively. Figure 4-32 plot shows copper deportment into the 0.30 mm fractions for the Caida ore.

When the metal RER is one, equal mass transfer of gangue and metal occurs into the fines fraction, and there is no preferential deportment of metal. When the metal RER is above one, preferential deportment of metal into the fines fraction is indicated, and the larger the positive RER number, the stronger the metal enrichment tendency. When the metal RER is below one, preferential deportment of gangue into the fines fraction is indicated, and metal enrichment occurs in the plus 0.30 mm coarse fraction material.

In Figure 4-30, crushed Ballarat ore shows that a significant proportion, from 25 % to greater than 40 % of the gold in the crusher ore feed, is deported into the minus 0.30 mm fines fraction. No grade-by-size gold deportment upgrade into the minus 0.30 mm fines occurred for the SELFRAG, rolls crusher and VSI crushing modes due to the calculated upgrade ratio being below 1. Similarly, for Cadia ore, Figure 4-31 shows that a significant proportion, from approximately 25% to greater than 40% of gold contained in the crushed ore feed, is concentrated into the minus 0.30 mm fines fraction due to the calculated upgrade ratio above below 1. Figure 4-31 also identifies that preferential gold by size deportment occurs into the minus 0.3 mm fines for all crushing modes, particularly for the SELFRAG and, to a lesser extent, the VSI. Figure 4-32 shows that the Cadia ore copper deportment by size response was similar to gold. With copper grade-by-size-based deportment only slightly lower into the fines fraction and metal enrichment ratio lower in the screen undersize fractions size.

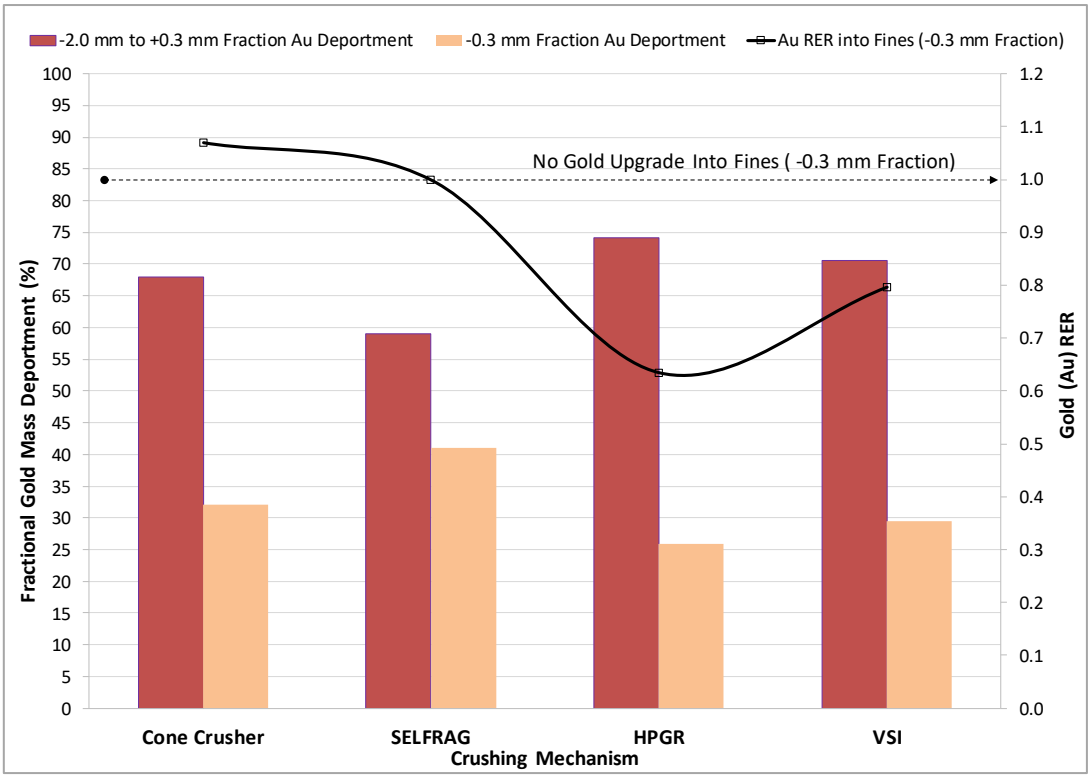

Figure 4-30. Ballarat ore gold metal deportment and gold RER response by crushing mode (adapted from McGrath et al., 2018)

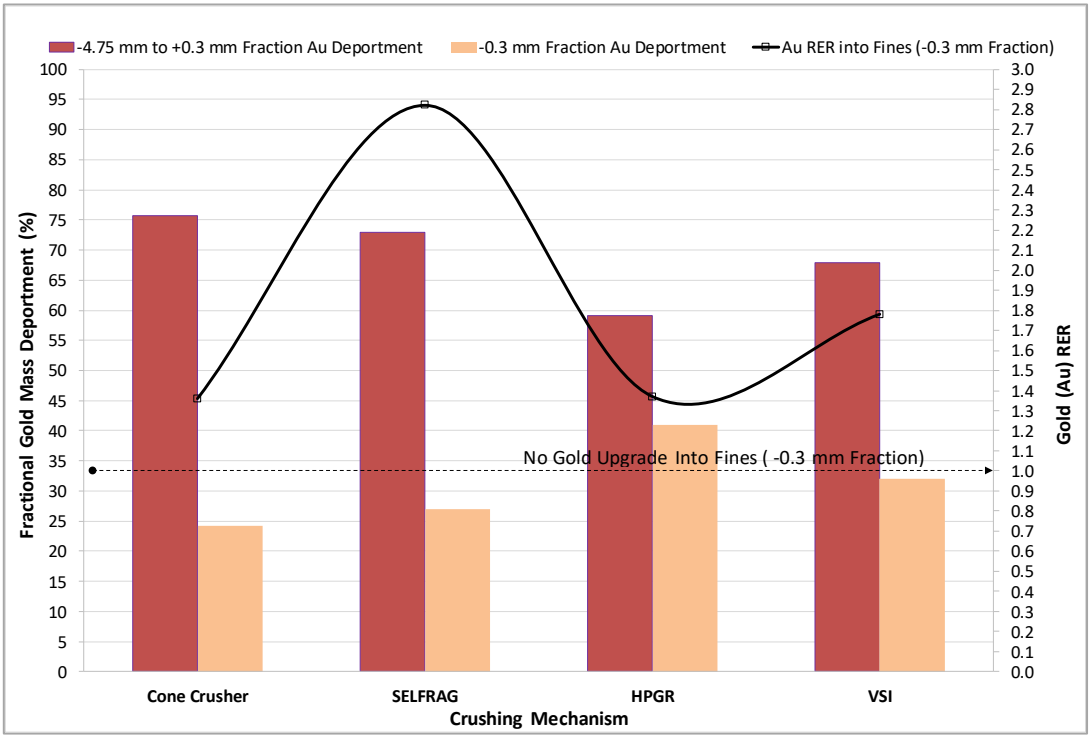

Figure 4-31. Cadia copper-gold ore gold metal deportment and gold RER response by crushing mode

Figure 4-32. Cadia copper-gold ore copper metal deportment and copper RER response by crushing mode

4.4.4 Metallurgy efficiency of concentration by density analysis

The metallurgy efficiency of metal concentration for crushed Ballarat and Cadia ore samples is characterised using the GRAT experimental balanced sink-float data shown in Appendix two and three. The metallurgy efficiency of metal concentration response is estimated from the relationship between the RER parameter value versus the metal recovery into sinks over the GRAT density classification range. The shape and extent of the predicted LSR modelled fitted lines in Figure 4-33, Figure 4-34 and Figure 4-35 suggest the amenability for metal deportment into the sink fractions over the GRAT HLS density range. The RER parameter value calculation is subject to gangue rejection. This information is useful in understanding density separation responses, also linked to the natural grade heterogeneity of ores and their amenability to transfer metal between density separation fraction products.

The Ballarat and Cadia plots shown in Figure 4-33, Figure 4-34, and Figure 4-35 have LSR technique predicted lines of best fit produced using a power function described in section 3.9, equation 4 and a spherical function described in section 3.9, equation 9. The power function produced a predicted best fit line for the cone, SELFRAG and VSI bivariate data. A spherical function gave the predicted best-fitting line for the rolls crusher bivariate data. Thus, it is

observed from the evidence shown in Figure 4-33, Figure 4-34, and Figure 4-35 that standard LSR modelling functions produce good lines of best fit to the GRAT observed data.

4.4.4.1 Crushed Ballarat ore efficiency of concentration by density

The crushed Ballarat ore comparative response for the metallurgical efficiency of gold concentration is described in Figure 4-33 for different crushing modes. The predicted lines of best fit in Figure 4-33 for the different crushing modes are produced by LSR modelling. The predicted lines of best fit provide a graphical expression of the strength of Ballarat ore to preferentially concentrate metal into multiple density fractions during coarse particle gangue rejection (CPGR). The LSR modelling technique used in predicting gold enrichment versus recovery into sink best-fit line used the power function (section 3.9, equation 4) for the cone, SELFRAG and VSI modes. A spherical function (section 3.9, equation 9) gave the predicted best-fitting line for the HPGR mode bivariate data. The shape and extent of the different crushing mechanisms generated by LSR lines of best fit characterised the preferential metal deportment into the sink fractions over the GRAT HLS density partition range. The LSR model lines of best fit suggested the extent of the density-based preferential metal separation in improving the metallurgical efficiency of concentration.

The lines of best fit in Figure 4-33 show the comparative response relationship between the gold RER parameter values versus sink gold recovery for selected crushing modes. Subsequentially, the lines of best fit suggest the strength of preferential grade by density deportment response within HLS fractions, characterised by the rate of change in gold deportment into sink product with accepted mass pull, over the GRAT density partition range.

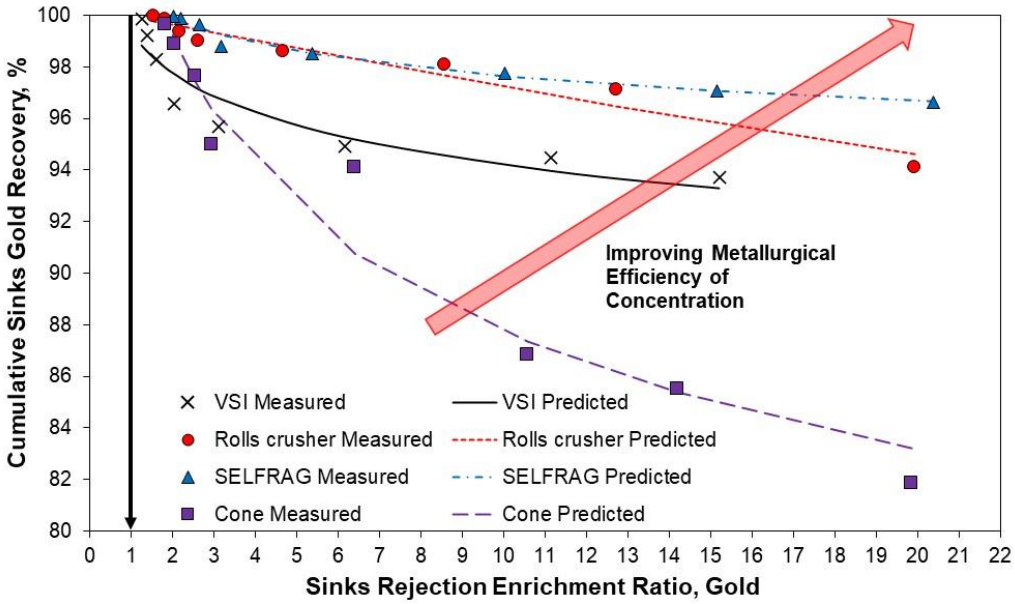

Figure 4-33. Ballarat ore LSR model fitted lines for HLS sink gold recovery versus RER metric by crushing mode (Bode et al., 2019)

For the Ballarat ore, it is observed in Figure 4-33 that the rolls crusher curve is comparable to that of SELFRAG over part of the GRAT density partition range. The LSR lines of best fit suggest that the rolls crusher and SELFRAG crushed products have a low proportion of composite or incompletely liberated gold particles and a similar degree of silicate gangue liberation from gold-bearing particles. The shape and extent of the rolls crusher and SELFRAG crushing mode lines of best fit indicate a strong preferential density-based separation response and, therefore, high metallurgical efficiency of concentration-response. Figure 4-33 shows the shape and extent of the line of best fit for the cone crushing mode. To a lesser extent, the VSI curve infers a relative lower metallurgical efficiency of concentration responses compared to other crushing modes plots. The results suggest that different fine crushing breakage modes influence changes in the CPGR and metal pre-concentration operations due to gangue and metal-bearing sulfide particle liberation.

The statistical quality of the gold separation response fitted LSR lines of best fit for crushed Ballarat ore is provided in Table 4-18 for the different crushing modes. The results indicate good strength of fit for each of the developed models. In addition, the ME, RMSE and correlation coefficients show that the model predictions can be used to estimate the metallurgy efficiency of metal concentration in HLS sink fractions over the density range investigated.

Table 4-18: Ballarat ore sink gold recovery versus RER LSR fitted lines descriptive statistics by crushing mode (Bode et al., 2019)

Statistic	Cone	SELFRAG	Rolls	VSI
ME	0.001142	-0.000017	-0.000005	-0.000091
RMSE	0.489	0.064	0.139	0.269
R^2	0.9524	0.9772	0.9518	0.8752

The crushing modes lines of best fit shown in Figure 4-33 demonstrate that different fine crushing modes can significantly influence the gold grade and metal recovery response in gravity separation. Furthermore, the statistical quality information contained in Table 4-18 suggests that the LSR modelling provides reliable predictions for the metallurgy efficiency of concentration direction, influenced by differences in the specified crushing mode liberation characteristics. This information is useful in understanding density separation responses linked to an ore's natural grade heterogeneity and amenability to transfer metal between density separation fraction products after breakage by selected crushing mode.

4.4.4.2 Crushed Cadia ore efficiency of concentration by density

The crushed Cadia ore comparative response for the metallurgical efficiency of gold and copper concentration is described in Figure 4-34 and Figure 4-35 for different crushing modes. The predicted lines of best fit provide a graphical expression of the strength of Cadia ore to preferentially concentrate metal into multiple density fractions during coarse particle gangue rejection (CPGR). The lines of best fit in Figure 4-34 and Figure 4-35 show the relationship between the gold RER parameter values versus sink gold recovery for selected crushing modes. Subsequentially, the lines of best fit suggest the strength of preferential grade by density deportment response within HLS fractions, characterised by the rate of change in gold and copper deportment into sink product with accepted mass pull, over the GRAT density partition range.

Two different model functions were used to predict the lines of best fit for selected crushing mode predicted and measured values, plotted in Figure 4-34 and Figure 4-35; these were power and spherical equations. The power function (section 3.9, equation 4) LSR technique predicted lines of best fit for cone, SELFRAG and VSI curved and a spherical function for the HPGR (section 3.9, equation 9).

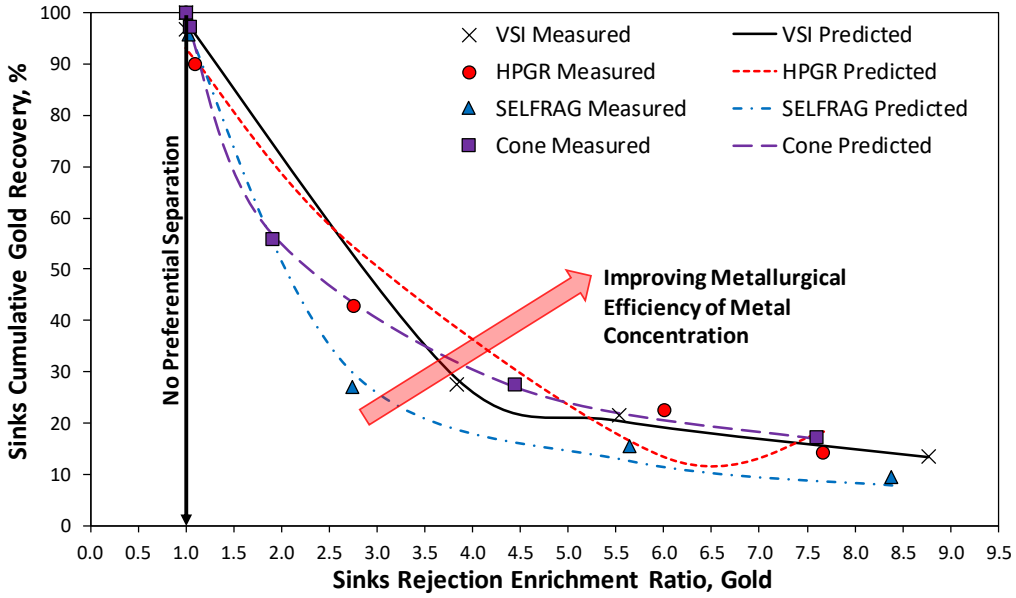

Figure 4-34. Cadia ore LSR model fitted lines for HLS sink gold recovery versus RER metric by crushing mode

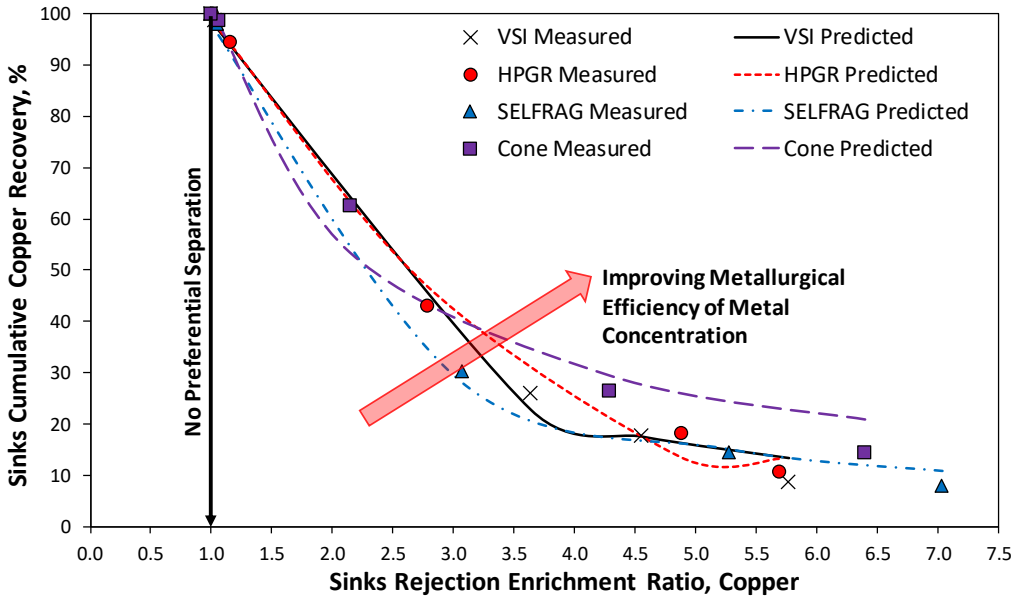

Figure 4-35. Cadia ore LSR model fitted lines for HLS sink copper recovery versus RER metric by crushing mode

The Cadia ore gold and copper results are shown in Figure 4-34, and Figure 4-35 infer a much weaker metallurgy efficiency of metal concentration-response for gold and copper for all crushing mode products investigated. Consequently, the Cadia copper-gold ore HLS metal separation results, over the GRAT density partition range examined, suggest low separation efficiency and higher misclassification due to composite particles. However, Figure 4-34 and Figure 4-35 show evidence that some fine crushing modes offer a weak preferential metal

deportment response over the examined GRAT HLS density partition range. However, different size fractions or different crushing modes may produce a more substantial preferential grade by density response.

The statistical quality of the gold and copper separation response fitted LSR lines of best fit for crushed Cadia ore is provided in Table 4-19 and Table 4-20 for the different crushing modes. The results shown in these tables indicate good strength of fit for the developed models. Furthermore, the ME, RMSE and correlation coefficients suggest that the models are good estimators of the metallurgy efficiency of metal concentration in HLS sink fractions over the density range investigated.

Table 4-19: Cadia ore sink gold recovery versus RER LSR fitted lines descriptive statistics by crushing mode

Statistic	Cone	SELFRAG	HPGR	VSI
ME	-0.047877	-0.370031	-0.000052	-0.043445
RMSE	0.236	0.878	3.353	0.447
R^2	0.9998	0.9976	0.9540	0.9993

Table 4-20: Cadia ore sink copper recovery versus RER LSR fitted lines descriptive statistics by crushing mode

Statistic	Cone	SELFRAG	HPGR	VSI
ME	0.559814	0.294689	-0.000051	0.231009
RMSE	2.380	0.919	1.311	1.168
R^2	0.9775	0.9974	0.9939	0.9958

4.4.5 Metallurgy Parameter grade deportment by density analysis

Key metals were selected for preferential elemental deportment characterisation and analysis, namely: gold and copper. The elemental deportment response into specified classification product fractions was described by an Enrichment Deportment Response (EDR) (calculation is shown in section 3.11.1) value. The EDR variable characterises grade deportment by density for a single separation process. The EDR value for selected elements is a function of the RER and the cumulative weight sink percentage. The EDR value corresponds to the propensity of the gold-bearing sulfide ores to preferentially deport elements in specified HLS classification fractions. As with the RER and the EDR parameters are calculated as metallurgy functions subject to gangue rejection during a separation operation.

With EDR values determined from a mass balance of grade by mass contained in the sink–float fractions, at sequential density increments, for a GRAT density separation operation. The gold RER and EDR values calculated for density fractions are given for the Ballarat free-milling ore in Table 4-21, corresponding to cumulative mass yield values.

Table 4-21. RER and EDR response metrics for Ballarat ore preferential gold deportment by density for different fine crushing modes (Bode et al., 2019)

Sink Density Fraction (g/ml)	Cone			SELFRAG			Rolls			VSI		
	Mass (%)	Au RER	Au EDR	Mass (%)	Au RER	Au EDR	Mass (%)	Au RER	Au EDR	Mass (%)	Au RER	Au EDR
2.65	54.0	1.8	99.4	49.2	2.0	99.9	63.8	1.6	100.0	78.6	1.3	99.5
2.70	47.9	2.1	98.5	45.2	2.2	99.9	54.4	1.8	99.7	71.2	1.4	97.7
2.75	38.2	2.6	97.5	37.5	2.7	99.7	45.5	2.2	99.2	60.1	1.6	96.6
2.80	32.1	3.0	95.5	31.0	3.2	99.0	37.5	2.6	99.0	47.0	2.1	95.4
2.85	14.7	6.4	96.8	18.3	5.4	99.1	21.1	4.7	99.1	30.6	3.1	96.3
2.90	8.2	10.6	94.3	9.7	10.0	99.0	11.4	8.6	99.1	15.4	6.2	97.2
2.95	6.0	14.2	94.4	6.4	15.2	98.9	7.6	12.7	98.9	8.5	11.2	97.7
3.00	4.1	19.9	93.7	4.7	20.4	98.9	4.7	19.9	98.0	6.2	15.2	97.7

Table 4-21 density-based deportment results for Ballarat free-milling gold-bearing ore indicated substantial preferential metallurgical efficiency in metal concentration into HLS sink product fractions. All the crushing modes investigated for the Ballarat ore demonstrated high EDR response values approaching their maximum value of 100 across the GRAT selected density range. The EDR responses for the SELFRAG and HPGR products were similar and showed the highest potential for pre-concentration gravity separation, with the cone crusher product yielding the lowest potential. The VSI product HLS EDR values were between those of the HPGR and cone crusher results. The magnitude of the RER's values observed across the density partition range indicates that well-liberated gold particles were produced from each crushing mode investigated. The RER and EDR values for the VSI suggest that the VSI mode product contains the highest proportion of high-grade composite particles.

The gold RER, EDR, and sink mass pull, by specified density split responses into GRAT sink fractions for the Cadia copper-gold ore, are shown in Table 4-22. Table 4-22 Cadia ore gold

density-based deportment results indicated moderate preferential HLS metal concentration into sink product fractions.

Table 4-22. RER and EDR response metrics for Cadia ore preferential gold deportment by density for different fine crushing modes.

Sink Density Fraction (g/ml)	Cone			SELFRAG			HPGR			VSI		
	Mass (%)	Au RER	Au EDR	Mass (%)	Au RER	Au EDR	Mass (%)	Au RER	Au EDR	Mass (%)	Au RER	Au EDR
2.55	100.0	1.00	62.8	99.9	1.00	73.5	99.9	1.00	88.7	100.0	1.00	49.1
2.65	93.7	1.04	58.2	93.3	1.03	37.3	82.1	1.10	46.6	95.9	1.01	25.0
2.75	29.3	1.91	52.7	9.8	2.74	43.5	15.5	2.76	54.5	7.2	3.83	51.0
2.85	6.2	4.45	53.7	2.7	5.64	48.1	3.7	6.01	54.6	3.9	5.54	52.7
2.95	2.3	7.60	53.5	1.1	8.39	47.3	1.9	7.67	51.2	1.5	8.77	51.9

All the crushing modes investigated demonstrated EDR response values around the low to medium index range for the GRAT selected density range. The range of the EDR values suggests that there is exploitable separation potential for gold from the host rock, following different modes of fine crushing. The HPGR crusher, closely followed by the cone crusher, showed the highest gold pre-concentration by gravity separation responses, with the SELFRAG product having the lowest response. The VSI EDR responses were between the cone crusher and SELFRAG results. The RER values across the density partition range indicated a low probability of producing fully liberated metal particles within the crushed ore product. Comparing the RER and EDR values for the cone crusher with other crushing modes suggests that the cone crusher produces the highest proportion of high-grade composite particles. There is also evidence that the HPGR and SELFRAG modes produce low to high-grade composite particles, which is suggested by the high EDR values shown in the 2.55 SG fraction. The copper RER, EDR, and sink mass pull, by specified density split responses into GRAT sink fractions for the Cadia copper-gold ore, are shown in Table 4-23.

Table 4-23. RER and EDR response metrics for Cadia ore preferential copper deportment by density for different fine crushing modes

Sink Density Fraction (g/ml)	Cone			SELFRAG			HPGR			VSI		
	Mass (%)	Cu RER	Cu EDR	Mass (%)	Cu RER	Cu EDR	Mass (%)	Cu RER	Cu EDR	Mass (%)	Cu RER	Cu EDR
2.55	100.0	1.00	98.6	99.9	1.00	83.8	99.9	1.00	87.9	100.0	1.00	84.9
2.65	93.7	1.06	82.6	93.3	1.05	72.8	82.1	1.15	72.4	95.9	1.03	69.3
2.75	29.3	2.14	61.9	9.8	3.08	48.4	15.5	2.79	55.0	7.2	3.64	49.0
2.85	6.2	4.29	52.4	2.7	5.28	46.2	3.7	4.88	48.3	3.9	4.55	46.7
2.95	2.3	6.40	49.0	1.1	7.04	43.4	1.9	5.69	43.7	1.5	5.77	41.9

Table 4-23 demonstrates Cadia ore GRAT density-based separation RER and EDR metallurgy parameter responses. Observation of these parameters identifies that copper has overall higher responses than those shown for gold, for different crushing modes, over the HLS SG range investigated. This evidence suggests that gold and copper components in the same ore treated by the same breakage mode can demonstrate different responses for preferential grade by density deportment, indicating differences in the extent of valuable component liberation and CPGR. Table 4-22 and Table 4-23 show that the cone crushing mode produced the strongest EDR response for gold and copper, followed by the HPGR mode.

4.5 Summary

This study evaluated and compared the comparative response variability and the propensity for size and density separation operations between changes in metal-rich and gangue particles by the GRAT method. The GRAT method investigated metal deportment subject to gangue rejection in specific density fractions and particle size fractions produced by different crushing modes for Ballarat CGT and Calia CVO gold-bearing sulfide ores. Sub-samples of Ballarat ore were crushed by the laboratory scale Sala mortar cone crusher (Cone), rolls crusher (Rolls), SELFRAG Lab Selective Fragmentation (SELFRAG) and Vertical Shaft Impactor (VSI) modes. Cadia ore subsamples were crushed by the cone crusher, High Pressure Grinding Rolls (HPGR), SELFRAG and VSI, modes. Test work on Ballarat CGT and Calia CVO ore samples used different versions of the GRAT method described in Section 3 of this thesis.

Particle size distributions for the Ballarat and Cadia ore crushing mode products were predicted by the Rosin-Rammler (RR) modelling technique and shown by lines of best fit to experimental data from this study. The RR lines of best fit provided the ability to compare the physical and statistical properties of the size distributions produced by the different crushing modes treating Ballarat and Cadia ores. The Ballarat crushed ores RR lines of best fit revealed that the SELFRAG produced a significantly coarser particle size distribution (PSD) below approximately (~) 600 microns and a finer PSD above 600 microns when compared to the mechanical mode RR lines of best fit. The RR lines of best fit indicate that the size difference between the cone, HPGR, and VSI modes is minimal. The Cadia crushed ores RR lines of best fit revealed that, when compared to other crushing modes, the HPGR crusher produces a finer PSD across the size classes studied. When compared to mechanical modes, the SELFRAG has a coarser PSD across all size classes.

The comparative response gold size by size distributions in Ballarat crushed ore for selected crushing modes revealed that the rolls crusher had a stronger gold deportment into coarser particles than other crushing modes. The rolls crusher grade by size results revealed that the -2.0/+1.18 mm size fraction material indicated the strongest gold particle preferential deportment response. An examination of the Cadia crushed ore gold and copper distribution by size revealed that the SELFRAG mode produced the strongest gold deportment tendency into fines compared to all other crushing mode products studied. Similarly, the SELFRAG copper preferential deportment into the fine fraction was stronger than all other crushing mode products studied but weaker than gold. Overall, for Cadia ores exploiting the propensity of the ore to preferentially deport metal into specific size fractions during breakage to achieve metal pre-concentration and gangue rejection is less confident than for Ballarat ore. However, better preferential grade-by-size metal deportment may be achieved in different specific size fractions during breakage than those used in the presented GRAT separation tests

A heavy liquid separation (HLS) comparative response study on gold-bearing ore samples from Ballarat and Cadia revealed significant variability and preferential grade separation performance between metal-rich and gangue particles in specific density fractions with particle size. This study observed that the extent of gangue rejection was strongly influenced by the natural heterogeneity of an ore's mineralisation and its interaction with a crushing mode. Both Ballarat and Cadia ores demonstrated that different crushing modes indicated

distinct intergranular breakage characteristics that could strongly influence valuable and waste materials liberation, demonstrated by gravity separation results.

The comparative response charts of the accumulative metal deportment by mass into HLS float and sinks fractions for Ballarat and Cadia ores for different crushing modes depicted the metal loss versus mass pull into the HLS float relationship, characterising the gangue rejection response. Observations showed that the Ballarat crushed ore produced strong gangue rejection responses across all crushing modes, resulting in a strong metal pre-concentration response. In contrast, Cadia ore densimetric comparative response data suggested significantly lower gold and copper pre-concentration responses.

Following HLS sequential density separation of Ballarat ore, the HPGR and SELFRAG crushed products were determined to have a low proportion of composite or incompletely liberated gold particles. Consequentially, these crushing mode gold by density deportment results suggests a similar degree of silicate gangue liberation from gold-bearing particles. The HPGR and SELFRAG crushing modes produced evidence for a strong preferential density-based separation response, suggesting the highest metallurgical performance of concentration-response. The sequential density separation results for Cadia ore provided evidence of metallurgical performance in the concentration-response for copper and gold. The concentration-response was minimal for all four crushing comminution modes investigated. The most promising gravity separation was observed on the SELFRAG product concentrating gold and copper into the fines. Over the GRAT density partition range, the Cadia copper-gold ore HLS results revealed a higher degree of misclassification in binary composite particles with silicates.

This study investigated the natural propensity to reject gangue into floats is referred to as the gangue rejection response or Rejection Enrichment Ratio (RER). Metal pre-concentration is a function of preferential grade by density deportment into sinks specific gravity fractions and is subject to the strength of the RER response. Further, this study evaluated the new Enrichment Deportment Response (EDR) parameter. The EDR parameter measures preferential grade by density deportment response and is a function of the RER value and product cumulative weight recovery, calculated for each separation operation.

The EDR values are used to characterise and quantify the GRAT HLS CPGR and metal pre-concentration separation response per specified separation faction for Ballarat and Cadia crushed ores. Elemental EDRs were calculated for separation fractions produced during the GRAT gravity separation process. The EDR value represents the propensity of specified elements contained in the gold-bearing sulfide ore to deport into specified density fractions during breakage preferentially. The EDR value is comparable to a separation step metallurgical separation performance of the concentration operation, where the highest separation performance for completely liberated metal and gangue from the ore is measured at an EDR value of 100.

The Ballarat ore demonstrated very high EDR responses for all crushing modes investigated over the density range examined in the Ballarat version of the GRAT methodology. Excluding the level of variation between individual crushing modes, the EDR values were all in the high 90's up to 100, indicating a strong grade deportment by density response into the HLS sinks products. The GRAT results suggest that coarse gold particles are liberated by all crushing modes investigated. The SELFRAG and HPGR modes yielded comparable and highest EDR values, indicating a high degree of metal and gangue liberation in particles, with gravity separation having the greatest potential for coarse particle metal pre-concentration. Based on the RER and EDR values calculated from VSI data, it is suggested that this crushing mode product contains the highest proportion of high-quality composite particles. The cone crushing mode, by contrast, has the highest proportion of low-grade composite particles.

Cadia ore metal density-based deportment results indicated moderate preferential metallurgical performance in HLS metal concentration into sink product fractions. All the crushing modes investigated demonstrated EDR response values around the medium index range for the GRAT selected density partition range. Still, the range of the EDR values suggests that there is exploitable gravity separation potential for gold and copper from the host rock for selected modes of fine crushing. Cadia ore copper EDR values show an overall stronger EDR than those achieved for gold.

Cadia polymetallic ore gold EDR responses by density for the HPGR and cone crushing modes were similar and also produced the highest grade by density yield-response into sinks compared to other crushing modes investigated in this thesis. The SELFRAG crushing mode

produced the lowest relative potential for the gold magnitude of preferential deportment into sink fractions during density separation, indicated by comparatively lower EDR by density values. The VSI EDR by density responses were generally between the cone crusher and SELFRAG results. A comparison of both the RER and EDR values determined from the GRAT grade by density deportment analysis suggested that the HPGR and cone crushed products contained the highest proportion of high-grade composite particles. Where the RER and EDR values suggest the VSI crushed product contains slightly lower grade composite particles than either the HPGR and cone crushing produces. There is evidence that the SELFRAG product has highly liberated gold particles, but the lowest overall proportion of high-grade composite particles. This is suggested by a high gold RER value, but a lower EDR value in the particles having a specific gravity higher than 2.95. This evidence suggests that the SELFRAG breakage pattern does not effectually liberate gold from the host rock to the same extent as other fine crushing modes investigated. The Cadia ore heterogeneity and texture appear to negatively influence the SELFRAG breakage efficiency in gold liberation from waste minerals during comminution. Evidence from the gold RER and EDR values suggests that selective metal liberation by different crushing modes varies

A comparison of the crushing mode product copper EDR responses by density for the Cadia polymetallic ore showed the cone crusher mode produces the higher copper EDR values, and the VSI produces the weakest responses. The HPGR copper EDR responses by density are slightly lower than that achieved by the cone crusher mode. The SELFRAG EDR values by density were lower than those produced by other crushing modes examined in this thesis. This evidence suggests that the SELFRAG breakage pattern does not liberate copper in the rock during comminution to the same extent as other fine crushing modes. The Cadia ore heterogeneity and texture appear to negatively influence the SELFRAG breakage efficiency in gold liberation from waste minerals during comminution. However, similar to gold GRAT observations, evidence suggests that the SELFRAG mode produces a lower ratio of highly liberated metal particles, indicated by a higher copper RER value but a lower EDR value in the 2.95 specific gravity separation response. Evidence from the copper RER and EDR values suggests that selective metal liberation by different crushing modes varies. Also, comparative RER and EDR value evidence for different valuable metal components, such as gold and

copper in the Cadia ore, suggests differences in metal liberation responses, following different crushing modes of comminution.

This comparative study showed significant differences between crushing modes in their coarse particle gangue rejection (CPGR) and preferential grade deportment responses by size and density strategies on Ballarat and Cadia ore styles. These results suggest that different crushing modes could produce better results for size-based classification or density-based beneficiation processes, dependent on the ore style. Furthermore, these findings are important to resource exploitation and downstream processing strategy.

Chapter 5. Statistical analysis of separation performance

Ballarat and Cadia ore breakage behaviour and elemental separation deportment characterisation have shown that different modes of fine crushing treatment influence preferential grade-by-size and grade-by-density deportment responses. Therefore, there is an anticipation that the interaction of gravity separation processes on products produced by different crushing modes results in significant changes in Enrichment Deportment Response (EDR) values. In this chapter, statistical analysis techniques are employed to identify the significance of changes in gravity separation operation EDR parameter values linked to the crushing mode and gold-bearing ore type.

5.1 Background

Parametric statistical analysis methods were used to compare means and variances for the gold and copper Enrichment Deportment Response (EDR) values, calculated from the experimental results produced by the Ballarat and Cadia versions of the gangue rejection amenability test (GRAT). The GRAT densimetric results were produced from Ballarat CGT and Cadia CVO ore samples, crushed by selected laboratory crushing modes. Crushing mechanisms used were laboratory-scale Sala mortar cone (cone) crusher, SELFRAG Lab Selective Fragmentation (SELFRAG), rolls crusher, High Pressure Grinding Rolls (HPGR) and Vertical Shaft Impactor (VSI) crusher modes. The EDR value quantifies the extent of the metallurgical efficiency of the concentration operation response from a specified separation operation.

Statistical techniques were employed to evaluate the GRAT Ballarat and Cadia ore sample EDR generated densimetric data results for specified crushing modes Subsequentially, various comparative statistical analysis techniques were used to draw conclusions for changes in

preferential grade by density deportment response and gravity separation efficiency using evidence of variation in the EDR metric. It is recognised that the influence of different crushing mode breakage on changes in density separation efficiency in the concentration operation during gangue rejection may, however, not be statistically significant between crushing modes treating the same ore type.

This study uses statistical methods to evaluate similarities and differences in empirical gravity results. These results are obtained from the interaction between two gold-bearing ore types, four selected crushing modes, and gravity separation techniques. The EDR data produced from the experimental gravity methods are not comparable due to the difference in the gravity technique used on each ore type. The following assumptions that are relevant to clarifying the study's aim are:

(1) different versions of the GRAT method can adequately assess the Ballarat Castlemaine Goldfields Limited, Victoria, Australia orogenic ore and the Cadia East, NSW, Australia porphyry copper-gold ore;

(2) the EDR calculated values can be calculated from data produced from the Ballarat and Cadia versions of the GRAT method for all crushing modes treating Ballarat and Cadia gold-bearing ore type samples;

(3) all crushing mode products are gravity separated under the same conditions for each ore type.

(4) That the GRAT data collected has no bias.

(5) That the GRAT data collected is reliable.

In this investigation, different statistical techniques evaluated crushing mode EDR data. The ANOVA uses F-tests to test the compared crushing mode EDR variance and equality of mean (equal means). A t-tests technique is used to test upgrade versus cumulative recovery slope of regression line relationships. These tests assume the sample population is normally distributed, has homogeneity of variance and has independent comparison groups (Napier-Munn, 2014).

5.2 Comparison of Enrichment Deportment Response by crushing mode

Section 3.11.1 describes the method used to calculate the Enrichment Deportment Response parameter values using log-transformed data. The log-transformed data is understood to produce normal data sets useful (Napier-Munn, 2014). In Figure 5-1 and Figure 5-2, bar charts compare the different crushing modes influence on the EDR response in crushed Ballarat and Cadia ore sub-samples, following the GRAT combined size and heavy liquid density separations operations described in

Figure 3-11. Ballarat ore GRAT methodology flowsheet (adapted from McGrath et al., 2018)

and Figure 3-12. The bars in the charts represent the overall arithmetic mean EDR response derived from the interaction between different crushing modes, gravity separation techniques, and gold-bearing ore geological styles. A standard error of the mean (SEM) is associated with each bar in the charts. The standard deviation (SD) of the data sample is divided by the square root of the sample size to calculate the SEM (Napier-Munn, 2014). The SEM error bars information (typically T-shaped) adds another degree of detail to the displayed mean bar information. The Error Bars are used to show estimated error or uncertainty to offer a general idea of how precise an EDR mean measurement is or how precisely the EDR mean value is reported correctly (Box, Hunter, & Hunter, 1978). Given that the GRAT data sample sizes are equal for SEM value calculations, as a rule-of-thumb, if the T-shaped bars overlap, the corresponding confidence level is 95% that the difference between the compared EDR means is not statistically significant. Therefore, The SEM bars in Figure 5-1 and Figure 5-2 show the difference between each crushing mode mean EDR value, with the precision of those means (Box et al., 1978).

Gold EDR responses in Figure 5-1 show the SELFRAG Lab Selective Fragmentation (SELFRAG) and rolls crusher (Rolls) have comparable and higher metallurgical efficiency of the concentration responses than the Sala mortar cone crusher (cone) and Vertical Shaft Impactor (VSI) crushing modes. The overlapping of the SEM error bars in Figure 5-1 implies that the difference in mean EDR values between SELFRAG and rolls crushers is not statistically significant at a 95 percent confidence level. Conversely, Figure 5-1 shows that the comparative cone and VSI crusher mean gold EDR value difference is statistically significant at a 95 percent confidence level, owing to the minimal SEM error bars overlap. Comparing all

crushing mode SEM error bars suggests that at a 95% confidence level, the cone crusher has the highest uncertainty in the precision of the gold EDR mean value and the SELFRAG the lowest uncertainty.

In Figure 5-1, the SELFRAG and HPGR modes EDR means indicate their crushed products contain a low proportion of composite or incompletely liberated particles, with a similar degree of silicate gangue liberation from gold-bearing particles. This evidence suggests that the SELFRAG and HPGR breakage patterns achieved a higher efficiency of metallurgical separation of gold in the GRAT sink fractions over the density partition range measured. Conversely, Figure 5-1 shows that the cone and, to a lesser extent, the VSI crushing modes have rock fracture liberation patterns that result in a higher proportion of composite or incompletely liberated particles, decreasing density separation performance.

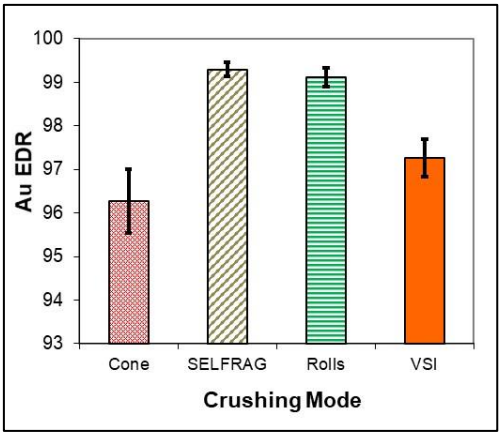

Figure 5-1. Ballarat ore gold EDR values by crushing mode, with fitted SEM bars

Figure 5-2 shows two bar charts, with SEM error bars, for the Cadia ore gold and copper mean EDR values impacted by different crushing modes. These bar charts depict mean metal EDR values generated by GRAT gravity separation operations on crushed ore using a cone, SELFRAG, High Pressure Grinding Rolls (HPGR), and VSI crushing modes.

A comparison of the gold EDR bars suggests that the HPGR and the cone crusher products achieve comparably higher preferential gold deportment by density response than either the SELFRAG or VSI mode products. This result in gold deportment implies that the SELFRAG and VSI crushed products contain a comparable higher proportion of composite or incompletely gold-containing and gangue liberated particles than either the HPGR or cone crusher products. However, the overlapping of the SEM error bars in Figure 5-2 implies that the difference between the cone crusher and HPGR mean gold EDR values are not statistically

significant at a 95 percent confidence level. Figure 5-2 suggests that the SELFRAG and VSI gold mean EDR values are similar. The VSI EDR value indicates that these breakage modes produced a relatively lower degree of silicate gangue liberation from gold-bearing particles than other crushing modes.

In Figure 5-2, the EDR values suggest that the HPGR breakage pattern allowed a higher degree of silicate gangue liberation from gold-bearing particles relative to other breakage modes. This high degree of liberation resulted in a higher gold metallurgical separation performance into the GRAT sink fractions over the density partition range measured.

The copper EDR bars in Figure 5-2 suggests that the cone crusher products achieve a comparably higher preferential copper deportment by density response than either the HPGR, SELFRAG or VSI crushing mode products. This copper deportment result implies that the HPGR, SELFRAG, and VSI crushed products contain a higher proportion of composite or incompletely gold-containing and gangue liberated particles than the cone crusher products. The overlapping of the SEM error bars in Figure 5-2 implies that the difference between the HPGR, SELFRAG and VSI crushed product means copper EDR values are not statistically significant at a 95 percent confidence level.

In Figure 5-2, The EDR values suggest that the cone crusher breakage pattern allowed a higher degree of silicate gangue liberation from copper-bearing particles relative to other breakage modes. This high degree of liberation resulted in a higher copper metallurgical separation performance into the GRAT sink fractions over the density partition range measured.

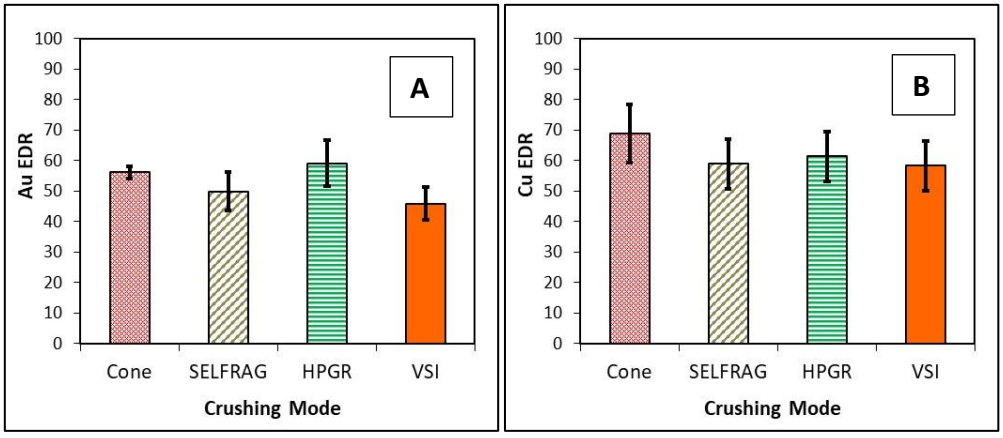

Figure 5-2. Cadia ore gold (A) and copper (B) EDR values by crushing mode, with fitted SEM bars

5.3 Variation test between crushing modes by ANOVA F-test technique

An ANOVA-F Test was performed, along with a blocking analysis, on gold and copper EDR values calculated for different crushing modes on sink-float ore samples from Ballarat and Cadia (Box et al., 1978). Without blocking for each density fraction, it is not possible to conclude that there is a significant difference between each of the four crushing modes for improving EDR values with certainty. The F-test with blocking analysis consists of these hypotheses:

H_0: EDR value does not depend on the type of crushing mode employed in breakage.

H_1: EDR value does depend on the type of crushing mode employed in breakage.

The ANOVA F-test, blocked for Ballarat HLS sink gold EDR values produced by different crushing modes, as shown in Figure 5-1. With blocking for each density fraction, the significance of the difference between each of the four crushing modes on gold EDR variance and block out density fraction variance is considered.

Table 5-1. ANOVA - F Test for gold EDR response on Ballarat ore sample with blocking for the impact of different crushing mode

	Density Fraction									
Treatment	SG 2.65	SG 2.70	SG 2.75	SG 2.80	SG 2.85	SG 2.90	SG 2.95	SG 3.00	Mean	Variance
Cone	99	98	98	95	97	94	94	94	96.27	4.39
SELFRAG	100	100	100	99	99	99	99	99	99.29	0.20
Rolls	100	100	99	99	99	99	99	98	99.11	0.34
VSI	99	98	97	95	96	97	98	98	97.26	1.49
Mean	99.70	98.94	98.25	97.19	97.83	97.42	97.48	97.07	97.99	3.21
Difference	1.71	0.96	0.26	-0.79	-0.15	-0.56	-0.51	-0.92		

		Variance of Means	2.38
		F Ratio =>	**5.92**
Number of Treatments	4	Degrees of Freedom (Sum of all data points)	28
Reduce for Estimating Error	1	Fewer Degrees of Freedom	3
Degrees of Freedom (No. levels less 1)	3	Significance level (Selected)	0.05
Number of Density Fractions Sampled	8	**F Distribution (Critical Value)**	**2.99**

When the variation between density fractions is blocked out, it can be concluded that there is a significant difference between each of the four crushing modes gold EDR values between density splits, since the F ratio of 5.92 is higher than the F-Critical value of 2.99. Therefore, the null hypothesis (H_0) is rejected; changes in the crushing mode, and associated changes in ore breakage pattern, significantly influence EDR responses within density fraction groups. Consequently, there is strong evidence of differences in preferential gold deportment into sinks density fractions resulting from the application of different crushing modes.

The ANOVA F-test, blocking the Cadia HLS sink gold EDR values for different crushing modes, is described in Figure 5-2. With blocking for each density fraction, the significance of the difference between each of the four crushing modes on gold EDR variance and block out density fraction variance can be considered. When blocking out the variation between density fractions, it can be concluded that the difference is discernible since the F Ratio of 3.00 is higher than the F Critical value of 2.99, and therefore the null hypothesis is rejected. Consequently, there is weak evidence of differences in preferential gold deportment into sinks density fractions resulting from the application of different crushing modes.

Table 5-2. ANOVA - F Test for gold EDR response on Cadia ore sample with blocking for the impact of different crushing mode

	Density Fraction						
Treatment	SG 2.55	SG 2.65	SG 2.75	SG 2.85	SG 2.95	Mean	Variance
Cone	63	58	53	54	53	56.16	18.31
SELFRAG	73	37	43	48	47	49.93	191.77
HPGR	89	47	54	55	51	59.10	283.69
VSI	49	25	51	53	52	45.93	139.09
Mean	68.51	41.77	50.39	52.27	50.97	52.78	94.47
Difference	15.73	-11.01	-2.39	-0.51	-1.81		

		Variance of Means	35.47
		F Ratio =>	**3.00**
Number of Treatments	4	Degrees of Freedom (data points)	28
Reduce for Estimating Error	1	Fewer Degrees of Freedom	3
Degrees of Freedom (No. levels less 1)	3	Significance level (Selected)	0.05
Number of Density Fractions Sampled	8	**F Distribution (Critical Value)**	**2.99**

The ANOVA F-test, blocked for Cadia HLS sink copper EDR values for different crushing modes, is described in Figure 5-3. With blocking for each density fraction, the significance of the difference between each of the four crushing modes on copper EDR variance can be considered and block out density fraction variance. When blocking out the variation between density fractions, it can be concluded that the difference is not discernible since the F Ratio of 1.20 is lower than the F Critical value of 2.99, so the null hypothesis cannot be rejected. Consequently, there is insufficient evidence of differences in preferential copper deportment into sinks density fractions resulting from the application of different crushing modes. It is worth examining further through a standard F-Test approach.

Table 5-3. ANOVA - F Test for copper EDR response on Cadia ore sample with blocking for the impact of different crushing mode

	Density Fraction						
Treatment	SG 2.55	SG 2.65	SG 2.75	SG 2.85	SG 2.95	Mean	Variance
Cone	99	83	62	52	49	68.91	447.57
SELFRAG	84	73	48	46	43	58.94	331.27
HPGR	88	72	55	48	44	61.43	337.63
VSI	85	25	51	53	52	53.08	451.47
Mean	88.80	63.20	54.08	49.89	46.99	60.59	286.07
Difference	28.21	2.60	-6.51	-10.70	-13.60		

Variance of Means	43.01
F Ratio =>	**1.20**

Number of Treatments	4	Degrees of Freedom (data points)	28
Reduce for Estimating Error	1	Fewer Degrees of Freedom	3
Degrees of Freedom (No. levels less 1)	3	Significance level (Selected)	0.05
Number of Density Fractions Sampled	8	**F Distribution (Critical Value)**	**2.99**

The EDR results determined for the Cadia ore sample investigated under the GRAT density fractionation conditions are used in a standard F-test analysis. A standard F-test, derived from Napier-Munn (2014) without blocking, is used to further test for evidence of any significant difference in copper EDR value groups, in density fractions or by the application of different crushing modes. In the typical F-Test approach, the sum of squares within groups (SSW), a measure of within groups variability, and the sum of squares between groups (SSB), a measure of between-group variability, is examined for significance by calculating the associated p-values. Table 5-4 shows the null hypothesis that is tested for the variance within groups (sW) being either greater than or less than or equal to the variance between groups. In Table 5-4, a significance level (error) of 0.05 is nominated, which indicates a 5 % risk of concluding that a significant difference exists when, in fact, there is no actual difference. If the Table 5-4 p-value is less than or equal to the error, the null hypothesis(s) is rejected, concluding that not all the population means are equal by group type. It is observed by the probability value(s) (p-value), per hypothesis test, that there is no evidence against the stated null hypothesis(s), so fail to reject them. There is insufficient evidence to conclude that the application of different crushing modes caused changes in the copper EDR responses, either within the specified density partition range investigated or by the influence of different crushing modes.

In Table 5-4 statistical data analysis, the SST is the total sum of squares (Napier-Munn, 2014). The SST parameter is denoted as the squared differences between the observed dependent variable and its mean (Napier-Munn, 2014). the number of degrees of freedom (df) is the number of observations in the final calculation of a statistic that are free to change (Napier-Munn, 2014).

Table 5-4. ANOVA - F Test for the impact of different crushing mode treatments no improve copper EDR response on Cadia ore sample.

HYPOTHESIS TESTING

Null Hypothesis	*p-value*	*Error*
H_0: sW - sB = 0	0.6876	0.0500
H_0: sW - sB >= 0	0.3438	
H_0: sW - sB <= 0	0.6562	

SUMMARY

Groups	*n*	*df*	*df*	*Sum*	*Mean*	*Variance*	*SSW*
Cone	5	4	16	344.5563831	68.91	447.57	6271.77
SELFRAG	5	4		294.708168	58.94	331.27	
HPGR	5	4		307.152536	61.43	337.63	
VSI	5	4		265.4103098	53.08	451.47	

VARIANCE ANALYSIS

Source	*SS*	*% SS*	*df*	*VAR*	*F*	*P Value*	*F Critical*
Between Groups (SSB)	645.1817	9.33%	3	215.0606	0.5486	0.6562	3.2389
Within Groups (SSW)	6271.7733	90.67%	16	391.9858			
Total (SST)	6916.9550		19				

5.4 Statistical comparison of metal deportment response by crushing mode

Differences in nominated metal gravity separation response in Ballarat and Cadia crushed ores for selected crushing mode products are statistically analysed. The significance of the influence of different crushing modes on preferential gold and copper deportment into specified sink products by density separation was investigated using the Student's t-test (t-test) for analysis of regression line slopes for Ballarat and Cadia ore samples. Alternately, the variables compared in the analysis were the metal RER parameter versus cumulative metal recovery over the GRAT density partition range. The statistically analyse method compares two independent samples by testing the significance of the slope of the regression line.

The t-test selected in this study implements a paired comparison using a linear regression t-test methodology to determine whether the slope of the regression line differs significantly

from zero or if the slopes are equal. This approach is a variant of the typical t-test application used to examine the differences between the means of two groups. The variables compared in the analysis were metal recovery and the metal RER into GRAT sink fractions over the density partition range.

In this thesis, a paired t-test method compares the slopes between two linear regression lines. A two-sample t-test method can compare the slopes of fitted regression lines through a statistical approach using unpooled and pooled variance assessment (Zaiontz, 2013). The paired t-test comparison of slopes method determines whether there is any significant difference in the regression line slopes between two different crushing mode sample populations. The slope regression comparison hypothesis tests whether the slopes (β1 and β2) for cumulative metal recovery into sink versus natural log (ln) metal cumulative Rejection Enrichment Ratio (RER) ratios are equal, i.e., test the following null and alternative hypotheses:

H_0: $\beta_1 = \beta_2$ or $\beta_1 - \beta_2 = 0$

H_1: $\beta_1 \neq \beta_2$ or $\beta_1 - \beta_2 \neq 0$

Since the linear equation will not fit the observations exactly, estimated values must be used. These estimates are found using the method of least squares. By using these estimated values, each data pair may be modelled using Equation 15.

$$Y = a + bx + \varepsilon \tag{15}$$

Note that a and b are the estimates of the population parameters α and β. The 'Ɛ' value (error or residual) represents the discrepancies between the estimated values (a + bX) and the actual values 'Y'.

To conduct the hypothesis test for the population slope *β*, we use the t-test statistic value Equation 16 stated by Zaiontz (2013), which compares regression lines slopes with the t value and is calculated by:

$$t = \frac{b_1 - b_2}{\sqrt{S_{b1}^2 - S_{b2}^2}} \sim T\left(n_1 + n_2 - 4\right) \tag{16}$$

Where b_1 and b_2 are the slopes and the S_{b1} and S_{b2} is the standard error of the slopes for each of the regression lines. The calculated t value is compared to the Student's t-distribution, T value, where $n_1 + n_2 - 4$ equals the degrees of freedom (DF), and if the H_0 is true, then Zaiontz (2013) states that the slope difference of the regression lines is equal to zero, Equation 17:

$$\beta_1 - \beta_2 \sim N\left(0, Sb_1 - Sb_2\right)$$

$$\beta_1 - \beta_2 \sim \mathrm{N}(0, \mathrm{S_{b1}} - \mathrm{S_{b2}}) \tag{17}$$

Where it is, it is assumed that the least-squares errors or residuals are normally distributed (N) and if there is no difference in the slope, they would be equal to 0. Zaiontz (2013) states that the standard error of the slope is shown in Equation 18.

$$\mathrm{S_{b1-b2}} = \sqrt{S_{b1}^2 - S_{b2}^2} \tag{18}$$

In Equation 18, the $\mathrm{S_{b1-b2}}$ parameter is the standard error of the slope (Zaiontz 2013). If the two error variances (S^2) are equal, then the estimates of the error variances can be pooled, weighing each by their degrees of freedom. If the two slope error variances are equal, then pool the estimates of the error variances, weighing each by their degrees of freedom, shown by equation 19 and equation 20 given by Zaiontz (2013), where:

$$S_{Res}^2 = \frac{(n_1-2){S_{y\cdot x_1}}^2+(n_2-2){S_{y\cdot x_2}}^2}{n_1-n_2-4} \tag{19}$$

or

$$\mathrm{S_{b1-b2}} = \mathrm{S_{Res}} \times \sqrt{\left(\frac{1}{S_{x1}^2(\mathrm{n_1}-1)} + \frac{1}{S_{x2}^2(\mathrm{n_2}-1)}\right)} \tag{20}$$

Where $S_{y.x1}^2$ and $S_{y.x2}^2$ are the standard error for the line of best fit, n_1 and n_2 are the sizes of the respective samples, S_{Res}^2 is the variance of the pooled residuals (Zaiontz 2013).

5.4.1 Null hypothesis testing

The difference in slope of regression line variance between specified crushing modes is investigated in this thesis gold upgrade versus cumulative recovery regression analysis using statistical t-test pooled and unpooled results. The statistical t-test analysis pooled and

unpooled results are used to test the null hypothesis (H_0). The H_0 states that there is no significant difference between compared crushing mode metal upgrade versus the cumulative recovery slope of regression line relationships. Data for the statistical t-test analysis is derived from the GRAT gravity separation tests on Ballarat and Caida gold-bearing ores, described in Chapter 3 of this thesis. The statistical pooled and unpooled results provide t-values and p-values which are used, with a chosen significance level, alpha of 0.05, to indicate whether the H_0 should be rejected in favour of the alternative hypothesis (H_1). Typically, for the H_0 to be rejected, the calculated p-value is less than or equal to the selected significance level (α) is ≤ 0.05 (95% Confidence level), and the calculated t value is greater than the tabulated critical t-value (t > t-crit), there is a statistically significant difference between the two variables. If the p-value is greater than alpha, you fail to reject the null hypothesis; there is not enough evidence to conclude that the results are not significantly different between the two crushing more slope variables (Box, 1978). If it is less than alpha, you reject the null hypothesis (Box, 1978). In this study, rejecting the H_0 indicates a significant difference between the slope of the regression line for compared crushing mode variables. If the test statistic t value is less than the critical t-value of 2.18 and the p-value result is greater than α, then fail to reject the H_0, or a relationship exists between the comparison of crushing mode slope data (Box, 1978). Failing to reject the H_0 indicates the crushed ore GRAT gravity results did not provide sufficient evidence to conclude that the results are not significantly different between the selected crushing mode slope variables compared.

5.4.2 Ballarat ore gold gravity separation statical variance analysis between crushing modes

For a Ballarat ore sub-sample crushed by specified modes, Figure 5-3 graphically depicts least-squares linear regression analysis of scatter plots for the gravimetric separation relationship between sink's gold (Au) RER versus cumulative gold recovery performance across the HLS density partition range. Figure 5-3 observed graphical evidence and regression equation variable data suggest that the SELFRAG, rolls crusher, and VSI have similar predicted linear slope characteristics, with slopes of -1.4, -1.8, and -2.2 identified in respective line functions. Comparing SELFRAG, rolls crusher, and VSI slope and extent of the regression lines rise over run variables implies a strong gold separation performance for all crushing modes. However, the cone crusher mode linear rate of change slope value is significantly higher than the other crushing modes, with a value of -7.1, suggesting a real and lower difference in gold

preferential deportment into sinks fractions against that achieved by other crushing mode products. Where crushing mode comparisons show similarities between the slope and extent of the regression lines rise over run variables there is an assumption that the gold gravity separation performance is similar. Similar regression line rise over run variables suggests that SELFRAG, rolls crusher, and VSI modes produce similar breakage patterns between the waste and valuable component minerals. However, this assumption needs to be tested for statistical significance. As a result, compared crushing mode slope variables can be t-tested to compare relationships between gravity separation responses in different crushing mode products.

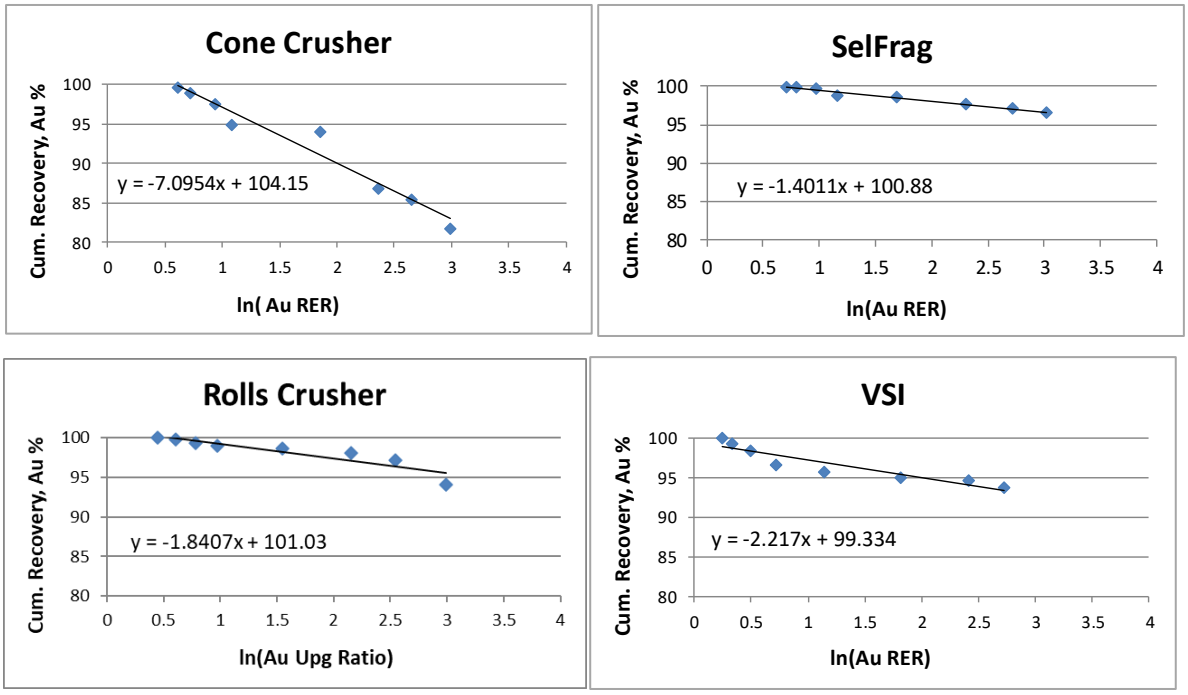

Figure 5-3. Ballarat sink gold RER response as a metal upgrade versus cumulative recovery relationship by different crushing modes

Table 5-5 shows the statistical quality information for the crushing mode comparisons shown in Figure 5-3. The results show a high regression correlation coefficient, denoted by the R^2 values, for all the crushing modes, indicating strong robustness in modelling the grade versus recovery relationship. The SELFRAG RMSE value suggests the lowest potential for bias between the sample data mean, and the population mean, with the cone crusher having the highest potential for bias.

Table 5-5: Ballarat cumulative gold RER and recovery relationship descriptive statistics

Statistic	Cone	SELFRAG	Rolls	VSI
ME	-0.0004	-0.0049	0.0018	0.0004
RMSE	0.463	0.064	0.249	0.273
R^2	0.957	0.9770	0.8464	0.8714

A t-test pooled versus unpooled variance method is used in hypothesis testing to compare data relationships described in Figure 5-3 for different crushing mode products. The data for the statistical t-test analysis is derived from this thesis gravity separation test work on Ballarat gold-bearing ores, with this data described in regression line plots shown in Figure 5-3. The pooled test is used when the variances of the two data populations are equal and the unpooled test is used when the variances of the two populations are unequal.

In the pooled variance assessment method, it is considered that "no difference" is observed between two compared crushing mode sample fitted regression line proportions, when the value is 0. A value of 0 means the observed difference will not result in the rejection of the null hypothesis (Zaiontz, 2013). If the value in H_0 is a number other than 0, then the unpooled procedure is considered for testing for a specific difference (e.g. the difference between two sample proportions (Zaiontz, 2013). In considering the "pooled" or "unpooled" procedure information, the two-sample SD's are compared (Zaiontz, 2013). As a general rule-of-thumb: if the larger sample SD is more than double the smaller sample SD, the unpooled method information has more evidentiary weight in t-test assessment (Zaiontz, 2013).

Gold upgrade versus cumulative recovery regression analysis statistical t-test pooled, and unpooled results for the Cadia sample ore linear regression pair comparisons are shown in Table 5-6 and Table 5-7. The t-test analysis of regression line slopes between the Cone vs. SELFRAG, Cone vs. Rolls, Cone vs. VSI and SELFRAG vs. VSI crushing modes suggest we would reject the H_0 in favour of the alternative hypothesis H_1. The null hypothesis H_0 is rejected since both the test statistic t value is higher than the critical t-value of 2.18 and the p-value less than alpha, 0.05. The statistical results are shown in Table 5-6, and Table 5-7 suggest that the H_0 cannot be rejected for evidence of a significant difference between the Rolls vs. SELFRAG and VSI vs. Rolls. Subsequently, failing to reject the H_0 indicates the crushing mode compared

variables did not provide sufficient evidence to conclude that the results are not significantly different between the crushing mode slope variables compared.

The evidence for rejecting the H_0 comparisons between the cone versus other crushing modes is strong based on the comparative difference between the t-value and t-crit value data presented in Table 5-6 and Table 5-7. However, Table 5-6 and Table 5-7 show weaker evidence for rejecting the H_0 for the comparison between the SELFRAG vs. VSI crushing modes, due to the p-value being close to the alpha value and the t-value of 2.28 being slightly larger than the t-crit value of 2.18, thereby reducing confidence that the decision that the difference between the regression line relationships is statistically significant. Table 5-6 and Table 5-7 information suggest that there is insufficient evidentiary weight to support using the unpooled method information based on the SD data. Therefore, the pooled method has more evidentiary weight in this t-test assessment.

Table 5-6. Fitted parameters and t-test statistics for crushing mode comparisons of Ballarat ore gold RER and recovery relationships using a pooled error variance analysis method

Statistic	Cone vs. SELFRAG	Cone vs. Rolls	Cone vs. VSI	Rolls vs. SELFRAG	VSI vs. Rolls	SELFRAG vs. VSI
S^2_{Res}	1.167	1.475	1.542	0.352	0.727	0.419
S_{b1-b2}	0.6278	0.6858	0.6979	0.3406	0.4728	0.3698
t	9.07	7.66	6.99	1.29	0.80	2.21
df	12	12	12	12	12	12
alpha	0.05	0.05	0.05	0.05	0.05	0.05
p-value	0.00000	0.00001	0.00001	0.22116	0.44149	0.04760
t-crit	2.18	2.18	2.18	2.18	2.18	2.18
Sig.	yes	yes	yes	no	no	yes

Table 5-7. Fitted parameters and t-test statistics for crushing mode comparisons of Ballarat ore gold RER and recovery relationships using an unpooled error variance analysis method

Statistic	Cone vs. SELFRAG	Cone vs. Rolls	Cone vs. VSI	Rolls vs. SELFRAG	VSI vs. Rolls	SELFRAG vs. VSI
sb1-b2	0.618	0.691	0.704	0.332	0.473	0.359
t	9.21	7.61	6.93	1.32	0.80	2.28
df	12	12	12	12	12	12
alpha	0.05	0.05	0.05	0.05	0.05	0.05
p-value	0.000001	0.000006	0.000016	0.2101	0.4413	0.0420
t-crit	2.18	2.18	2.18	2.18	2.18	2.18
Sig.	yes	yes	yes	no	no	yes

The paired t-values produced from the comparison of selected crushing modes are shown in Figure 5-4 using values taken from Table 5-6 and Table 5-7 for gold deportment statistical analysis results. The graphically displayed t-values allow comparison of the relative error difference between compared crushing modes and the Critical t-value.

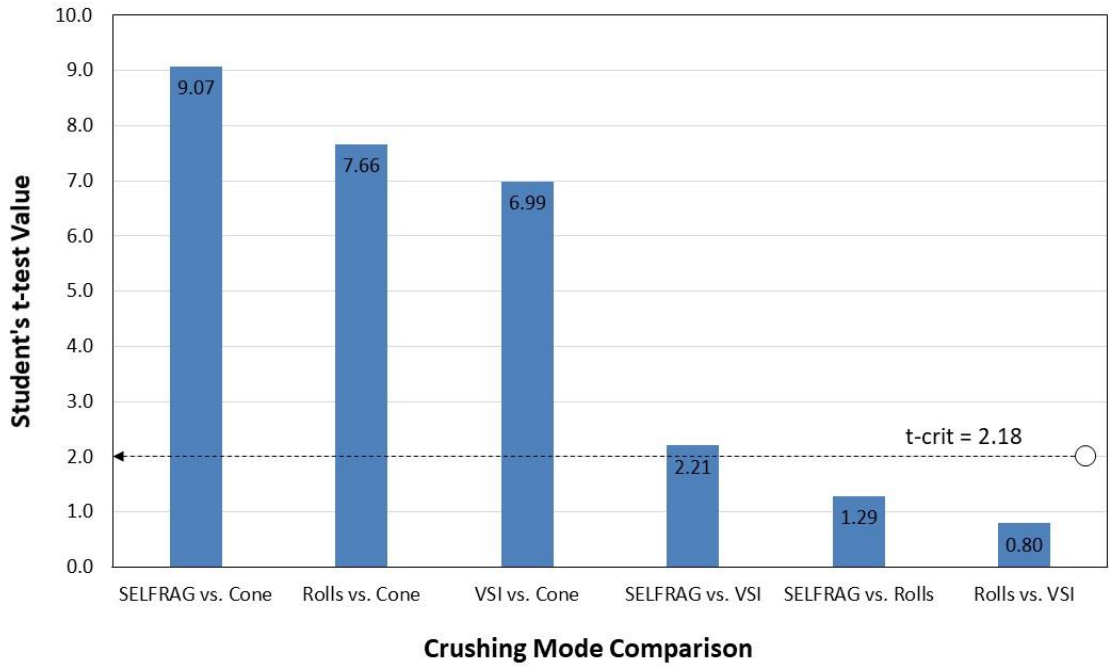

Figure 5-4. Ballarat ore Pair t-values for gold RER and gold cumulative recovery relationship as a function of crushing mode

5.4.3 Cadia ore metal gravity separation statical variance analysis between crushing modes

For Cadia ore sub-samples crushed by specified modes, Figure 5-5 graphically depicts least-squares linear regression analysis of scatter plots for the gravimetric separation relationship between sink's gold (Au) RER versus cumulative gold recovery performance across the HLS density partition range. The number of sample points available for use in this regression analysis is low, which reduces confidence in the statical analysis. However, Figure 5-5 graphical and mathematical evidence suggests that the cone and HPGR modes have similar predicted regression line characteristics, with respective line function slopes of approximately -28.5 and -27.5. Also, Figure 5-5 indicates that the SELFRAG and VSI modes have similar predicted linear slope characteristics, with slopes of approximately -15.7 and -17.0. These crushing mode comparisons showing similarities between the slope and extent of the regression lines rise over run variables may imply a gold separation performance relationship. Still, the compared crushing mode slope variables can be t-tested for hypothesis testing to

better understand relationships better. Similar regression line rise over run variables may indicate that comparable crushing modes produce similar breakage patterns between the waste and valuable component minerals.

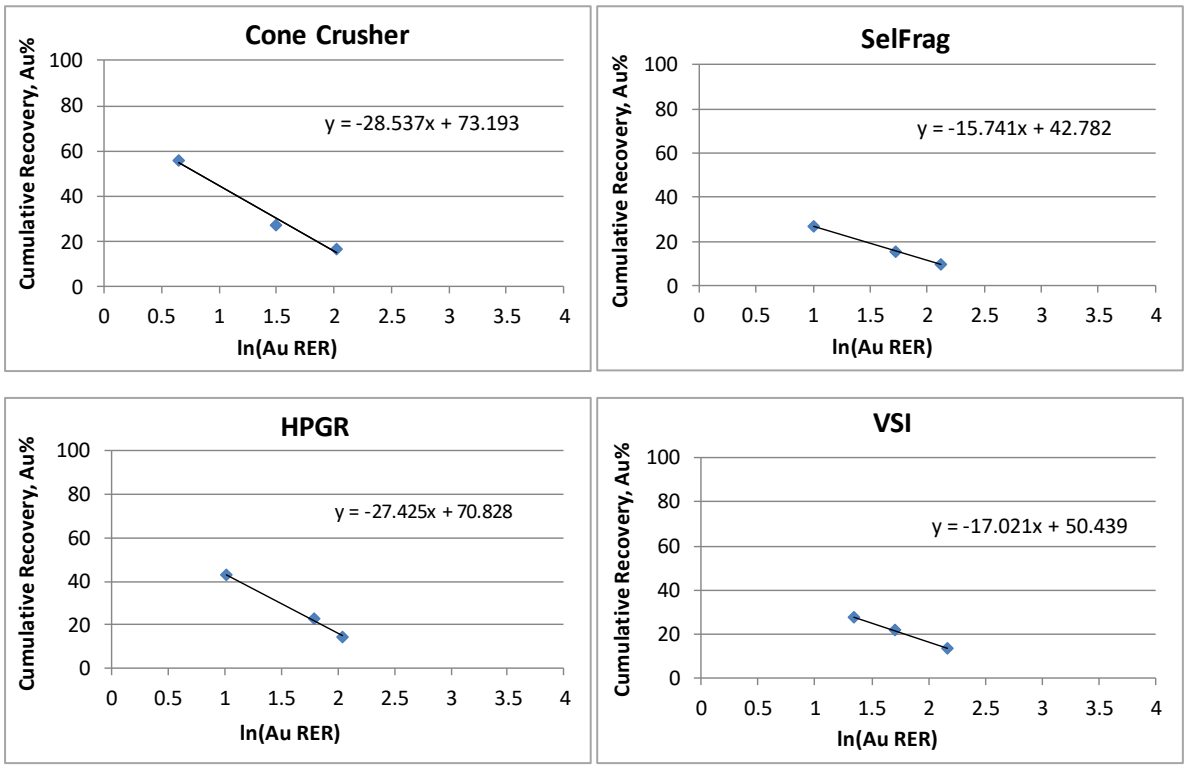

Figure 5-5. Cadia sink gold RER response as a metal upgrade versus cumulative recovery relationship by different crushing modes

Table 5-8 compares the statistical information for the crushing mode regression lines comparisons, described in Figure 5-5. The results show a high regression correlation coefficient, denoted by the R^2 values, for all the crushing modes, indicating strong robustness in modelling the grade versus recovery relationship. The SELFRAG and VSI RMSE values suggest the lowest potential for bias between the sample data mean and the population mean. The cone crusher has the highest potential for bias.

Table 5-8. Cadia cumulative gold RER and recovery relationship descriptive statistics

Statistic	Cone	SELFRAG	HPGR	VSI
ME	-0.0004	0.0003	-0.0003	0.0003
RMSE	1.228	0.051	0.367	0.088
R^2	0.9831	0.9999	0.9972	0.9993

A t-test procedure for pooled versus unpooled variance method is used in hypothesis testing to compare data relationships described in Figure 5-5 for different crushing mode products.

Table 5-9 and Table 5-10 describe the statistical t-test pooled and unpooled results for the Cadia sample ore linear regression pair comparisons for gold upgrade versus cumulative recovery regression study. The t-test analysis of regression line slopes between the HPGR vs. SELFRAG and HPGR vs. VSI crushing modes suggests evidence to reject the H_0 in favour of the alternative hypothesis H_1. The H_0 is rejected since the t value is more significant than the critical t-value of 4.30 and the p-value less than alpha 0.05. However, the statistical results shown in Table 5-9 and Table 5-10 suggest that the H_0 cannot be rejected for evidence of a significant difference between the Cone vs. SELFRAG, Cone vs. HPGR, Cone vs. VSI and the SELFRAG vs. VSI. Therefore, failing to reject the H_0 indicates the Cadia ore GRAT gravity results did not provide sufficient evidence to conclude that the results are not significantly different between the selected crushing mode slope variables compared.

Table 5-9. Fitted parameters and t-test statistics for Cadia ore sample crushing mode comparisons for gold RER and recovery relationship using pooled error variance

Statistic	Cone vs. SELFRAG	Cone vs. HPGR	Cone vs. VSI	HPGR vs. SELFRAG	VSI vs. HPGR	SELFRAG vs. VSI
S^2_{Res}	6.794	7.390	6.817	0.619	0.642	0.047
S_{b1-b2}	4.194	4.538	5.183	1.432	1.731	0.457
t	3.05	0.25	2.22	8.16	6.01	2.80
df	2	2	2	2	2	2
alpha	0.05	0.05	0.05	0.05	0.05	0.05
p-value	0.0927	0.8292	0.1564	0.0147	0.0266	0.1072
t-crit	4.30	4.30	4.30	4.30	4.30	4.30
Sig.	no	no	no	yes	yes	no

Table 5-10. Fitted parameters and t-test statistics for Cadia ore sample crushing mode comparisons for gold RER and recovery relationship using unpooled error variance

Statistic	Cone vs. SELFRAG	Cone vs. HPGR	Cone vs. VSI	HPGR vs. SELFRAG	VSI vs. HPGR	SELFRAG vs. VSI
sb1-b2	3.745	4.015	3.768	1.473	1.528	0.490
t	3.42	0.28	3.06	7.93	6.81	2.62
df	2	2	2	2	2	2
alpha	0.05	0.05	0.05	0.05	0.05	0.05
p-value	0.0760	0.8078	0.0924	0.0155	0.0209	0.1204
t-crit	4.30	4.30	4.30	4.30	4.30	4.30
Sig.	no	no	no	yes	yes	no

The evidence for failing to reject the H_0 comparisons between the Cone vs. SELFRAG, Cone vs. HPGR, Cone vs. VSI, and the SELFRAG vs. VSI crushing modes is weak based on the p-value

data shown in Table 5-9 and Table 5-10. Failing to reject the H_0 is due to the p-values number indicating lower to significantly lower than 95% confidence level in these crushing mode t-tests comparisons. Not to fail to reject the H_0 would mean the chosen alpha (α) should be larger than the existing 0.05 alpha level, reducing confidence in the decision regarding the relationship between each of the paired modes assessed.

Figure 5-6 shows the Cadia ore gold t-values for the linear regression crushing mode paired t-tests comparisons. Figure 5-6, t-value results suggest a significant difference between the SELFRAG vs HPGR and VSI and HPGR crushing mode results for RER versus cumulative gold recovery and subsequentially preferential grade by density deportment. However, there is no supporting evidence for a significant difference between the SELFRAG vs. Cone, SELFRAG vs. VSI, VSI vs. cone or the HPGR vs. Cone crushing modes.

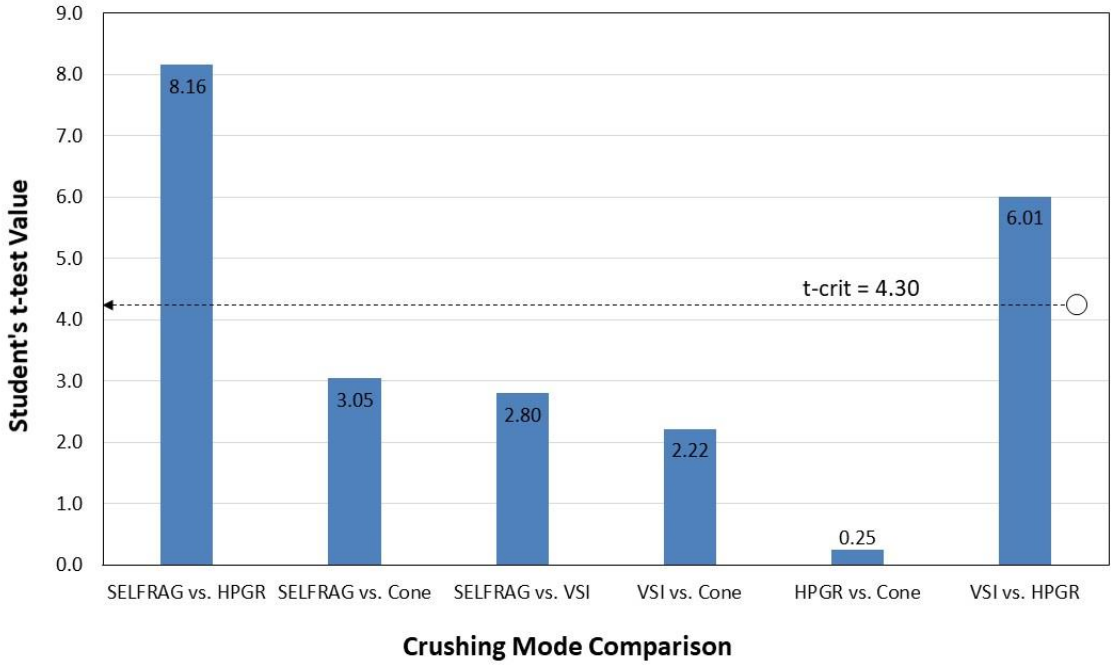

Figure 5-6. Cadia ore Pair t-values for gold RER and gold cumulative recovery relationship as a function of crushing mode

Figure 5-7 graphically describes linear regression analysis plots for the gravity separation relationship between sink's Copper (Cu) RER versus cumulative gold recovery performance over the HLS density partition range for the Cadia ore sample crushed by specified modes. Figure 5-7 graphical and mathematical evidence suggests that the cone and SELFRAG modes have similar predicted linear slope characteristics, with slopes of 49.7 and 47.9 identified in respective line functions. Also, Figure 5-7 suggests that the VSI and HPGR modes have similar

predicted linear slope characteristics, with slopes of 53.7 and 52.3. Comparing the Cone vs. SELFRAG against the VSI vs. HPGR slope and extent of the regression line's rise over run variables implies that the cone and SELFRAG modes have a slightly stronger copper separation performance than the VSI and HPGR modes. These crushing mode comparisons showing similarities between the slope and extent of the regression lines rise over run variables may imply a copper separation performance relationship. Still, the compared crushing mode slope variables need to be t-tested for hypothesis testing to better understand relationships. Similar regression line rise over run variables may indicate that comparable crushing modes produce similar breakage patterns between the waste and valuable component minerals.

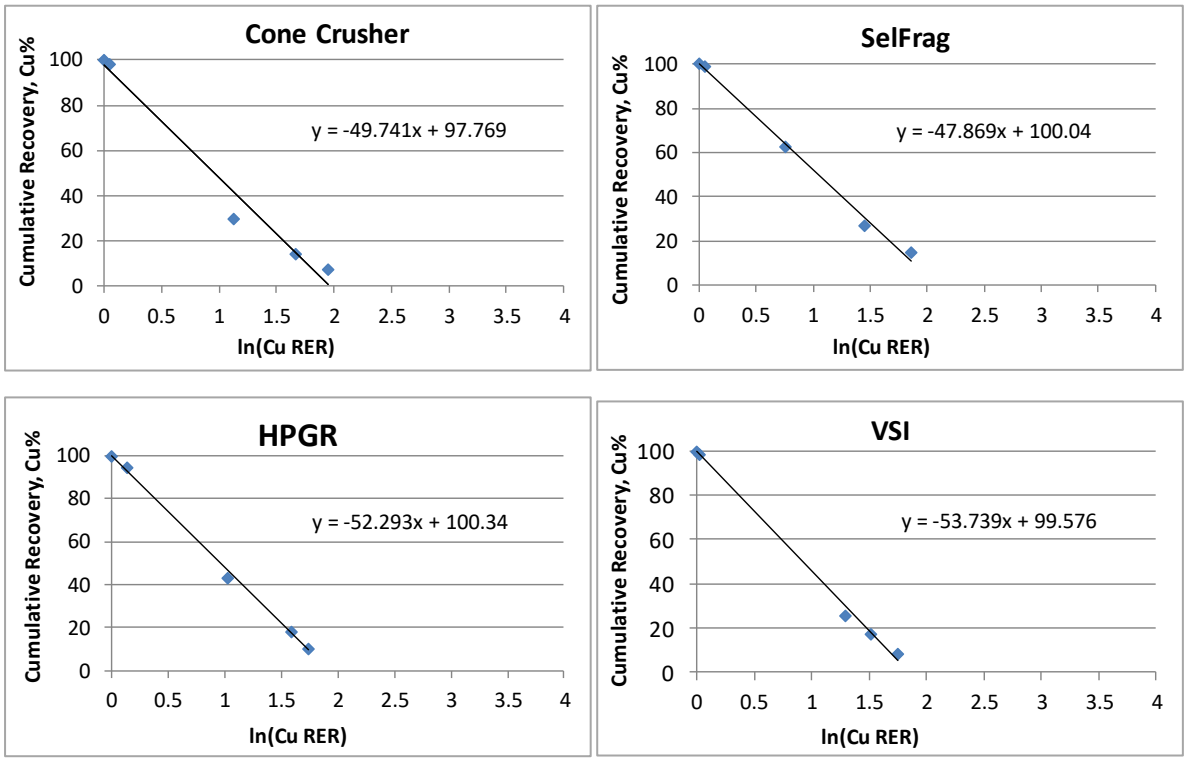

Figure 5-7: Cadia sink copper RER response as a metal upgrade versus cumulative recovery relationship by different crushing modes

Figure 5-7 shows that the predicted linear slopes appear similar, indicating a similar preferential metal deportment response. In addition, similar slopes are shown for the cone and SELFRAG modes and the HPGR and VSI modes. This evidence may indicate that similar crushing modes have similar breakage patterns between the waste and valuable component minerals.

Table 5-11 shows the statistical quality information for the crushing mode regression line comparisons, described in Figure 5-7. The results show a high regression correlation

coefficient, denoted by the R^2 values, for all the crushing modes except for the HPGR, which shows a moderate reduction. The R^2 values shown in Table 5-11 for Figure 5-7 indicate strong robustness in modelling the grade versus recovery relationship. All the crushing mode RMSE values suggest a higher potential for bias between the sample data mean, and the population mean.

Table 5-11. Cadia cumulative copper RER and recovery relationship descriptive statistics

Statistic	Cone	SELFRAG	HPGR	VSI
ME	-0.0002	-0.0005	7.1661	-0.1207
RMSE	2.837	1.044	3.993	0.896
R^2	0.9756	0.9957	0.9368	0.9976

Copper upgrade versus cumulative recovery regression analysis statistical t-test pooled and unpooled results for the Cadia sample ore linear regression pair comparisons are shown in Table 5-12 and Table 5-13. The statistical results shown in Table 5-12 and Table 5-13 suggest that the H_0 cannot be rejected for evidence of a significant difference between the Cone vs. SELFRAG, Cone vs. HPGR, Cone vs. VSI, HPGR vs. SELFRAG, VSI vs. HPGR and the SELFRAG vs. VSI. Therefore, failing to reject the H_0 indicates the Cadia ore GRAT gravity results did not provide sufficient evidence to conclude that the results are not significantly different between the selected crushing mode slope variables. The H_0 is not rejected since all the test statistic t value is under the critical t-value of 2.45. However, the p-values are high to very high in all the t-tests comparisons reducing confidence in the decision regarding the relationship between the paired modes assessed.

Table 5-12. Fitted parameters and t-test statistics for Cadia ore sample crushing mode comparisons for copper RER and recovery relationship using pooled error variance

Statistic	Cone vs. SELFRAG	Cone vs. HPGR	Cone vs. VSI	HPGR vs. SELFRAG	VSI vs. HPGR	SELFRAG vs. VSI
S^2_{Res}	38.083	7.531	38.339	36.536	7.787	38.339
S_{b1-b2}	5.061	2.383	5.036	5.045	2.406	5.036
t	0.37	1.86	0.79	0.51	0.60	0.79
df	6	6	6	6	6	6
alpha	0.05	0.05	0.05	0.05	0.05	0.05
p-value	0.7242	0.1128	0.4575	0.6311	0.5698	0.4575
t-crit	2.45	2.45	2.45	2.45	2.45	2.45
sig	no	no	no	no	no	no

Table 5-13. Fitted parameters and t-test statistics for Cadia ore sample crushing mode comparisons for copper RER and recovery relationship using unpooled error variance

Statistic	Cone vs. SELFRAG	Cone vs. HPGR	Cone vs. VSI	HPGR vs. SELFRAG	VSI vs. HPGR	SELFRAG vs. VSI
sb1-b2	4.893	2.375	4.901	4.791	2.393	4.901
t	0.38	1.86	0.82	0.53	0.60	0.82
df	6	6	6	6	6	6
alpha	0.05	0.05	0.05	0.05	0.05	0.05
p-value	0.7152	0.1119	0.4459	0.6135	0.5677	0.4459
t-crit	2.45	2.45	2.45	2.45	2.45	2.45
sig	no	no	no	no	no	no

The evidence for failing to reject the H_0 comparisons between Cone vs. SELFRAG, Cone vs. HPGR, Cone vs. VSI, HPGR vs. SELFRAG, VSI vs. HPGR, and the SELFRAG vs. VSI crushing modes is weak based on the p-value data shown in Table 5-13 and Table 5-12. Failing to reject the H_0 is due to the p-values number indicating lower to significantly lower than 95% confidence level in these crushing mode t-tests comparisons. Not failing to reject would mean the chosen alpha (α) should be larger than the existing 0.05 alpha level. However, increasing the alpha reduces the confidence in the H_0 decision regarding the relationship between each of the paired modes assessed.

Figure 5-8 shows Cadia ore sample t-values for the linear regression pair t-tests comparisons as a function of different crushing modes. Figure 5-8 t-value results suggest no supporting evidence for a significant difference between the crushing mode results for RER versus cumulative gold recovery and subsequentially preferential grade by density deportment.

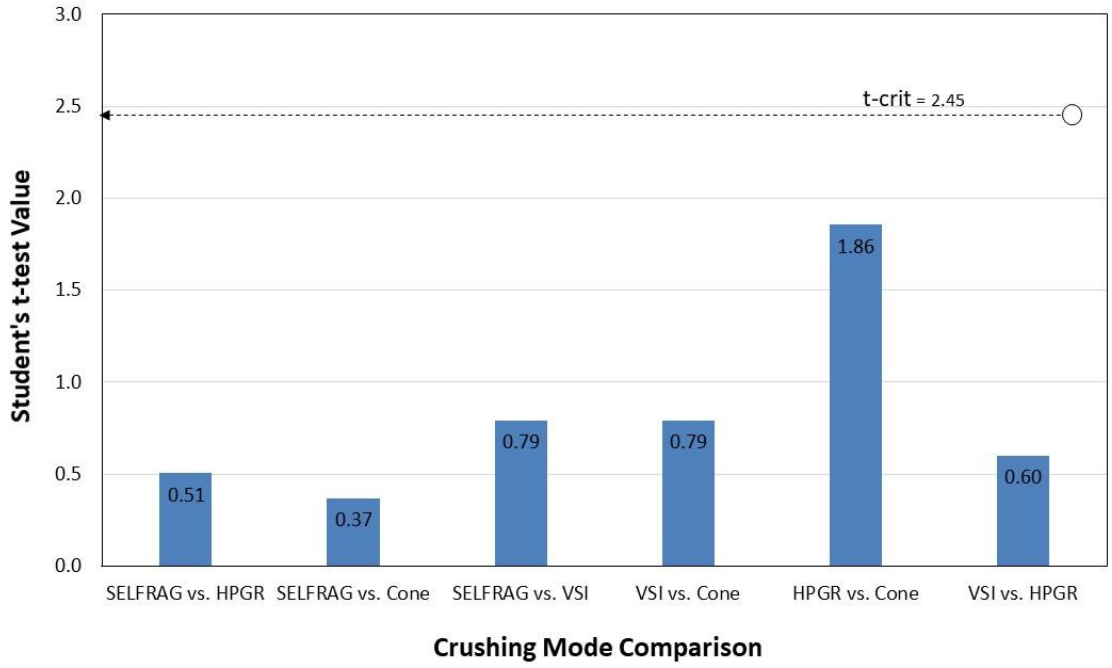

Figure 5-8. Cadia ore Pair t-values for copper RER and copper cumulative recovery relationship as a function of crushing mode

5.5 Summary

The interaction between sub-samples of the as-received gold-bearing ores received from the Ballarat CGT and Cadia CVO mining operations and different crushing modes of comminution was investigated using parametric statistical analysis methods. These methods were used to compare means and variances for the metallurgical efficiency of concentration responses, described by EDR values, from grade by density experimental separation operation observations. In this thesis, comminution was induced by laboratory scale cone crusher, SELFRAG, rolls crusher, HPGR and VSI crusher mechanisms. In this study, statistical analysis of the gold and copper EDR parameter variance was conducted to assess the magnitude of grade deportment by density separation operation, influenced by crushing methods and controlled by the natural mineralogy and textures present in the ore-deposit styles itself. In addition, grouped GRAT Ballarat and Cadia ore EDR results from specified crushing mode gravity studies were used to analyse variance between groups of means and compare regression line slopes using various statistical techniques.

Bar chart comparisons for Ballarat fine crushed ore show EDR responses that indicate the SELFRAG and HPGR modes have comparable and higher preferential gold department by density responses than the cone and VSI crushing modes. The SELFRAG and HPGR modes

produced a lower proportion of composite or incompletely liberated particles and a similar degree of silicate gangue liberation from gold-bearing particles. By comparison, the cone and, to a lesser extent, the VSI has liberation patterns that produce a higher proportion of composite or incompletely liberated particles.

Bar chart visual comparisons for Cadia fine crushed ore show EDR responses that indicate the HPGR, and the cone modes have comparable and higher preferential gold department by density responses than the SELFRAG and VSI crushing modes. This finding suggests that the HPGR and cone mode products contain a similar proportion of composite or incompletely liberated particles. The SELFRAG and VSI gold EDR suggested a similar and relatively lower degree of silicate gangue liberation from gold-bearing particles. The copper EDR values for different crushing modes indicate that the HPGR and cone modes produce a higher degree of silicate gangue liberation from copper-bearing particles. The copper EDR values for the SELFRAG, HPGR and VSI indicate a similar and higher proportion of composite or incompletely liberated particles.

An ANOVA F-test with blocking effect for Ballarat HLS sink gold EDR values for different crushing modes was completed. This test principally performs a one-way ANOVA after accounting for the variability among the density fraction 'blocks'. It is observed that when the variation between density fractions is blocked out, it can be concluded that there is a significant difference between each of the four crushing modes for the gold EDR values between density splits.

An ANOVA F-test with blocking for Cadia HLS sink gold EDR values for different crushing modes was completed. The F-test showed weak evidence of differences in preferential gold deportment into density fractions resulting from the application of different crushing modes.

An ANOVA F Test was completed with blocking effect for Cadia HLS sink copper EDR values for different crushing modes. Without blocking, it may not rightly be concluded that there is a significant difference between each of the four crushing modes for improving EDR values. There is insufficient evidence of differences in preferential copper deportment into density fractions resulting from the application of different crushing modes.

T-test analysis of the metal upgrade versus cumulative recovery slope of regression line relationships between specified crushing modes was performed on the gravity separation densimetric data produced from Ballarat and Cadia crushed ore samples. The t-test analysis results were used to test the null hypothesis (H_0), which states that there is no significant difference between selected compared crushing mode metal upgrade versus cumulative recovery slope of regression slopes. This statistical approach compared crushing modes to determine whether their specific breakage patterns induce significant differences, at a 95% confidence level, in preferential gold and copper grade by density deportment into sinks during breakage. The variables compared in the statistical analysis were the calculated metal RER parameter and cumulative metal recovery over the GRAT density partition range.

The t-test analysis of Ballarat ore gravity separation results for the gold slope of regression line relationships identified that compared SELFRAG versus (vs.) cone, rolls vs. cone, VSI vs. cone and SELFRAG vs. VSI crushing modes evidence led to the rejection of the H_0. Also, the t-test results show that there is weak evidence for a significant difference between the SELFRAG and VSI crushing modes. There is no supporting evidence for a significant difference between the SELFRAG vs. rolls or the rolls vs. the VSI crushing modes, as these crushing mode comparisons failed to reject the H_0.

The t-test analysis of Cadia ore gravity separation results for gold upgrade versus cumulative recovery slope of regression line relationships between specified crushing modes identified compared crushing modes both rejected and failed to reject the H_0. In this analysis, comparisons for the HPGR vs. SELFRAG and HPGR vs. VSI crushing modes showed rejection of the H_0. There is no supporting evidence for a significant difference between the Cone vs. SELFRAG, Cone vs. HPGR, Cone vs. VSI and the SELFRAG vs. VSI crushing modes, as these crushing mode comparisons failed to reject the H_0. However, evidence for failing to reject the H_0 is weak based on the p-value data.

The t-test analysis of Cadia ore gravity separation results for copper upgrade versus cumulative recovery slope of regression line relationships for different comparisons failed to reject the H_0. In this analysis, comparisons for the SELFRAG vs. HPGR, SELFRAG vs. cone, SELFRAG vs. VSI, VSI vs. cone, HPGR vs. cone, and VSI vs. HPGR crushing modes showed

statistical evidence of failure to reject the H_0 and no supporting evidence for a significant difference. However, evidence for failing to reject the H_0 is weak based on the p-value data.

Chapter 6. Enrichment Deportment Index (EDI) determination and application

Previous research has shown that crusher selection can improve metal and gangue liberation and gravity separation performance in coarse-scale (millimetre) particles. However, the improvements are highly dependent on the ore's geological style. Furthermore, there has been little research on a suitable metallurgical parameter for characterising gravity separation efficiency as a rock-based attribute or index until this thesis. Therefore, a linear least-squares regression modelling-based methodology is used to derive an index value for preferential grade by density deportment response. This index value predicts mineral gravity separation performance linked to the interaction of specific gold-bearing sulfide ores with different crushing modes and separation techniques.

6.1 Background

This study developed a linear least-squares regression model to derive a new parameter describing gravity separation performance for the overall magnitude of grade deportment across specific density fractions. The new parameter is called the Enrichment Deportment Index (EDI). The EDI parameter characterises densimetric data derived from the gangue rejection amenability test (GRAT). The Densimetric data was obtained for various gold-bearing sulfide ore styles, crushing modes (mechanical and SELFRAG), and the two different GRAT methodologies described in Chapter 3 of this thesis. The EDI parameter value describes the strength of a crushed gold ore's natural preferential grade by density deportment response across a mass pull range into the sinks. Therefore, the EDI parameter is a suitable interpretative technique for ore gravity separation performance characterisation. The EDI parameter describes the separation behaviour through indexing and racking the magnitude of the gravity classification responses.

It is well understood in the mining industry that coarse particle waste rejection from an active mining operation's run-off mine ore stream might affect downstream operations such as comminution, flotation, and leaching. For this reason, indexing and ranking an ore's gravity separation characteristics are beneficial to the mining industry. Characterisation of an ore's natural preferential deportment grade by density response after coarse-scale breakage allows

the identification of business value-adding strategies in mining and beneficiation. In addition, the EDI parameter value can be ranked to allow comparison of control variables, such as ore style, crushing mode, and gravity technique, in the metallurgical characterisation of gravity separation performance.

The variability and the extent of preferential grade by density deportment, following the interaction between different crushing modes, gold-bearing ores, and SG classification scheme, can be quantified by the EDI parameter value. The new EDI parameter is a function of the GRAT data calculated RER values and associated cumulative mass pulls at specified sequential density fraction intervals. The EDI parameter value describes the mathematical rate of change for the relationship between the RER parameter values and the cumulative weight (CW) reporting into the HLS sink fractions.

6.2 Enrichment Deportment Index (EDI) parameter determination

Ballarat orogenic ore gold grade deportment plots for the GRAT density classification results are shown in Figure 6-1. The plots use a linear function (Section 3.9, equation 3) LSR technique to predict best-fit lines, describing the propensity for gold deportment after breakage for the different crushing mode data. Crushing mechanisms investigated were the Sala mortar cone crusher (cone), SELFRAG Lab Selective Fragmentation (SELFRAG), rolls crusher (Rolls), and vertical shaft impactor (VSI) crusher modes. The EDI values for the crushing modes shown in Table 6-2 are very high, averaging 97.5. This high average EDI value suggests that nearly all the gold contained in the rock is transferred into the sink fractions over the GRAT density test work range. It is also observed that the best fit lines produced for the different crushing modes are all very close together. The proximity of the lines suggests that each crushing mode product contained a similar degree of gangue and metal liberated particles. The shape and extent of the lines indicated that the Ballarat ore has a naturally high propensity to release highly liberated gold particles upon breakage, regardless of the crushing mode used. Still, the EDI values shown in Table 6-2 provide evidence that differences exist between crushing modes and changes in the ore's amenability for coarse particle gangue rejection (CPGR), which may be exploitable in mine operational practice. Table 6-2 identifies that the crushing mode influenced the propensity for preferential gold deportment into the sink fractions. The EDI numeric value relative to 100 decreases from higher to lower in the following order: SELFRAG>Rolls>VSI>cone. In this case, the cone crushing mode produces the lowest recovery

of gold into sink fractions, indicating a relatively higher proportion of silicate in mineral associations with gold particles.

Cadia porphyry ore gold and copper grade deportment plots for the GRAT density classification results are shown in Figure 6-2 and Figure 6-3, respectively. These plots show LSR lines of best fit, which describe the propensity for gold and copper deportment after breakage by the cone crusher, SELFRAG, High Pressure Grinding Rolls (HPGR) and VSI modes. The best-fit lines EDI values indicate a low preferential metal (grade) deportment response for both gold and copper into the HLS density fractions. The average EDI values for gold and copper, shown in Table 6-4 and Table 6-6 are 51.3, and 46.9, respectively. Comparing the gold and copper average EDI values suggests that gold has only a slightly better grade deportment potential than copper. Information in Table 6-4 and Table 6-5 identifies the extent which individual crushing modes influence the propensity for preferential gold deportment into the sink fractions. Based on Table 6-4 and Table 6-5 results for the EDI numeric value, ordering the gold EDI results from higher to lower for the different crushing modes gives cone>HPGR>VSI>SELFRAG. Similarly, copper deportment into the sink fractions decreases in the following order of crushing mode: cone>HPGR>SELFRAG>VSI.

The Ballarat crushed ore EDI results indicate that the SELFRAG mode achieves the highest metal concentration, closely followed by the HPGR, then the VSI and cone crusher modes, respectively. Comparing differences in the EDI values for the different crushing modes provides evidence that the SELFRAG and HPGR comminution modes produce a higher degree of gangue particle liberation. By comparison, there is an indication from the Cadia EDI values for different crushing modes that suggests that the cone, HPGR, VSI and SELFRAG, modes produce a similarly high proportion composite particle with silicates. Therefore, Cadia ore EDI values indicate a relatively moderate to a low likelihood of metal deportment during density separation into the HLS sink fractions. Gold is the most substantial evidence for preferential grade by density deportment and pre-concentration. The Cadia EDI values indicate the cone crusher produces a stronger metal deportment tendency to the sink fraction than other crushing modes.

The statically quality of the LSR best fit lines for the Ballarat and Cadia ore RER versus mass pull relationship into the HLS sink is shown in Table 6-1, Table 6-3, Table 6-4, Table 6-5 and

Table 6-6. Overall, the results indicate the excellent strength of the developed models in predicting the line of best fit for the variables considered. In addition, the ME, RMSE and correlation coefficients indicate that the developed models can estimate the gold and copper percentage accepted to sink by the EDI parameter.

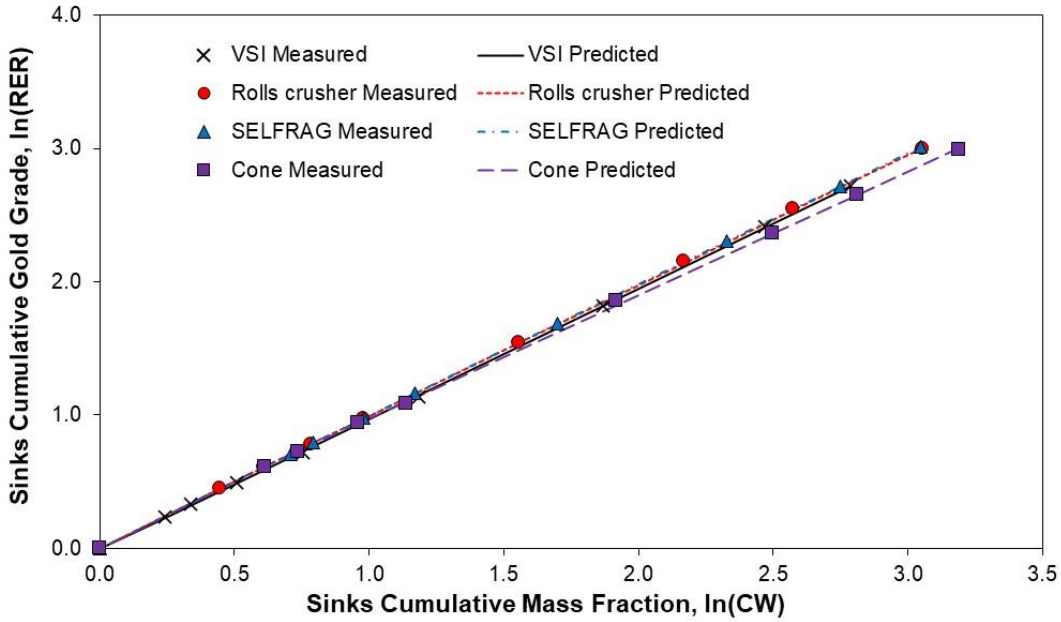

Figure 6-1. Ballarat ore preferential gold grade by Cumulative Weight (CW) deportment response (Bode et al., 2019)

Table 6-1: Ballarat ore preferential gold grade vs. CW descriptive statistics (Bode et al., 2019)

Statistic	Cone	SELFRAG	Rolls	VSI
ME	-0.010	-0.002	-0.003	0.002
RMSE	0.009	0.002	0.003	0.003
R^2	0.9991	1.0000	0.9999	0.9999

Table 6-2. Ballarat ore gold grade vs. CW deportment slope and EDI responses by crushing mode (Bode et al., 2019)

Breakage Mode	Slope (b)	EDI
Cone	0.947	94.7
SELFRAG	0.990	99.0
Rolls	0.987	98.7
VSI	0.974	97.4

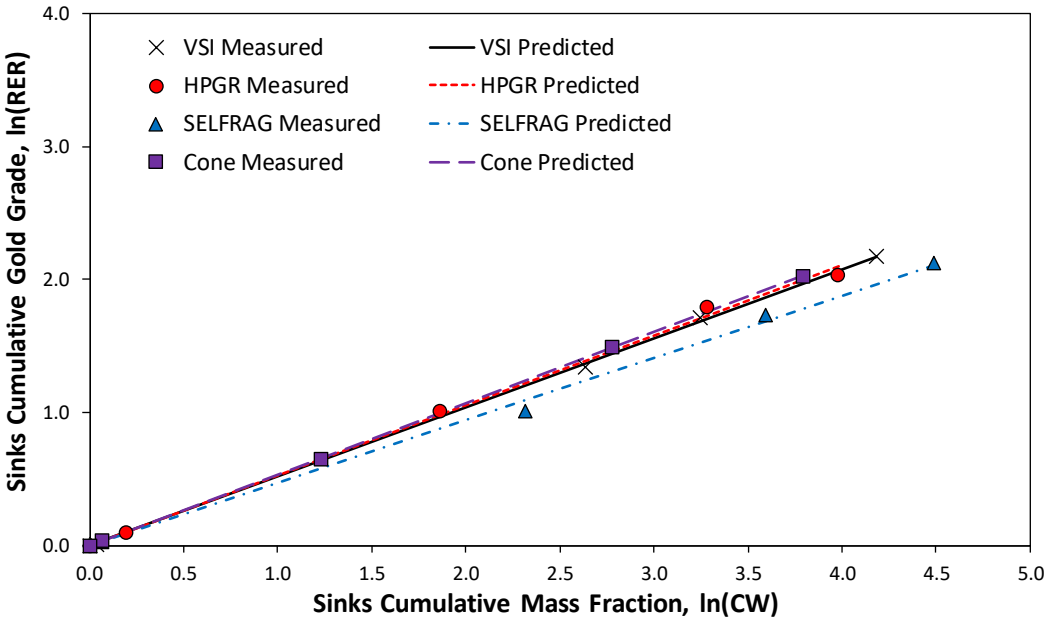

Figure 6-2. Cadia ore preferential gold grade by CW deportment response

Table 6-3: Cadia ore preferential gold grade vs. CW descriptive statistics

Statistic	Cone	SELFRAG	HPGR	VSI
ME	0.001	0.008	-0.003	0.003
RMSE	0.002	0.018	0.019	0.007
R^2	1.0000	0.9978	0.9975	0.9996

Table 6-4. Cadia ore gold grade vs. CW deportment slope and EDI responses by crushing mode

Breakage Mode	Slope (b)	EDI
Cone	0.535	53.5
SELFRAG	0.470	47.0
HPGR	0.528	52.8
VSI	0.520	52.0

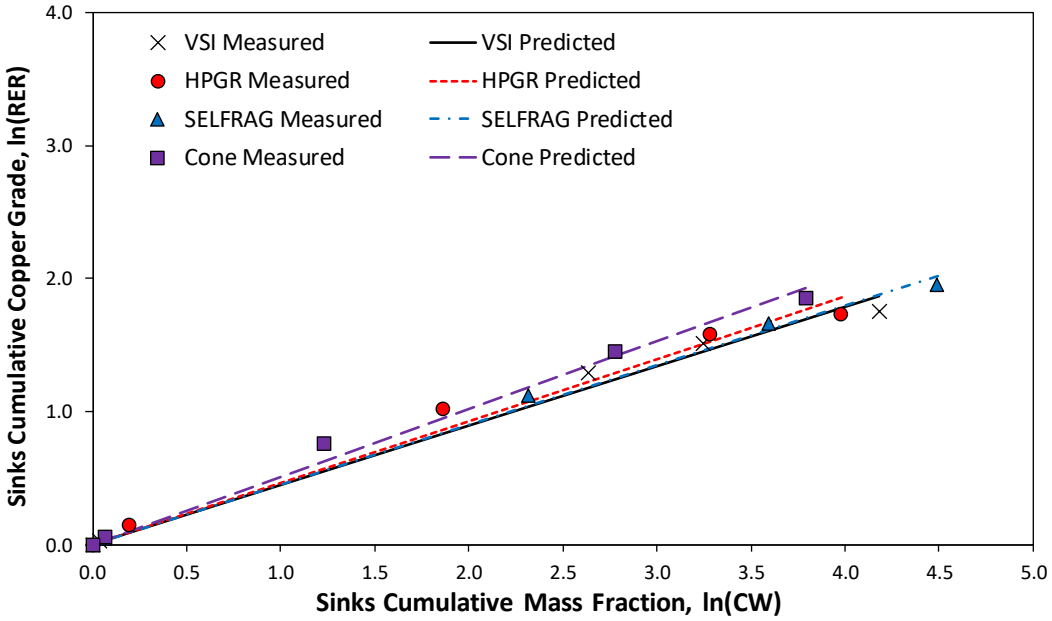

Figure 6-3. Cadia ore preferential copper grade by CW deportment response

Table 6-5: Cadia ore preferential copper grade vs. CW descriptive statistics

Statistic	Cone	SELFRAG	HPGR	VSI
ME	-0.025	-0.013	-0.028	-0.013
RMSE	0.032	0.023	0.042	0.035
R^2	0.9905	0.9958	0.9830	0.9891

Table 6-6. Cadia ore copper grade vs. CW deportment slope and EDI responses by crushing mode

Breakage Mode	Slope (b)	EDI
Cone	0.509	50.9
SELFRAG	0.451	45.1
HPGR	0.467	46.7
VSI	0.447	44.7

6.3 EDI characterisation of Ballarat and Cadia crushed ores

EDI values derived for different ore types and fine crushing breakage modes can be used in generating partition curves to describe metal deportment between HLS float and sink fractions as a function of cumulative weight or mass yield (pull) to sink. In addition, the partition curves can be used to describe the grade by density classification and variability of CPGR and metal pre-concentration relationships.

Comparative response of the accumulative metal yield into sinks and the grade deportment into floats and sinks against sinks mass pull is shown via partition lines for different crushing

modes in Figure 6-4 for crushed Ballarat gold ore. Similarly, in Figure 6-5 and Figure 6-6, the same type of information is shown for crushed Cadia ore.

The partition curves are produced using EDI values, provided in Section 6.2 of this thesis. The EDI values characterise the extent of CPGR and the metal pre-concentration response as a function of sink mass pull. Figure 6-4, Figure 6-5, and Figure 6-6 curves show that when optimising the overall CPGR beneficiation strategy, the implications of variability from ore mineralogical heterogeneity, texture, grade, and mode of breakage must be investigated. As these variables significantly influence differences in gravity, separation response shown by changes in the shape and extent of the partition curves and their consideration will maximise the preconcentration potential of different valuable components.

Figure 6-4 shows the partition curves generated for the Ballarat free-milling gold-bearing sulfide ore sample. Excellent separation performance is achieved with the Ballarat ore, and the misplacements of the gold in float and sink fractions are minimal. Metal deportment is shown to change with mass pull, depending on the method of particle breakage. Overall, the Ballarat ore sample demonstrates strong amenability for gangue rejection and metal pre-concentration in the float and sink fractions for all crushing modes examined.

Figure 6-4 indicates that overall, considering gold grade and recovery, the HPGR crushing mode achieves a better CPGR response for the Ballarat ore sample. Figure 6-5 and Figure 6-6 show that the cone crushing mode achieves the best CPGR response for the Cadia ore sample.

Figure 6-5 and Figure 6-6 show the partition curves generated for the Cadia polymetallic gold-bearing sulfide ore sample. Compared to the Ballarat results, lower separation performance is achieved with the Cadia ore due to the higher misplacements of the gold and copper in float and sink fractions during the HLS process. In addition, metal deportment is shown to change with mass pull, depending on the method of particle breakage. Overall, the Cadia ore sample demonstrates weaker amenability for gangue rejection and metal pre-concentration in the float and sink fractions, respectively, for all crushing modes examined.

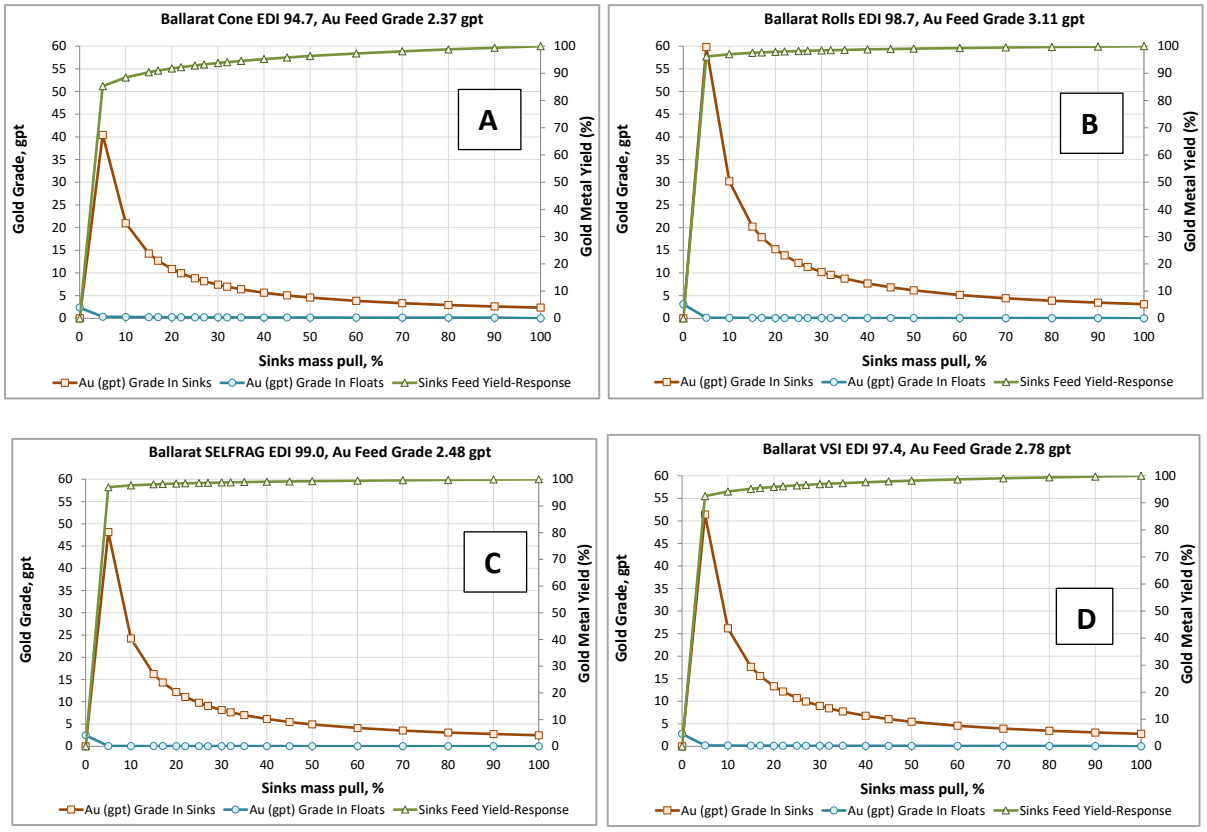

Figure 6-4. Ballarat ore gold EDI response grade versus mass density partition curves for (A) Cone crusher, (B) Rolls crusher, (C) SELFRAG, and (D) VSI crushing modes

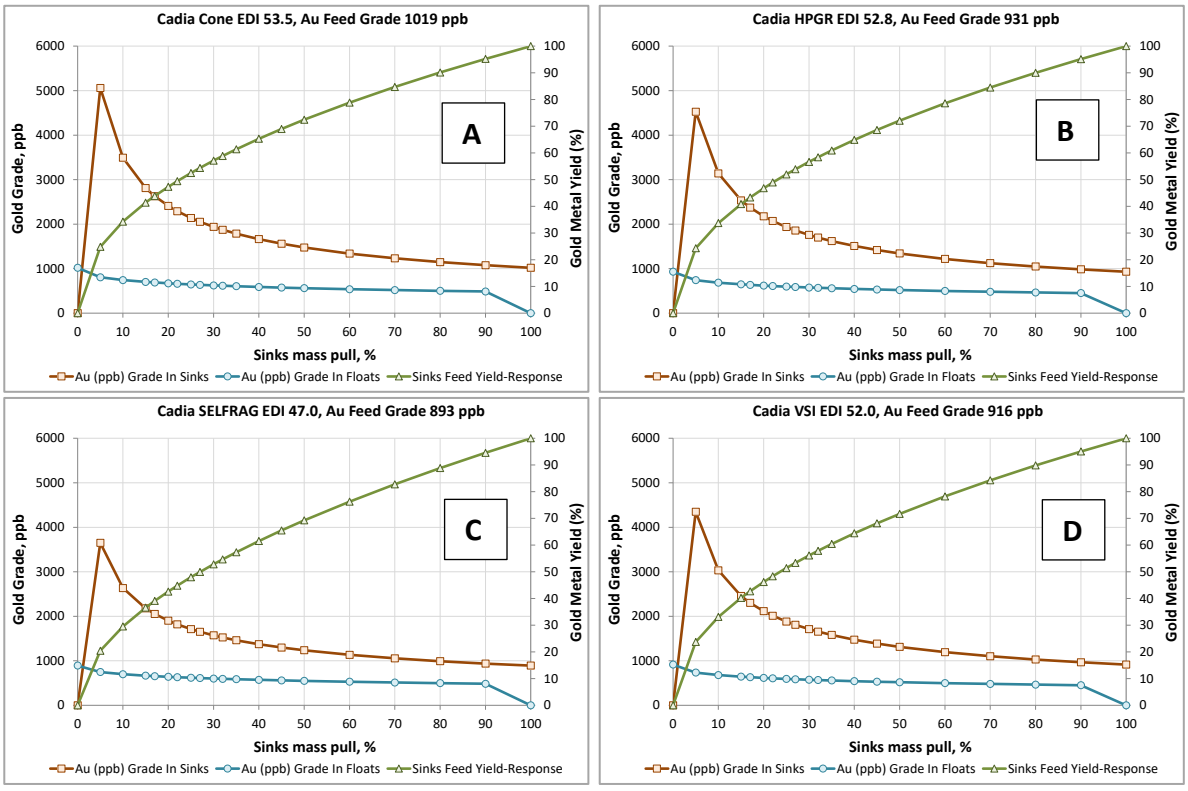

Figure 6-5. Cadia ore gold EDI response grade versus mass density partition curves for (A) Cone crusher, (B) HPGR, (C) SELFRAG, and (D) VSI crushing modes

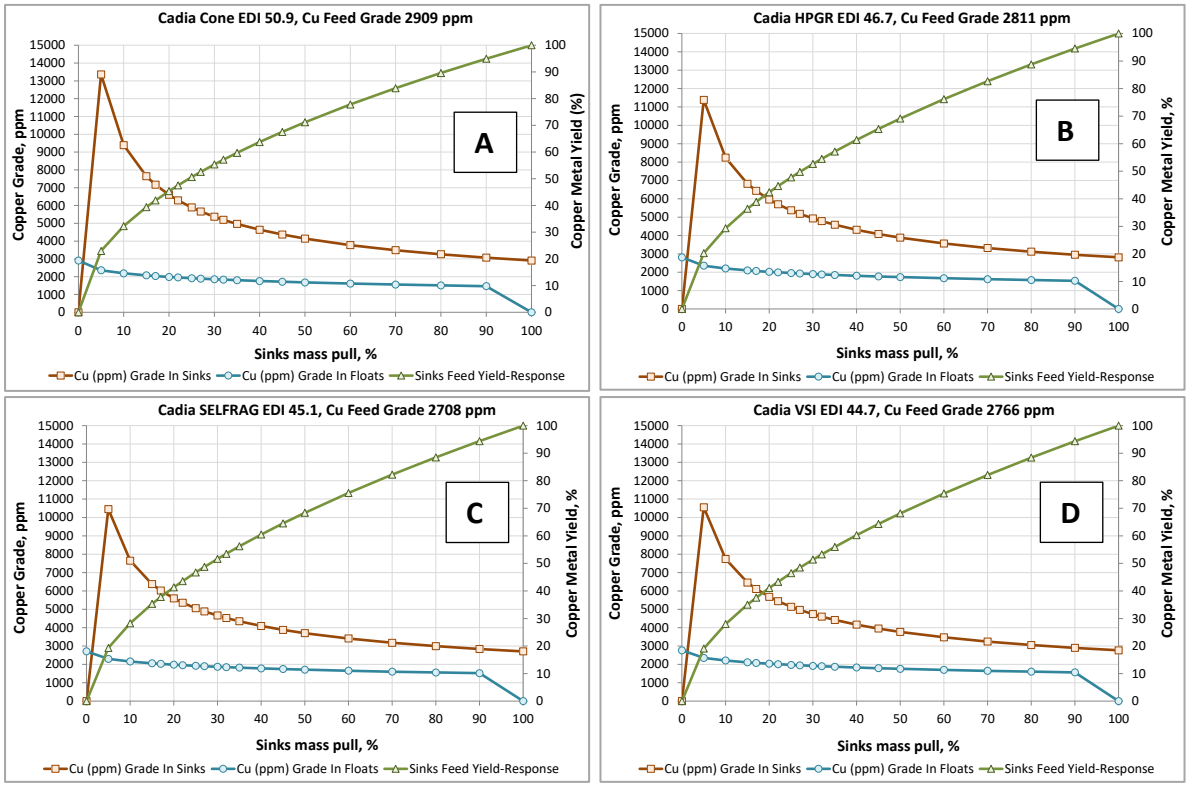

Figure 6-6. Cadia ore copper density EDI value predicted grade versus mass pull partition curves for (A) Cone crusher, (B) HPGR, (C) SELFRAG, and (D) VSI crushing mode responses

6.3.1 Validate EDI response predictions against actual gravity results

The EDI parameter approach was validated in this thesis by comparing EDI predicted gold (Au) and copper (Cu) metal yields at different mass pulls to sinks from calculated partition curves. Where the EDI parameter predicts the metal enrichment ratio at different mass pulls linked to the specific gravity separation operations. The EDI predicted Au and Cu metal yields were compared against the GRAT measured densimetric metal yield results. The EDI parameter calculated metal yields, and GRAT measured metal yields were obtained from the Ballarat and Cadia balanced GRAT densimetric classification results for selected gold-bearing ore shown in Appendix 2 and 3.

A comparison of observed measured and predicted yield values show variability in some instances. The variability may arise from but is not limited to:

1. The sampling practises.
2. Analytical and mass measurement errors in experimental results.
3. Error in the least-squares regression analysis approach to determining the EDI parameter.

Table 6-7 shows the Ballarat ore GRAT measured, and EDI predicted gold yields at different gravity separation mass pulls from density classification studies for selected fine crushing modes. Table 6-7 observed results indicate reasonable agreement between measured and predicted values.

Table 6-7. Ballarat density classification measured and predicted gold yields per specified separation class

Sink Density Fraction (g/ml)	Cone			SELFRAG			Rolls			VSI		
	Cum. Sink Mass (%)	Meas. Au Yield (%)	Pred. Au Yield (%)	Cum. Sink Mass (%)	Meas. Au Yield (%)	Pred. Au Yield (%)	Cum. Sink Mass (%)	Meas. Au Yield (%)	Pred. Au Yield (%)	Cum. Sink Mass (%)	Meas. Au Yield (%)	Pred. Au Yield (%)
2.65	54.0	99.6	96.8	49.2	100.0	99.3	63.8	99.98	99.4	78.6	99.88	99.4
2.70	47.9	98.9	96.2	45.2	99.9	99.2	54.4	99.83	99.2	71.2	99.23	99.1
2.75	38.2	97.6	95.0	37.5	99.7	99.0	45.5	99.36	99.0	60.1	98.31	98.7
2.80	32.1	95.0	94.1	31.0	98.8	98.8	37.5	98.98	98.7	47.0	96.58	98.1
2.85	14.7	94.1	90.3	18.3	98.5	98.3	21.1	98.61	98.0	30.6	95.67	97.0
2.90	8.2	86.8	87.6	9.7	97.8	97.7	11.4	98.09	97.2	15.4	94.92	95.3
2.95	6.0	85.5	86.2	6.4	97.1	97.3	7.6	97.12	96.7	8.5	94.50	93.8
3.00	4.1	81.9	84.4	4.7	96.6	97.0	4.7	94.12	96.1	6.2	93.70	93.0

Napier-Munn (2014) described an F-test method to compare the measured and predicted yields fitted to mass pull to identify the accuracy and reliability of the EDI parameter in predicting separation performance. This method described a common null hypothesis (Ho) test to analyse variance by the F-test evaluating the equality of two variances between two groups. In this analysis, the null hypothesis is rejected when the calculated F-test p-value, or probability value, is smaller than the F-test alpha (α) level (Napier-Munn, 2014). The null hypothesis should not be rejected if the calculated f value is smaller than the test critical F Value, taken from the published F-table (Napier-Munn, 2014). The F-test analysis shown in Table 6-8 for Table 6-7 data determines whether the variances of the Ballarat measured and predicted gold yield classification data are statistically different. In Table 6-8 a one-tailed F-test analysis is used to test statistical differences, as described by Snedecor & Cochran (1983). The one-tailed tests suggest whether the measured gold yield variance is greater than or less

than the EDI parameter gold predicted variance (Snedecor and Cochran, 1983; Napier-Munn, 2014). Acronyms used in the F-test included the standard deviation (S) of a sample, sample number (n), and degrees of freedom (df) (Napier-Munn, 2014). The F-test findings show there is not enough evidence to reject the null hypothesis, and thereby the variances of the gold yield measured and predicted value groups are equal. This analysis identifies the EDI parameter as a reasonable predictor of the measured gold yield in sink fractions over the density range investigated for different crushing mode products assessed.

Table 6-8. F-test assessment of the gold measured and predicted yields in Ballarat density classification products by crushing mode

Statistic	Cone	SELFRAG	Rolls	VSI
S Measured 1	6.761	1.297	1.918	2.302
n Measured 1	8	8	8	8
df Measured 1	7	7	7	7
S Predicted 2	4.842	0.894	1.243	2.481
n Predicted 2	8	8	8	8
df Predicted 2	7	7	7	7
F Ratio of Variances	1.950	2.105	2.379	0.861
α	0.05	0.05	0.05	0.05
One-tailed Test (Left Tail)				
Lower Critical F Value	0.264	0.264	0.264	0.264
p-value	0.801	0.826	0.862	0.424
Decision	Do not reject H_o	Do not reject H_o	Do not reject H_o	Do not reject H_o
One-Tailed test (Right Tail)				
Upper Critical F Value	3.787	3.787	3.787	3.787
p-value	0.199	0.174	0.138	0.576
Decision	Do not reject H_o	Do not reject H_o	Do not reject H_o	Do not reject H_o

Table 6-9 and Table 6-10 show Cadia measured and predicted results for gold and copper yields produced from this Thesis densimetric classification studies for selected crushing modes. Table 6-9 and Table 6-10 results indicate reasonable observed agreement between measured and predicted values. However, the statistical significance of the apparent relationship requires testing.

Similar to the Ballarat data statical analysis, an F-test methodology was used to compare the Cadia measured and predicted gold and copper yields for different mass pulls, respectively. In addition, this methodology estimated the accuracy and reliability of the EDI parameter in

predicting separation performance. The F-test findings show there is insufficient evidence to reject the null hypothesis. Therefore, the variances of both the gold and copper yield measured and predicted value groups are equal. Subsequentially, this analysis identifies the EDI parameter as a reasonable predictor of the measured gold yield in sink fractions over the density range investigated for different crushing mode products assessed.

Table 6-9. Cadia density classification measured and predicted gold yields per specified density separation fraction

Sink Density Fraction (g/ml)	Cone			SELFRAG			HPGR			VSI		
	Cum. Sink Mass (%)	Meas. Au Yield (%)	Pred. Au Yield (%)	Cum. Sink Mass (%)	Meas. Au Yield (%)	Pred. Au Yield (%)	Cum. Sink Mass (%)	Meas. Au Yield (%)	Pred. Au Yield (%)	Cum. Sink Mass (%)	Meas. Au Yield (%)	Pred. Au Yield (%)
2.55	100.0	100.0	100.0	99.9	100.0	99.9	99.9	100.0	100.0	100.0	100.0	100.0
2.65	93.7	97.3	97.0	93.3	95.8	96.4	82.1	90.0	91.1	95.9	96.9	98.0
2.75	29.3	55.9	56.5	9.8	26.9	29.2	15.5	42.8	41.5	7.2	27.4	28.3
2.85	6.2	27.6	27.4	2.7	15.4	14.7	3.7	22.5	21.1	3.9	21.5	21.1
2.95	2.3	17.1	17.3	1.1	9.4	9.2	1.9	14.3	15.4	1.5	13.4	13.3

Table 6-10. Cadia density classification measured and predicted copper yields per specified density separation fraction

Sink Density Fraction (g/ml)	Cone			SELFRAG			HPGR			VSI		
	Cum. Sink Mass (%)	Meas. Cu Yield (%)	Pred. Cu Yield (%)	Cum. Sink Mass (%)	Meas. Cu Yield (%)	Pred. Cu Yield (%)	Cum. Sink Mass (%)	Meas. Cu Yield (%)	Pred. Cu Yield (%)	Cum. Sink Mass (%)	Meas. Cu Yield (%)	Pred. Cu Yield (%)
2.55	100.0	100.0	100.0	99.9	100.0	99.9	99.9	100.0	99.9	100.0	100.0	100.0
2.65	93.7	98.9	96.9	93.3	98.1	96.3	82.1	94.7	90.0	95.9	98.7	97.7
2.75	29.3	62.8	54.7	9.8	30.2	27.9	15.5	43.2	37.0	7.2	26.1	23.3
2.85	6.2	26.7	25.5	2.7	14.4	13.8	3.7	18.3	17.3	3.9	17.7	16.6
2.95	2.3	14.5	15.7	1.1	7.9	8.4	1.9	10.6	12.1	1.5	8.8	9.8

Table 6-11. F-test assessment of the gold measured and predicted yields in Cadia density classification products by crushing mode

Statistic	Cone	SELFRAG	HPGR	VSI
S Measured 1	38.397	44.653	39.070	42.852
n Measured 1	5	5	5	5
df Measured 1	4	4	4	4
S Predicted 2	38.297	44.683	39.436	43.111
n Predicted 2	5	5	5	5
df Predicted 2	4	4	4	4
F Ratio of Variances	1.005	0.999	0.981	0.988
α	0.05	0.05	0.05	0.05
One-tailed Test (Left Tail)				
Lower Critical F Value	0.157	0.157	0.157	0.157
p-value	0.502	0.499	0.493	0.495
Decision	Do not reject H_o	Do not reject H_o	Do not reject H_o	Do not reject H_o
One-Tailed test (Right Tail)				
Upper Critical F Value	6.388	6.388	6.388	6.388
p-value	0.498	0.501	0.507	0.505
Decision	Do not reject H_o	Do not reject H_o	Do not reject H_o	Do not reject H_o

Table 6-12. F-test assessment of the copper measured and predicted yields in Cadia density classification products by crushing mode

Statistic	Cone	SELFRAG	HPGR	VSI
S Measured 1	39.682	45.402	41.968	45.231
n Measured 1	5	5	5	5
df Measured 1	4	4	4	4
S Predicted 2	39.154	45.167	41.100	45.328
n Predicted 2	5	5	5	5
df Predicted 2	4	4	4	4
F Ratio of Variances	1.027	1.010	1.043	0.996
α	0.05	0.05	0.05	0.05
One-tailed Test (Left Tail)				
Lower Critical F Value	0.157	0.157	0.157	0.157
p-value	0.510	0.504	0.516	0.498
Decision	Do not reject H_o	Do not reject H_o	Do not reject H_o	Do not reject H_o
One-Tailed test (Right Tail)				
Upper Critical F Value	6.388	6.388	6.388	6.388
p-value	0.490	0.496	0.484	0.502
Decision	Do not reject H_o	Do not reject H_o	Do not reject H_o	Do not reject H_o

6.4 Summary

A new parameter, called the EDI parameter, has been derived to quantify the extent of the gravity separation performance and measure the overall magnitude of grade deportment by density response as a relative index value. The EDI parameter value is determined from the slope the of LSR linear model line of best fit for bivariate data, comparing the RER parameter values versus CW or mass pull into the sink's fractions. In this thesis, the EDI parameter describes the mathematical rate of change in the relationship between the RER and CW variables, determined from the GRAT method HLS separation operations. The EDI parameter value is the enrichment rate of change relative to mass deportment into the sink as a function of ore type and mode of comminution. The EDI parameter quantifies the propensity of ore to preferentially deport metal into specific gravity separation product fractions through a single estimator metric.

In this study, an EDI parameter value of 100 implies a perfect separation of valuable components into a separation density sink product with no waste minerals present. Conversely, an EDI value of 0 implies no separation between the valuable component and waste minerals during classification operation. Subsequentially, after the EDI equals 100 percent, the gravity classification efficiency must decline in proportion to the progressive addition of waste minerals to the metal value concentrate.

Generally, high EDI values are predicted for the Ballarat ore, indicating strong preferential deportment of the gold into the HLS sink product, relative to mass pull, for all crushing modes. The high EDI values suggest that a high proportion of the gold contained in the crushed parent rock is preferentially transferred into the sink during the GRAT. The high EDI values also indicate that a high degree of gold particle liberation is achieved during fine crushing.

For the Ballarat ore, the influence of the different crushing modes on improving the propensity for preferential gold deportment into the sink fractions decreases in the following: SELFRAG>HPGR>VSI>cone. For this ore, the cone crushing mode produced the lowest recovery of gold into the sink fractions, indicating a relatively higher proportion of silicate in mineral associations with gold particles.

For the Cadia ore, generally low EDI values are predicted for gold and copper, indicating weaker preferential deportment of those metals into the HLS sink product, relative to mass pull, for all crushing modes. In addition, the low EDI values suggest a low separation efficiency of the ore valuable metals into the sink during densimetric separation. Finally, the low gold and copper EDI values may also suggest that a lower degree of valuable component particle liberation was produced by selected fine crushing investigated on Cadia ore.

For the Cadia ore, the influence of the different comminution modes on improving the propensity for preferential gold deportment into the sink fractions decreases in the following order: cone>HPGR>VSI>SELFRAG. For copper, the propensity for preferential gold deportment into the sink fractions is cone>HPGR>SELFRAG>VSI.

This thesis demonstrated that the EDI values could predict metal grade and yield partition curves for metal deportment between HLS float and sink fractions and metal yield into sinks at different HLS sink mass pulls. The EDI value describes the strength of the coarse particle gangue rejection (CPGR) and metal pre-concentration responses in a single metric. It is related to the metallurgical efficiency of the concentration operation. The determination of predicted grade and yield versus density mass pull partition curves describes the variability of CPGR and metal pre-concentration relationships, influenced by ore type and the equipment mode of particle comminution. Subsequentially, the EDI parameter can be a method to access separation efficiency from partition curves.

In Section 6.3.1, validation of the Ballarat and Cadia ore EDI predicted values for gold and copper metal yields into sinks was compared against measured GRAT experimental yield results at different sinks mass yields linked to specific gravity (SG) separation operations. The measured GRAT experimental yield values were calculated by mass balancing the GRAT data, shown in Appendix 2 and 3. The statistical evidence from this comparison suggested good agreement between the EDI parameter predicted metal yield values and the GRAT measured data metal yields at different density separation operations. This study implies that the EDI value can describe the strength of the preferential metal (grade) deportment by density response, in a single parameter, as a real effect. Subsequently, the EDI parameter can estimate changes in selected grade and metal yield responses in selected gravity product fractions during classification at different sink percentage mass yields across a density range.

Furthermore, separate EDI parameter values for different valuable metals can be determined for a gold-bearing ore to predict their magnitude of gravity classification responses during fine crushing.

The Ballarat orogenic and Cadia copper-gold ore produced significant variability in EDI parameter values for the metals of interest, demonstrating sensitivity to changes between the interaction of ore type, crusher mode and density-base separation. The EDI parameter value is demonstrated as capable of indexing and ranking a gravity separation operation preferential grade by density deportment response, linked to the interaction between specific gold-bearing sulfide ores and different fine crushing regimes. In addition, the EDI parameter response value is suitable for identifying gravity separation performance pre-concentration responses for valuable components in ore, following the fine crushing of ore, for mineral resources not yet processed.

Chapter 7. Conclusion and recommendations

This chapter summarises the thesis conclusions alongside the objectives used to test the hypothesis and recommendations for future work.

7.1 Problem statement validation, hypothesis testing and claims for novel contributions

This thesis validated the problem statement described in Section 1.2 by the work completed and summarised in Section 7.1.1 below. The problem statement expressed that mathematically derived parameters that quantitatively predict preferential metal deportment between metal-rich and gangue particles in specific density fractions remain inadequate, principally for particle sizes above 1.18 millimetres. This study demonstrated mathematically derived parameters capable of quantifying, indexing, and ranking the propensity of gold-bearing sulfide ore to preferentially concentrate metal into specific density fractions after the breakage in gold-bearing ore particle sizes up to 4.75 mm.

The extent to which the study results hold for the thesis hypothesis is confirmed in sections 4.4 and 6.2. In these sections, metallurgical parameters coined the “rejection enrichment ratio” (RER), and “enrichment deportment response” (EDR) demonstrated predictions for the grade enrichment ratio and preferential grade by density deportment response during coarse particle gangue rejection (CPGR) in the gravity separation process. In addition, the metallurgy parameter coined “enrichment deportment index” (EDI) parameter was determined by

mathematical technique as the uniform response value for the EDR parameter values. The EDI parameter measures the gravity process magnitude of grade deportment by density response during gangue rejection. The EDI parameter value can numerically predict grade deportment response into float and sink fractions across a specified density split range at different mass pulls for a gold-bearing ore after breakage by various fine crushing mechanisms. The EDI parameter was used to calculate metal yields in float and sinks fractions to compare against measured yields for specific density fractions to validate the accuracy of EDI parameter predictions for crushed Ballarat and Cadia ores.

7.2 Characterising and quantifying ore for preferential metal deportment responses

This research demonstrated a new analytical method capable of characterising and quantifiably measuring preferential gold deportment responses in density separations, as a function of gangue liberation and rejection, for a variety of fine crushed products. The methodology focused on measuring preferential grade by density deportment response in crushed gold-bearing sulfide ore by characterising gravity separation performance with new metallurgical parameters. The new parameters developed in this thesis were calculated from the gangue rejection amenability test (GRAT) classification data produced from the interaction of mechanical and non-mechanical mode breakage, gold-bearing ore styles and gravity separation techniques. The GRAT methodology was shown sensitive enough to indicate the natural amenability of Ballarat and Cadia ores to exhibit changes in the propensity for metal concentration by variation of the separation density with particle size in the particle size range 4.75 mm to 0.30 mm, after mechanical and non-mechanical modes breakage.

This research showed that classification method responses evaluated are a function of the interaction of the natural heterogeneity of an ore's mineralisation and preferential breakage induced by the selected crushing mode. The researched characterisation method also relied on constructed plotted partition curves and least-squares regression modelling to support these study findings for variability between crushing mode interaction with ore and separation scheme. The partition curves for Ballarat and Cadia GRAT data identified key performance factors, including the separation specific gravity (SG) cutpoints, ’coarse particle gangue rejection’ (CPGR) separation response and the preferential metal (grade) deportment by density response for gold and copper.

The study has demonstrated the ability of new a mathematical approach capable of characterising the GRAT gravity separation empirical data. This dissertation developed three metallurgy parameters to describe gravity separation metallurgical efficiency of metal concentration for particle sizes of ≤4.75 mm. These parameters were coined the rejection enrichment ratio (RER), enrichment deportment response (EDR) and enrichment deportment index (EDI). The RER and EDR parameters provided a statistically robust prediction of the grade enrichment ratio and preferential grade by density deportment response within sink fractions during gangue removal. Where preferential grade by density deportment response, during gravity separation, describes the propensity for the gold-bearing ores to exhibit preferential breakage leading to the concentration of metal into either specific size or SG fractions. The EDI parameter characterised the overall magnitude of preferential metal deportment response as a uniform response value for the EDR results produced from sequential heavy liquid separation (HLS) processes.

The comparative response of the GRAT method size and density separation performance results for Ballarat and Cadia gold-bearing sulfide ores commuted by different crushing modes identified:

i. Ballarat and Cadia gold-bearing sulfide ore size by size gold or copper preferential deportment response showed significant gold deportment by size variation between metal-rich and gangue particles in size fractions for all the different crushing modes studied.

ii. Ballarat ore gold RER results suggested an overall weak preferential grade by size deportment response. The SELFRAG RER values indicate a weak to moderate gold pre-concentration potential into the sieve oversize (O/S) below a 600 micron particle size, as did the cone crusher above a particle size of 212 microns. Conversely, the rolls crusher and VSI RER results suggested gold pre-concentration into the screen undersize U/S below a 600 micron particle size.

iii. Ballarat gold-bearing sulfide ore preferential grade by size deportment EDR response results indicated strong gold responses under the influence of all the different crushing modes studied. The SELFRAG and rolls crusher produced comparable and the

best results among the crushing modes investigated in this study. Subsequential, the SELFRAG and HPGR modes crushed products produced the highest gangue liberation and metal pre-concentration opportunity during gravity separation.

iv. Cadia gold RER results suggested an overall moderate preferential grade by size deportment response. The SELFRAG mode achieves the strongest comparative response, most notable below a particle size of 850 microns.

v. Cadia gold-bearing sulfide ore preferential grade by size deportment EDR investigations indicated weak to moderate gold and copper responses for the different crushing modes studied.

vi. The Cadia ore gold EDR values showed that the HPGR and the cone crushing modes produced the highest potential for gold pre-concentration by density separation compared to the other crushing modes. In addition, the cone crusher product RER and EDR values suggested the highest proportion of high-grade composite particles. Conversely, there is evidence that the HPGR and SELFRAG modes produce a low proportion of highly liberated particles, as evidenced by higher EDR values and low metal yield in their respective HLS separation fractions.

vii. Heavy liquid separation (HLS) studies on gold-bearing ore samples from Ballarat and Cadia mines revealed significant preferential grade by density deportment variation between metal-rich and gangue particles in specific density fractions influencing CPGR and preconcentration potential during gravity separation.

viii. The Ballarat sequential density separation results suggest a high separation efficiency into sinks for gold deportment across the density range for all four crushing comminution modes. With strong potential for gangue rejection during gravity separation.

ix. For Ballarat ore, this thesis suggested that the cone crusher produced a comparatively weaker preferential gold deportment by density response into sinks relative to other crushing modes responses, indicating a higher proportion of silicate locking in mineral associations with gold particles.

x. The Cadia ore GRAT density fractionation research data identified that the SELFRAG crusher produced a higher proportion of composite particles, with lower gold content when compared to the cone crusher and HPGR grade and recovery plots which suggest a higher proportion of composite particles with relatively higher gold content. Furthermore, compared to other crushing mode results, the cone crusher showed a higher potential to pre-concentrate gold by size through recovering particles in a size range of around 2.36 mm.

xi. High EDI values were predicted for the Ballarat ore gold response, indicating strong preferential deportment of the gold into the HLS sink product, relative to mass pull, for all crushing modes. The high EDI values suggest a high separation efficiency of the ore valuable metal into the sink during densimetric separation.

xii. Lower EDI values are predicted for the Cadia ore gold and copper response, indicating weaker preferential deportment of those metals into the HLS sink product, relative to mass pull, for all crushing modes. The low EDI values suggest a low separation efficiency of the ore valuable metals into the sink during densimetric separation. Low separation efficiency suggests a lower degree of valuable component particle liberation is present in crushed materials.

This comparative response study found significant differences in the Ballarat and Cadia ores preferential grade by size deportment and preferential grade by size deportment responses for different crushing modes. These findings imply that different crushing modes may produce better results for size-based classification or density-based beneficiation processes depending on the ore type. In addition, these findings could affect the mining approach and downstream processing strategy used to exploit ore resources.

7.3 Statistical analysis techniques to identify the significance of changes in the EDR Response

In this thesis, bar chart comparisons, ANOVA F-test, and t-test analysis statistical methods were used to evaluate and compare the variance between groups of EDR parameter means. As well as metal upgrade versus cumulative recovery slope of regression line relationships derived from the GRAT densimetric data produced by the interaction of ore type, crushing mode, and gravity separation technique. This statistical analysis discovered:

(1) Gold EDR response bar chart comparisons for Ballarat fine crushed ore by different crushing modes indicate the SELFRAG and rolls crusher modes have comparable and higher preferential gold deportment by density response than the cone and VSI crusher modes.

(2) Gold EDR response bar chart comparisons for Cadia fine crushed ore by different crushing modes suggest that both the HPGR and the cone crusher achieve comparably higher preferential gold deportment by density response than the SELFRAG or VSI mode products.

(3) Copper EDR response bar chart comparisons for Cadia fine crushed ore by different crushing modes showed the cone crushed products achieve a comparably higher preferential copper deportment by density response than the HPGR, SELFRAG or VSI crushing mode products.

(4) An ANOVA F-test for Ballarat HLS sink gold EDR values for different crushing modes found a significant difference in compared test for equal means between density splits. With SELFRAG and rolls crusher modes showing comparable and higher preferential gold preferable deportment by density responses than the cone and VSI crushing modes.

(5) An ANOVA F-test for Cadia HLS sink gold EDR values for different crushing modes found weak evidence of differences in the compared test for equal means between density splits. Thus, there is insufficient evidence of differences in preferential copper deportment into density fractions resulting from the application of different crushing modes.

(6) An ANOVA F-test for Cadia HLS sink copper EDR values for different crushing modes found weak evidence of differences in the compared test for equal means between density splits. Thus, there is insufficient evidence of differences in preferential copper deportment into density fractions resulting from the application of different crushing modes.

(7) The gravity separation densimetric data collected from Ballarat crushed ore samples were subjected to a t-test study of the metal upgrade versus cumulative recovery slope of regression line relationships between specified crushing modes. The evidence for rejecting the H_0 comparisons between the cone crusher versus other crushing modes is strong. However, the H_0 cannot be rejected for evidence of a significant difference between the Rolls vs. SELFRAG and VSI vs. Rolls.

(8) The gravity separation densimetric data collected from Cadia crushed ore samples were subjected to a t-test study of the metal upgrade versus cumulative recovery slope of regression line relationships between specified crushing modes. For gold comparisons, H_0 cannot be rejected for evidence of a significant difference between the Cone vs. SELFRAG, Cone vs. HPGR, Cone vs. VSI and the SELFRAG vs. VSI. For copper, similar null hypothesis results to those of gold crushing mode comparisons are achieved. In the gold and copper comparisons, the HPGR vs. SELFRAG and HPGR vs. VSI crushing modes suggest there is evidence to reject the H_0. Several limitations of this statistical analysis include:

I. It is unclear whether the same statistical results would have been reached if a bigger ore sample mass or data set had been produced and analysed as part of this thesis work. Alternatively, the statistical interpretation of the influence of the identical crushing modes explored in this thesis on the density-based magnitude of grade deportment reaction could not vary if the EDR results were obtained from various locations in the ore resource.

II. Another limitation was that despite significant differences between the EDR responses for different crushing modes, the EDR values for the Ballarat and Cadia ore results are still very similar in terms of their central statistical measures. Therefore, it is not clear evidence that the SELFRAG and HPGR modes would continue to deliver the best separation for Ballarat ore or, similarly, the HPGR and the cone modes on Cadia ores.

7.4 Applicability and accuracy of Enrichment Deportment Index parameter

The linear least-squares model, designated as the “EDI” parameter, characterises the magnitude of preferential metal deportment as a function of gangue rejection, where an increasing EDI value indicates a stronger propensity for the element to concentrate into

higher SG fractions following breakage preferentially. The EDI value allows ranking the interaction between the ore characteristics, the crushing mode breakage mechanism, and the preferential metal by density deportment response in achieving gold pre-concentration by gangue rejection. Knowledge of the EDI response allows better exploitation of opportunities for valuable metal pre-concentration by removing typically coarse, competent siliceous materials by coarse gangue rejection. By reducing the gangue component in tumble milling in the circulating load, a subsequent reduction in energy intensity can lead to significant unit gold productivity gains through a reduction in energy consumption per unit metal produced.

In this study, EDI values have indicated that different crushing modes significantly influence preferential gold by density deportment in Ballarat ore and, to a lesser extent, copper or gold grade by recovery in the Cadia ore. Improved understanding of early-stage metal pre-concentration through density-based coarse waste rejection processes is particularly useful in its implications for later decisions for selecting crushing equipment and mineral processing circuit operating strategy.

7.5 Recommendations

Future research should address the following areas:

- Conduct similar research on different gold-bearing ore mineralogy and textual characteristics using new metallurgy parameters described in this thesis as the "rejection enrichment ratio" (RER), "enrichment deportment response" (EDR), and "enrichment deportment index" (EDI). This study will enable mineralogical and textural data to be compared, gaining a better understanding of the interaction between specific gold-bearing sulfide ores and different fine crushing regimes to quantitatively predict enrichment and preferential metal deportment by density in gravity separation operations

- A more extensive database of metallurgy parameter information for RER, EDR, and EDI behaviour for gold-bearing ore resources is required to test the predictions generated in this study.

- Conduct similar research on gold-bearing ore types using industrial crushing modes at different energy levels that correspond to industrial conditions to thoroughly test and validate predictions developed in this study for future industrial applications.

- Conduct similar research using RER, EDR and EDI metallurgy parameters in mapping mineral preferential grade by density response over a resource deposit. This study will enable populating these parameters as three-dimensional distributions in an orebody for use in mine plans and metallurgy process models.

- Conduct similar research using RER, EDR, and EDI responses with characterisation and analysis of particle shape using X-ray microtomography. This study will provide a pathway to automated geometallurgy mapping of ore resources.

- Comparing the EDI predicted metal grade and recovery against actual measured densimetric results over different gold-bearing ore types and larger ore sample sizes.

- Conduct similar research in future work to include mine site field testing, scaleup and pilot demonstration.

- Conduct similar research using RER, EDR and EDI metallurgy parameters on different ore minerals for various metals. This research will improve understanding of gravity-based preconcentration and characterisation using this research methodology.

References

ABS (Australian Bureau of Statistics)., 2012. (various years), Australian Industry, cat. no. 8155.0, Canberra.

ABS (Australian Bureau of Statistics)., 2016. Estimates of Industry Multifactor Productivity, cat. no. 5260.0.55.002, Canberra, Australia.

ABS (Australian Bureau of Statistics)., 2018. Estimates of Industry Multifactor Productivity, 2017-18, cat. no. 5260.0.55.002, Canberra.

Aktaş, Z., Karacan, F. and Olcay, A., 1998. Centrifugal float–sink separation of fine Turkish coals in dense media. Fuel Process. Technol. 55 (3), pp.235–250.

Akerstrom, B.J.S., Waters, T., Bubnich, J., and D Seaman, D., 2018. Cleaner circuit optimisation at Cadia operations.

Aldrich, C., 2013. Consumption of steel grinding media in mills – A review. Minerals Engineering, 49(0), pp.77-91.

Anticoi, H., Guasch, E., Ahmad Hamid, S., Oliva, J., Alfonso, P., Bascompta, M., Sanmiquel, L., Escobet, T., Escobet, A., Parcerisa, D. and Peña-Pitarch, E., 2018. An improved high-pressure roll crusher model for tungsten and tantalum ores. Minerals, 8(11), 483.

Anticoi, H., Guasch, E., Oliva, J., Alfonso, P., Bascompta, M. and Sanmiquel, L., 2019. High-pressure grinding rolls: model validation and function parameters dependency on process conditions. Journal of materials research and technology, 8(6), pp.5476-5489.

Ballantyne, G. and Powell, M., 2014. Benchmarking comminution energy consumption for the processing of copper and gold ores. Minerals Engineering, 65: pp.109-114.

Bamber, A.S., Klein, B., Pakalnis, R.C. and Scoble, M.J., 2008. Integrated mining, processing and waste disposal systems for reduced energy and operating costs at Xstrata Nickel's Sudbury Operations. Mining Technology, 117(3), pp.142-153.

Banisi, S., Laplante, A.R. and Marois, J., 1991. A study of the behaviour of gold in industrial and laboratory grinding. CIM Bull, pp.72-78.

Barbery, G. and Leroux, D., 1988. Prediction of particle composition distribution after fragmentation of heterogeneous materials. International Journal of mineral processing, 22(1-4), pp.9-24.

Baumgartner, R., 2012. Geometallurgy–Optimising the resource.

Bazin, C., Grant, R., Cooper, M. and Tessier, R., 1994. A method to predict metallurgical performances as a function of fineness of grind. Minerals Engineering, 7(10), pp.1243-1251.

Bearman, R.A., 2013. Step change in the context of comminution. Minerals Engineering, 43, pp.2-11.

Bengtsson, M. and Evertsson, C.M., 2008. Modelling of output and power consumption in vertical shaft impact crushers. International Journal of Mineral Processing, 88(1-2), pp.18-23.

Bengtsson, M., Svedensten, P. and Evertsson, C.M., 2006, September. Characterization of compressive breakage behaviour. In Proceedings of the XXIII international mineral processing Congress, Istanbul, Turkey (pp. 3-8).

Bode, P., 2017. AMIRA P420F Gold Processing Technology - Crushing, Liberation & Pre-concentration of Gold Ores progress report: Development of a novel approach to characterise effect of different modes of particle breakage on coarse gangue rejection. Perth, Western Australia.

Bode, P., McGrath, T.D.H. and Eksteen, J.J., 2019. Characterising the effect of different modes of particle breakage on coarse gangue rejection for an orogenic gold ore. Mineral Processing and Extractive Metallurgy, pp.1-14.

Bohling, G., 2007. Introduction to geostatistics. Kansas Geological Survey Open File Report no, 26, pp.50.

Bonnici, N., Hunt, J.A., Walters, SG, Berry, R. and Collett, D., 2008, September. Relating textural attributes to mineral processing-Developing a more effective approach for the Cadia east Cu-Au porphyry deposit. In Proceedings of the ninth international congress for applied mineralogy conference (ICAM) (pp. 4-5).

Bonnici, N.K., 2012. The mineralogical and textural characteristics of copper-gold deposits related to mineral processing attributes (Doctoral dissertation, University of Tasmania).

Box, G.E., Hunter, W.H. and Hunter, S., 1978. Statistics for experimenters (Vol. 664). New York: John Wiley and sons.

Bearman, R.A., 2013. Step change in the context of comminution. Minerals Engineering, 43, pp.2-11.

Bowman, D.J. and Bearman, R.A., 2014. Coarse waste rejection through size based separation. Minerals Engineering, 62, pp.102-110.

Bracey, R., 2012. Novel Comminution Devices Report. Brisbane: Julius Kruttschnitt Mineral Research Centre, University of Queensland, Brisbane.

Bru, K., Touzé, S., Auger, P., Dobrusky, S., Tierrie, J. and Parvaz, D.B., 2018. Investigation of lab and pilot scale electric-pulse fragmentation systems for the recycling of ultra-high performance fibre-reinforced concrete. Minerals engineering, 128, pp.187-194.

Burns, R. and Grimes, A., 1986. The application of pre-concentration by screening at Bougainville Copper Limited. Paper presented at the Proceedings of the AUSIMM Mineral Development Symposium, Madang, Papua New Guinea.

Burt, R.O., 1984. Gravity concentration technology.

Carrasco, C., Keeney, L. and Napier-Munn, T., 2016a. Methodology to develop a coarse liberation model based on preferential grade-by-size responses. Minerals Engineering, 86, pp.149-155.

Carrasco, C., Keeney, L., Napier-Munn, T.J. and François-Bongarçon, D., 2016b. Managing uncertainty in a Grade Engineering® industrial pilot trial. Minerals Engineering, 99, pp.1-7.

Carrasco, C., Keeney, L. and Walters, S., 2016c. Development of a novel methodology to characterise preferential grade-by-size deportment and its operational significance. Minerals Engineering, 91 pp.100-107.

Carrasco, C., Keeney, L., Napier-Munn, T. and Bode, P., 2017. Unlocking additional value by optimising comminution strategies to process Grade Engineering® streams. Minerals Engineering, 103, pp.2-10.

Chibaya, A., 2013. Geometallurgical Analysis-Implications on Operating Flexibility.

Choi, W.Z., 1986. A combined size reduction and liberation model of grinding (Doctoral dissertation, Virginia Polytechnic Institute and State University).

Choi, W.Z., Adel, G.T. and Yoon, R.H., 1987. Size reduction/liberation model of grinding including multiple classes of composite particles. Mining, Metallurgy & Exploration, 4(2), pp.102-108.

Choi, W.Z., Adel, G.T. and Yoon, R.H., 1988. Liberation modeling using automated image analysis. International Journal of Mineral Processing, 22(1-4), pp.59-73.

Clark, I., 2010. Statistics or geostatistics? Sampling error or nugget effect? Journal of the Southern African Institute of Mining and Metallurgy, 110(6), pp.307-312.

Daniel, M.J., 2007, Energy efficient mineral liberation using HPGR technology, PhD Thesis, Julius Kruttschnitt Mineral Research Centre, Department of Mining and Metallurgical Engineering, University of Queensland

Dominy, S.C., Murphy, B. and Gray, A.H., 2011, September. Characterisation of gravity amenable gold ores—Sample representivity and determination methods. In Proceedings International Geometallurgy Conference; The Australasian Institute of Mining and Metallurgy: Melbourne, Australia (pp. 281-292).

Dominy, S.C., O'Connor, L., Parbhakar-Fox, A., Glass, H.J. and Purevgerel, S., 2018. Geometallurgy—A route to more resilient mine operations. Minerals, 8(12), p.560.

Drozdiak, J.A., 2011. A pilot-scale examination of a novel high pressure grinding roll/stirred mill comminution circuit for hard-rock mining applications (Doctoral dissertation, University of British Columbia).

Drozdiak, J.A., Klein, B., Nadolski, S. and Bamber, A., 2011. A Pilot-scale examination of a high pressure grinding roll/stirred mill comminution circuit. In Autogenous and Semi-autogenous Grinding Technology Conference, Vancouver.

Drzymala, J. Mineral Processing. Foundations of Theory and Practice of Minerallurgy, 1st ed.; Oficyna Wydawnicza Politechniki Wroclawskiej: Wroclaw, Poland, 2007

Drzymala, J., Tyson, D. and Wheelock, T.D., 2007. Presentation of particle beneficiation test results on an equal basis when yield and recovery are involved. Mining, Metallurgy & Exploration, 24(3), pp.145-151.

Ehrig, K., Liebezeit, V. and Macmillan, E., 2017. Metallurgical QAQC–who needs it? The Olympic Dam experience. Proceedings of the Metallurgical Plant Design and Operating Strategies, Perth, Australia, pp.11-12.

Eksteen, J. J., 2015. AMIRA P420E Project progress report. Perth, Western Australia.

Ericsson, M., Drielsma, J., Humphreys, D., Storm, P. and Weihed, P., 2019. Why current assessments of 'future efforts' are no basis for establishing policies on material use—a response to research on ore grades. Mineral Economics, 32(1), pp.111-121.

Esmaeelnejad, L., Siavashi, F., Seyedmohammadi, J. and Shabanpour, M., 2016. The best mathematical models describing particle size distribution of soils. Modeling Earth Systems and Environment, 2(4), pp.1-11.

Evertsson, C.M., 2000. Cone crusher performance. Chalmers Tekniska Hogskola (Sweden).

Fraser, A., 2020. ESTIMATION OF NOMINAL TOP SIZE USING ROSIN-RAMMLER REGRESSION.

Foggiatto, B., Bueno, M., Lane, G., McLean, E., & Chandramohan, R., 2014. The economics of large scale ore sorting. IMPC 2014, Santiago, Chile.

Gay, S.L., 2004. A liberation model for comminution based on probability theory. Minerals Engineering, 17(4), pp.525-534.

Ghaffari, H. (2004, November 23). Scavenging flotation tailings using a continuous centrifugal gravity concentrator. University of British Columbia. Retrieved from https://circle.ubc.ca/handle/2429/15609

Ghorbani, Y., Mainza, A.N., Petersen, J., Becker, M., Franzidis, J.P. and Kalala, J.T., 2013. Investigation of particles with high crack density produced by HPGR and its effect on the redistribution of the particle size fraction in heaps. Minerals Engineering, 43, pp.44-51.

Giurco, D., Prior, T., Mudd, G. M., Mason, L., & Behrisch, J., 2010. Peak minerals in Australia: A review of changing impacts and benefits: Institute for Sustainable Futures, UTS & Department of Civil Engineering, Monash University.

Goodall, W.R., 2008. Characterisation of mineralogy and gold deportment for complex tailings deposits using QEMSCAN®. Minerals Engineering, 21(6): 518-523.

Goovaerts, P., 1997. Geostatics for natural resources evaluation. Oxford University Press.

Gray, A.H., Davies, M., Theletsane, G., 2014. Coarse liberation and recovery of free gold and gold Sulfidecarriers for energy reduction in process plants. In: 12th AusIMM Mill Operators Conference 2014. T. A. I. o. M. a. Metallurgy. Townsville, Queensland.

Grigg, N., Delemontex, G., 2014. Higher grades and better recovery through pre-concentration of precious and base metal ores. IMPC 2014, Santiago, Chile.

Guimarães, C. and Durão, F., 2003. 2D simulation model of mineral particles yielded by discriminatory size reduction. Minerals engineering, 16(12), pp.1339-1348.

Guldris Leon, L., Hogmalm, K.J. and Bengtsson, M., 2020. Understanding Mineral Liberation during Crushing Using Grade-by-Size Analysis—A Case Study of the Penuota Sn-Ta Mineralization, Spain. Minerals, 10(2), p.164.

Gy, P.M., 1992. Sampling of heterogeneous and dynamic material systems: theories of heterogeneity, sampling and homogenizing (Vol. 10). Elsevier.

Hanusch, M., Aguilar, J., Hund, K.L., Bogoev, J., Baskaran, G.C. and Hayman, J.J., 2019. Digging Beneath the Surface: An Exploration of the Net Benefits of Mining in Southern Africa (No. 138997, pp. 1-108). The World Bank.

Holland-Batt, A.B., 1990. Interpretation of Spiral and Sluice Tests, Trans. Instn. Mining and Metallurgy, Vol. 99, pp. C1-C20.

Huang, W., 2019. Selective breakage of mineralised particles by high voltage pulses.

Hunt, J., Berry, R. and Bradshaw, D., 2011. Characterising chalcopyrite liberation and flotation potential: Examples from an IOCG deposit. Minerals Engineering, 24(12), pp.1271-1276.

Hunt, J., Berry, R. and Walters, S., 2010, January. Using mineral maps to rank potential processing behaviour. In 25th International Mineral Processing Conference, Brisbane, Australia (pp. 2899-2905).

Iyakwari, S., 2014. Application of near infrared sensors to minerals pre-concentration (Doctoral dissertation, University of Exeter).

Keeney, L. and Walters, SG, 2011, January. A methodology for geometallurgical mapping and orebody modelling. In GeoMet 2011-1st AusIMM International Geometallurgy Conference 2011 (pp. 217-225). Australasian Institute of Mining and Metallurgy.

King, R.P., 1994. Comminution and liberation of minerals. Minerals Engineering, 7(2-3), pp.129-140.

Lakshmanan, V.I. and Gorain, B. eds., 2019. Innovations and Breakthroughs in the Gold and Silver Industries: Concepts, Applications and Future Trends. Springer Nature.

Laplante, A., Woodcock, F., & Huang, L., 2000. Laboratory procedure to characterize gravity-recoverable gold. TRANSACTIONS-SOCIETY FOR MINING METALLURGY AND EXPLORATION INCORPORATED, 308, pp.53-59.

Laplante, A. R., 2000. A Standardized Test to Determine Gravity Recoverable Gold. Department of Mining and metallurgical Engineering, McGill University.

Laplante, A., Dunne, R., 2002a. The gravity recoverable gold test and flash flotation, In Proceedings of 34th Annual Canadian Mineral Processors Operators Conference. McGill University & Newcrest Mining Limited, Ottawa, p. Paper 7.

Laplante, A.R. and Dunne, R., 2002b. The GRG Test and Flash Flotation. Proc. of34lh Ann. Meet. of Canadian Mineral Processors, pp.105-124.

Laplante, A.R. and Shu, Y., 1992. The use of a laboratory centrifugal separator to study gravity recovery in industrial circuits. In Proc. 24th Annual Meeting of the Canadian Mineral Processors.

Laplante, A., Shu, Y. and Marois, J., 1996. Experimental characterization of a laboratory centrifugal separator. Canadian metallurgical quarterly, 35(1), pp.23-29.

Maré, E., Beven, B. and Crisafio, C., 2015. Developments in nonmagnetic physical separation technologies for hematitic/goethitic iron ore. In Iron Ore (pp. 309-338). Woodhead Publishing.

Marsden, J. and House, I., 2006. The chemistry of gold extraction. SME.

McGrath, T.D.H., Eksteen, J.J. and Bode, P., 2018. Assessing the amenability of a free milling gold ore to coarse particle gangue rejection. Minerals Engineering, 120, pp.110-117.

Middlemiss, S.N., 2004. Microscale fracture studies in geological materials with implications for mineral liberation. The University of Utah.

Mitchell, P. and Steen, J., 2017. Productivity in mining.

Minerals Council of Australia., 2017. Cost competitiveness challenge. Retrieved from http://www.minerals.org.au/resources/gold/cost_competitiveness_challenge

Minnitt, R.C.A. and Assibey-Bonsu, W., 2009. A comparison between the duplicate series analysis and the heterogeneity test as methods for calculating Gy'ssampling constants, K and alpha. In Fourth World Conference on Sampling & Blending. The Southern African Institute of Mining and Metallurgy.

Mitchell, P., Michael, B., Higgins, L., Steen, J., Henderson, C., Kastelle, T., Moran, C., MacAulay, S. and Kunz, N., 2014. Productivity in mining: Now comes the hard part, a global survey.

Mudd, G. M., 2007a. Gold mining in Australia: linking historical trends and environmental and resource sustainability. Environmental science & policy, 10(7), pp.629-644.

Mudd, G.M., 2007b. The sustainability of mining in Australia: key production trends and their environmental implications. Department of Civil Engineering, Monash University and Mineral Policy Institute, Melbourne.

Mudd, G.M. and Ward, J.D., 2008, December. Will sustainability constraints cause" peak minerals. In 3rd International Conference on Sustainability Engineering and Science: Blueprints for Sustainable Infrastructure. Auckland, New Zealand.

Mukherjee, A.K., 2009. A new method for evaluation of gravity separation processes. Mineral Processing & Extractive Metallurgy Review, 30(3), pp.191-210.

Murphy, B., van Zyl, J., and Domingo, G., 2012. Underground pre-concentration by ore sorting and coarse gravity separation. Paper presented at the Narrow vein mining conference.

Napier-Munn, T., 2014. Statistical methods for mineral engineers-How to design experiments and analyse data, 5. Julius Kruttschnitt Mineral Research Centre.

Norgate, T. and Haque, N., 2010. Energy and greenhouse gas impacts of mining and mineral processing operations. Journal of Cleaner Production, 18(3), pp.266-274.

Norgate, T., Haque, N., Wright, S. and Jahanshahi, S., 2010. Opportunites and technologies to reduce the energy and water impacts of deteriorating ore reserves, Sustainable Mining Conference, Kalgoorlie, Western Goldstralia, pp.128-137.

Norgate, T., Jahanshahi, S. and Rankin, W., 2007. Assessing the environmental impact of metal production processes. Journal of Cleaner Production, 15(8-9), pp.838-848.

Novak, J. and Moran, A., 2011. Submission to inquiry into the Mineral Resource Rent Tax Bill 2011 and related bills.

Okrusch, M., 2018. MINERALOGY: An Introduction to Minerals, Rocks, and Mineral Deposits. SPRINGER.

Parian, M., Mwanga, A., Lamberg, P. and Rosenkranz, J., 2018. Ore texture breakage characterization and fragmentation into multiphase particles. Powder Technology, 327, pp.57-69.

Parapari, P.S., Parian, M., Forsberg, F. and Rosenkranz, J., 2020. Characterization of ore texture crack formation and liberation by quantitative analyses of spatial deformation. Minerals Engineering, 157, p.106577.

Parapari, P.S., Parian, M. and Rosenkranz, J., 2020. Breakage process of mineral processing comminution machines–An approach to liberation. Advanced Powder Technology, 31(9), pp.3669-3685.

Parker, T., 2016. The effects of high voltage pulse treatment on ore characteristics and separation performances of a porphyry copper ore.

Parvaz, D.B., Weh, A. and Mosaddeghi, A., 2015, September. A Pre-concentration Application for SELFRAG High Voltage Treatment. In 14th European Symposium on Comminution and Classification (ESCC 2015), Chalmers University of Technology, Gothenburg, Sweden, pp.7-10.

Pérez-Barnuevo, L., Pirard, E., and Castroviejo, R., 2012. Textural descriptors for multiphasic ore particles. Image Analysis & Stereology, 31(3), pp.175-184.

Petrie, M.P., Hernan, M.M. and Valle, M.E., 2017. Annual Qualified Persons Report for the Ballarat Gold Mine, Australia for the Year Ended 31 March 2017 LionGold Corp Ltd.

Pitard, F.F., 1993. Pierre Gy's sampling theory and sampling practice: heterogeneity, sampling correctness, and statistical process control. CRC Press.

Pleysier, R., 2018. Ore sampling nomogram plot, Reported for CSIRO Minerals Laboratory, Waterford, Perth.

PorterGeo. Cadia Valley Operations - Ridgeway, Cadia Quarry/Extended, Cadia Hill, Cadia East/Far East Big Cadia. 2018 [cited 14 Aug]; Retrieved from: http://www.portergeo.com.au/database/mineinfo.asp?mineid=mn228.

Prior, T., Giurco, D., Mudd, G., Mason, L. and Behrisch, J., 2012. Resource depletion, peak minerals and the implications for sustainable resource management. Global Environmental Change, 22(3), pp.577-587.

Redwood, N. and Scott, M., 2016. Application of Enterprise Optimisation Considering Grade Engineering® Strategies. Cooperative Research Centre Optimising Resource Extraction (CRC ORE).

Resabal, V., 2017. Investigation of the breakage mechanism in high speed disk-type impeller stirred mills and its influence on the mineral liberation.

Rosin, P. and Rammler, E., 1933. The laws governing the fineness of powdered coal (Las leys queue governing la finer del carbon purverulento). J. Inst. Fuel, 7, pp.29-36.

Sakuhuni, G., Altun, N., Klein, B., & Tong, L., 2016. A novel laboratory procedure for predicting continuous centrifugal gravity concentration applications: The gravity release analysis. International Journal of Mineral Processing, 154, pp.66-74.

Sakuhuni, G., Tong, L. and Klein, B., 2014. Gravity release analysis and its application on Myra Falls zinc flotation tails, XXVII International Mineral Processing Congress-IMPC 2014. Gecamin Digital Publications.

Sandu, S. and Syed, A., 2008. Trends in energy intensity in Australian industry. Canberra, Australia: ABARE.

Sarkar, B., Das, A. and Mehrotra, S., 2008. Study of separation features in floatex density

Shirley, P., 2009. Pre-concentration applications.

Scott, G., 2006. Microwave pretreatment of a low grade copper ore to enhance milling performance and liberation. The University of Stellenbosch.

Snedecor, G.W. and Cochran, W.G., 1983. Statistical Methods. 6th Edition, Oxford and IBH, New Delhi.

Solomon, N., 2011. Effect of HPGR on platinum bearing ores and the flotation response as compared to the conventional ball mill (Master's thesis, University of Cape Town).

Syed, A., Grafton, Q. and Kalirajan, K., 2013. Productivity in the Australian mining sector. BREE, Canberra, Commonwealth of Australia.

Syed, A., Grafton, R.Q., Kalirajan, K. and Parham, D., 2015. Multifactor productivity growth and the Australian mining sector. Australian Journal of Agricultural and Resource Economics, 59(4), pp.549-570.

Taggart, A., 1951. Elements of ore dressing, John Wiley& Sons. Inc., New York, pp.44-48.

Topp, V., Soames, L., Parham, D. and Bloch, H., 2008. Productivity in the mining industry. Australian Productivity Commission.

Topp, V., 2008. Productivity in the mining industry: measurement and interpretation.

Tungpalan, K., Wightman, E., Keeney, L. and Manlapig, E., 2021. A geometallurgical approach for predicting separation performance. Minerals Engineering, 171, p.107065.

Vatandoost, A., Fullagar, P., Walters, S. and Kojovic, T., 2009, January. Towards petrophysical characterization of comminution behavior. In Procceilings 41st Annual Meeting of the Canadian Mineral Processors (pp. 619-640).

Vizcarra, T., Wightman, E., Johnson, N. and Manlapig, E., 2010. The effect of breakage mechanism on the mineral liberation properties of Sulfideores. Minerals Engineering, 23(5), pp.374-382.

Von Ketelhodt, L., 2009. Viability of optical sorting of gold waste rock dumps. In World Gold Conference (pp. 271-278).

Walters, SG, 2011, January. Integrated industry relevant research initiatives to support geometallurgical mapping and modelling. In GeoMet 2011-1st AusIMM International Geometallurgy Conference 2011 (pp. 273-278). AusIMM: Australasian Institute of Mining and Metallurgy.

Walters, SG, 2016. Driving productivity by increasing feed quality through application of innovative Grade Engineering® technologies. Grade Engineering White paper. Retrieved from: <http://www.crcore.org.au/main/images/docs/papers/Walters-2016-Grade-Engineering-Whitepaper.pdf>.

Wang, Y. and Forssberg, E., 2007. Enhancement of energy efficiency for mechanical production of fine and ultra-fine particles in comminution. China Particuology, 5(3), pp.193-201.

Wang, E., Shi, F. and Manlapig, E., 2011. Pre-weakening of mineral ores by high voltage pulses. Minerals Engineering, 24(5), pp.455-462.

Wang, E., Shi, F. and Manlapig, E., 2012. Experimental and numerical studies of selective fragmentation of mineral ores in electrical comminution. International Journal of Mineral Processing, 112, pp.30-36.

Webster, R., 2005. SPATIAL VARIATION, SOIL PROPERTIES. In: D. Hillel (Ed.), Encyclopedia of Soils in the Environment. Elsevier, Oxford, pp.1-13.

Webster, R. and Oliver, M.A., 2007. Geostatistics for environmental scientists. John Wiley & Sons.

Weatherwax, T., 2007. Integrated mining and pre-concentration systems for nickel sulfide ores (Doctoral dissertation, University of British Columbia).

Wills, B.A., Wills' mineral processing technology: An introduction to the practical aspects of ore treatment and mineral recovery. 7th edn. 2006, Butterworth-Heinemann, Oxford, U.K.

Wills, B.A. and Finch, J., 2015. Wills' mineral processing technology: an introduction to the practical aspects of ore treatment and mineral recovery. Butterworth-Heinemann.

Wills, B.A. and Napier-Munn, T.J., 2006. An introduction to the practical aspects of ore treatment and mineral recovery. Wills' Mineral Processing Technology, pp.267-352.

Wilson, R. and Hawk, J., 1999. Impeller wear impact-abrasive wear test. Wear, 225, pp.1248-1257.

Woodcock, F. and Laplante, A.R., 1993. A laboratory method to measure free gold content. In Proceedings of Randol Gold Seminar (pp. 151-155).

Yamashita, A.S., Thivierge, A. and Euzébio, T.A., 2021. A review of modeling and control strategies for cone crushers in the mineral processing and quarrying industries. Minerals Engineering, 170, p.107036.

Zaiontz, C., 2013. Real Statistics resource pack. Available: www. real-statistics. com/free-download/real-statistics-resource-pack/.(September 2016).

Zhou, J. and Gu, Y., 2016. Geometallurgical characterization and automated mineralogy of gold ores. In Gold ore processing (pp. 95-111). Elsevier.

Zhou, J., Jago, B. and Martin, C., 2004. Establishing the process mineralogy of gold ores. Technical bulletin: 03.

Zhou, M., 2016. Size-by-Size Optimization of Dry Gravity Separation Using a 3-Inch Knelson Concentartor. McGill University (Canada).

APPENDIX 1

Sampling Nomogram Plot (Reported by CSIRO Minerals Laboratory, Waterford, Perth)

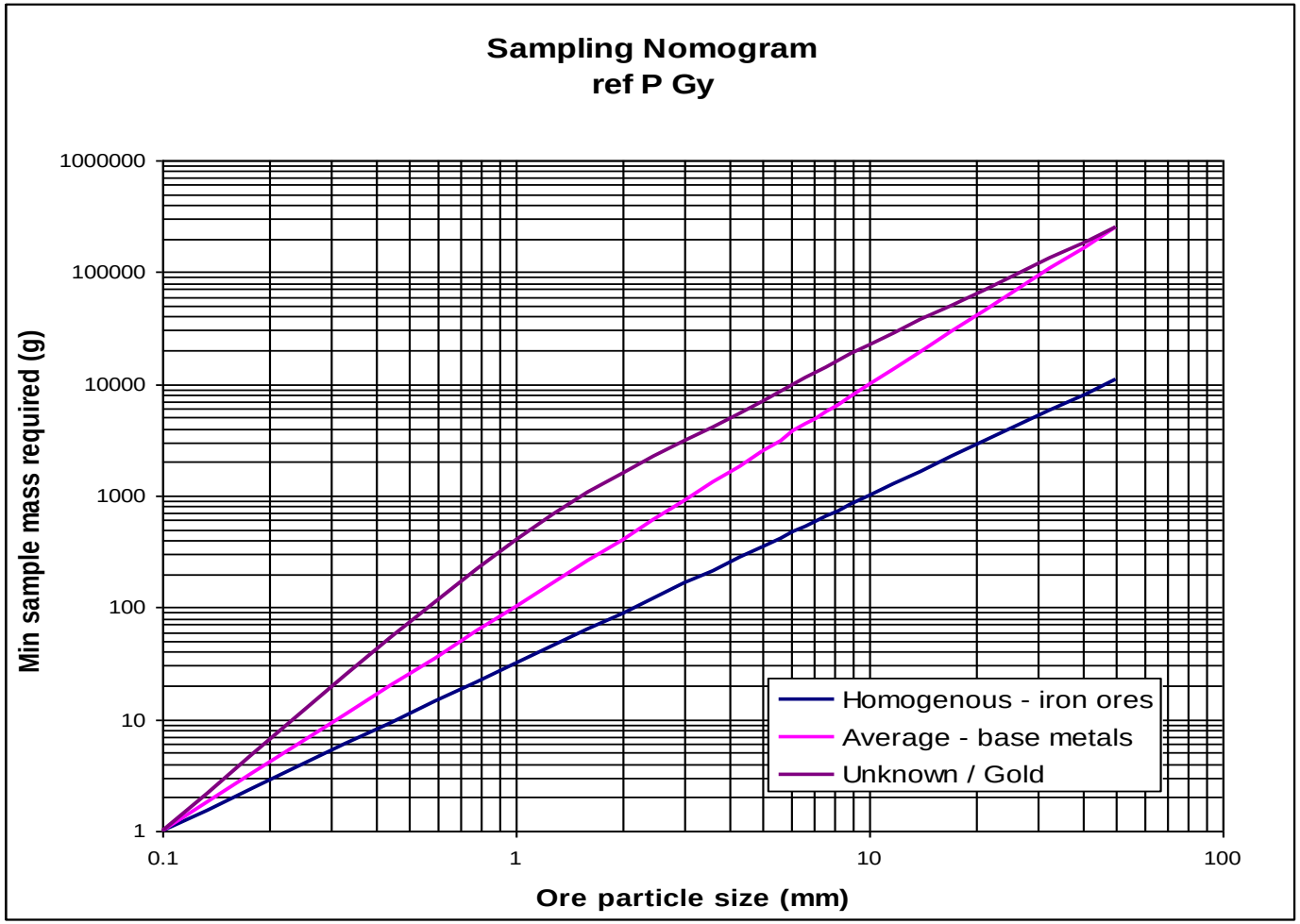

CSIRO Sampling nomogram Plot –(Pleysier, 2018)

APPENDIX 2

Ballarat crushed ore metallurgical balanced GRAT classification data

SAMPLE	Mass	Au	As	Fe	S	Between STAGE Deportment				
	g	ppm	ppm	%	%	Yield	Au	As	Fe	S
Cone Crush										
Assay Head										
Cone Crush Size by Size Analysis										
Calc. Head	19434.40	1.64	2426	3.78	0.36	100.00%	100.00%	100.00%	100.00%	100.00%
+1180	5032.80	1.25	2217	3.02	0.40	25.90%	19.72%	23.66%	20.68%	28.98%
+600	3746.00	1.40	3007	3.19	0.41	19.28%	16.50%	23.89%	16.25%	21.94%
+300	3200.50	2.27	3425	5.76	0.40	16.47%	22.77%	23.24%	25.07%	18.47%
+212	868.53	3.23	3190	3.68	0.40	4.47%	8.82%	5.88%	4.35%	5.01%
+150	962.42	1.57	2860	3.78	0.39	4.95%	4.74%	5.84%	4.95%	5.41%
+106	785.09	1.26	2440	3.75	0.38	4.04%	3.09%	4.06%	4.01%	4.30%
+75	894.84	3.22	2310	3.75	0.38	4.60%	9.04%	4.38%	4.57%	4.84%
+53	506.70	1.85	1860	3.92	0.33	2.61%	2.94%	2.00%	2.70%	2.41%
+38	405.92	1.95	1850	4.26	0.34	2.09%	2.49%	1.59%	2.35%	1.99%
+25	267.35	2.01	1430	4.19	0.28	1.38%	1.68%	0.81%	1.52%	1.08%
-25	2764.24	0.95	792	3.60	0.14	14.22%	8.20%	4.64%	13.54%	5.58%
Cone Crush Size by Float - Sink Analysis for 2.0 - 1.8 mm Fraction										
Calc. Head	4669.93	1.25	2217	3.02	0.40	25.90%	19.72%	23.66%	20.68%	28.98%
3.0 g/ml sink	154.31	31.25	59800	22.70	9.80	0.86%	16.32%	21.09%	5.14%	23.49%
2.95 g/ml sink	80.69	1.04	3680	11.40	0.63	0.45%	0.28%	0.68%	1.35%	0.79%
2.90 g/ml sink	69.43	1.15	2150	9.49	0.41	0.39%	0.27%	0.34%	0.97%	0.44%
2.85 g/ml sink	307.73	0.34	941	6.34	0.19	1.71%	0.35%	0.66%	2.86%	0.88%
2.80 g/ml sink	726.56	0.13	298	4.42	0.10	4.03%	0.32%	0.49%	4.71%	1.13%
2.75 g/ml sink	265.05	1.56	294	4.64	0.24	1.47%	1.40%	0.18%	1.80%	0.99%
2.70 g/ml sink	469.72	0.25	73	3.04	0.09	2.60%	0.40%	0.08%	2.09%	0.66%
2.65 g/ml sink	339.95	0.17	127	1.70	0.08	1.89%	0.19%	0.10%	0.85%	0.42%
2.65 g/ml Final Float	2256.49	0.02	9	0.28	0.01	12.51%	0.18%	0.04%	0.91%	0.18%
1.8 - 0.6 mm Fraction										
Calc. Head	3275.49	1.40	3007	3.19	0.41	19.28%	16.50%	23.89%	16.25%	21.94%
3.0 g/ml sink	118.95	36.30	79900	24.30	10.20	0.70%	15.51%	23.05%	4.50%	20.00%
2.95 g/ml sink	56.61	0.76	1210	12.60	0.48	0.33%	0.16%	0.17%	1.11%	0.45%
2.90 g/ml sink	26.95	2.89	969	10.80	0.22	0.16%	0.28%	0.06%	0.45%	0.10%
2.85 g/ml sink	249.88	0.16	639	6.81	0.14	1.47%	0.14%	0.39%	2.65%	0.58%
2.80 g/ml sink	631.21	0.04	88	3.96	0.04	3.71%	0.10%	0.13%	3.89%	0.42%
2.75 g/ml sink	195.48	0.14	56	3.72	0.04	1.15%	0.10%	0.03%	1.13%	0.13%
2.70 g/ml sink	342.46	0.07	33	2.62	0.03	2.02%	0.08%	0.03%	1.40%	0.17%
2.65 g/ml sink	147.60	0.22	52	1.43	0.04	0.87%	0.12%	0.02%	0.33%	0.10%
2.65 g/ml Final Float	1506.35	0.00	5	0.34	<0.001	8.86%	0.02%	0.02%	0.79%	0.00%
0.6 - 0.3 mm Fraction										
Calc. Head	3107.00	2.27	3425	5.76	0.40	16.47%	22.77%	23.24%	25.07%	18.47%
3.0 g/ml sink	185.70	27.40	52500	20.80	5.88	0.98%	16.46%	21.30%	5.42%	16.21%
2.95 g/ml sink	72.90	7.25	10500	12.10	1.32	0.39%	1.71%	1.67%	1.24%	1.43%
2.90 g/ml sink	153.20	0.46	245	7.24	0.10	0.81%	0.23%	0.08%	1.56%	0.23%
2.85 g/ml sink	150.70	7.81	112	50.04	0.03	0.80%	3.81%	0.04%	10.57%	0.07%
2.80 g/ml sink	562.20	0.05	54	3.40	0.02	2.98%	0.09%	0.07%	2.68%	0.17%
2.75 g/ml sink	224.50	0.10	69	3.25	0.03	1.19%	0.07%	0.03%	1.02%	0.10%
2.70 g/ml sink	254.70	0.31	43	2.15	0.01	1.35%	0.26%	0.02%	0.77%	0.04%
2.65 g/ml sink	191.50	0.21	26	0.96	0.01	1.02%	0.13%	0.01%	0.26%	0.03%
2.65 g/ml Final Float	1311.60	0.01	7	0.85	0.01	6.95%	0.02%	0.02%	1.56%	0.20%

SAMPLE	Mass	Au	As	Fe	S	Between STAGE Deportment				
	g	ppm	ppm	%	%	Yield	Au	As	Fe	S
SELFRAG										
Assay Head										
SELFRAG Size by Size Analysis										
Calc. Head	15995.50	3.60	2932	3.39	0.42	100.00%	100.00%	100.00%	100.00%	100.00%
+1180	2716.70	6.15	2149	2.93	0.32	16.98%	28.96%	12.45%	14.65%	12.82%
+600	4849.60	1.97	2648	3.04	0.38	30.32%	16.58%	27.38%	27.13%	27.36%
+300	3299.40	3.92	3751	3.42	0.43	20.63%	22.45%	26.39%	20.78%	20.98%
+212	1176.23	2.14	3700	3.62	0.50	7.35%	4.36%	9.28%	7.84%	8.70%
+150	963.38	4.94	3480	3.68	0.51	6.02%	8.26%	7.15%	6.53%	7.26%
+106	713.74	3.26	3320	3.83	0.56	4.46%	4.04%	5.05%	5.03%	5.91%
+75	707.07	4.33	3080	4.01	0.59	4.42%	5.30%	4.64%	5.22%	6.17%
+53	520.11	2.93	2670	4.37	0.55	3.25%	2.64%	2.96%	4.19%	4.23%
+38	289.28	3.49	2930	4.98	0.62	1.81%	1.75%	1.81%	2.65%	2.65%
+25	140.66	4.57	3210	5.33	0.65	0.88%	1.11%	0.96%	1.38%	1.35%
-25	619.33	4.23	1450	4.03	0.28	3.87%	4.54%	1.92%	4.60%	2.56%
SELFRAG Size by Float - Sink Analysis for 2.0 - 1.8 mm Fraction										
Calc. Head	2552.34	6.15	2149	2.93	0.32	16.98%	28.96%	12.45%	14.65%	12.82%
3.0 g/ml sink	75.91	203.95	67800	23.15	9.00	0.51%	28.58%	11.68%	3.44%	10.75%
2.95 g/ml sink	36.02	1.35	1580	12.65	0.56	0.24%	0.09%	0.13%	0.89%	0.31%
2.90 g/ml sink	82.02	0.20	970	9.84	0.37	0.55%	0.03%	0.18%	1.58%	0.47%
2.85 g/ml sink	114.76	0.42	590	6.42	0.16	0.76%	0.09%	0.15%	1.44%	0.28%
2.80 g/ml sink	434.97	0.04	180	3.99	0.06	2.89%	0.03%	0.18%	3.40%	0.41%
2.75 g/ml sink	158.05	0.27	170	4.32	0.13	1.05%	0.08%	0.06%	1.34%	0.31%
2.70 g/ml sink	176.08	0.05	70	3.02	0.03	1.17%	0.02%	0.03%	1.04%	0.08%
2.65 g/ml sink	209.06	0.06	20	1.61	<0.001	1.39%	0.02%	0.01%	0.66%	0.00%
2.65 g/ml Final Float	1265.49	0.01	10	0.34	0.01	8.42%	0.01%	0.03%	0.85%	0.20%
SELFRAG Size by Float - Sink Analysis for 1.8 - 0.6 mm Fraction										
Calc. Head	4405.84	1.97	2648	3.04	0.38	30.32%	16.58%	27.38%	27.13%	27.36%
3.0 g/ml sink	191.97	41.50	58400	22.50	7.95	1.32%	15.21%	26.32%	8.76%	24.84%
2.95 g/ml sink	68.44	1.06	1010	12.30	0.42	0.47%	0.14%	0.16%	1.71%	0.47%
2.90 g/ml sink	161.89	0.70	632	9.05	0.24	1.11%	0.22%	0.24%	2.97%	0.62%
2.85 g/ml sink	454.04	0.40	269	4.92	0.08	3.12%	0.35%	0.29%	4.53%	0.59%
2.80 g/ml sink	487.51	0.13	121	3.15	0.04	3.35%	0.12%	0.14%	3.11%	0.32%
2.75 g/ml sink	291.96	0.79	107	3.84	0.06	2.01%	0.44%	0.07%	2.27%	0.29%
2.70 g/ml sink	346.62	0.14	89	3.56	0.04	2.39%	0.09%	0.07%	2.50%	0.23%
2.65 g/ml sink	32.85	0.17	61	1.90	0.03	0.23%	0.01%	0.00%	0.13%	0.02%
2.65 g/ml Final Float	2370.56	0.00	16	0.24	<0.001	16.31%	0.00%	0.09%	1.15%	0.00%
SELFRAG Size by Float - Sink Analysis for 0.6 - 0.3 mm Fraction										
Calc. Head	3245.30	3.92	3751	3.42	0.43	20.63%	22.45%	26.39%	20.78%	20.98%
3.0 g/ml sink	219.60	56.55	54500	20.90	6.09	1.40%	21.90%	25.95%	8.59%	20.10%
2.95 g/ml sink	65.70	0.71	1060	10.50	0.22	0.42%	0.08%	0.15%	1.29%	0.22%
2.90 g/ml sink	95.90	1.25	375	8.14	0.12	0.61%	0.21%	0.08%	1.46%	0.17%
2.85 g/ml sink	300.60	0.15	129	4.62	0.04	1.91%	0.08%	0.08%	2.60%	0.18%
2.80 g/ml sink	371.30	0.06	56	3.60	0.02	2.36%	0.04%	0.05%	2.50%	0.11%
2.75 g/ml sink	223.30	0.17	77	3.32	0.02	1.42%	0.07%	0.04%	1.39%	0.07%
2.70 g/ml sink	257.00	0.10	39	2.11	0.02	1.63%	0.05%	0.02%	1.02%	0.08%
2.65 g/ml sink	174.70	0.06	24	0.09	0.02	1.11%	0.02%	0.01%	0.03%	0.05%
2.65 g/ml Final Float	1537.20	0.00	5	0.66	0.00	9.77%	0.01%	0.02%	1.90%	0.00%

SAMPLE	Mass	Au	As	Fe	S	Between STAGE Deportment				
	g	ppm	ppm	%	%	Yield	Au	As	Fe	S
Rolls crusher										
HPGR Size by Size Analysis										
Calc. Head	7391.21	1.97	2343	3.49	0.39	100.00%	100.00%	100.00%	100.00%	100.00%
+1180	1639.77	3.15	2136	3.05	0.39	22.19%	35.44%	20.22%	19.38%	22.36%
+600	1592.94	1.86	2423	3.08	0.39	21.55%	20.28%	22.29%	19.04%	21.56%
+300	1138.08	2.36	4027	4.59	0.55	15.40%	18.39%	26.47%	20.23%	22.06%
+212	435.20	1.65	3110	3.70	0.49	5.89%	4.93%	7.82%	6.24%	7.48%
+150	370.65	1.45	2750	3.60	0.46	5.01%	3.67%	5.89%	5.17%	5.98%
+106	281.03	2.56	2440	3.60	0.45	3.80%	4.94%	3.96%	3.92%	4.43%
+75	302.64	1.30	2250	3.55	0.41	4.09%	2.69%	3.93%	4.17%	4.35%
+53	214.78	1.31	1830	3.71	0.39	2.91%	1.93%	2.27%	3.09%	2.94%
+38	145.85	1.27	1670	3.87	0.35	1.97%	1.27%	1.41%	2.19%	1.79%
+25	110.06	1.44	1680	3.93	0.35	1.49%	1.09%	1.07%	1.68%	1.35%
-25	1160.21	0.68	699	3.31	0.14	15.70%	5.38%	4.68%	14.89%	5.70%
HPGR Size by Float - Sink Analysis for 2.0 - 1.8 mm Fraction										
Calc. Head	1594.53	3.15	2136	3.05	0.39	22.19%	35.44%	20.22%	19.38%	22.36%
3.0 g/ml sink	45.71	104.20	66200	22.10	11.70	0.64%	33.60%	17.97%	4.03%	19.29%
2.95 g/ml sink	33.40	5.62	2730	11.60	1.05	0.46%	1.32%	0.54%	1.54%	1.26%
2.90 g/ml sink	49.70	0.60	1580	8.92	0.41	0.69%	0.21%	0.47%	1.77%	0.73%
2.85 g/ml sink	117.12	0.07	819	6.26	0.13	1.63%	0.06%	0.57%	2.92%	0.55%
2.80 g/ml sink	282.98	0.03	184	4.10	0.02	3.94%	0.06%	0.31%	4.63%	0.20%
2.75 g/ml sink	106.95	0.09	225	3.81	0.07	1.49%	0.07%	0.14%	1.62%	0.27%
2.70 g/ml sink	135.28	0.05	146	2.80	0.01	1.88%	0.04%	0.12%	1.51%	0.05%
2.65 g/ml sink	126.61	0.07	38	1.21	<0.001	1.76%	0.06%	0.03%	0.61%	0.00%
2.65 g/ml Final Float	696.78	<0.001	19	0.27	<0.001	9.69%	0.00%	0.08%	0.75%	0.00%
HPGR Size by Float - Sink Analysis for 1.8 - 0.6 mm Fraction										
Calc. Head	1537.00	1.86	2423	3.08	0.39	21.55%	20.28%	22.29%	19.04%	21.56%
3.0 g/ml sink	59.23	45.15	59700	21.00	9.33	0.83%	19.01%	21.16%	5.00%	20.08%
2.95 g/ml sink	64.20	0.66	1110	10.40	0.40	0.90%	0.30%	0.43%	2.68%	0.93%
2.90 g/ml sink	53.31	0.87	585	7.25	0.13	0.75%	0.33%	0.19%	1.55%	0.25%
2.85 g/ml sink	140.19	0.14	197	5.00	0.02	1.97%	0.14%	0.17%	2.82%	0.10%
2.80 g/ml sink	218.33	0.06	168	3.72	0.02	3.06%	0.09%	0.22%	3.26%	0.16%
2.75 g/ml sink	93.34	0.23	85	3.71	0.01	1.31%	0.15%	0.05%	1.39%	0.03%
2.70 g/ml sink	138.74	0.22	47	2.67	<0.001	1.95%	0.22%	0.04%	1.49%	0.00%
2.65 g/ml sink	160.15	0.02	34	0.74	<0.001	2.25%	0.02%	0.03%	0.48%	0.00%
2.65 g/ml Final Float	609.51	0.00	2	0.15	<0.001	8.55%	0.01%	0.01%	0.37%	0.00%
HPGR Size by Float - Sink Analysis for 0.6 - 0.3 mm Fraction										
Calc. Head	817.30	2.36	4027	4.59	0.55	15.40%	18.39%	26.47%	20.23%	22.06%
3.0 g/ml sink	70.30	25.50	45700	20.20	6.03	1.32%	17.13%	25.83%	7.67%	20.70%
2.95 g/ml sink	18.70	3.36	1520	11.70	0.52	0.35%	0.60%	0.23%	1.18%	0.47%
2.90 g/ml sink	43.00	0.43	411	8.18	0.13	0.81%	0.18%	0.14%	1.90%	0.27%
2.85 g/ml sink	111.40	0.18	120	4.84	0.03	2.10%	0.19%	0.11%	2.91%	0.16%
2.80 g/ml sink	143.70	0.09	58	3.45	0.02	2.71%	0.13%	0.07%	2.68%	0.14%
2.75 g/ml sink	104.40	0.06	53	3.33	0.03	1.97%	0.06%	0.04%	1.87%	0.15%
2.70 g/ml sink	75.90	0.12	39	2.25	0.02	1.43%	0.09%	0.02%	0.92%	0.07%
2.65 g/ml sink	82.50	0.03	23	0.93	0.02	1.55%	0.02%	0.02%	0.41%	0.08%
2.65 g/ml Final Float	167.40	0.00	4	0.76	0.00	3.15%	0.00%	0.01%	0.69%	0.00%

SAMPLE	Mass	Au	As	Fe	S	Between STAGE Deportment				
	g	ppm	ppm	%	%	Yield	Au	As	Fe	S
VSI										
Assay Head										
VSI Size by Size Analysis										
Calc. Head	4918.53	2.92	2703	4.04	0.46	100.00%	100.00%	100.00%	100.00%	100.00%
+1180	1092.67	2.11	2405	4.69	0.56	22.22%	16.06%	19.77%	25.82%	26.77%
+600	1213.45	4.78	3269	4.91	0.58	24.67%	40.34%	29.84%	30.01%	31.05%
+300	789.16	2.57	3415	2.44	0.43	16.04%	14.11%	20.27%	9.71%	14.87%
+212	345.49	5.51	3050	3.60	0.44	7.02%	13.23%	7.93%	6.26%	6.65%
+150	248.21	1.14	3060	3.53	0.43	5.05%	1.96%	5.71%	4.41%	4.67%
+106	183.45	1.12	2830	3.75	0.44	3.73%	1.42%	3.91%	3.46%	3.53%
+75	181.07	2.42	2630	3.81	0.42	3.68%	3.05%	3.58%	3.47%	3.33%
+53	129.77	1.47	2560	4.10	0.42	2.64%	1.33%	2.50%	2.68%	2.38%
+38	94.68	1.84	2470	4.40	0.42	1.92%	1.21%	1.76%	2.10%	1.74%
+25	49.20	2.95	2340	4.61	0.40	1.00%	1.01%	0.87%	1.14%	0.86%
-25	591.39	1.53	871	3.68	0.16	12.02%	6.29%	3.87%	10.94%	4.14%
VSI Size by Float - Sink Analysis for 2.0 - 1.8 mm Fraction										
Calc. Head	746.06	2.11	2405	4.69	0.56	22.22%	16.06%	19.77%	25.82%	26.77%
3.0 g/ml sink	39.38	34.30	40700	21.50	9.06	1.17%	13.75%	17.66%	6.24%	22.86%
2.95 g/ml sink	11.40	0.19	1550	12.10	0.57	0.34%	0.02%	0.19%	1.02%	0.42%
2.90 g/ml sink	74.14	0.14	902	8.26	0.28	2.21%	0.10%	0.74%	4.52%	1.33%
2.85 g/ml sink	114.29	0.36	447	4.64	0.08	3.40%	0.42%	0.56%	3.91%	0.59%
2.80 g/ml sink	147.54	0.09	141	4.07	0.04	4.39%	0.14%	0.23%	4.43%	0.38%
2.75 g/ml sink	120.47	0.80	235	3.72	0.08	3.59%	0.98%	0.31%	3.30%	0.62%
2.70 g/ml sink	66.94	0.81	49	3.14	0.05	1.99%	0.55%	0.04%	1.55%	0.21%
2.65 g/ml sink	66.20	0.02	49	1.17	0.07	1.97%	0.01%	0.04%	0.57%	0.30%
2.65 g/ml Final Float	105.70	0.07	2	0.36	0.01	3.15%	0.08%	0.00%	0.28%	0.07%
VSI Size by Float - Sink Analysis for 1.8 - 0.6 mm Fraction										
Calc. Head	731.25	4.78	3269	4.91	0.58	24.67%	40.34%	29.84%	30.01%	31.05%
3.0 g/ml sink	47.75	70.35	47900	21.90	7.96	1.61%	38.75%	28.55%	8.74%	27.60%
2.95 g/ml sink	23.52	1.13	1020	11.30	0.38	0.79%	0.31%	0.30%	2.22%	0.65%
2.90 g/ml sink	55.10	0.24	698	8.10	0.22	1.86%	0.16%	0.48%	3.73%	0.88%
2.85 g/ml sink	136.05	0.06	136	4.76	0.06	4.59%	0.09%	0.23%	5.41%	0.59%
2.80 g/ml sink	114.37	0.36	62	3.78	0.05	3.86%	0.48%	0.09%	3.61%	0.42%
2.75 g/ml sink	95.56	0.05	53	3.80	0.06	3.22%	0.05%	0.06%	3.03%	0.42%
2.70 g/ml sink	116.02	0.06	45	2.58	0.03	3.91%	0.07%	0.07%	2.50%	0.25%
2.65 g/ml sink	48.05	0.78	94	1.27	0.05	1.62%	0.43%	0.06%	0.51%	0.17%
2.65 g/ml Final Float	94.83	0.00	3	0.32	0.01	3.20%	0.00%	0.00%	0.25%	0.07%
VSI Size by Float - Sink Analysis for 0.6 - 0.3 mm Fraction										
Calc. Head	872.40	2.57	3415	2.44	0.43	16.04%	14.11%	20.27%	9.71%	14.87%
3.0 g/ml sink	59.50	36.25	49200	10.40	6.03	1.09%	13.56%	19.92%	2.82%	14.20%
2.95 g/ml sink	17.40	2.11	936	7.57	0.29	0.32%	0.23%	0.11%	0.60%	0.20%
2.90 g/ml sink	16.20	0.40	348	4.75	0.12	0.30%	0.04%	0.04%	0.35%	0.08%
2.85 g/ml sink	86.40	0.05	142	3.44	0.04	1.59%	0.03%	0.08%	1.35%	0.14%
2.80 g/ml sink	112.10	0.03	67	3.20	0.02	2.06%	0.02%	0.05%	1.63%	0.09%
2.75 g/ml sink	78.50	0.38	57	3.26	0.03	1.44%	0.19%	0.03%	1.17%	0.08%
2.70 g/ml sink	58.10	0.06	40	2.20	0.02	1.07%	0.02%	0.02%	0.58%	0.05%
2.65 g/ml sink	57.40	0.03	28	0.96	0.02	1.06%	0.01%	0.01%	0.25%	0.05%
2.65 g/ml Final Float	386.80	0.00	5	0.54	0.00	7.11%	0.00%	0.01%	0.95%	0.00%

APPENDIX 3

Cadia crushed ore metallurgical balanced GRAT classification data

Cone Crush Density Fractionation Summary

Assay Head

SAMPLE	Mass	Au	Cu	Mo	Fe	S	Between STAGE Deportment					
	g	ppb	ppm	ppm	%	%	Yield	Au	Cu	Mo	Fe	S
Cone Crush Density Fractionation Summary Analysis												
Calc. Head	24492.3	1019	2909	11	4.23	0.52	100.00%	100.00%	100.00%	100.00%	100.00%	100.00%
2.95 g/ml sink	552.5	7745	18618	27	17.76	7.91	2.26%	17.14%	14.44%	5.32%	9.48%	34.44%
2.85 g/ml sink	968.7	2701	8974	22	8.37	1.57	3.96%	10.48%	12.20%	7.68%	7.83%	11.95%
2.75 g/ml sink	5645.1	1250	4545	16	5.68	0.62	23.05%	28.26%	36.01%	33.34%	30.96%	27.70%
2.65 g/ml sink	15774.3	655	1636	9	3.25	0.20	64.41%	41.42%	36.22%	51.81%	49.50%	25.01%
2.55 g/ml sink	1540.6	435	522	3	1.49	0.07	6.29%	2.68%	1.13%	1.84%	2.22%	0.90%
2.55 g/ml Final Float	11.0	380	40	1	0.67	0.04	0.045%	0.017%	0.001%	0.004%	0.007%	0.003%

Cone Crush Size by Size Fractionation Summary

Assay Head

Cone Crush Size by Size Fractionation Summary Size by Size Analysis												
Calc. Head	29817.3	1106	3043	12	4.33	0.58	100.00%	100.00%	100.00%	100.00%	100.00%	100.00%
-4.75mm +3.35mm	6160.5	758	2906	11	4.17	0.49	20.66%	14.17%	19.73%	18.89%	19.93%	17.49%
-3.35mm +2.36mm	5947.9	1062	2875	10	4.21	0.49	19.95%	19.16%	18.85%	17.53%	19.43%	16.78%
-2.36mm +1.70mm	3752.7	1159	2831	12	4.20	0.48	12.59%	13.19%	11.71%	12.32%	12.23%	10.51%
-1.70mm +1.18mm	3025.6	964	2869	13	4.23	0.50	10.15%	8.85%	9.57%	11.40%	9.93%	8.75%
-1.18mm +850µm	1862.4	1202	2894	12	4.22	0.54	6.25%	6.79%	5.94%	6.48%	6.09%	5.81%
-850µm +600µm	1473.9	1153	2975	11	4.27	0.59	4.94%	5.15%	4.83%	4.55%	4.88%	5.05%
-600µm +425µm	1285.0	927	2868	10	4.16	0.59	4.31%	3.61%	4.06%	3.51%	4.14%	4.42%
-425µm +300µm	984.4	1606	3093	9	4.32	0.72	3.30%	4.80%	3.36%	2.51%	3.30%	4.13%
-300µm	5325.0	1503	3740	15	4.86	0.88	17.86%	24.28%	21.95%	22.81%	20.07%	27.05%

SelFrag Crush Density Fractionation Summary

Assay Head

SAMPLE	Mass	Au	Cu	Mo	Fe	S	Between STAGE Deportment					
	g	ppb	ppm	ppm	%	%	Yield	Au	Cu	Mo	Fe	S
SelFrag Crush Density Fractionation Summary Analysis												
Calc. Head	24989.8	893	2708	11	4.12	0.44	100.00%	100.00%	100.00%	100.00%	100.00%	100.00%
2.95 g/ml sink	279.7	7487	19056	14	20.87	9.60	1.12%	9.39%	7.87%	1.44%	5.68%	24.43%
2.85 g/ml sink	404.0	3337	10990	17	10.09	1.95	1.62%	6.04%	6.56%	2.61%	3.96%	7.16%
2.75 g/ml sink	1771.6	1450	6027	17	6.81	0.86	7.09%	11.52%	15.78%	11.33%	11.72%	13.84%
2.65 g/ml sink	20870.7	736	2203	10	3.73	0.28	83.52%	68.82%	67.93%	80.93%	75.76%	53.15%
2.55 g/ml sink	1649.0	570	758	6	1.77	0.09	6.60%	4.21%	1.85%	3.66%	2.84%	1.40%
2.55 g/ml Final Float	14.8	237	438	5	2.69	0.19	0.059%	0.016%	0.010%	0.028%	0.039%	0.026%

SelFrag Crush Size by Size Fractionation Summary

Assay Head

SelFrag Crush Size by Size Fractionation Summary Size by Size Analysis												
Calc. Head	27631.6	1106	3043	12	4.33	0.58	100.00%	100.00%	100.00%	100.00%	100.00%	100.00%
-4.75mm +3.35mm	7321.9	694	2418	10	4.05	0.34	26.50%	16.64%	21.06%	21.23%	24.77%	15.63%
-3.35mm +2.36mm	6177.8	693	2554	13	4.03	0.38	22.36%	14.01%	18.77%	24.80%	20.84%	14.82%
-2.36mm +1.70mm	3832.4	863	2740	10	4.14	0.42	13.87%	10.83%	12.49%	11.20%	13.29%	10.06%
-1.70mm +1.18mm	3121.7	1176	2757	10	4.12	0.45	11.30%	12.02%	10.24%	9.52%	10.75%	8.84%
-1.18mm +850µm	1742.0	1092	3003	10	4.12	0.50	6.30%	6.22%	6.22%	5.24%	6.00%	5.49%
-850µm +600µm	1256.6	1249	3293	10	4.31	0.66	4.55%	5.14%	4.92%	3.70%	4.53%	5.17%
-600µm +425µm	911.0	1479	3481	10	4.39	0.79	3.30%	4.41%	3.77%	2.67%	3.35%	4.50%
-425µm +300µm	626.3	1826	4054	8	4.77	1.11	2.27%	3.74%	3.02%	1.49%	2.50%	4.34%
-300µm	2641.8	3121	6209	25	6.32	1.88	9.56%	26.98%	19.51%	20.14%	13.97%	31.14%

HPGR Crush Density Fractionation Summary

Assay Head

SAMPLE	Mass	Au	Cu	Mo	Fe	S	Between STAGE Deportment					
	g	ppb	ppm	ppm	%	%	Yield	Au	Cu	Mo	Fe	S
HPGR Crush Density Fractionation Summary Analysis												
Calc. Head	24645.3	931	2811	11	4.00	0.47	100.00%	100.00%	100.00%	100.00%	100.00%	100.00%
2.95 g/ml sink	459.4	7142	15997	22	17.87	7.54	1.86%	14.30%	10.61%	3.63%	8.32%	29.96%
2.85 g/ml sink	464.5	4061	11453	22	9.64	1.86	1.88%	8.22%	7.68%	3.59%	4.54%	7.47%
2.75 g/ml sink	2895.9	1605	5961	20	6.22	0.82	11.75%	20.26%	24.92%	20.25%	18.25%	20.52%
2.65 g/ml sink	16407.7	660	2174	11	3.64	0.27	66.58%	47.21%	51.48%	64.54%	60.44%	38.54%
2.55 g/ml sink	4384.2	523	837	5	1.90	0.09	17.79%	9.99%	5.30%	7.96%	8.42%	3.50%
2.55 g/ml Final Float	33.8	106	341	3	1.10	0.05	0.137%	0.016%	0.017%	0.033%	0.038%	0.014%

HPGR Crush Size by Size Fractionation Summary

Assay Head

HPGR Crush Size by Size Fractionation Summary Size by Size Analysis												
Calc. Head	35145.3	1106	3043	12	4.33	0.58	100.00%	100.00%	100.00%	100.00%	100.00%	100.00%
-4.75mm +3.35mm	3880.9	835	2846	12	4.01	0.43	11.04%	8.34%	10.33%	11.05%	10.24%	8.14%
-3.35mm +2.36mm	5029.8	763	2784	12	4.03	0.43	14.31%	9.88%	13.10%	14.38%	13.34%	10.57%
-2.36mm +1.70mm	3719.3	817	2856	14	4.02	0.46	10.58%	7.82%	9.93%	12.09%	9.84%	8.46%
-1.70mm +1.18mm	3825.1	1150	2794	11	3.98	0.44	10.88%	11.32%	9.99%	9.84%	10.00%	8.34%
-1.18mm +850µm	2688.3	899	2760	11	3.95	0.45	7.65%	6.22%	6.94%	7.34%	6.99%	5.96%
-850µm +600µm	2260.3	931	2821	10	4.00	0.51	6.43%	5.42%	5.96%	5.17%	5.94%	5.67%
-600µm +425µm	1878.9	1239	2742	9	3.99	0.55	5.35%	5.99%	4.82%	4.03%	4.93%	5.10%
-425µm +300µm	1362.8	1161	2916	9	4.03	0.69	3.88%	4.07%	3.72%	3.07%	3.61%	4.65%
-300µm	10500.0	1516	3586	13	5.08	0.83	29.88%	40.95%	35.21%	33.04%	35.10%	43.11%

VSI Crush Density Fractionation Summary

Assay Head

SAMPLE	Mass	Au	Cu	Mo	Fe	S	Between STAGE Deportment					
	g	ppb	ppm	ppm	%	%	Yield	Au	Cu	Mo	Fe	S
VSI Crush Density Fractionation Summary Analysis												
Calc. Head	26194.9	916	2766	10	4.14	0.45	100.00%	100.00%	100.00%	100.00%	100.00%	100.00%
2.95 g/ml sink	399.8	8036	15950	17	18.89	8.56	1.53%	13.38%	8.80%	2.59%	6.96%	28.90%
2.85 g/ml sink	618.6	3158	10408	18	9.49	1.70	2.36%	8.14%	8.89%	4.18%	5.41%	8.86%
2.75 g/ml sink	856.8	1659	7087	20	6.92	0.96	3.27%	5.92%	8.38%	6.57%	5.47%	6.96%
2.65 g/ml sink	23234.6	717	2265	10	3.75	0.28	88.70%	69.43%	72.64%	84.06%	80.40%	54.24%
2.55 g/ml sink	1078.5	692	865	6	1.75	0.11	4.12%	3.11%	1.29%	2.57%	1.74%	1.02%
2.55 g/ml Final Float	6.6	466	419	15	4.81	0.57	0.025%	0.013%	0.004%	0.037%	0.029%	0.032%

VSI Crush Size by Size Fractionation Summary

Assay Head

VSI Crush Size by Size Fractionation Summary Size by Size Analysis												
Calc. Head	31942.1	1106	3043	12	4.33	0.58	100.00%	100.00%	100.00%	100.00%	100.00%	100.00%
-4.75mm +3.35mm	7399.2	698	2842	12	4.28	0.40	23.16%	14.63%	21.63%	22.86%	22.92%	16.18%
-3.35mm +2.36mm	5213.9	860	2673	10	4.07	0.39	16.32%	12.69%	14.34%	13.32%	15.36%	10.95%
-2.36mm +1.70mm	3501.1	942	2786	10	4.07	0.43	10.96%	9.33%	10.03%	8.93%	10.31%	8.16%
-1.70mm +1.18mm	3368.4	936	2735	9	3.99	0.41	10.55%	8.93%	9.48%	8.23%	9.72%	7.40%
-1.18mm +850µm	2177.5	1078	2702	9	4.12	0.47	6.82%	6.65%	6.05%	5.24%	6.50%	5.60%
-850µm +600µm	1833.1	1212	2737	10	4.11	0.55	5.74%	6.29%	5.16%	4.85%	5.45%	5.47%
-600µm +425µm	1556.3	1142	2706	9	4.08	0.61	4.87%	5.03%	4.33%	3.78%	4.59%	5.14%
-425µm +300µm	1145.3	1359	2978	8	4.44	0.84	3.59%	4.41%	3.51%	2.40%	3.68%	5.24%
-300µm	5747.2	1969	4305	20	5.17	1.15	17.99%	32.04%	25.46%	30.40%	21.48%	35.86%

APPENDIX 4

Statements of contribution of co-authors

STATEMENT OF CONTRIBUTION OF CO-AUTHORS

To whom it may concern

I, **Paul Bode**, the primary author of the following three publications produced from this thesis, contributed to the conception, design, data collection, analysis and interpretation and wrote the manuscript of all the three publications. These are:

- **Bode, P.,** 2017. AMIRA P420F Gold Processing Technology - Crushing, Liberation & Pre-concentration of Gold Ores progress report: Development of a novel approach to characterise the effect of different modes of particle breakage on coarse gangue rejection. Perth, Western Australia.
- **Bode, P.,** McGrath, T., & Eksteen, J., (2019). Characterising the effect of different modes of particle breakage on coarse gangue rejection for orogenic gold ore. In World Gold Conference, Perth, WA, 11-13 September 2019 (pp. 285-302).
- **Bode, P.,** McGrath, T.D.H. and Eksteen, J.J., 2019. Characterising the effect of different modes of particle breakage on coarse gangue rejection for an orogenic gold ore. Mineral Processing and Extractive Metallurgy, pp.1-14.

Signature of Candidate:

I, as a co-author, endorse that this level of contribution by the candidate indicated above is appropriate.

Dr Teresa McGrath
Signature:

Prof Jacques Eksteen
Signature: